

# smartCrystals<sup>®</sup> - investigations on preparation, preservation and long-term stability

Dissertation zur Erlangung des akademischen Grades des  
Doktors der Naturwissenschaften (Dr. rer. nat.)

eingereicht im Fachbereich Biologie, Chemie, Pharmazie  
der Freien Universität Berlin

vorgelegt von

Loaye Al Shaal

aus Damaskus

Juni 2011

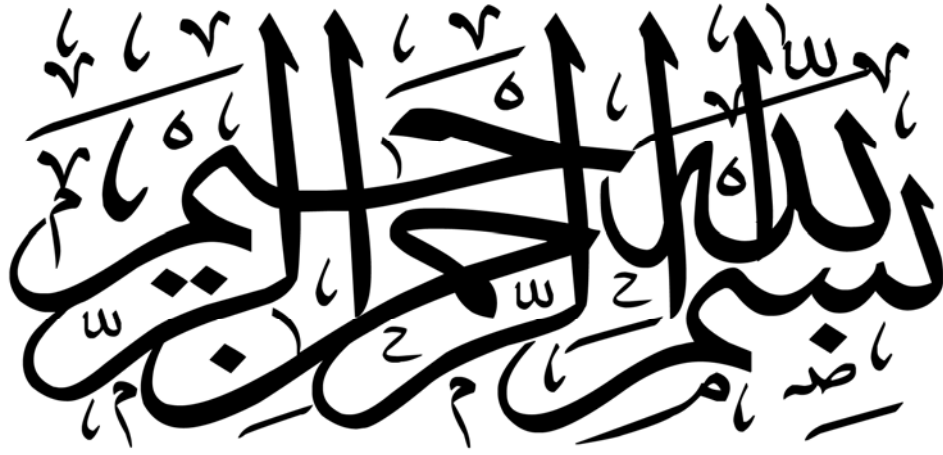
The work of this thesis was performed at the department of Pharmaceutical Technology, Biopharmaceutics & NutriCosmetics at the Freie Universität Berlin under the supervision of Prof. Dr. Rainer H. Müller from February 2008 until May 2011.

1<sup>st</sup> Reviewer: Prof. Dr. Rainer H. Müller

2<sup>nd</sup> Reviewer: Prof. Dr. Michael Dittgen

Date of defense: 07. July 2011





To my mother and father with love and gratitude

Das Fehlen einer besonderen Kennzeichnung oder eines entsprechenden Hinweises auf ein Warenzeichen, ein Gebrauchsmuster oder einen Patentschutz lässt nicht den Schluss zu, dass über die in dieser Arbeit angegebenen Dinge frei verfügt werden kann.

<b>1</b>	<b>INTRODUCTION</b>	<b>5</b>
1.1	THE SKIN	5
1.2	AGEING OF THE SKIN	6
1.3	FLAVONOIDS	7
1.4	DRUG SOLUBILITY	10
1.5	NANOSUSPENSIONS AND NANOCRYSTALS	11
1.5.1	<i>Bottom-up technologies</i>	12
1.5.2	<i>Top-down technologies</i>	13
1.5.2.1	Pearl milling	13
1.5.2.2	Homogenization in water	13
1.5.2.3	Homogenization in water-liquid mixtures and non aqueous media	13
1.5.3	<i>Combination technologies</i>	14
<b>2</b>	<b>AIMS &amp; OBJECTIVES</b>	<b>17</b>
2.1	FORMULATION DEVELOPMENT OF NANOSUSPENSIONS	17
2.2	NANOSUSPENSIONS INCORPORATION IN SEMI-SOLID DOSAGE FORM	17
2.3	<i>IN VITRO</i> EVALUATION	17
<b>3</b>	<b>MATERIALS &amp; METHODS</b>	<b>18</b>
3.1	MATERIALS	18
3.1.1	<i>Hesperetin</i>	18
3.1.2	<i>Apigenin</i>	18
3.1.3	<i>Stabilizing agents</i>	19
3.1.3.1	Tween 80	19
3.1.3.2	Poloxamer 188	20
3.1.3.3	Plantacare <sup>®</sup> 2000 UP	20
3.1.3.4	Inutec <sup>®</sup> SP1	21
3.1.4	<i>Preservatives</i>	21
3.1.4.1	Caprylyl glycol	21
3.1.4.2	Cetylperidinium Chloride (CPC)	22
3.1.4.3	Ethanol	22
3.1.4.4	Euxyl <sup>®</sup> K 700 (EUX700)	22
3.1.4.5	Euxyl <sup>®</sup> K 702 (EUX702)	23
3.1.4.6	Euxyl <sup>®</sup> PE 9010 (EUX9010)	23
3.1.4.7	Glycerin	24
3.1.4.8	Hydrolite <sup>®</sup> -5 (Pentylene glycol)	24
3.1.4.9	MultiEx naturotics	25
3.1.4.10	Propylene glycol	26
3.1.4.11	Phenonip <sup>®</sup>	26
3.1.4.12	Rokonsal <sup>®</sup> PB-5	27

3.1.4.13	Triclosan.....	27
3.1.4.14	D-alpha tocopheryl polyethylene glycol 1000 succinate (TPGS).....	28
3.1.5	2,2-diphenyl-1-picrylhydrazyl (DPPH).....	29
3.1.6	Gelling agents.....	30
3.2	METHODS.....	30
3.2.1	Determination of refractive index (RI).....	30
3.2.2	Production of nanosuspensions by high pressure homogenization (HPH).....	30
3.2.2.1	Operation principle of a piston-gap type high pressure homogenizer.....	30
3.2.2.2	Preparation of nanosuspensions.....	31
3.2.3	Production of smartCrystals <sup>®</sup> .....	32
3.2.4	Characterization of drug nanosuspensions.....	32
3.2.4.1	Laser Diffractometry (LD).....	32
3.2.4.2	Photon Correlation Spectroscopy (PCS).....	33
3.2.4.3	Zeta potential.....	34
3.2.4.4	Light microscopy.....	35
3.2.5	Determination of the antioxidant activity.....	35
3.2.6	Drug assay.....	35
3.2.6.1	Hesperetin.....	36
3.2.6.2	Apigenin.....	36
3.2.7	In vitro dissolution behavior.....	36
3.2.8	Saturation solubility.....	36
3.2.9	X-ray diffraction (XRD).....	37
3.2.10	Semi-solid dosage form development.....	37
<b>4</b>	<b>RESULTS &amp; DISCUSSION.....</b>	<b>38</b>
4.1	HESPERETIN.....	38
4.1.1	Refractive index (RI).....	38
4.1.2	Screening of stabilizers.....	38
4.1.3	Reproducibility.....	44
4.1.4	Preservative screening.....	45
4.1.4.1	Addition preservatives after homogenization.....	46
4.1.4.2	Addition preservatives before homogenization.....	50
4.1.4.3	Optimised addition of preservatives.....	58
4.1.5	Antifoaming agents effect.....	59
4.1.6	Scale-up.....	62
4.1.6.1	Batch production using Avestin C50.....	63
4.1.6.2	Production of smartCrystals <sup>®</sup> (CT).....	69
4.1.7	Screening of gelling agents.....	75
4.1.8	Long term physical Stability.....	75
4.1.8.1	Long term physical stability of hesperetin nanosuspensions in different stabilizers.....	75

4.1.8.2	Long term physical stability of lab scale preserved batches .....	79
4.1.8.3	Long term physical stability of hesperetin nanosuspensions in presence of antifoaming agent .....	91
4.1.8.4	Long term physical stability of hesperetin nanosuspensions incorporated in different gels .....	94
4.1.8.5	Long term physical stability of scaled up nanosuspensions .....	95
4.1.9	<i>Saturation solubility</i> .....	118
4.1.10	<i>Antioxidant activity</i> .....	119
4.1.11	<i>X-ray diffraction (XRD)</i> .....	124
4.1.12	<i>In vitro release</i> .....	125
4.1.12.1	Cellulose acetate membranes .....	125
4.1.13	<i>Chemical stability</i> .....	126
4.2	<b>APIGENIN</b> .....	131
4.2.1	<i>Refractive index</i> .....	131
4.2.2	<i>Screening of stabilizers</i> .....	131
4.2.3	<i>Reproducibility</i> .....	131
4.2.4	<i>Preservative screening</i> .....	132
4.2.5	<i>Scale-up (smartCrystals®)</i> .....	138
4.2.5.1	Ethanol and glycols .....	140
4.2.5.2	Synthetic established single preservatives .....	143
4.2.5.3	Combinations of preservatives .....	144
4.2.5.4	Surface active agents .....	147
4.2.5.5	Zeta potential (ZP) .....	149
4.2.6	<i>Incorporation in gels</i> .....	150
4.2.7	<i>Long term physical stability</i> .....	150
4.2.7.1	Long term physical stability of lab scale preserved batches .....	151
4.2.7.2	Long term physical stability of apigenin nanosuspensions incorporated in gels .....	163
4.2.7.3	Long term physical stability of smartCrystals® .....	163
4.2.8	<i>Saturation solubility</i> .....	177
4.2.9	<i>Antioxidant activity</i> .....	177
4.2.10	<i>X-ray diffraction (XRD)</i> .....	182
4.2.11	<i>In vitro release</i> .....	183
4.2.12	<i>Chemical stability</i> .....	184
<b>5</b>	<b>SUMMARY/ZUSAMMENFASSUNG</b> .....	<b>186</b>
5.1	SUMMARY .....	186
5.2	ZUSAMMENFASSUNG .....	187
<b>6</b>	<b>REFERENCES</b> .....	<b>190</b>
<b>7</b>	<b>PUBLICATION LIST</b> .....	<b>201</b>
<b>8</b>	<b>ACKNOWLEDGMENTS</b> .....	<b>204</b>



<b>9</b>	<b>CURRICULUM VITAE .....</b>	<b>206</b>
	<i>Personal data .....</i>	<i>206</i>
	<i>Educational background and Certificates .....</i>	<i>206</i>
	<i>Work Experiences.....</i>	<i>207</i>
	<i>Teaching Experiences .....</i>	<i>207</i>
<b>10</b>	<b>LIST OF FIGURES AND TABLES: .....</b>	<b>208</b>
	10.1 FIGURES: .....	208
	10.2 TABLES:.....	221

# 1 Introduction

In the last two decades the aging theories were thoroughly studied. Aging is the progressive random accumulation of different, deleterious changes that increase the chance of ailment and mortality with increased age [1, 2]. Aging changes are generally related to development, genetic defects, environment, disease, and an inborn aging process. These changes limit the human life expectancy at birth to a maximum of about 85 years.

In 1956, Harman D. proposed that free radicals cause cumulative oxidative damage to cells, hence aging and subsequently death of cells occurs [3]. These free radicals are normally produced in the organism, with cellular constituents. Among the highly exposed tissues to oxidative stress in the body, skin, the largest organ and an important protective barrier between the environment and the inner milieu, is the one to be highly considered [4].

## 1.1 The skin

Morphologically, skin is divided into epidermis, dermis, and subcutaneous tissue (Fig. 1). The epidermis is the most exterior layer composed mainly of keratinocytes, pigment producing melanocytes, and antigen presenting Langerhans cells.

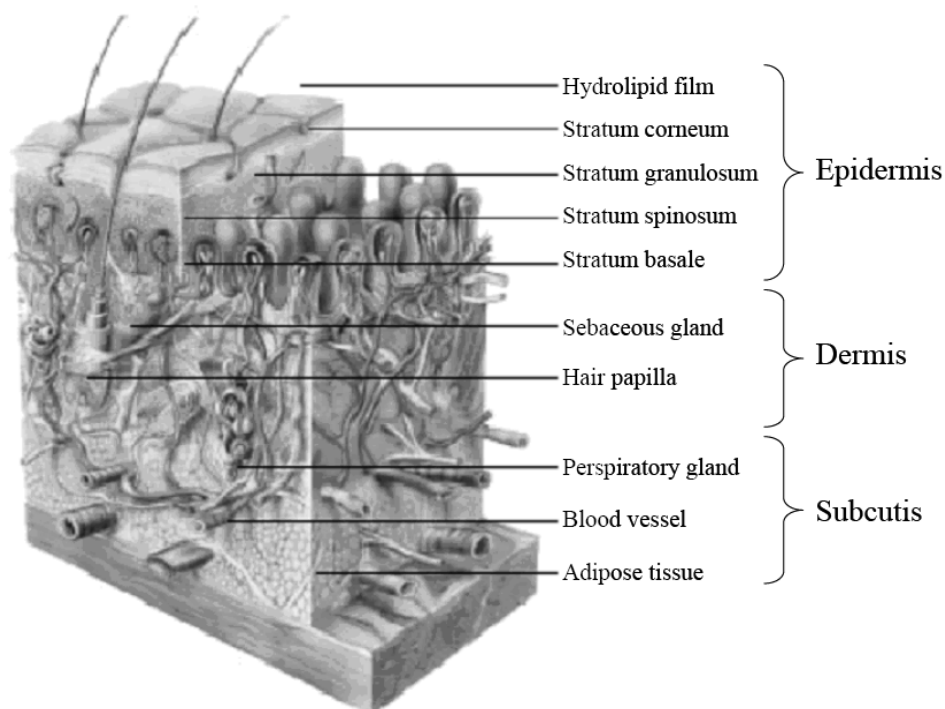


**Fig. 1** The morphology of human skin [5]

The epidermis is mainly responsible for the barrier function and mechanical resistance. A basement membrane separates the epidermis from the dermis, which is composed primarily of extracellular matrix proteins, produced by resident fibroblasts. The dermis is composed of a dense network of elastin and collagen fibers, which provide the mechanical properties of the skin. Furthermore, blood vessels, lymph vessels, nerves, cells of the immune defense system and adnexa (e.g. sweat glands, sebaceous glands, hairs) are located in the dermis and contribute to its functions (e.g. nutrition supply of the avascular epidermis, thermoregulation). The skin acts as a barrier in two directions, controlling the loss of water, electrolytes and other body constituents, while preventing the entry of harmful or unwanted molecules from the external environment [6].

The vascular supply to the skin resides in the dermis. The subcutaneous tissue consists of fat cells that underline the connective tissue framework. Cells are equipped with an impressive repertoire of antioxidant enzymes, as well as small antioxidant molecules mostly derived from dietary fruits and vegetables [7].

## 1.2 Ageing of the skin

Chronologically aged skin appears thin, smooth, dry, unblemished, with some loss of elasticity. The most obvious sign of aged skin is wrinkling. These ageing wrinkles develop from the flattening of the dermo-epidermal junction, the effect of gravity and the absence of elastic properties of the skin.

The keratinization in skin takes longer in elderly people [8, 9]. A diminution in the quantitative structure of collagen can be recognized in aged skin [10]. In order to maintain skin hydration, Hyaluronan-bound water in the dermis and in the viable areas of the epidermis is a crucial factor. In aged skin epidermal hyaluronan decline significantly although the total amount of hyaluronan remains stable in the dermis. An ongoing depletion in size of the hyaluronan polymer and lymphatic vessel atrophy in the skin as a function of age has been reported [11, 12]. It is now beyond doubt that oxidants are generated in vivo and can cause significant harm [13-16].

Photodamaged skin is highly correlated to increased epidermal thickness, and modifications of the connective tissue organization. The aggregation of amorphous elastin-containing material that stay under the epidermal dermal junction is regarded the main manifestation of photoaged skin. The changes in the fibrillar organization of collagen and elastin was observed intensely in photoaged skin, compared to sun-protected chronologically aged skin [17]. The

degree of skin pigmentation and the accumulated sun exposure affect the severity of photoaging.

In general, the morphological and histological characteristics of photoaged skin are different from the chronologically aged one. However, emerging evidence indicates that many of the molecular alterations that occur in human skin following acute UV irradiation closely resemble those observed in chronologically aged, as compared to young skin.

Skin undergoes oxidative stress from both exogenous and endogenous sources [18]. Exogenous sources contain environmental factors such as air pollutants, ionizing and non-ionizing radiation [18, 19], while endogenous sources consist of reactive species formed from activated neutrophils and phagocytes as well as enzymes which produce active oxygen metabolites [20]. The effect of the environment, particularly UV irradiation; is of a great importance regarding the oxidative stress on the skin and hence skin aging [21].

Skin has an antioxidant system of its own, which plays a main role in neutralizing the wrecking effect of reactive oxygen species (ROS) [22]. The previously mentioned system comprises of enzymatic antioxidants like catalase, superoxide dismutase (SOD) and glutathione peroxidase. Non-enzymatic antioxidants include Vitamin E, ascorbate glutathione and uric acid [23]. However, it was noticed that the activity of the antioxidant enzymes reduces with aging while an increasing in the oxidizing compounds was observed [24, 25].

Presently, more than 300 ageing theories have been published [26]. Many of them are connected as the biological processes in the body and the factors affecting ageing are crosslinked. In addition, many DNA and genetic theories were postulated and the most prominent one is the one described by Hayflick [27].

The most prominent ageing theory is the free radical theory postulated by Harman [24, 28]. Reactive oxygen species, such as superoxide radical, hydrogen peroxide, singlet oxygen and hydroxyl radical can cause oxidative damage to cellular macromolecules such as proteins, carbohydrates, lipids and nucleic acids and are thus cytotoxic.

### 1.3 Flavonoids

The polyphenolic flavonoids have the diphenylpropane ( $C_6C_3C_6$ ) skeleton. The family includes monomeric flavanols, flavanones, anthocyanidins, flavones, and flavonols (Fig. 2). Along with the phenylpropanoids or hydroxycinnamic acid derivatives ( $C_6C_3$ ) (Fig. 2F), flavonols and to a lesser extent flavones are found in almost every plant [29]. While flavanones and flavones are often found together (e.g., in citrus fruits) and are connected by

specific enzymes, there is a certain mutual exclusion between flavones and flavonols in many plant families and anthocyanins are almost absent in flavanone-rich plants [30].

Plant polyphenols are multifunctional and can act as reducing agents, hydrogen donating antioxidants, and singlet oxygen quenchers.

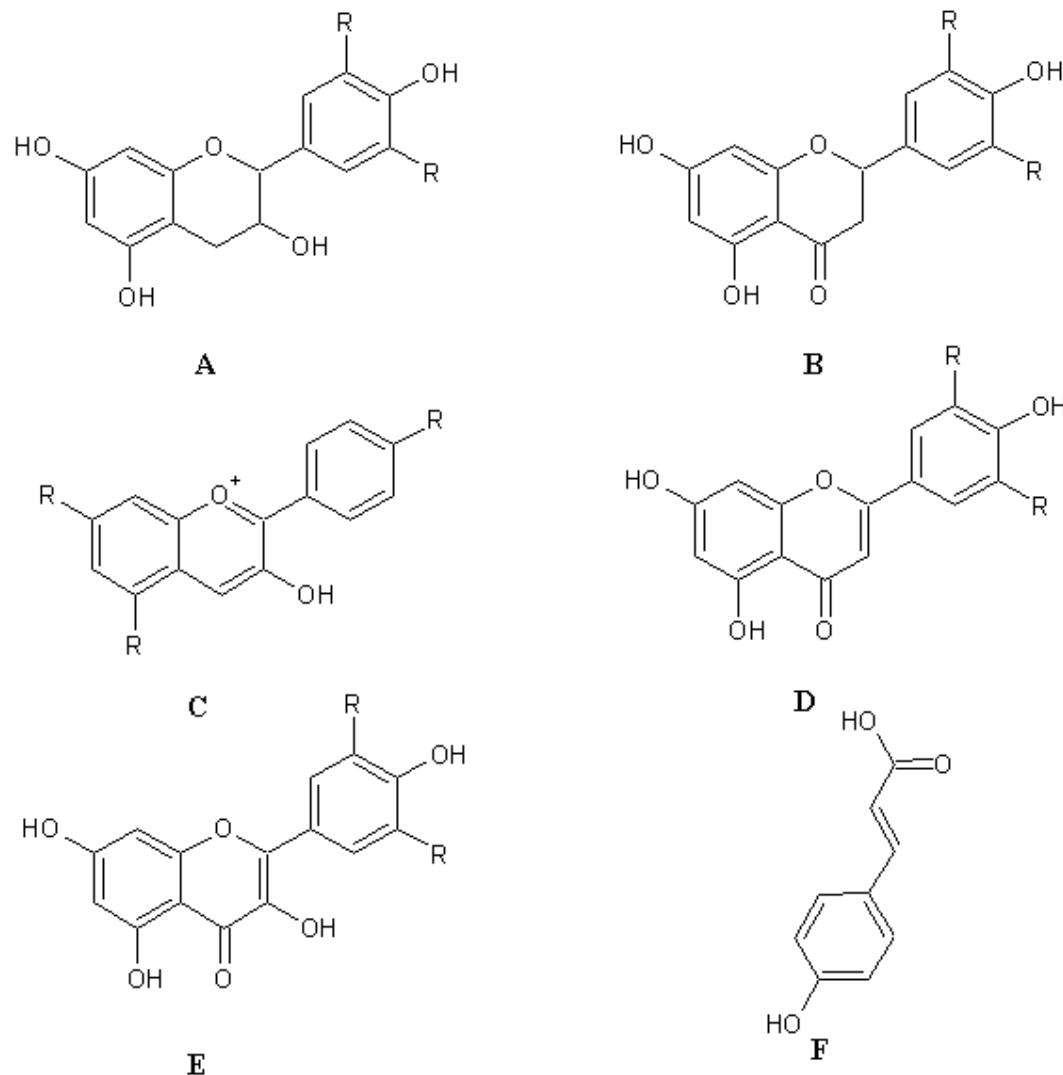


**Fig. 2** Chemical structure of the flavonoid family: (A) flavanols, (B) flavanones, (C) anthocyanidins, (D) flavones, (E) flavonols, (F) hydroxycinnamic acid.

The chemical properties of polyphenols in terms of the availability of the phenolic hydrogens as hydrogen donating radical scavengers predicts their antioxidant activity.

The biological, pharmacological, and medicinal properties of the flavonoids have been extensively reviewed [31, 32]. Flavonoids and other plant phenolics are reported, in addition to their free radical scavenging activity [33], to have multiple biological activities [34, 35] including vasodilatory [36], anticarcinogenic, antiinflammatory, antibacterial, immunostimulating, antiallergic, antiviral, and estrogenic effects, as well as being inhibitors of

phospholipase A2, cyclooxygenase, and lipoxygenase [34, 37-41] (about which a considerable amount of work has been published), glutathione reductase, [42] and xanthine oxidase [43].

The chemistry of the flavonoids is predictive of their free radical scavenging activity because the reduction potentials of flavonoid radicals are lower than those of alkyl peroxy radicals and the superoxide radical, Flavonoids as antioxidants means that flavonoids may inactivate these oxyl species and prevent the deleterious consequences of their reactions [39] Their antioxidant activity is also reported as scavengers of superoxide radical [44-47], although there is conflicting evidence [48, 49], peroxy radical scavengers [50], inhibitory effects on lipid peroxidation [51]; inhibition of LDL oxidation induced by copper ions and macrophages [52] with half-maximal inhibition induced by compounds ranging in concentration from 1-10  $\mu$ M.

Many in vitro studies have defined the antioxidant potential of the polyphenols as direct radical scavengers and as agents capable of enhancing the resistance to oxidation of low density lipoproteins implicated in the pathogenesis of coronary heart disease. All the major polyphenolic constituents of food (Table 1) show greater efficacy in these systems as antioxidants on a mole for mole basis than the antioxidant nutrients vitamin C, vitamin E, and 3-carotene [53].

**Table 1 Different types of flavonoids used as antioxidants**

<b>Type of flavonoids</b>	<b>Commonly used compounds</b>
<b>Flavones</b>	luteolin apigenin
<b>Flavanones</b>	hesperetin naringenin
<b>Flavonols</b>	quercetin kaempferol
<b>Flavanols</b>	catechin epicatechin
<b>Anthocyanidin (flavylium salts)</b>	cyaniding cyanin and their glycosides

Due to the phenolic nature of flavonoids they are considerably polar but at the same time they exhibit poor solubility in water, thus have limited absorption [54].

In many cases poorly soluble actives, pharmaceuticals and cosmetics, have bioavailability problems at their desired site of action, especially when the actives are simultaneously poorly soluble in aqueous and non-aqueous (organic) media [55-57]. In most cases, the poorly soluble actives are lipophilic; hence, in principle the molecules show a good permeability through lipophilic membranes.

## 1.4 Drug solubility

Poor solubility is generally related to a slow dissolution velocity. Thus, when the few dissolved molecules have permeated a membrane in the body, dissolution from the crystals of the active is not fast enough to replace the permeated molecules (Fig. 3, left). The rate-limiting step for absorption of such drugs is the dissolution velocity. These drug are the so called class II drugs of the biopharmaceutical classification system (BCS) [58-60]. One approach to overcome this problem is the production of nanocrystals. Nanocrystals possess an increased dissolution velocity due to their large surface area  $A$ , but also because in addition they exhibit an increased saturation solubility  $C_s$  [61-66] (Fig. 3, right). Apart from fast dissolution, the increased saturation solubility  $C_s$  leads to an increased concentration gradient at membranes further promoting permeation (Fig. 3, right).

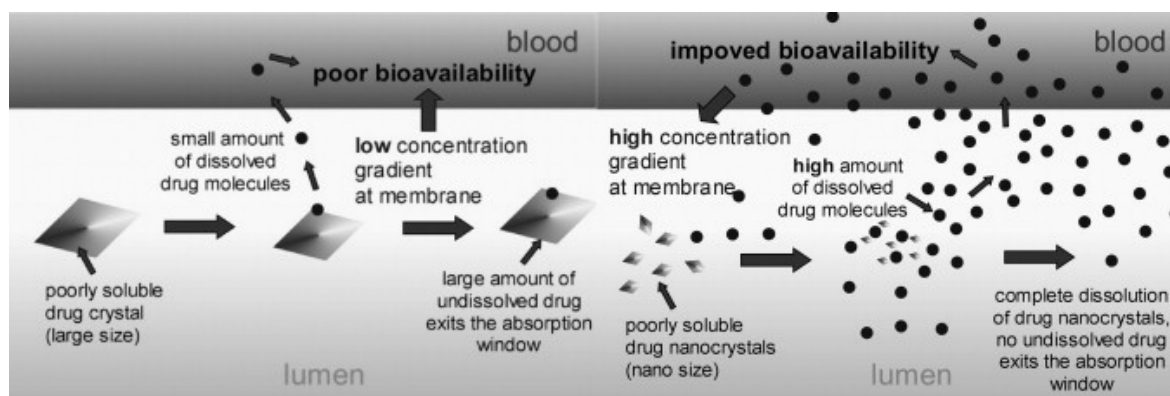


**Fig. 3 Left: poor solubility of BCS class II drug due to low-dissolution velocity and low-concentration gradient at membrane; right: improved bioavailability by production of nanocrystals, processing an increased saturation solubility and a high dissolution velocity which leads to a high-concentration gradient at the membranes [67]**

According to the biopharmaceutical classification system (BCS), poorly soluble drugs are classified under BCS class II (poor solubility and high permeation) and class IV (poor solubility, poor permeability), which generally have oral bioavailability problems [56, 57, 68]. There are many ways to increase the solubility of poorly soluble drugs, e.g. solubilization. But these methods are limited to drugs with certain properties in regard to their chemistry (e.g., solubility in certain organic media) or for example to their molecular size or conformation

(e.g., molecules to be incorporated into the cyclodextrin ring structure [69, 70]). Apart from that, the usage of surfactants or cosolvents is also possible, but sometimes leads to increased side effects (e.g., Cremophor EL increases the toxicity of Taxol<sup>®</sup>, HP- $\beta$ -cyclodextrin is the cause of nephrotoxicity of itraconazole in Sporanox<sup>®</sup> [71]).

With regard to dermal application a prolonged contact time due to the adhesive properties of nanoparticulate materials on the skin can be achieved. Furthermore, the increased saturation solubility can promote penetration of the active ingredient due to an increased concentration gradient between dermal formulation and the skin.

In principle, there is little difference between the penetration problems of dermal drugs and dermal cosmetic actives. The requirements regarding formulation characteristics (e.g. nanocrystal size), physical stability, tolerability/toxicity and desired controlled increased penetration are identical or at least similar (of course still having in mind the less strict regulatory hurdles for cosmetics).

To elucidate the principle production and formulation parameters affecting the size characteristics and physical stability of dermal nanocrystals, the active Hesperetin was used to produce nanocrystals.

## 1.5 Nanosuspensions and nanocrystals

As the penetration problems of dermal drugs and dermal cosmetic actives are similar [67], nanocrystals were meanwhile introduced to the cosmetic market by PharmaSol GmbH Berlin (e.g. products from Juvena Switzerland, e.g. series Juvedical and la prairie product platinum rare). Important formulation characteristics are nanocrystal size, repulsive charge (zeta potential), physical stability in the formulation in vitro (e.g. in presence of preservatives) as well in vivo (e.g. presence of electrolytes in the gut), to avoid aggregation and subsequent loss of nanocrystal special properties.

Since 2000 more than five products entered the pharmaceutical market (e.g. Emend<sup>®</sup>, TriCor<sup>®</sup> etc.) [72], about 20 are presently in clinical phases [56].

It could be shown that dermal application of rutin and hesperidin increased the bioactivity in the skin by up to a factor 500, compared to water soluble derivatives of the original molecules [73]. The first cosmetic product with rutin nanocrystals entered the market in 2007 (line JUVEDICAL, Juvena Switzerland). The same principle can also be employed for the improved delivery of dermal drugs.

Nanocrystals can be produced in two different ways, the “Bottom-up” and “Top-down” technologies. In the “Bottom-up” technology the production starts from molecules dissolved



in a solvent followed by precipitation. i.e. adding the solution to a non-solvent (e.g. NanoMorph™). Scaling-up the “Bottom-up” technology can be relatively easy when using e.g. static blenders. However, major disadvantages of this technology are the use organic solvents (costs for removal, potential residues in the product), and the difficulty to avoid crystal growth to the  $\mu\text{m}$  range, and long-term preservation of the crystal size in the nanosuspensions. Therefore all the nanocrystals products on the pharmaceutical market (about 6) are based on top down technology.

Top-down technologies are better applicable in pharmaceutical industry. Nanocrystals can be produced using two different wet milling methods, low energy milling technology (Nanosystems/élan [74]) or high pressure homogenization (Dissocubes® technology [75]). In low energy milling the grinding of the particles takes place by beads or pearls. High pressure homogenization (HPH) forces the particles to pass through a tiny gap (5-10  $\mu\text{m}$ , depending on the applied pressure) with high velocity causing the particle size reduction by cavitation, particle collision and shear forces. A second generation of drug nanocrystals (smartCrystals®) was introduced by using a combination of both technologies. The particles are firstly pre-milled by pearl milling, and subsequently passed through a high pressure homogenizer [76]. There is only limited data published about the scale up of this nanocrystals production technology. The reasons are that the technology is relatively young (at beginning of the 1990s), and most of the research is less performed in academia, most in industry and the data are held confidential.

### 1.5.1 Bottom-up technologies

The particles are generated by precipitation, as for example by Sucker are in most cases crystalline in nature; in contrast to this, the company Knoll (nowadays owned by Abbott, the new name is “Soliqs”) created amorphous particles by a precipitation technique [77]. The product is NanoMorph™.

The advantage of the precipitation techniques is that relatively simple equipment can be used. However, there are some major general disadvantages of the precipitation techniques. The drug needs to be soluble in at least one solvent (thus excluding all new drugs that are simultaneously poorly soluble in aqueous and in organic media). The solvent needs to be miscible with at least one non-solvent. Solvent residues need to be removed, thus increasing production costs.

It is a little bit tricky to preserve the particle characteristics (i.e. size, especially the amorphous fraction).

## 1.5.2 Top-down technologies

There are basically two top-down techniques, which mean starting from a large sized powder and performing a size diminution [78, 79]:

### 1.5.2.1 Pearl milling

Liversidge and co-workers developed the milling process to yield the so-called NanoCrystals<sup>®</sup>. The mills used by the élan Company are basically containers with small pearls, beads, or balls which can have different sizes, a typical size being 1-2 mm. In the milling process, the pearls are moved, either by using a stirrer or by moving the milling container itself. This process is accompanied by the erosion of milling material from the pearls, a phenomenon well known for these mills and documented in the literature [79].

### 1.5.2.2 Homogenization in water

Homogenization in water is performed either using microfluidizers as high pressure homogenizers (SkyePharma Canada Inc.) or piston-gap homogenizers. In microfluidizer, a frontally collision of two fluid streams under pressure up to 1700 bar leads to particle collision, shear forces and cavitation forces. The collision chambers are designed as Y type or Z type. A major disadvantage of microfluidizers is the required long production time. The company SkyePharma Canada Inc applies this technology to produce submicron particles of poorly soluble drugs [78]. Cavitation was employed as the most important effect to diminish particles in a piston-gap homogenizer. In this homogenizer types, the dispersion (emulsion or suspension) passes a very tiny gap with an extremely high velocity. Prior to entering the gap, the suspension is contained in a cylinder with a relatively large diameter compared to the width of the following gap. In the APV LAB 40, the diameter of the cylinder is about 3 cm, it narrows to about roughly 3 - 25  $\mu\text{m}$  (varies with applied pressure) when the suspension enters the homogenization gap. The cavitation and shear forces in the gap were sufficiently high to break particles which were distinctly larger than the gap width. Therefore it is possible to disrupt relatively large sized powders (up to 200  $\mu\text{m}$ ) [78-80].

Homogenization with piston-gap homogenizers has good potential to be used as a production technique because it fulfills the key industrial features such as large scale production and various regulatory aspects [78, 79].

### 1.5.2.3 Homogenization in water-liquid mixtures and non aqueous media

The DissoCubes<sup>®</sup> patent describes homogenization in pure water as a dispersion medium; the cavitation is seen as being responsible for the diminution of the particles. The basic of the

Nanopure<sup>®</sup> technology is that homogenization was performed against these teachings, leading to a comparable or even improved product. Under the Nanopure<sup>®</sup> technology, not only drugs, but also polymers can be processed, leading to a product with a mean diameter in the nanometer range (nanoparticles) or a size of a few micrometers (both particle ranges are covered).

Nonaqueous dispersion media can be used to produce oral formulations, for example, drug nanocrystals dispersed in liquid PEG 600 or miglyol oil which can be directly filled into soft gelatin capsules, sealed hard gelatine capsules or HPMC capsules. Nanosuspensions in mixtures of water with water-miscible liquids (e.g., ethanol, isopropanol) can be used in the granulation process for tablet production; the solvent mixture evaporates much better than water.

Another option of the Nanopure<sup>®</sup> technology is the production of aqueous polymer particle dispersions with a diameter of a few micrometers or in the nanometer range. This could be an alternative to polymer dispersions (e.g. Surelease<sup>®</sup>, ethyl cellulose) for the coating of tablets which are now produced by using solvents. Aqueous shellac dispersions produced with Nanopure<sup>®</sup> technology have already been described [79].

### 1.5.3 Combination technologies

In 2001, Baxter Healthcare Company presented their NANOEDGE<sup>®</sup> technology at the annual meeting of the American Association of Pharmaceutical Scientists (AAPS) in Denver. NANOEDGE<sup>®</sup> is an aqueous suspension of drug nanoparticles suitable for intravenous injection. The particles are prepared basically by a high pressure homogenization process, which means either by microfluidization or homogenization in water using piston-gap homogenizers, or alternatively, by a new production process developed by Baxter [79]. This process is called the “microprecipitation method,” and is a combination of precipitation followed by a process with high energy input (e.g., homogenization).

The problem of the precipitation technique - continuing crystal growth after precipitation - has been overcome because the particles are only an intermediate product to undergo subsequent diminution/annealing.

Another combination technology has been developed by Petersen using ball milling and subsequent high pressure homogenization (CT). Using the CT technology, performance (e.g. physical stability) of nanocrystals could be distinctly improved, as example for dermal application. Nanocrystals can increase the penetration of poorly soluble cosmetic and pharmaceutical actives into the skin. The increased saturation solubility leads to an increased

concentration ingredient, thus promoting passive penetration. Molecules penetrated into the skin are very fast replaced by new molecules dissolving from the nanocrystal depot in the cream. The first four cosmetic nanocrystal products with rutin were launched by Juvena. As compared to the water-soluble rutin glucoside, the original rutin molecule as smartCrystal formulation possesses a 500 times higher bioactivity (as measured by sun protection factor (SPF)). The same principle can be applied to poorly soluble pharmaceutical drugs of interest for dermal application. Dermal application of nanocrystals is protected by a US and PCT patent application.

In multi-dose vials also these oral nanosuspensions need to be preserved. For example, the oral nanosuspension sodium benzoate as preservative [81]. However, many preservatives can impair the physical stability of suspensions, macro- but even more pronounced the highly dispersed nanosuspensions. Therefore in this study, the effect of various preservatives on the stability of hesperetin nanosuspensions was investigated, to identify the best or most suitable preservatives.

In order to obtain good microbial stability aqueous systems need to be preserved. Nanocrystals are provided as aqueous concentrates for incorporation into dermal formulations, for reasons of safety preservation is essential. However, many preservatives can destabilize suspensions, especially highly dispersed systems as nanosuspensions. The influence of different preservatives with different chemical properties on the physical stability of hesperetin and apigenin nanosuspensions was investigated to assess the physical stability. The particle size and particle size distribution were measured directly after the addition of the preservatives and over the time at three different temperatures. Based on zeta potentials, observed data and considering the chemical structure of the preservatives, a general guideline for the choice of preservatives for nanosuspensions should be outlined.

Hesperetin is the aglycon of hesperidin, an antioxidant [82-84]. It possesses additionally antiallergic, anti-inflammatory properties [85, 86]. Pharmaceutically it can be applied as protective agent against skin cancer because it acts as scavenger of free radicals [82]. Hesperetin is under investigation as a dermally applied cosmetic ingredient in antiaging but also pharmaceutical products. As hesperetin is a very poorly water soluble compound it can be transferred to nanocrystals to make it biologically active [87].

Hesperetin has antioxidative [83, 88, 89] and also antiallergic properties [90]. It is common knowledge, that oxidative stress, but also inflammation play a key role in the aging process [91], thus hesperetin, capable to prevent both, is thought to be a very effective anti aging compound.

Thus, hesperetin has not only a potential as oral, but also as dermal anti aging compound, thought to be even more effective than its already very effective glycoside hesperidin, which has strong antioxidative but no anti inflammatory properties [90]. Hesperetin has an even lower solubility than hesperidin (1.4 µg/ml versus 20 µg/ml of hesperidin), the molecule has more lipophilic character, and should therefore penetrate even better when the solubility problem and the low dissolution velocity can be overcome by nanocrystal production. In this study, nanosuspensions of hesperetin were produced by high pressure homogenization employing four different stabilizers. The stabilizers were of different class, i.e. low molecular weight stabilizers (i.e. surfactants) and high molecular weight polymers (i.e. steric stabilizers). The obtained nanocrystals were characterized in terms of size (laser diffractometry, photon correlation spectroscopy, light microscopy) and particle charge (zeta potential). To assess the physical stability a short-term study was performed storing the differently stabilized nanosuspensions at three different temperatures, to elucidate which type of stabilization proved to be most effective.

Apigenin is an active bioingredient found naturally in many citrus fruits [92] as well as vegetables like basil, oregano, tarragon, cilantro and parsley [93, 94]. It is used as traditional or alternative medicine and possesses anti-inflammatory, analgesic [95, 96], free radical scavenging [97], anti-carcinogenic activity [98] and antihistamine action. It has been shown to possess growth inhibitory properties in breast, colon, skin, thyroid leukemia and pancreatic cancer cell lines [99, 100]. However, its use is still limited due to their low water solubility especially when they are poorly soluble in both aqueous and organic solvents.

## **2 Aims & Objectives**

### **2.1 Formulation development of nanosuspensions**

- Develop poorly soluble flavonoid nanocrystals on a lab scale suitable for oral, dermal and mucosal application using various stabilizers.
- Investigate the physical (nanoparticles size distribution) and chemical (drug content) stability of the formulated nanosuspensions.
- Examine the effect of the anti-foaming agents on the physical and chemical stability of the nanosuspensions
- Optimize the preservatives to be used and the incorporation method.
- Investigate the physical (nanoparticles size distribution) and chemical (drug content) stability of the preserved nanosuspensions.
- Scale-up the production from small lab scale to large batches reaching 3 kg.

### **2.2 Nanosuspensions incorporation in semi-solid dosage form**

- Prepare apigenin and hesperetin gels containing drug nanocrystals using the various GRAS listed excipients.
- Characterize the products to identify the suitability of the used excipients.

### **2.3 *In vitro* evaluation**

- Perform the *in vitro* characterization of the nanosuspensions with respect to particle size analyses, morphology, physical stability, and investigate the influence of physicochemical characteristics of different nanosuspensions such as degree crystallinity of nanocrystals, solubility and dissolution behavior.
- Evaluate the drug release from the nanosuspensions and solid dosage forms using Franz diffusion cells.
- Investigate the antioxidant activity of the prepared nanosuspensions and the original raw powder in the suspension form.
- Antioxidant activity using 2,2-Diphenyl-1-Picrylhydrazyl (DPPH) method.
- Investigate the physical (nanoparticles size distribution) and chemical (drug content) stability of the lab and large preserved scale batches.
- Investigate the improvement in dissolution rate and saturation solubility of the prepared poorly soluble nanocrystals.

## 3 Materials & Methods

### 3.1 Materials

#### 3.1.1 Hesperetin

The flavonoid hesperetin (Fig. 4) is a flavanone, an aglycon of hesperidin. Hesperetin is the predominant flavonoid in lemons and oranges. The peel and membraneous parts of these fruits have the highest hesperetin concentrations. Therefore, orange juice containing pulp is richer in the flavonoid than that without pulp. Sweet oranges (*Citrus sinensis*) and tangelos are the richest dietary sources of hesperetin. Hesperetin is classified as a citrus bioflavonoid.

Hesperetin, rutin and other flavonoids are thought to reduce capillary permeability and to have anti-inflammatory action. They are collectively known as vitamin P and may have a contribution to the total antioxidant activity and act as detoxifiers. There is no official recommended dosage of Vitamin P, but an amount of 500 mg per day is indicated for supplementation [101]. It is considered that it lowers down cholesterol levels if it taken with vitamin C. It is also known to have pharmacological actions e.g. antihistaminic and antiviral. These substances, however, are not vitamins per definition and thus are no longer referred to, except in older literature, as vitamin [86].

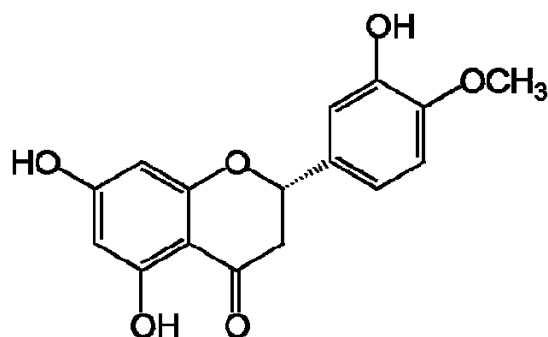


**Fig. 4** Chemical structure of hesperetin

It is soluble in organic solvents such as ethanol (1 mg/ml), dimethyl sulfoxide (DMSO) (30 mg/ml), dimethylformamid (DMF) (30 mg/ml). It is sparingly soluble in aqueous buffers and insoluble in water [87]. Hesperetin was purchased from Exquim, S.A. (Spain).

#### 3.1.2 Apigenin

Apigenin (Fig. 5), 5,7-Dihydroxy-2-(4-hydroxyphenyl)- 4H-1-benzopyran-4-on, is a flavonoid from vegetables (e.g. parsley, peppermint, perilla) and fruits (e.g. lemon, berries) [102]. As compared with other flavonoids, such as quercetin, apigenin is relatively nontoxic

and nonmutagenic. More interestingly, it has been found that apigenin can inhibit skin cancer induced by chemicals and UV radiation in mice [103, 104]. It is a naturally occurring pigment and appear as a light beige to light brown crystalline powder with a melting point of 315°C. Apigenin is a potent inhibitor of epidermal ornithine decarboxylase (ODC), a tumor promotion marker, that is induced by either UV radiation [103] or 12-O-tetradecanoylphorbol-13-acetate (TPA) [104].

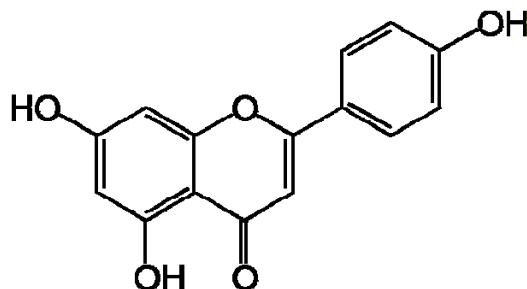


**Fig. 5 Chemical structure of apigenin**

It is abundantly found and distributed in parsley. Other important properties of apigenin are significant scavenging properties on oxidizing species such as OH radical, superoxide radical, and peroxy radical [105]. It is soluble in ethanol (0.3 mg/ml) DMSO (15 mg/ml), DMF (25 mg/ml) and in alkaline solution and insoluble in water [106]. Apigenin was purchased from Exquim, S.A. (Spain).

### **3.1.3 Stabilizing agents**

#### **3.1.3.1 Tween 80**

Polysorbate 80 (Polyoxyethylen(20)sorbitan monooleate), Tween 80 was purchased from the company Uniqema (Belgium). It is a non-ionic surfactant with a relatively low toxicity and HLB value of 15 [107]. For example for oral application, the product Combantrin<sup>®</sup> tablet and oral suspension (Pfizer Consumer Healthcare 2000) contains this surfactant. Fig. 6 represents the structure of the molecule.



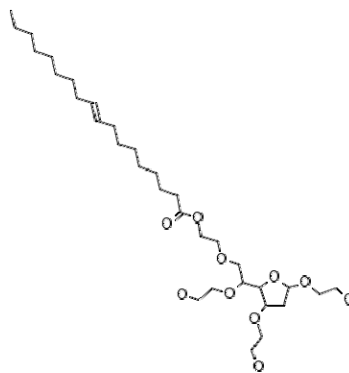
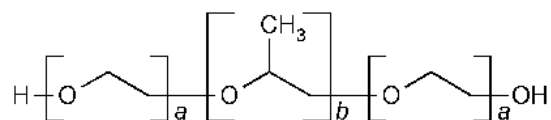


**Fig. 6 Molecular structure of Tween 80**

### 3.1.3.2 Poloxamer 188

Poloxamer 188 is a white or almost white waxy powder, microbeads or flakes with a melting point around 50°C. As all poloxamers, it is very soluble in water and alcohol. Chemically, poloxamer is a synthetic block copolymer of  $\alpha$ -Hydro- $\omega$ -hydroxypoly (oxyethylene) poly (oxypropylene) poly (oxyethylene) with the general formula shown in Fig. 7.



$$a = \text{ca. } 80, b = \text{ca. } 27$$

**Fig. 7 Molecular structure of poloxamer 188**

It has an average molecular weight from 7680 to 9510. Poloxamer 188 has an HLB value of 29 [107]. Poloxamer 188 was ordered as Lutrol<sup>®</sup> F68 from BASF AG (Germany).

### 3.1.3.3 Plantacare<sup>®</sup> 2000 UP

Plantacare<sup>®</sup> 2000 UP is a colorless viscous liquid. It is a fatty alcohol glycoside. The fatty chain consists of C6 max. 1%, C8: 33 - 40 %, C10: 21 - 28 %, C12: 27 - 32 %, C14: 9 - 12 %, C16: max. 1% (Fig. 8). Plantacare<sup>®</sup> 2000 UP was obtained from Cognis (Germany).

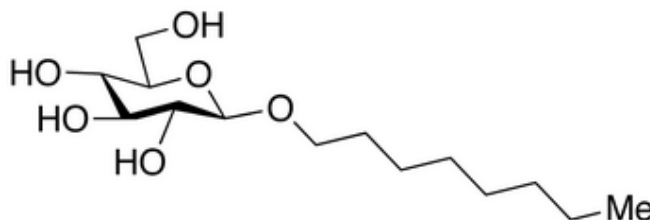


**Fig. 8 Molecular structure of Plantacare<sup>®</sup> 2000 UP**

### 3.1.3.4 Inutec® SP1

Inutec® SP1 is inulin lauryl carbamate (Fig. 9) which is white crystalline powder with a melting point of 170°C. It is a non-ionic, polymeric-based surfactant system derived from chicory inulin. It can be used as an emulsion stabilizer for o/w emulsions, as a dispersant for hydrophobic particles and in the production of foams. Inutec® SP1 was purchased from Orafti Bio Based Chemicals (Belgium).

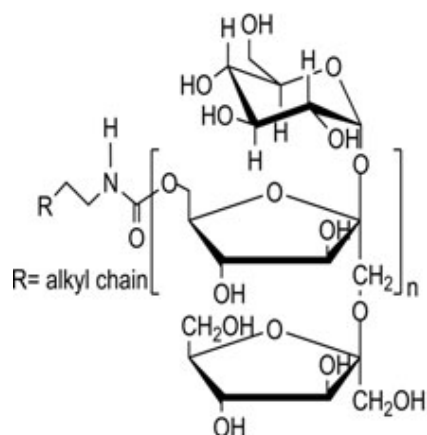


Fig. 9 Molecular structure of Inutec® SP1

## 3.1.4 Preservatives

### 3.1.4.1 Caprylyl glycol

1,2-Octanediol (Fig. 10), linear diol containing two primary hydroxyl groups, has bacteriostatic and bacteriacidal properties which are useful in cosmetics as a preservative [108]. It is also used in coating materials, paper mills and water circulation systems for the effective preservation against bacteria and fungi. It is used as an emollient, humectant, and wetting agent in cosmetic and skin care products. Alcohols are very weak acids as they lose  $\text{H}^+$  in the hydroxyl group.

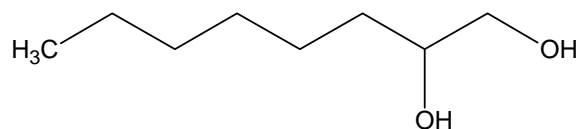


Fig. 10 Molecular structure of caprylyl glycol (1,2-Octanediol)

It has an average molecular weight of 160 with a melting point of 36°C. Caprylyl glycol was obtained from ACIMA AG für Chemische Industrie (Switzerland).

### 3.1.4.2 Cetylperidinium Chloride (CPC)

CPC (Fig. 11) is called or is present in commercial products such as 1-palmitylpyridinium chloride. It is a cationic quaternary ammonium compound in some types of mouthwashes, toothpastes, lozenges, throat sprays, anti-sore throat sprays, breath sprays, and nasal sprays.

CPC has the molecular formula  $C_{21}H_{38}NCl$  and at its pure form is in a solid state at room temperature. It has a melting point of  $77^{\circ}C$  when anhydrous or  $80\text{--}83^{\circ}C$  in its monohydrate form. It is freely soluble in water but insoluble in acetone, acetic acid, or ethanol. It has a pyridine-like odor. Concentrated solutions are destructive to mucous membranes. It is toxic when swallowed and very toxic when inhaled. Its CMC (critical micelle concentration) is 0.00124 M, corresponding to 0.042% in water [107]. CPC was purchased from Sigma-Aldrich (Germany).

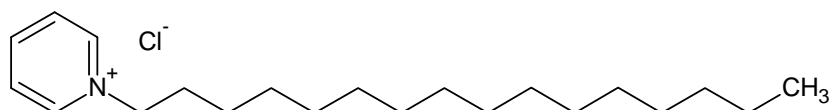


Fig. 11 Molecular structure of CPC

### 3.1.4.3 Ethanol

Although ethanol is primarily used as a solvent, it is also employed in solutions as an antimicrobial preservative. Topical ethanol solutions are used as penetration enhancers and as disinfectants. Ethanol has also been used in transdermal preparations in combination with Labrasol as a co-surfactant [109]. It has a boiling point of  $78.15^{\circ}C$  and is miscible with chloroform, ether, glycerin and water (Fig. 12) [107]. Ethanol was purchased from CG Chemikalien GmbH & Co. KG (Germany).

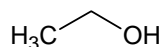
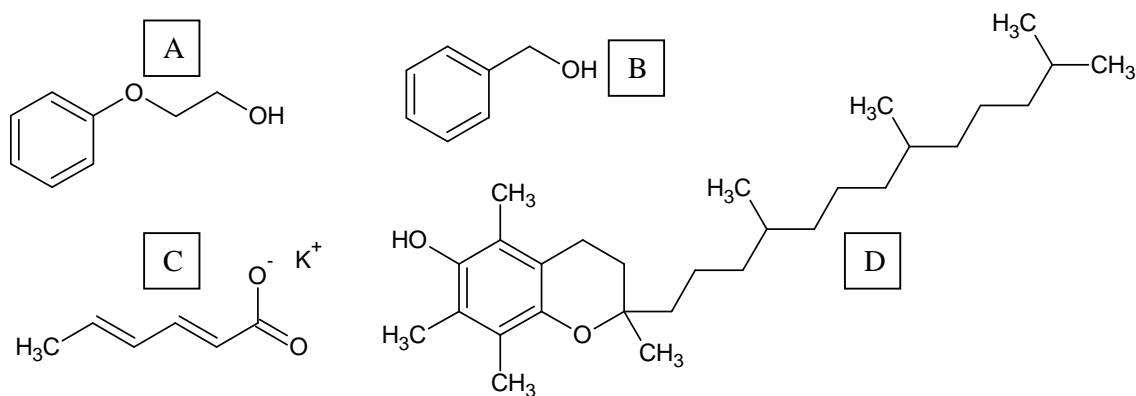


Fig. 12 Molecular structure of ethanol

### 3.1.4.4 Euxyl® K 700 (EUX700)

EUX700 is a liquid cosmetic preservative (Fig. 13), which can be used in leave-on as well as rinse-off products. It was developed for use in cosmetic formulations with a skin-friendly pH value up to 5.5. If pH values exceed 5.5 after the addition of EUX700 then it remains stable but becomes ineffective. EUX700 was obtained from Schülke & Mayr GmbH (Germany).



**Fig. 13** Molecular structures of compounds present in EUX700: Phenoxyethanol (A), Benzyl alcohol (B), Potassium sorbate (C) and Tocopherol (D)

### 3.1.4.5 Euxyl® K 702 (EUX702)

EUX702 (Fig. 14) was developed for use in cosmetic formulations with a skin- friendly pH value of up to 6. EUX702 is particularly effective in non-ionic systems. It has a broad, balanced spectrum of effect against bacteria, yeasts and mould fungi. EUX702 was obtained from Schülke & Mayr GmbH (Germany).

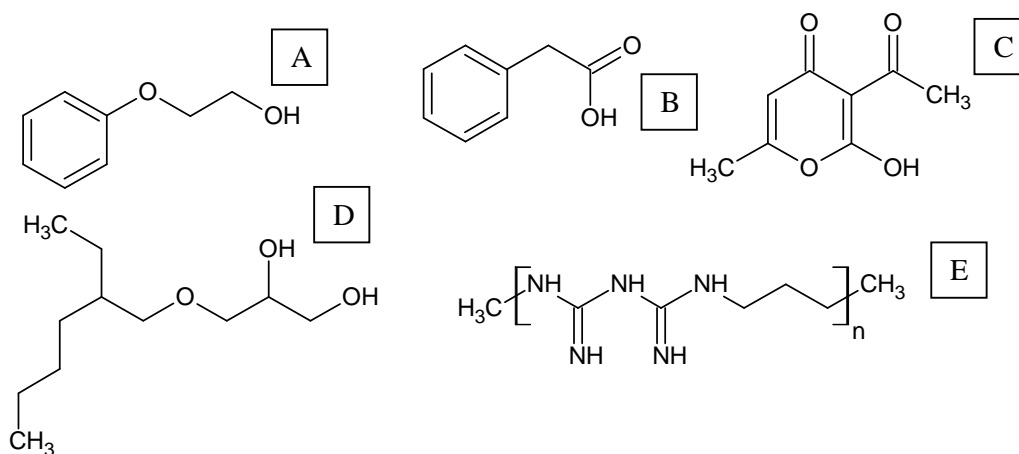


**Fig. 14** Molecular structures of components present in EUX702 containing Phenoxyethanol (A), Benzyl acid (B), Dehydroacetic acid (C), Ethylhexylglycerin (D) and polyaminopropyl biguanide (E)

### 3.1.4.6 Euxyl® PE 9010 (EUX9010)

EUX9010 (Fig. 15) is a liquid cosmetic preservative based on phenoxyethanol and ethylhexylglycerin. The combination of 10% ethylhexylglycerin affects the interfacial tension at the cell membrane of microorganisms, improving the preservative activity of phenoxyethanol. EUX9010 has a broad, balanced spectrum of effect against bacteria, yeasts

and mould fungi. It is a colorless liquid with a characteristic odor. EUX9010 was purchased from Schülke & Mayr GmbH (Germany).

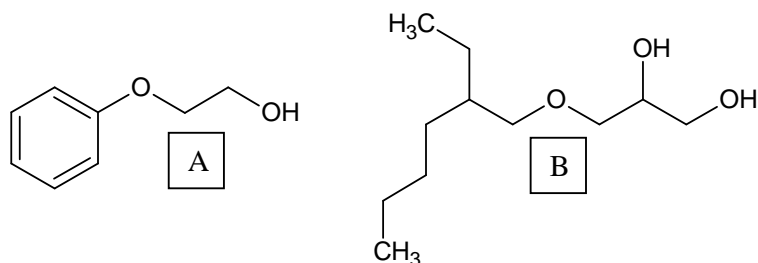
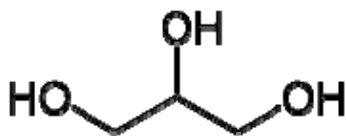


**Fig. 15** Molecular structures of compounds present in EUX9010: Phenoxyethanol (A) and Ethylhexylglycerin (B)

### 3.1.4.7 Glycerin

Glycerin (1,2,3-Propantriol) (Fig. 16) is used in a wide variety of pharmaceutical formulations including oral, otic, topical and parenteral preparations. In topical pharmaceutical formulations and cosmetics, glycerin is used primarily for its humectants and emollient properties. In parenteral formulations, glycerin is used mainly as a solvent [107].

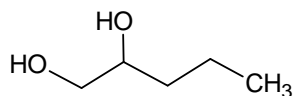
As other alkandiols, glycerin possesses the ability to preserve the preparations. It has an antimicrobial activity when used in concentrations of more than 20% [107]. Glycerin was ordered from Merck (Germany).



**Fig. 16** Molecular structure of glycerin

### 3.1.4.8 Hydrolite®-5 (Pentylene glycol)

Hydrolite®-5 is a Colorless liquid, very low in odor. It is water-soluble and oil-soluble. Hydrolite®-5 (Fig. 17) is an organic compound humectant used in cosmetics and beauty products that is also secondarily used as a solvent and preservative. It can have moisture-binding and antimicrobial properties. Hydrolite®-5 was purchased from Dragoco Gerberding & Co AG (Germany).

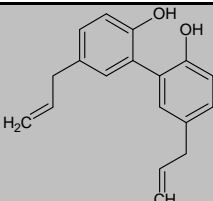
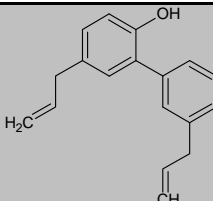
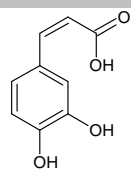
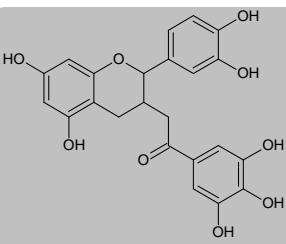
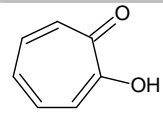
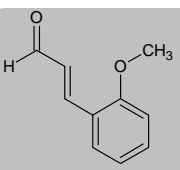
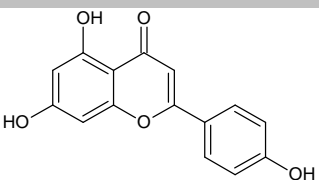
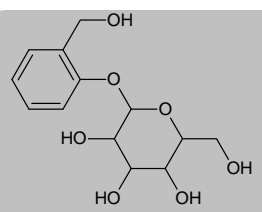


**Fig. 17** Molecular structure of Hydrolite-5

### 3.1.4.9 MultiEx naturotics

It is a mixture of natural preservative extracted from plants (Table 2) i.e. magnolia biondii bark extract, propolis extract, camellia sinensis leaf extract, thujopsis dolabrata

Table 2 MultiEx Naturotics compounds

INCI name	Ingredient(s)	
Magnolia biondii bark extract		magnolol
		honokiol
Propolis extract		3-(3,4-dihydroxyphenyl)prop-2-enoic acid
Camellia sinensis leaf extract		2-[2-(3,4-dihydroxyphenyl)-5,7-dihydroxy-3,4-dihydro-2H-1-benzopyran-3-yl]-1-(3,4,5-trihydroxyphenyl)ethan-1-one
Thujopsis dolabrata branch extract		tropolone
Citrus grandis (grapefruit) fruit extract		O-methoxycinnamaldehyde
Chamomilla recutita (matricaria) flower/leaf extract		apigenin
Salix alba (willow) bark extract		D-salicin

extract, citrus grandis (grapefruit) fruit extract, chamomilla recutita (chamomile) extract, salix alba (willow) bark extract. multiEx naturotics was obtained from Biospectrum Inc. (Korea).

### 3.1.4.10 Propylene glycol

Propylene glycol (Fig. 18) has become widely used as a solvent and a preservative in a variety of parenteral and nonparenteral pharmaceutical formulations. As an antiseptic it is not similar to ethanol, and active against molds. Propylene glycol was purchased from Sigma-Aldrich Chemie GmbH (Germany).

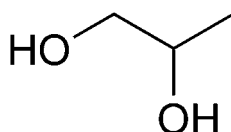


Fig. 18 Molecular structure of propylene glycol

### 3.1.4.11 Phenonip®

Phenonip® (Fig. 19) is a preservative that works in a multitude of applications. It has the same composition of Rokonsal® PB-5 but with different percentages. It is a clear liquid and the application concentrations vary from 0.3% to 1% by weight depending on the formulation. Phenonip® is used to inhibit a full range of microbial growth in creams, lotions, salt scrubs, dusting powders and liquid soap bases. Phenonip® is effective against Gram-positive and Gram-negative bacteria, yeasts and molds. Pheninop® is oil soluble and it can be used in emulsions and anhydrous formulations [110]. Phenonip® was purchased from Nipa Laboratories Inc. (UK).

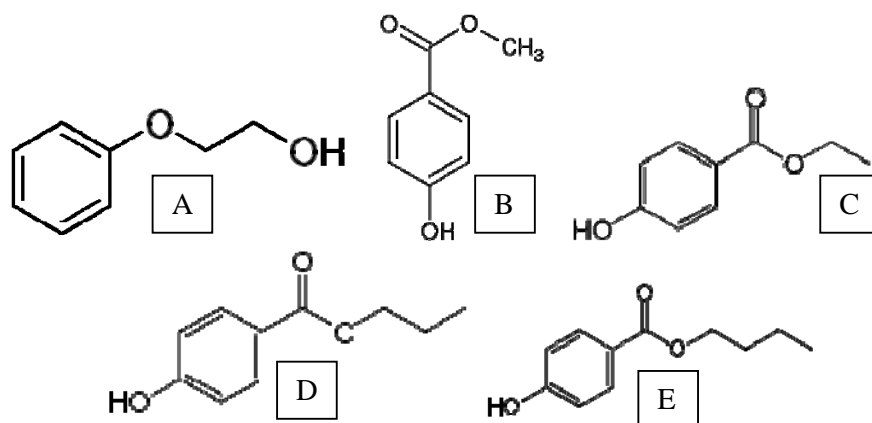


Fig. 19 Molecular structures of compounds present in Phenonip® ( A, Phenoxyethanol, B, Methylparaben, C, Ethylparaben, D, Propylparaben, E, Butylparaben)

### 3.1.4.12 Rokonsal® PB-5

Rokonsal® PB-5 (Fig. 20) consists of a combination of methyl-, ethyl- propyl- and butylparabens in phenoxyethanol. It does not contain formaldehyde or formaldehyde-releasing substances and conforms to the regulations of the EC cosmetics law. The parabenes as basic actives of Rokonsal® PB-5 become deactivated by nonionic or highly ethoxylated surfactants [111]. Rokonsal® PB-5 was obtained from ISP Biochema Schwaben GmbH (Germany).

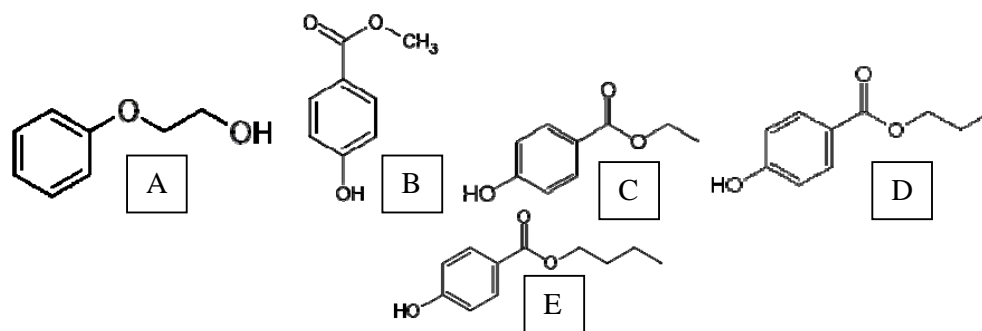


Fig. 20 Molecular structures of components present in Rokonsal® PB-5 (A, Phenoxyethanol, B, Methylparaben, C, Ethylparaben, D, Propylparaben, E, Butylparaben)

### 3.1.4.13 Triclosan

Triclosan (Fig. 21) is a potent wide spectrum antibacterial and antifungal agent. It is a polychlorophenoxy phenol. This organic compound is a white powdered solid with a slight aromatic/phenolic odor. It is a chlorinated aromatic compound which has functional groups representative of both ethers and phenols. Phenols often show anti-bacterial properties. Triclosan is only slightly soluble in water (12 mg/l), but highly soluble in ethanol, diethyl ether, and stronger basic solutions such as 1 M sodium hydroxide [107].

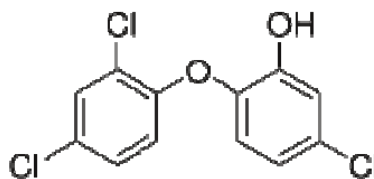


Fig. 21 Molecular structure of triclosan

Triclosan acts as a biocide, with multiple cytoplasmic and membrane targets. At lower concentrations, however, triclosan appears bacteriostatic and is seen to target bacteria mainly by inhibiting fatty acid synthesis. Triclosan binds to the bacterial enoyl-acyl carrier protein reductase enzyme (ENR), which is encoded by the gene *FabI*. This binding increases the enzyme's affinity for nicotinamide adenine dinucleotide (NAD<sup>+</sup>). This results in the formation



of a stable ternary complex of ENR-NAD<sup>+</sup>-triclosan, which is unable to participate in fatty acid synthesis. Fatty acids are necessary for reproducing and building cell membranes. Humans do not have an ENR enzyme, and thus are not affected. TCL was obtained from Alfa Aesar GmbH & CO KG (Germany).

#### 3.1.4.14 *D-alpha tocopheryl polyethylene glycol 1000 succinate (TPGS)*

Surfactants are not classical preservatives but as surface active agents have negative effect on the bacterial membranes – especially at high concentrations [112], it is worth to study the presence of high concentrations of these surfactants such as Plantacare<sup>®</sup> 2000 UP and TPGS. TPGS (Fig. 22) is a water-soluble form of vitamin E derived from natural sources. TPGS is prepared by the esterification of polyethylene glycol 1000 to the acid group of crystalline d-alpha tocopheryl acid succinate. TPGS is a surfactant that can be used as an emulsifier, solubilizer, bio-availability enhancer and a vehicle for a lipid-based drug formulation. With its unique properties, TPGS is widely used as an excipient in drug formulations and is rapidly expanding into the beverage and functional food markets [107]. TPGS was purchased from Eastman (UK).

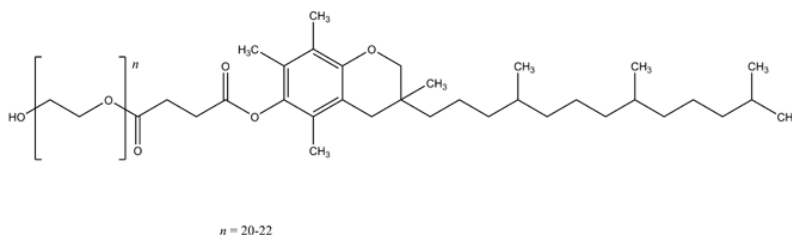


**Fig. 22** Molecular structure of TPGS

For each preservative there is a suggested concentration range specified by the manufacturer or in the literature (Table 3). Clearly, the anti-microbial effect is higher at high concentrations, but at the same time the potential stability impairment increases as well. For example, glycerol competes for the hydration water with the steric stabilizers (e.g. poloxamer). With less hydrates stabilizer layers the stabilization of the suspension will be reduced. Therefore, it was decided to use the highest possible concentration to study the maximum impairment effect of the preservatives on the physical stability of the nanosuspensions.

Table 3 List of preservatives and preservative mixtures used and their concentration ranges

preservative used	effective concentration for preservation	references
caprylyl glycol	0.5 - 1.0%	[113]
cetylperidinium chloride	1.0%	[114]
ethanol	20.0%	[107]
Euxyl® K 700	0.5 - 1.5%	[115]
Euxyl® K 702	0.2 - 1.0%	[116]
Euxyl® PE 9010	0.5 - 1.0%	[117]
glycerol	20.0 - 50.0%	[107, 118]
Hydrolite® -5	3.0 - 5.0%	[119]
multiEx Naturotics	0.5 - 2.0%	[120]
propylene glycol	20.0%	[107]
propylene glycol + Hydrolite® -5	5% + 3%	[107]
propylene glycol + glycerol	14% + 11%	[107]
Phenonip®	0.5 - 1.0%	[110]
Rokonsal® PB-5	0.3 - 1.0%	[111]
triclosan	< 0.3%	[121]
TPGS	2.5%	[122]

### 3.1.5 2,2-diphenyl-1-picrylhydrazyl (DPPH)

DPPH<sup>•</sup> is a free radical that is often used to measure the antioxidant behavior of investigated materials (Fig. 23). DPPH<sup>•</sup> has an absorption band at 515 nm which disappears upon reduction by an antiradical compound. DPPH<sup>•</sup> was purchased from Sigma-Aldrich (Germany).

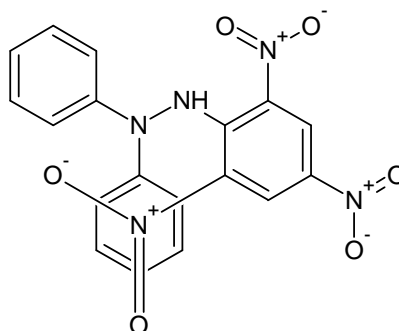


Fig. 23 Molecular structure of DPPH<sup>•</sup>

### 3.1.6 Gelling agents

Three different types of gelling agents viz 10% Tylose<sup>®</sup> 10000 P<sub>2</sub> (HEC), 8% Tylose<sup>®</sup> 30000 YP2 (HEC), 8% CMCNa, 1% Carbopol<sup>®</sup> Ultrez 10 polymer, 1% Carbopol<sup>®</sup> Ultrez 20 polymer and 1% Carbopol<sup>®</sup> Ultrez 21 polymer were selected. All Tylose<sup>®</sup> polymers were purchased from SE Tylose GmbH & Co. KG (Germany); CMCNa was purchased from Spectrum (USA) and Carbopol<sup>®</sup> Ultrez polymers were obtained from The Lubrizol Corporation (USA).

## 3.2 Methods

### 3.2.1 Determination of refractive index (RI)

Refractive index is defined as the ratio of light velocity in vacuum to that in the referred medium, and is thus a ratio of two quantities of the same kind [123]. In order to determine the RI of solid substances, the RI of different dilutions of the same material in an appropriate solvent should be measured [124]. From the different dilutions and the related RI data a standard curve can be depicted. By extrapolating the latter to 100% concentration, the RI of the raw material can be obtained.

### 3.2.2 Production of nanosuspensions by high pressure homogenization (HPH)

#### 3.2.2.1 Operation principle of a piston-gap type high pressure homogenizer

Piston-gap homogenizers are based on a different homogenization principle than jet stream homogenizers. A liquid/dispersion is streaming through a narrow gap with a very high streaming velocity. A typical arrangement for this technology is to place the dispersion (emulsion or suspension) in a cylinder with a piston; a pressure is applied to the piston, pressing the suspension through a gap at the end of the cylinder. In the Micron LAB 40, the cylinder has a diameter of about 3.0 cm, and the narrow gap just has a width of only 25  $\mu\text{m}$ ; this narrowing by a factor of 120,000 leads to extremely high flow velocities up to 200-700 m/s depending on the pressure applied. The gap reduces in width with increasing pressure. For some homogenizer types, velocities up to 1000 m/s are given. According to the patent of DissoCubes<sup>®</sup>, the reason for disintegration of the particles is the cavitation occurring in this gap. According to the Hagen-Poiseuille equation, the flow rate in the system of different diameters is equal at each diameter.

In piston gap-homogenizer the macrosuspensions is forced through a very tiny homogenization gap in order to produce drug nanocrystals. According to the Bernoulli equation, the sum of static and dynamic pressure is constant at each diameter of the system:

$$P_s + \frac{1}{2}\rho V^2 = K \dots\dots\dots \text{Equation 11}$$

where  $P_s$ , is the static pressure,  $\frac{1}{2}\rho V^2$  is the dynamic pressure ( $P_{dyn}$ ),  $\rho$  is density of the fluid,  $V$  its velocity and  $K$  is a constant.

In the gap, the dynamic pressure drastically increases (i.e. also the streaming velocity), and simultaneously, the static pressure decreases and falls below the vapor pressure of the water at room temperature. This leads to the boiling of the water at room temperature, the formation of gas bubbles which implode when the liquid leaves the gap being under the normal pressure conditions again (cavitation). The formation of gas bubbles and their implosion cause shock waves, leading to the diminution of particles of a suspension.

During a milling process, the particles/crystals break preferentially at weak points, i.e. imperfections. With decreasing particle size, the number of imperfections is getting less and less, that means the crystals remaining are becoming more and more perfect. Thus, the force required to break the crystals increases with decreasing particle size. If the force (power density) in the homogenizer is equal to the interaction forces in the crystal, the particles cannot further be diminished, even when additional homogenization cycles are applied. That means the maximum dispersity at the given power density/homogenization pressure is reached. By definition the term “homogenization” includes reduction of particle or droplet size and simultaneous narrowing of the size distribution, that is, making the particle population not only smaller, but simultaneously more homogeneous in size.

### **3.2.2.2 Preparation of nanosuspensions**

A formulation screening was carried out to identify the most suitable formulation for further processing. Drugs were dispersed in water and stabilizers were added. Then a pre-suspension was prepared by stirring using an Ultra-Turrax T25 (Janke & Kunkel GmbH, Germany) at 8000 rpm for 10 seconds. A Micron LAB 40 (APV Deutschland GmbH, Germany) was used for the HPH. The suspension was processed using 2 homogenization cycles at 150 bar and 2 homogenization cycles at 500 bars as pre-milling. The final nanosuspensions were produced applying 20 homogenization cycles at 1500 bar. Dispersed drugs as microparticles were passed through a continuous Micron LAB 40 at room temperature applying the variable pressure profile described above. At certain cycles (normally each fifth homogenization cycle at 1500 bars), samples were withdrawn for particle size analyses. Profiles of the particle size reduction as function of cycle number were plotted to illustrate the homogenization effectiveness.

### 3.2.3 Production of smartCrystals®

The dispersion medium is prepared, the drug is suspended in the dispersion medium using an Ultra Turax T25 (Janke & Kunkel, Germany) for 10 second at 8,000 rpm. The resulting pre-mix was then transferred into the chamber of a pearl mill Bühler PML-2 (Bühler AG, Switzerland). The chamber was filled with 3 kg zircon oxide milling beads Yttrium stabilized, 0.4-0.6 mm in diameter. The bead/suspension ratio was 75:25. The mill was run for 7 passages; samples were after each pass subsequently characterized by particle size analysis.

### 3.2.4 Characterization of drug nanosuspensions

#### 3.2.4.1 Laser Diffraction (LD)

LD has rapidly become a preferred standard method for particle sizing in the pharmaceutical industry. This is due to its short analysis time, robustness, high precision, reproducibility, wide measurement range and flexibility of operation using liquid, spray and dry dispersion attachment. Most LD instruments employ a standard He-Ne laser light source (632.8 nm wave length) and consist of an optical system for Fourier transform of the diffracted light onto a position-sensitive detector. The light scattering pattern from nonspherical particles is very complex, varying as a function of the scattering angle, particle size and shape, and complex refractive index which depends both on the light refraction (real component) and absorption (imaginary component). However, the forward (Fraunhofer) diffraction depends only on the particle size, an azimuthally averaged tangential (Feret's) diameter. This diameter can be associated with the projected-equivalent diameter that is defined by the overall intensity of the diffracted light. The volume-equivalent diameter is not measured by the laser diffraction technique, although the volume particle size distribution is derived from the Fraunhofer diffraction pattern using a system of linear equations incorporated into the algorithm of the instrument. Algorithms, based on rigorous Mie scattering theory should be ideally applied for particles below 25  $\mu\text{m}$ , however this requires the knowledge of the complex refractive indices which are not available for most organic materials and are not directly measurable with the available instruments. Therefore, in practice, the dispersion errors with small particles and uncertainties introduced by the imaginary component of the refractive index may outweigh the inaccuracy associated with the simplified Fraunhofer theory.

For non-spherical particles, such as plates and needles oriented randomly, the volume diameter is typically overestimated because of the larger projection diameter for these shapes. Another error may originate from high concentration of particles analyzed/high obscuration of laser beam, leading to multiple light scattering and overestimation of particle fines

(undersizing the particle size distribution). This can be easily avoided by keeping the obscuration, usually monitored during measurements. In some instruments, the LD method is combined with multiangle and multi wave length light scattering measurements, which enable expansion of the dynamic measuring range and essentially become the multiangle static laser light scattering (LLS) method.

The equivalent diameter measured by LD is not directly related to the particle volume or surface and therefore care should be taken when interpreting these data for any pharmaceutical application. For the quality control purposes it is sufficient to establish a reliable correlation between the LD data and, for example, particle size distribution measured by image analysis or aerodynamic measurements. In the instances where the particle size of nanocrystals is measured when incorporated in the final dosage form, different formulation ingredients may strongly affect the data. Examples include assessment of powder blending and tablet homogeneity, measurements of nebulizer sprays, phase separation and aggregation in a suspension of metered dose inhalers and deaggregation in dry powder inhalers.

Particle size distribution of the nanosuspensions was examined by laser diffractometry Mastersizer 2000 (LD) (Malvern Instruments, UK). The LD data obtained were evaluated using the volume distribution diameters ( $d$ )10%, 50%, 90% and 99%. For results based on the Mie theory, the real refractive and imaginary refractive index was determined specifically for each substance. The diameter values 10% to 99% indicate the percentage of particles possessing a diameter equal or lower than the given size value.

#### ***3.2.4.2 Photon Correlation Spectroscopy (PCS)***

This method, also known as dynamic light scattering (DLS) or quasi-elastic light scattering, is primarily used to measure nanoparticulate systems such as e.g. emulsions, micelles, liposomes and nanosuspensions. When a laser beam is passed through liquid dispersion containing particles in Brownian motion induced by the dispersant molecules, it experiences fluctuations in its intensity due to interferences of waves in light scattering. In the PCS instrument, measurements of this fluctuation of intensity at a given scattering angle are used to infer the particle size or the “hydrodynamic diameter” of the dispersed particles. The PCS instruments measure the fluctuations in the intensity of the scattered light with time in order to generate an exponentially decaying autocorrelation function. This function is then analyzed for characteristic decay times, to determine the diffusion coefficient unique to the scattering dispersed particles and, in conjunction with the Stokes-Einstein equation, the hydrodynamic radius. The primary advantage of the PCS method is that it provides an absolute measurement

without the need of any further information about the composition and the optical properties of the particles in dispersion. The lower limit of the instrument depends on the laser power, the sensitivity of the detector and the signal-to-noise ratio and can be as low as 2 nm. Hence it can be used to measure the sizes of not only surfactant micelles and colloids but also macromolecules.

The data obtained using the instrument is usually in two formats depending on the type of algorithms used for the inversion of the autocorrelation function. A Gaussian distribution is typically used to represent unimodal dispersions. A more complex analysis is required for multimodal (e.g., bimodal) particle size distributions. Introduction of multimodality can lead to a significant complication because the equations used to calculate the particle size become more ambiguous and less stable. The algorithms used provide information about the mean particle size, widths and peak modes of the particle size distributions. The intensity-based data, collected by the instrument, can be reduced to a volume-weighted particle size distribution (PSD) within certain limits of reliability. However, large particles ( $>3 \mu\text{m}$ ) may completely distort the measurements and therefore a complementary analysis with LD or laser scattering instrument is recommended in order to corroborate the obtained results.

The particle size average of the nanosuspensions was analyzed by photon correlation spectroscopy (PCS) with a Zetasizer Nano ZS (Malvern Instruments, UK). PCS yields the mean particle size (z-average) and the polydispersity index (PdI) which is a measure of the width of the size distribution. The z-average and PI values were obtained by averaging of 10 measurements in 10 mm diameter cells at 25°C. Prior to the measurement, all samples were diluted with bi-distilled water to have a suitable scattering intensity.

#### ***3.2.4.3 Zeta potential***

Zeta potential (ZP) shows the charge on the particle surface which indicates the physical stability of dispersed systems. The ZP was measured by determining the electrophoretic mobility using the Malvern Zetasizer Nano ZS. The measurements were performed in distilled water adjusted to a conductivity of 50  $\mu\text{S}/\text{cm}$  with sodium chloride solution (0.9% w/v), to avoid changes in ZP values due to day-to-day variations occurring in the conductivity of the water. The ZP was calculated using the Helmholtz-Smoluchowski equation. The measurements were repeated three times at 25°C at field strength of 20 V/cm. Under these measuring conditions the measured ZP is equivalent to Stern potential.

In addition, the ZP was also measured in the original media of the nanosuspensions. This was conducted to measure the ZP as a measure for the thickness of the diffuse layer and used to predict stability of electrically stabilized nanosuspensions.

#### **3.2.4.4 Light microscopy**

Light microscopy was performed using an Orthoplan microscope (Leitz, Wetzlar, Germany). The employed magnification was 1000 fold (oil immersion) and each sample was investigated 3 times. The crystallinity was examined using polarized light.

#### **3.2.5 Determination of the antioxidant activity**

The antiradical activity of the flavonoids was measured according to the procedure described by Brandwilliams et al. [125]. Initially, a set of accumulative concentrations of DPPH<sup>•</sup> in methanol (0.01 mM-0.3 mM) was prepared in order to get the standard curve. Middle concentration was scanned for the maximum absorbance at different wave length using a UV-Vis spectrophotometer (UV-1700 PharmaSpec, Shimadzu, Japan). Definite amount of the flavonoids (0.1 ml of the 5% flavonoid suspensions) were mixed with 3.9 ml methanol solution of DPPH<sup>•</sup> (0.025 g/100 ml) and were measured with the spectrophotometer at different time intervals until the reaction reached a plateau. The time required to reach plateau was further defined as the steady state time ( $T_{\text{steady state}}$ ). The percentages of residual DPPH<sup>•</sup> were plotted against the ratios of the antioxidant to the DPPH<sup>•</sup>. Standard curve equation was then obtained using Microsoft Excel 2007 (Microsoft Corporation, USA). Efficient concentration required to decrease the DPPH<sup>•</sup> concentration by 50% ( $EC_{50}$ ) was subsequently calculated from the curve equation. The same procedure was applied for preserved nanosuspensions in order to study the effect of preservatives on the antioxidation potential. All measurements were done after reaching the steady state condition.

#### **3.2.6 Drug assay**

In order to determine the content of the active ingredient in the nanosuspensions high performance liquid chromatography (HPLC) was used. A modified method has been developed for each substance. The chromatographic system consisted of a KromaSystem 2000 (Kontron Instruments GmbH, Germany), a solvent delivery pump equipped with a 20  $\mu$ l loop and a rheodyne sample injector. The analytical columns and mobil phases were specific for each drug. A diode array detector (DAD 540) was used as UV detector.



### 3.2.6.1 Hesperetin

Concentration of dissolved hesperetin in collected medium was determined by HPLC. A modified method after Kanaze et al. was chosen for the assay [126]. The HPLC conditions were as following: column, Lichrospher 100-RP8 5 $\mu$ m, 125 x 4 mm); mobile phase: isocratic, methanol : water : acetic acid = 40 : 58 : 2 (v/v/v); flow rate: 1.0 mL/min; UV/Vis detector;  $\lambda$  max. at 288 nm, temperature 45°C.

### 3.2.6.2 Apigenin

Apigenin concentrations were determined by HPLC. The chromatographic system consisted of a Kontron Instrument KromaSystem 2000, a solvent delivery pump equipped with a 20  $\mu$ l loop and rheodyne sample injector. Hypersil BDS C18 (250 mm x 4 mm) analytical column; acetonitrile : Methanol : 0.1% Phosphoric acid = 17 : 33 : 50 as a mobile phase were used. Diode array detector (DAD-Kontron Instrument HPLC 540) was used as UV detector and operated at 340 nm; flow rate: 1.0 ml/min; temperature 25°C.

### 3.2.7 In vitro dissolution behavior

The dissolution test was performed using Franz diffusion cell (Crown scientific, USA) at 32°C with 6.0-6.5 ml of the receptor media. As a first medium, simple phosphate buffer saline (PBS) was used containing NaCl (8.00 g/L) : KCl (0.20 g/L) : Na<sub>2</sub>HPO<sub>4</sub> . 2H<sub>2</sub>O (1.44 g/L) : KH<sub>2</sub>PO<sub>4</sub> (0.24 g/L) and as a second medium, a mixture of PBS : ethanol : Polyethylene glycol 400 (40 : 20 : 40) was used [127]. Both media were stirred by a magnetic bar at 600 rpm. The test was carried out under sink conditions with infinite dose. A known amount of drug suspension (300  $\mu$ l) was applied to the cellulose acetate membrane filter with a pore size of 0.1  $\mu$ m (Sartorius AG, Germany). At specified times; samples were withdrawn from the dissolution chamber and were filtered through Sartorius® 0.1  $\mu$ m filters (Sartorius AG, Germany). An aliquot from each vial was withdrawn with a 1ml glass syringe (Poulten & Graf GmbH, Germany) and assayed by HPLC (HPLC, Kroma-System 2000, Kontron Instruments, Germany) to evaluate the amount of drug dissolved.

### 3.2.8 Saturation solubility

An excess amount of the nanosuspension or powder suspension with an active content of 5.0% was suspended in water. Samples were stored at 25°C shaking with 100 rpm in an Innova 4230 incubator shaker (New Brunswick Scientific, USA). Samples obtained were centrifuged using Heraeus biofuge 22R (Thermo Scientific, Germany) applying 23,800 g and subsequently filtered using 0.1  $\mu$ m pore cellulose acetate membranes (Sartorius AG, Germany). Applying the same method as determining drug content of the nanosuspensions,

dissolved drug was also determined by HPLC. A modified method has been developed for each substance. The chromatographic system consisted of a KromaSystem 2000 (Kontron Instruments GmbH, Germany), a solvent delivery pump equipped with a 20 µl loop and a rheodyne sample injector. The analytical columns and mobile phases were specific for each drug. A diode array detector (DAD 540) was used as UV detector.

### **3.2.9 X-ray diffraction (XRD)**

XRD was performed at room temperature with a Philips X-ray Generator PW 1830 (Philips, Netherlands) for bulk powder and the prepared nanosuspensions after drying. The diffraction angle range was between 0.6°-40° with a step size of 0.04° per 2 seconds. The diffraction pattern was measured at a voltage of 40 kV and a current of 25 mA.

### **3.2.10 Semi-solid dosage form development**

Preferred Hesperetin and Apigenin nanosuspensions will be then incorporated into semi-solid dosage forms such as gels. Various polymers will be used for formulations of these gels making them more feasible to be used by patients and customers. These developed gels will be then further characterized for appearance & particle size. The short term stability studies will be performed on final product under various stress conditions.

## 4 Results & Discussion

### 4.1 Hesperetin

#### 4.1.1 Refractive index (RI)

The refractive index was determined by applying the Saveyn et al. method [124] where two different solvents were used to carry out the test. For HESPERETIN, acetone and ethanol, while DMSO and ethanol were selected for apigenin to determine the RI. Data, obtained from the Saveyn et al. method, were compared to RI data calculated using the Clausius-Mossotti-equation and are shown in Table 4.1.1-1.

**Table 4** Calculated and measured RI for hesperetin. For the standard curve [ $y = \text{RI}$  related to the concentration of the substance,  $x = \text{concentration of the material in the defined solvent (mg/100 mL)}$ ]

	Method	Solvent	Standard curve equation	RI
Hesperetin	Saveyn et al.	Acetone	$y = 0.0023x + 1.3613$	1.591
		Ethanol	$y = 0.0026x + 1.3336$	1.593
	Clausius-Mossotti-equation			$1.593 \pm 0.02$

As a result, the RI of hesperetin is 1.593.

#### 4.1.2 Screening of stabilizers

The first step of screening the suitable stabilizers was to measure the contact angle. Compressed discs were prepared using a 1 cm diameter single punch tablet machine (Emil Korsch Maschinenfabrik, Berlin, Germany) from coarse flavonoids powder and a drop of selected surfactant solution (i.e. in water) was observed on the surface of the mentioned discs using a Contact Angle Meter G1 (Krüss, Hamburg, Germany). However, adding an adequate amount of binder (Kollidon VA 64, 2.5% w/w, BASF AG, Germany) to render the flavonoids into compressible powder had a bad impact on the test, which made the direct observation of the contact angle difficult. Still, using this method helps to discard some surfactants which may have insufficient wetting ability, hence less ability to stabilize the nanosuspensions.

The contact angles between the surfactant solutions and the discs are shown in Table 5. It is obvious that the contact angles of the surfactant solutions are less than the one from purified water alone. Plantacare® 2000 UP showed the highest wettability for hesperetin with a contact

angle of 10 as compared to poor contact angle for purified water (35). After obtaining a preliminary impression about the stabilization activity of the different stabilizers, an actual investigation was done by producing four nanosuspensions in the presence of four different stabilizers and by performing a long-term stability.

**Table 5 Contact angle of different aqueous surfactant solutions (1% w/w) and pure water with the compressed discs of hesperetin**

Solution	Contact angle (°)
Purified water	35 ± 0.6
Inutec <sup>®</sup> SP1	15 ± 0.5
Plantacare <sup>®</sup> 2000 UP	10 ± 1
Poloxamer 188	15 ± 0.3
Tween 80	20 ± 0.9

Table 6 shows the four different formulations which were prepared to scan the suitability of stabilizers. Nanosuspensions (40 g each) containing 5% (w/w) hesperetin stabilized with 1% (w/w) stabilizer were produced at 5°C.

**Table 6 Formulations of hesperetin nanosuspensions with different stabilizers (w/w)**

Materials	A	B	C	D
hesperetin	5%	5%	5%	5%
Inutec <sup>®</sup> SP1	1%	-	-	-
Plantacare <sup>®</sup> 2000 UP	-	1%	-	-
poloxamer 188	-	-	1%	-
Tween 80	-	-	-	1%
Purified water	94%	94%	94%	94%

Although the homogenizer is equipped with a water bath ring, during homogenization the product temperature increases and the nanosuspension should be cooled to 5°C. Pre-milling (PM) was performed at 300, 500 and 1000 bar for 2 cycles each to prevent any possible blockage to the homogenization gap. Using lower pressure enlarges the homogenization gap (e.g. 15 µm at 150 bar whereas 3 µm at 1500 bar [72]) and this allows breakage of larger particles and at the same time hinders its blockage. Pre-milling step was followed by actual homogenization at high pressure of 1,500 bar for 30 cycles.

In previous studies, increasing the pressure further up to 2,000 or 4,000 bar has a minimal effect on the reduction of particle size whereas wearing of the machine increases due to applying extremely high pressures [128, 129]. In addition, applying such high pressures in the industry is considered more costly than the benefit of it.

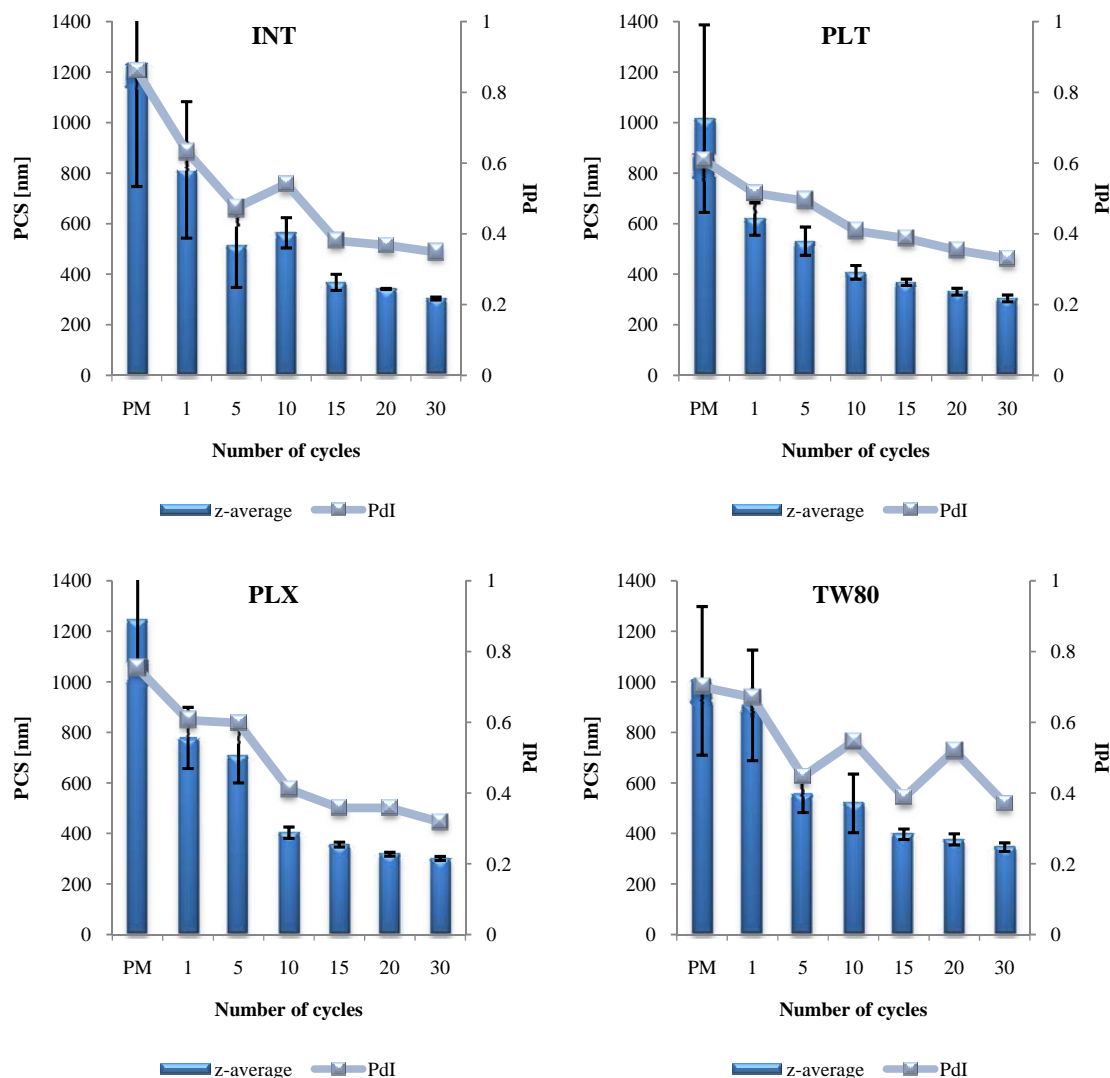
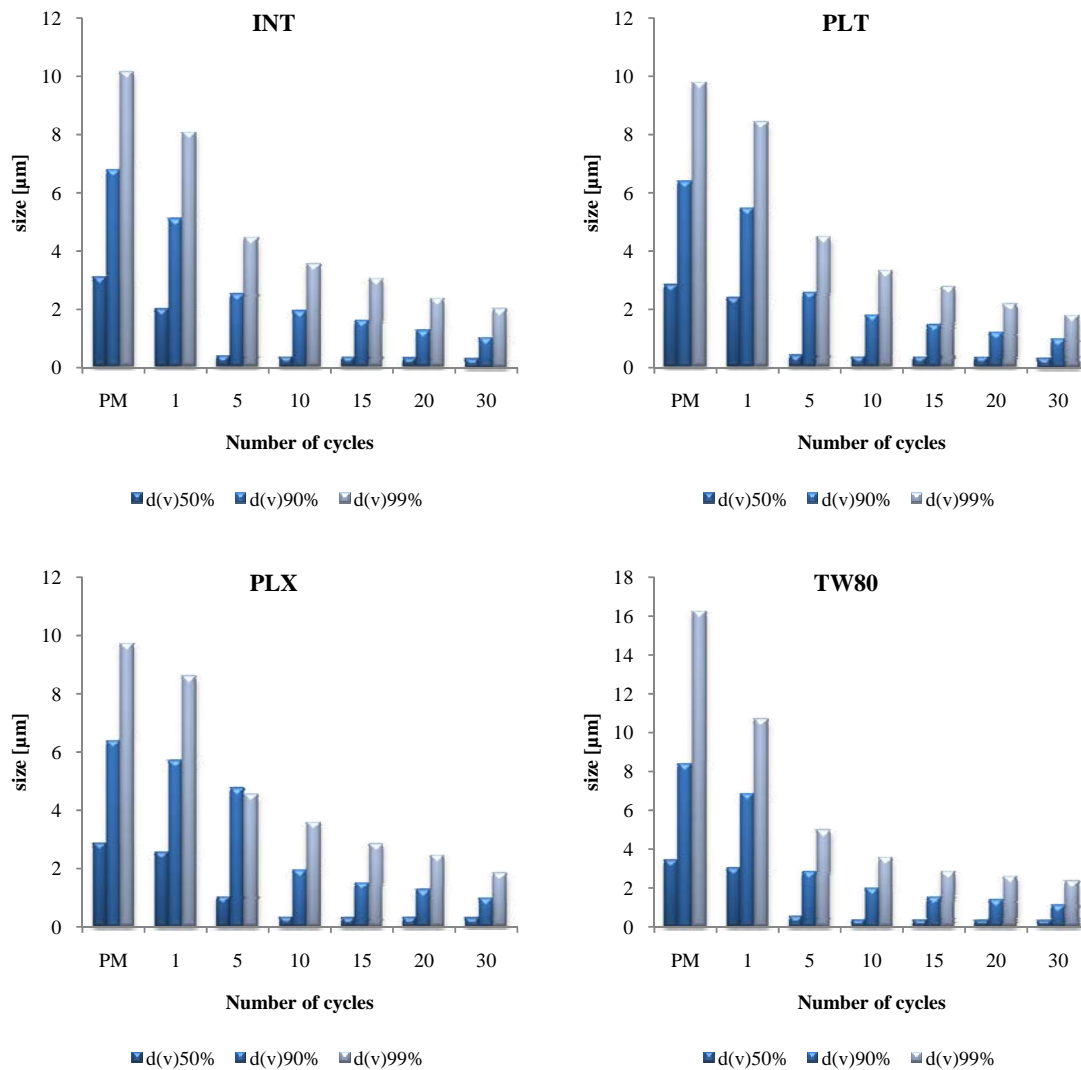


Fig. 24 Reduction in z-average (PCS) along with the decrease in polydispersity index (PdI) as function of homogenization cycles for the four stabilizers (INT= Inutec<sup>®</sup> SP1, PLT= Plantacare<sup>®</sup> 2000 UP, PLX= poloxamer 188 and TW80= Tween 80) (PM = pre-milling)

A continuous decrease in mean particle size (z-average) along with polydispersity index (PdI) was noticed as a function to number of cycles applied for all the stabilizers used. This constant reduction was observed till 20 cycles followed with a little change in particle size between 20 and 30 cycles. Hesperetin nanosuspensions stabilized with Plantacare<sup>®</sup> 2000 UP and Inutec<sup>®</sup> SP1 showed a more steady decrease in the particle size than that of poloxamer

188 and was least for Tween 80 (Fig. 24). Fluctuation in the PdI indicates slight reversible aggregations, which may appear during homogenization and de-aggregate in the next cycle. General reduction in PdI shows that at higher pressure after multiple cycles the larger particles are broken down and final size reduction of the bulk population takes place.

Laser diffractometry (LD) data (Fig. 25) confirm the obtained PCS results. It can be seen that the reduction in  $d(v)50\%$  was limited between the 15<sup>th</sup> and the 30<sup>th</sup> cycle. Whereas, further decrease in  $d(v)99\%$  was noticed in the same cycles range.



**Fig. 25** Reduction in LD diameter as function of homogenization cycles for the four stabilizers (INT= Inutec<sup>®</sup> SP1, PLT= Plantacare<sup>®</sup> 2000 UP, PLX= poloxamer 188 and TW80= Tween 80) (PM = pre-milling)

The order of the contact angle for hesperetin with different stabilizers was in the following order Plantacare<sup>®</sup> 2000 UP < Inutec<sup>®</sup> SP1  $\leq$  poloxamer 188 < Tween 80. In addition, the results of particle size and particle size distribution showed that Tween 80 was insufficient to

stabilize the produced hesperetin nanosuspensions in comparison to other stabilizers, which was in accordance to the results obtained from the contact angle measurements. On the other hand, Plantacare<sup>®</sup> 2000 UP was efficient in getting the lowest particle size of 350 nm. Hence, contact angle measurements assisted in selecting suitable stabilizer for production of nanocrystals.

Previous studies showed that, the final particle size after homogenization is normally determined by the pressure applied and number of homogenization cycles [130, 131]. The stabilizers play a role avoiding aggregation of the produced nanocrystals and hence maintaining the nanosuspension stability. Particles normally tend to aggregate after leaving the homogenizing gap in case they were not well stabilized. In order to achieve optimum stabilization the stabilizer should cover the surface of newly formed nanocrystals.

This phenomenon depends on the molecular weight, the de-aggregation velocity of the micelles to provide new monomeric surfactant for diffusion on new generated surfaces and the affinity between the particle surface and the stabilizer. Assuming that the stabilizer has no lack in the stabilizing capacity, the formed aggregation should be removed by applying addition cycles which will lead to covering the whole surface of particles. After 30 homogenization cycles, the z-average were around 300 nm for Inutec<sup>®</sup> SP1, Plantacare<sup>®</sup> 2000 UP and poloxamer 188, where it was around 350 nm for Tween 80. This implies aggregates formation in Tween 80 stabilized nanosuspension. Although the z-average for the nanocrystals stabilized with Tween 80 was higher than that of other stabilizers, observing the nanocrystals under the microscope showed no significant difference between them (Fig. 26). This could be due to the fact that the aggregates are very small and they are not accessible by light microscopy.

In order to have a clear understanding about the stability of the nanosuspension, zeta potential (ZP) has to be determined. Zeta potential should be measured in distilled water and in the original dispersion medium. Measuring the ZP in distilled water is measuring the Stern potential, which is in turn related to the Nernst potential. In other words, the higher the Nernst potential is, the higher is the Stern potential, thus higher ZP and as a result more stability.

However, the stabilizer may not totally desorb after diluting the sample with water which might affect the ZP measurement. This can be seen in a pronounced way with stabilizers such as poloxamer 188 and Inutec<sup>®</sup> SP1. Plantacare<sup>®</sup> 2000 UP stabilized nanosuspensions showed a ZP in distilled water of -48.3 mV, while the ZP data were between -30.0 to -36.0 mV for the other 3 stabilizers (Table 7). This can be due to desorption of Plantacare<sup>®</sup> 2000 UP to a high extent. On the other hand, measuring the ZP in the original dispersion medium is measuring

the thickness of the diffuse layer. Hence, the higher the measured ZP is, the thicker is the diffusion layer and thus the more stable is the suspension [132].

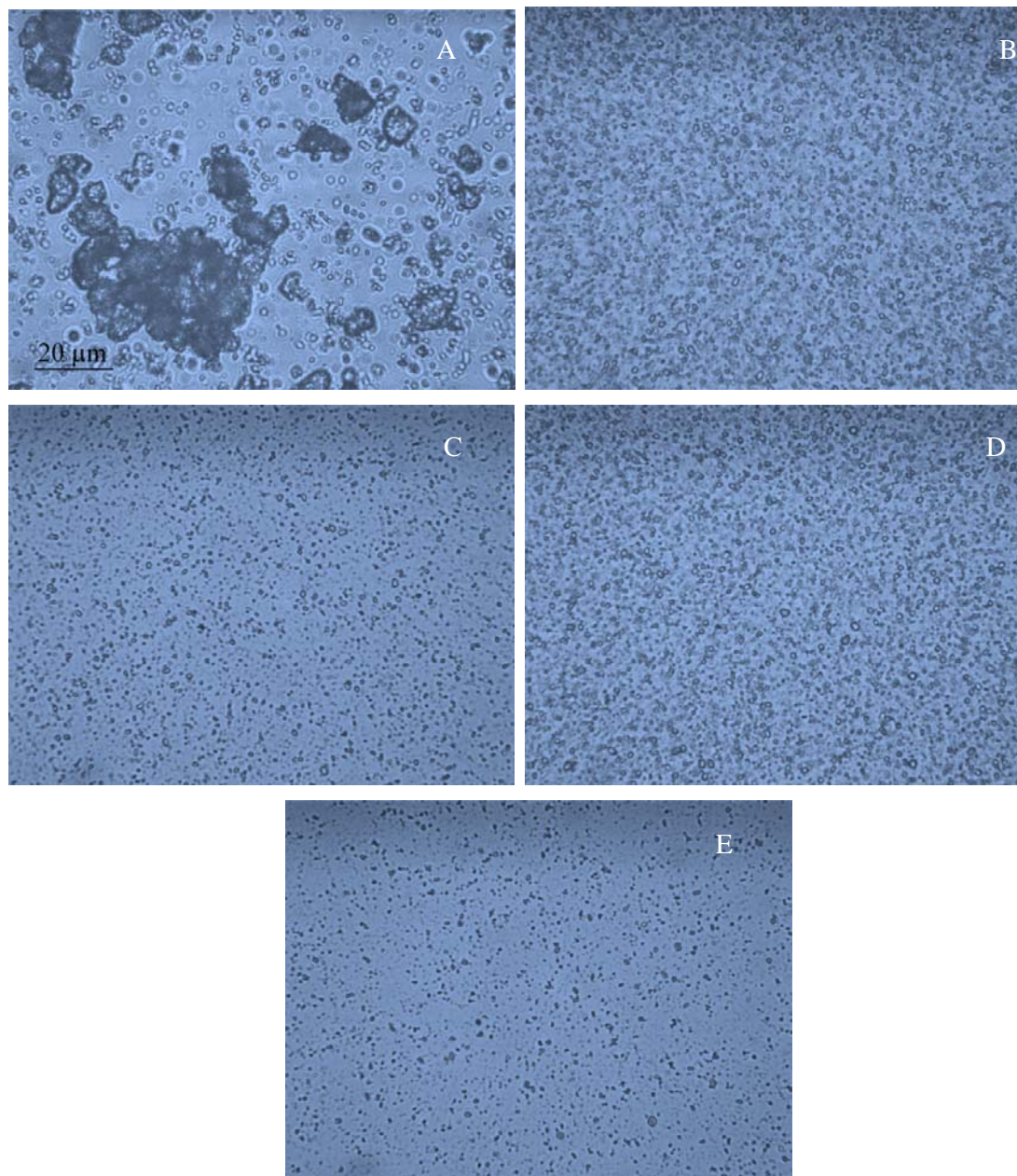


**Fig. 26** Microscopic pictures of hesperetin nanosuspensions with the four stabilizers: (A) the original hesperetin macrosuspension, (B) Inutec® SP1, (C) Plantacare® 2000 UP, (D) poloxamer 188 and (E) Tween 80 (magnification 1000 fold, bar = 20 µm)

Generally, an absolute ZP higher than 30 mV provides an optimum stability for the dispersed system, while nanosuspensions with an absolute ZP value above 20 mV are considered sufficiently stable. Whereas ZP around 20 mV provides only a short-term stability and around 5 mV are quickly aggregated systems [133]. However, the latter rule is only applicable when a low-molecular weight stabilizer is used but not for high-molecular weight stabilizers which



act as steric stabilizers. In the latter case an absolute value of ZP around 20 mV should be sufficient to stabilize the nanosuspension and hinder the formation of aggregates.

**Table 7 Zeta potential data for the hesperetin nanosuspensions using four different stabilizers.**

Type of stabilizer	Zeta potential (mV)	
	Water 50.0 $\mu$ S/cm and pH 5.8	Original dispersion medium
Inutec <sup>®</sup> SP1	-36.2	-22.0
Plantacare <sup>®</sup> 2000 UP	-48.3	-29.1
poloxamer 188	-34.7	-28.0
Tween 80	-30.6	-13.3

Inutec<sup>®</sup> SP1 shows a ZP of -36.2 mV in water and a ZP of -22.0 mV in the original dispersion medium, which indicates a thick adsorbed layer, thus a good stabilization. In addition, Plantacare<sup>®</sup> 2000 UP showed a high ZP not only in water with a value of -48.6 mV but also in the original dispersion medium with a value of -29.1 mV. This indicates a high stability during the storage period. poloxamer 188 exhibits a relatively high ZP of -34.7 mV for a non-ionic polymer, due to that the adsorption layer of poloxamer 188 might be thin, which provide less steric stabilization than Plantacare<sup>®</sup> 2000 UP. Hesperetin nanosuspensions stabilized with Tween 80 exhibited a low ZP value of -13.3 mV in the original dispersion medium and the stabilization may be more critical than other stabilizers.

From the previous data, the stabilization activity of the four stabilizers can be regarded in the following order: Plantacare<sup>®</sup> 2000 UP  $\geq$  Inutec<sup>®</sup> SP1 > poloxamer 188 > Tween 80. Thus Plantacare<sup>®</sup> 2000 UP was selected for further investigation and for development of topical dosage forms.

#### 4.1.3 Reproducibility

The reproducibility of hesperetin nanosuspensions using an Micron LAB 40 was tested by producing 3 different batches and the particle size was observed with the aid of PCS and LD. Fig. 27 shows comparative data for the prepared batches and measured with PCS (upper part) and LD (lower part). No difference can be seen between the three batches for both PCS and LD data. Hence, hesperetin nanosuspensions have a good reproducibility and this support the earlier work done about reproducibility of nanosuspensions produced with the APV LAB 40 [134].

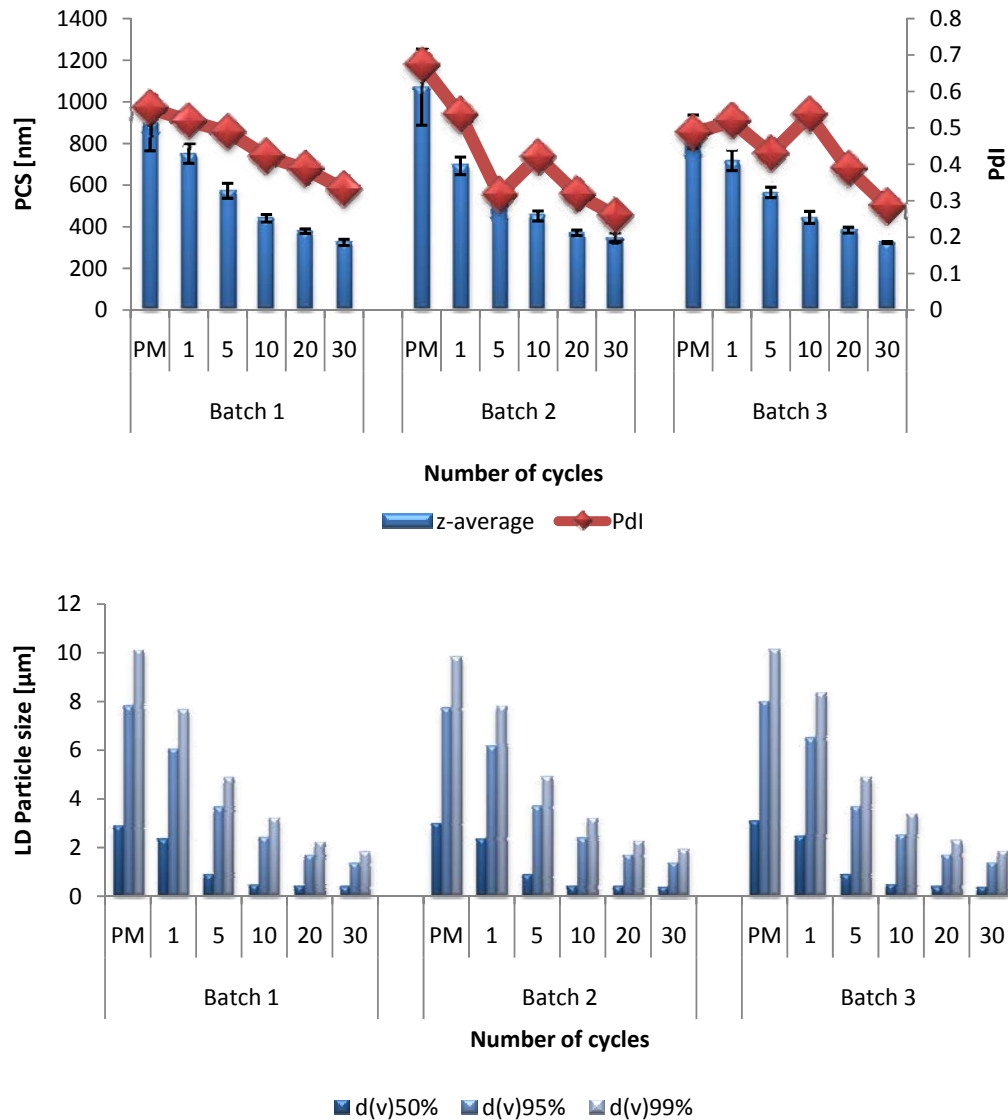


Fig. 27 PCS (upper) and LD (lower) particle size of three different batches of hesperetin nanosuspensions produced on the same day using Micron LAB 40

#### 4.1.4 Preservative screening

In order to obtain a stable product the microbial stability should be taken into account [135]. As Nanocrystals are provided in aqueous formulations to be incorporated in dermal products, preserving should be considered as a vital step in the formation of the product. However, many preservatives may have a negative effect on the stability of the product and more pronouncedly on the dispersed systems. Highly dispersed systems such as nanosuspensions are even more susceptible to the addition of such destabilizing agents.

The influence of six different preservatives with varied chemical characteristics was studied on the physical and chemical stability of the hesperetin nanosuspensions stabilized using

Plantacare<sup>®</sup> 2000 UP. The influence was studied by admixing the preservatives in two different ways.

- Adding the preservative to the suspension after homogenization
- Adding the preservative to the nanosuspensions before homogenization.

#### ***4.1.4.1 Addition preservatives after homogenization***

The physical stability of the suspensions is the first pre-requisite for selection of a preservative; the second selection criterion is that the selected preservative has a sufficient antimicrobial activity in the concentration used. The activity of a preservative depends on the system to be preserved, being reflected by concentration ranges specified for each preservative. Depending on the adsorption affinity of the preservative onto surfaces (more lipophilic preservatives have a higher tendency of adsorption), size of surface area (nanosuspension versus macrosuspension), and ability to remain in the water phase (more hydrophilic preservatives such as Hydrolite-5). In this study, for most cases, medium concentrations were investigated. For EUX9010, besides hydrolite-5 one of the suitable preservatives, a microbial challenge test by Dr. Rimpler GmbH was performed using hesperidin (= glycoside of hesperetin). Hesperidin nanosuspensions preserved with 1% EUX9010 are presently marketed as a cosmetic product (SmartCrystal - Lemon Extract, e.g. in Juvedical - Eye Optimizer, Juvena, Switzerland).

All nanosuspensions were produced by high pressure homogenization (HPH) in purified water after Muller et al. 1999 [66] using an APV Micron LAB 40 with a batch size of 40 g. The final formulations produced contained 5.0% (w/w) hesperetin and 1.0% (w/w) Plantacare<sup>®</sup> 2000 UP. At the end of the homogenization the selected preservatives were added to the nanosuspensions by simple admixing.

Characterization was carried out directly after production. Each preservative is advised to be used in a concentration range specified by the manufacturer or reported in the literature.

The particle size achieved using hesperetin nanosuspension stabilized with Plantacare<sup>®</sup> 2000 UP after 30 cycles was around 335 nm with a PdI of 0.390 being close to the previously published data. PCS was implemented to investigate the alteration in particle size because minor changes in the mean particle size of the nanosuspensions can be detected by this method (Standard deviation of optimized measuring conditions  $\pm 1\%$ ).

Figure 28 shows the particle sizes of the preserved nanosuspensions and the PdI directly after admixing the preservatives to the nanosuspension.

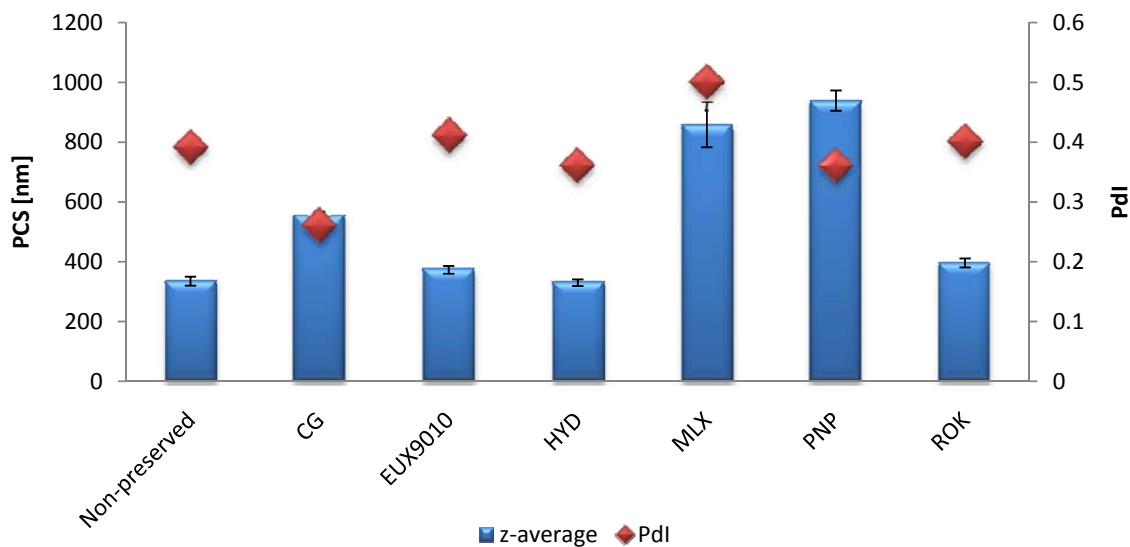


**Fig. 28** PCS diameter and polydispersityindex (Pdl) of the preserved nanosuspension directly after the addition of the preservative (CG= caprylyl glycol, EUX9010= Euxyl<sup>®</sup> PE 9010, HYD= hydrolite<sup>®</sup>-5, MLX= multiEx naturotics, PNP= Phenonip<sup>®</sup>, ROK= Rokonsal<sup>®</sup> PB-5)

With PCS measurements only particle sizes below approximately 3  $\mu\text{m}$  can be detected. The advantage of laser diffractometry (LD) measurements is that it provides has a board measuring range (e.g. 20 nm – 2000  $\mu\text{m}$ ) which enables to detect large particles or aggregates beside small sized bulk populations.

Figure 29 shows LD diameters  $d(v)50\%$ ,  $d(v)90\%$  and  $d(v)99\%$  of the preserved nanosuspensions after admixing preservatives to the nanosuspension.

From the data obtained by PCS it can be seen that particle sizes of nanosuspensions preserved with EUX9010, hydrolite<sup>®</sup>-5 and Rokonsal<sup>®</sup> PB-5 remained nearly unchanged after the addition of preservatives addition. The particle sizes were 373 nm, 330 nm and 396 nm, respectively. On the other hand, particle sizes of nanosuspensions preserved with caprylyl glycol, multiEx naturotics and Phenonip<sup>®</sup> were distinctly increased due to significant aggregations with particle diameters of 553 nm, 858 nm and 939 nm, respectively.

The LD data surprisingly do not show large agglomerations like PCS data except the nanosuspension preserved with multiEx naturotics (Fig. 29). This can be due to the fact that LD instrument has a build-in stirrer that de-aggregates loose agglomerations. That de-aggregation in the LD during the measurement took place and this could be proven when investigating the nanosuspensions by light microscopy.

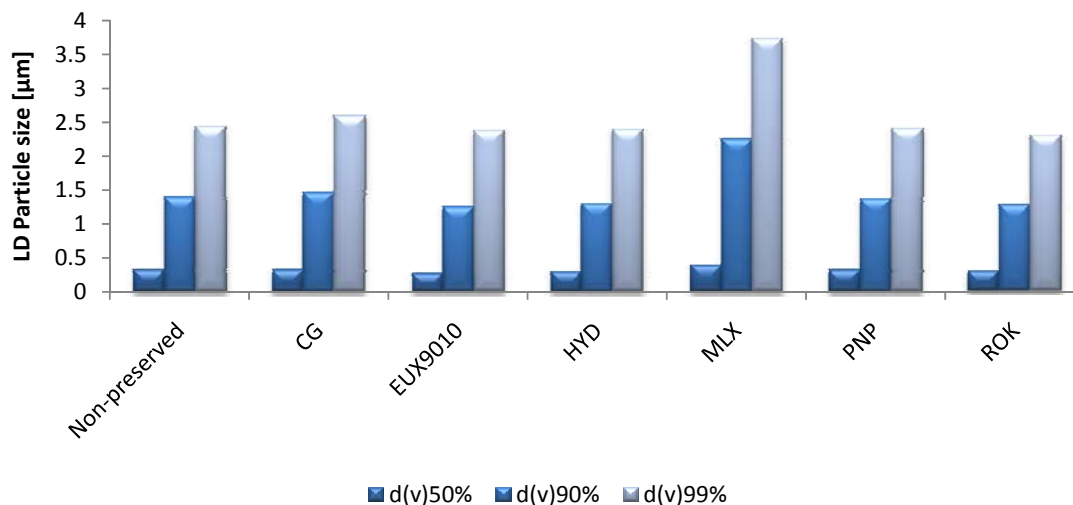


**Fig. 29** LD diameters 50%, 90% and 95% of the preserved nanosuspensions directly after addition of the preservative (CG= caprylyl glycol, EUX9010= Euxyl<sup>®</sup> PE 9010, HYD= hydrolite<sup>®</sup>-5, MLX= multiEx naturotics, PNP= Phenonip<sup>®</sup>, ROK= Rokonsal<sup>®</sup> PB-5)

Light microscopy is not able to give precise size information of nanocrystals in the lower nanometer size range due to the detection limit of the microscope, but it allows nicely to check for the presence of crystals or aggregates larger than 1 µm. In fig. 30, the pictures are put in order of increasing PCS diameter. Fig. 30A-C are the nanosuspensions which were found stable according to PCS and LD data, that means Hydrolite<sup>®</sup>-5, EUX9010 and Rokonsal<sup>®</sup> PB-5. Fig. 30D-F show the microscopic pictures of the preserved nanosuspensions being instable according to PCS, that means preserved with caprylyl glycol, multiEx naturotics and Phenonip<sup>®</sup>. The last three pictures show clear aggregates ranging from slight clumps to very pronounced agglomerates (multiEx naturotics, Fig. 30E). Looking at the pictures one has the impression that the aggregates are not condensed, they seem to be rather loose which would be in agreement with the de-aggregation during the LD measurement. These data demonstrate at the same time how important it is to complement LD measurements by simple microscopic pictures, which is often forgotten.

The zeta potential was measured in distilled water in order to measure Stern potential. The zeta potentials for all preserved nanosuspensions with Eux9010, Hydrolite-5, Rokonsal<sup>®</sup> PB-5 and Phenonip<sup>®</sup> were around -58.0 mV (Table 8). MultiEx naturotics possessed a distinctly lower ZP value of -32.0 mV. Preservative molecules adsorbed on a crystal surface can increase or decrease the zeta potential.

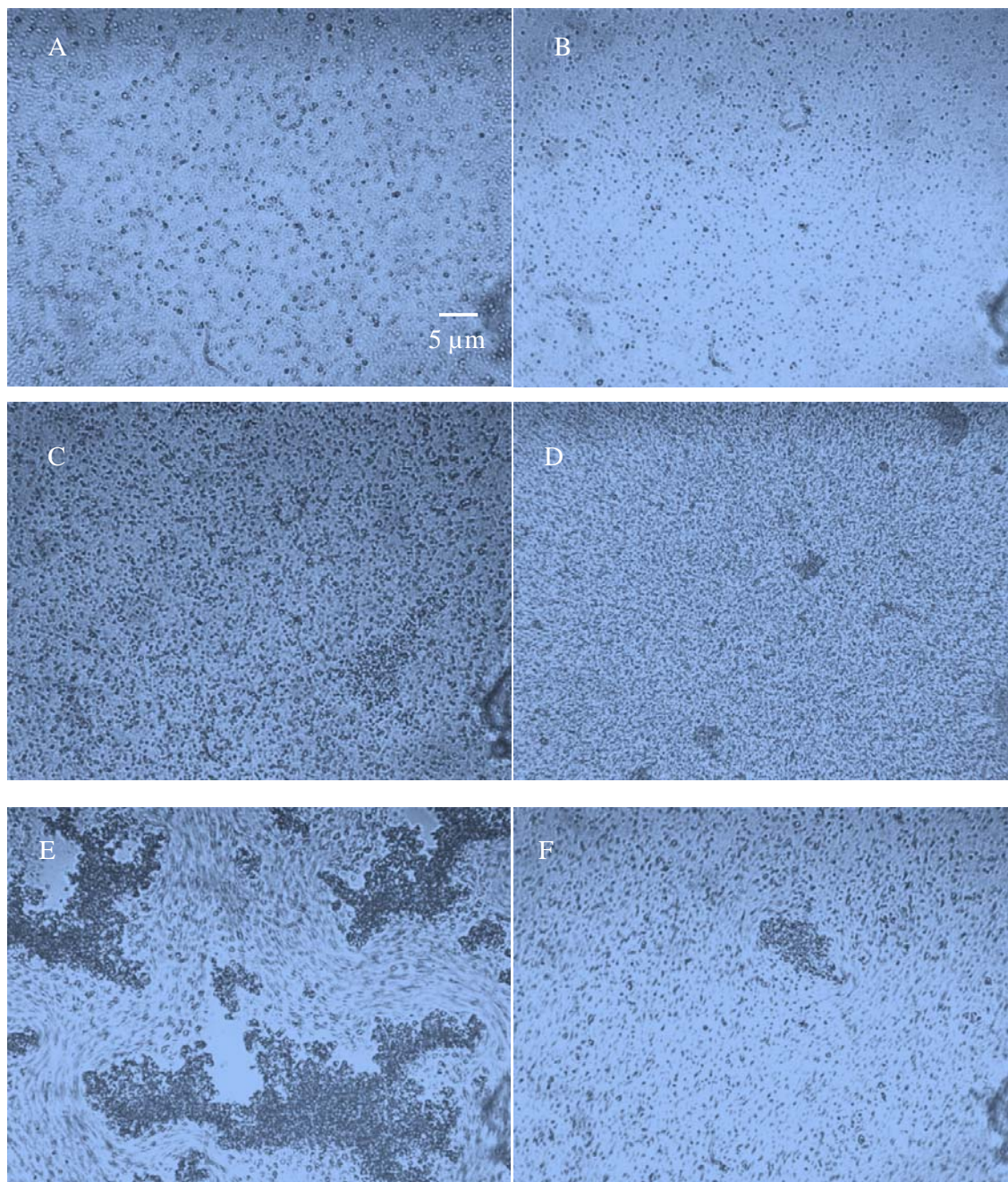


**Fig. 30** Light microscopy images of nanosuspensions preserved with: A) Hydrolite®-5, B) EUX9010, C) rokonsal PB-5, D) caprylyl glycol, E) multiEx naturotics, F) Phenonip®, (magnification 1000 fold, bar = 5  $\mu\text{m}$ )

In case of non-ionic compounds i.e. the preservatives used, generally a decrease in ZP takes place due to the shift of the plane of shear to a larger distance from the particle surface. The measured zeta potential of -58 mV for five of the preserved nanosuspensions could be interpreted this way, that dilution of the nanosuspension for the measurement in distilled water led to desorption of adsorbed preservatives. The charge of the original hesperetin nanocrystal was revealed being around -58 mV. For the nanocrystals preserved with multiEx

naturotics a lower zeta potential of -32.0 mV was observed. This could be explained by still adsorbed molecules of the preservative leading to the shift of plane of shear and the reduced measured zeta potential. This appears likely, when looking at the chemical structure of the preservatives. Hydrophobic compounds like magnolol and honokiol are likely to stay adsorbed on the hydrophobic crystal surface.

**Table 8 ZP values of the preserved hesperetin nanosuspensions**

Preservative	Zeta potential (mV)	
	Water 50.0 $\mu$ S/cm and pH 5.8	Original dispersion medium
Hydrolite <sup>®</sup> -5	-59.0	-33.3
Euxyl <sup>®</sup> PE 9010	-57.5	-29.0
Rokonsal <sup>®</sup> PB-5	-58.5	-32.6
caprylyl glycol	-55.3	-10.5
multiEx naturotics	-32.0	-28.2
Phenonip <sup>®</sup>	-58.6	-31.9

Measurements of ZP in the original dispersion medium are measurements of the diffuse layer. In order to obtain a stable nanosuspension an absolute ZP is to be greater than  $|30|$  mV. However, with steric stabilizers a value of  $|20|$  mV can be sufficient to stabilize the nanosuspension [136]. From table 8 it can be seen that all preserved nanosuspensions have ZP values around -30.0 except the nanosuspension preserved with caprylyl glycol, it was -10.5 mV. The zeta potentials above 30 mV for Hydrolite<sup>®</sup>-5, EUX9010 and Rokonsal<sup>®</sup> PB-5 are in agreement with the PCS data indicating long-term stability. The lowest value of -10.5 mV for caprylyl glycol is also in agreement with the observed instability. However, the preservatives multiEx naturotics and Phenonip<sup>®</sup> showed also a high ZP around -30 mV, but were not stable. This indicates that the zeta potential is not the only stability determining parameter. Rigidity and fluidity properties of the stabilizing surfactant film seem also to play a role.

#### **4.1.4.2 Addition preservatives before homogenization**

Adding the preservatives prior homogenization gives the option to preserve the product even during production. This may not be of that importance for lab scale production, but for industrial production the process of manufacturing might take from hours till 2 days. Electrolytes reduce the zeta potential and thus the repulsion of the particles, whereas non-ionic compounds do not. Therefore, to avoid a strong interaction of stabilizer and preservative, only non-ionic preservatives were selected. Among them, molecules were

selected which are currently preferred for use by manufacturers of cosmetic or dermal products (e.g. having less reports of undesired side effects such as allergy).

The preservatives were added to the macrosuspension prior to the homogenization process for the production of the nanosuspension. For the highest microbiological quality, all nanosuspensions were prepared with sterile water.

Based on theoretical considerations, a reduced efficiency of the stabilizer, due to a preservative presence, might lead to a more pronounced aggregation during the production process itself. Hence, the decrease in size from one cycle to the next will be less, when compared to the same suspension, being produced without preservative. The reason for this phenomenon is that the freshly diminished fine crystals leaving the homogenization gap will be less efficiently stabilized, leading to some re-aggregation of the particles. In addition, the ultrafine nanocrystals after cycle 30 might not be efficiently stabilized. Due to aggregation, the particle size of the produced nanosuspension will be above 300 nm, the size obtained previously for the non-preserved nanosuspension.

After pre-milling the nanocrystal size of the preservative-free hesperetin nanosuspensions were in the range of about 1000 nm. Figure 31 shows that there is a strong interference of the preservatives with the homogenization process, all the PCS sizes after PM are higher than 1800 nm. Slightly higher sizes to of 2000 nm were found for EUX9010, Rokonsal<sup>®</sup> PB-5 and Phenonip<sup>®</sup>, and just above 3000 nm for Hydrolite<sup>®</sup>-5. These preservatives were classified as “group 1” having the least interference. A very pronounced increase was found for both caprylyl glycol and multiEx naturotics: of about 8000 nm, which is actually outside the reliable measuring range of PCS. This classification was confirmed by looking at the PCS sizes after 5 homogenization cycles at 1,500 bar. The non-preserved hesperetin nanosuspension stabilized with Plantacare<sup>®</sup> 2000 UP exhibited a PCS size of 530 nm at cycle 5, group 1 in this study sizes around 1,000 nm. The nanosuspensions preserved with caprylyl glycol and multiEx naturotics had a PCS size of almost 2000 nm and 5,000 nm, respectively.

In general, the group 1 showed a steady decay in size and PdI with increasing the number of homogenization cycles, having lowest sizes and lowest PdI after 30 cycles (Fig. 31A-D). In contrast to this, there was practically no size reduction in the nanosuspensions preserved with caprylyl glycol and multiEx naturotics, where the PCS sizes stayed around 1,000 and 3,000 nm, respectively. In addition, the PdI showed no decrease (Fig. 31E, F).



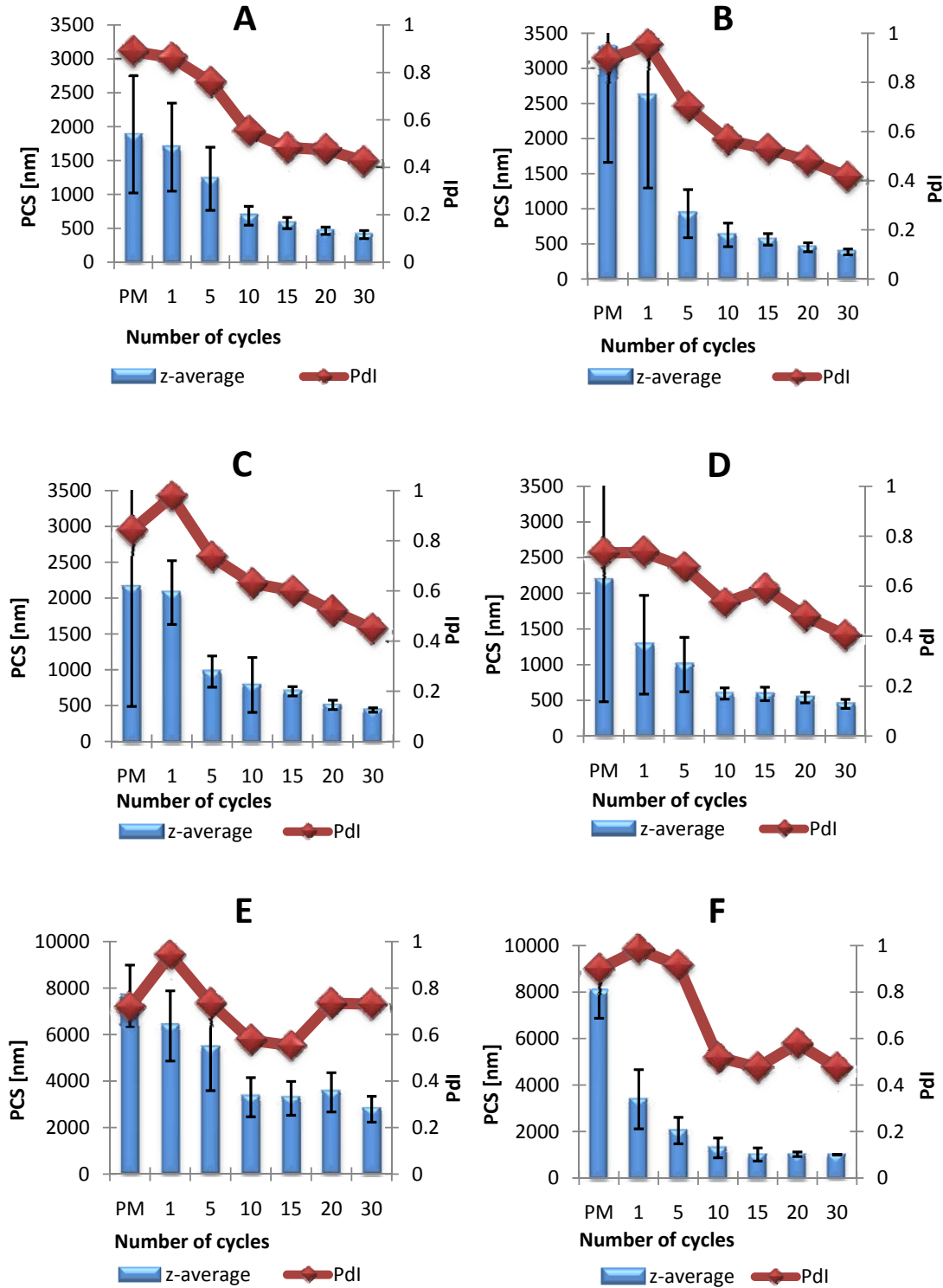


Fig. 31 Reduction in particle size (PCS) along with the decrease in polydispersity index (Pdl) as function of homogenization cycles for the six preservatives (A) EUX9010= Euxyl® PE 9010, (B) Hydrolite®-5, (C) Rokonsal® PB-5, (D) Phenonip®, (E) caprylyl glycol, and (F) multiEx naturotics (PM = pre-milling)

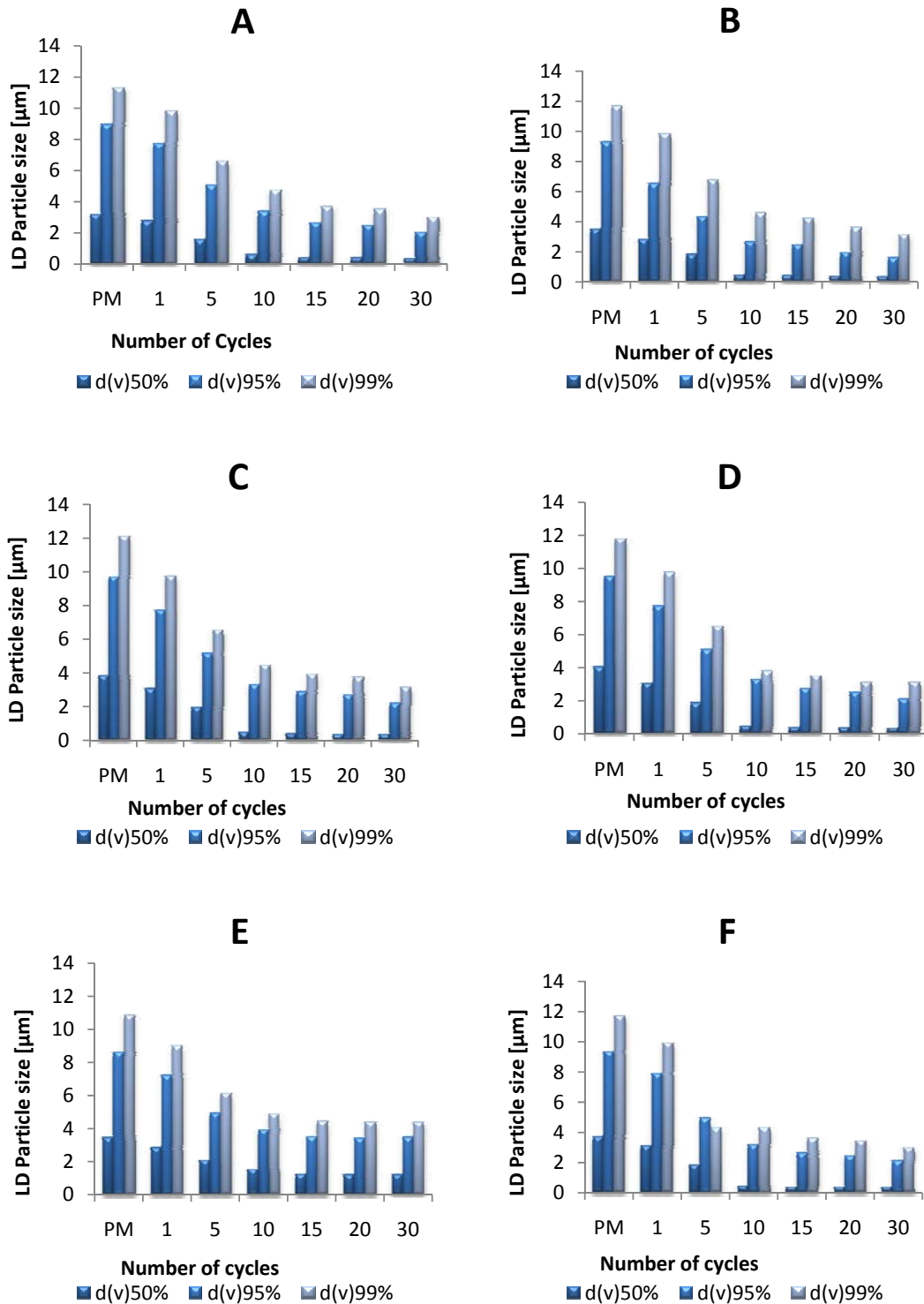
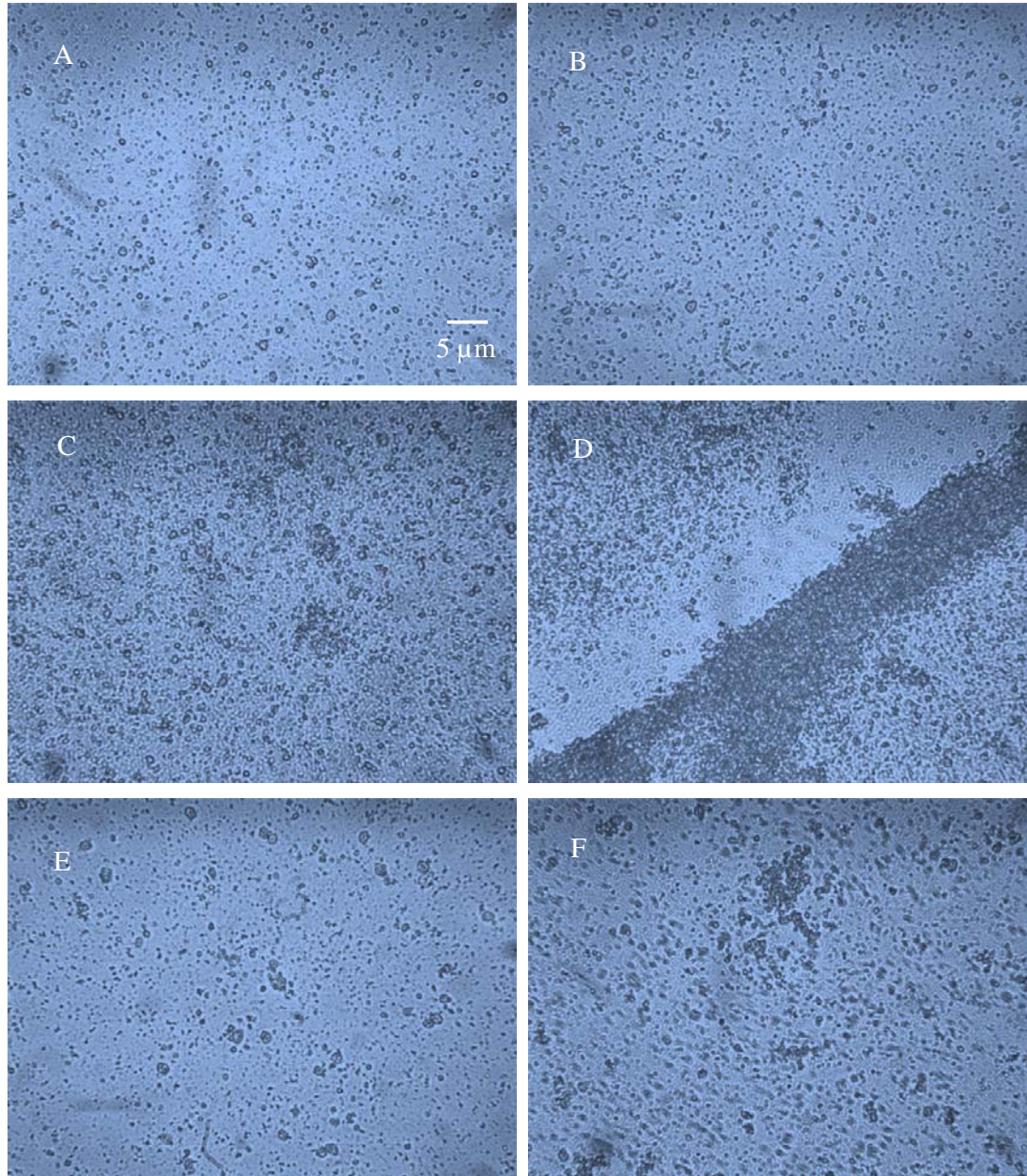


Fig. 32 LD diameters as a function of homogenization cycles for the six preservatives (A) EUX9010= Euxyl® PE 9010, (B) Hydrolite®-5, (C) Rokonsal® PB-5, (D) Phenonip®, (E) caprylyl glycol, and (F) multiEx naturotics (PM = pre-milling)

Obviously, the high energy input could not destroy the aggregates, or most likely, the aggregates were destroyed in the homogenisation gap, but re-aggregated immediately after leaving the gap because of the insufficient stabilizing efficiency of the stabilizer-preservative mixture.



**Fig. 33** Light microscopy images of nanosuspensions preserved with: (A) EUX9010= Euxyl® PE 9010, (B) Hydrolite®-5, (C) Rokonsal® PB-5, (D) Phenonip®, (E) caprylyl glycol, and (F) multiEx naturotics (magnification 1000 fold, bar = 5 μm)

These results could be used to place the best four preservatives in an order of least affecting the stability regarding the final size. After 20 cycles of HPH the preservatives Hydrolite®-5 and EUX9010 exhibited the lowest sizes, being 452 nm and 464 nm, respectively. The

Rokonsal<sup>®</sup> PB-5 preserved nanosuspension had a PCS diameter of 510 nm, and Phenonip<sup>®</sup> 540 nm. This order was confirmed by the sizes after 30 cycles, being 386 nm, 408 nm, 438 nm and 452 nm, respectively. Increasing the cycle number to 30 further reduced the size (in line with the theory) but the small size of 301 nm of the preservative-free nanosuspensions could not be reached. It might be approachable after other 10 or 20 cycles, but such a high cycle number is not applicable in an industrial production process, and was therefore not further investigated. Increasing the cycle number from 20 to 30 had no effect for the caprylyl glycol preserved system (1023 nm and 1007 nm) and only a limited effect in the multiEx naturotics system (3518 nm and 2791 nm).

Fig. 32 shows the decrease in the LD diameters with increasing cycle number. The  $d(v)_{50\%}$  changes relatively little from cycle 10 to cycle 30. The diameters 95% and 99% are sensitive measurements of remaining larger particles, large crystals and/or aggregates. They show a steady exponential decay with increasing cycle number, with generally the lowest values after 30 cycles (Fig. 32). Unlike multiEx naturotics suspension, which had identical values at 20 and 30 cycles (around 4.4  $\mu\text{m}$ ). Surprisingly the decay in the LD diameters was very similar for all investigated nanosuspensions. In contrast to the PCS data, the LD data do not reflect the clear difference between the group of the four least interfering preservatives (group 1) and caprylyl glycol and multiEx naturotics, which dramatically affect the stability of the hesperetin nanocrystals. A potential explanation is that the aggregates are relatively loose. The build-in stirrer in the LD instrument can de-aggregate loose aggregates, thus making them not accessible to the analysis. This potential interference of the build-in stirrer is a well known problem [137]. In contrast, there is no stirring in the PCS measuring cell. This leads to a clear differentiation by the measured sizes.

The presence of large aggregates in the CG and multiEx naturotics preserved nanosuspensions – despite the low LD diameters 95% and 99% - could clearly be proven by light microscopy (Fig. 33). Light microscopy could place the preservatives in the same order regarding stability preservation as PCS. The easy re-dispersability in LD measurements was also observed during short-term stability investigation. The short term stability carried out for 30 days revealed even a de-aggregation of the systems after a storage period of 96 h. This could be observed as a decrease in size (PCS and LD), which was not observed for the nanosuspension without preservatives. For example the size of the suspension preserved with Hydrolite<sup>®</sup>-5 decreased from about 390 nm to about 330 nm and the suspension preserved with EUX9010 decreased from 408 nm to 374 nm. For the other preservatives this effect was also observed

but in a less pronounced manner. These results indicate that the preservatives cause changes in the systems even after the production.

Interestingly, by measuring the Stern potentials (ZP in distilled water) for group 1, the four least interfering preservatives, are practically identical to the zeta potential measured for the non-preserved nanosuspension, i.e. around -50 mV (Table 9).

**Table 9 ZP values of the preserved nanosuspensions in distilled water and in original dispersion medium**

Preservative	Zeta potential (mV)	
	Water 50.0 $\mu$ S/cm and pH 5.8	Original dispersion medium
Euxyl <sup>®</sup> PE 9010	-51.5	-6.3
Hydrolite <sup>®</sup> -5	-50.5	-24.8
Rokonsal <sup>®</sup> PB-5	-51.5	-18.2
Phenonip <sup>®</sup>	-48.4	-18.6
caprylyl glycol	-43.7	-10.3
multiEx naturotics	-26.9	-3.1

This supports that the preservatives, potentially adsorbed on the crystal surface (inner Helmholtz layer), are desorbed in praxis from the surface of the particles. In this case the pure Nernst potential is measured, and thus it should be identical for all formulations (because the crystals consist of the same milled material). Nevertheless, the Stern potential of the destabilizing preservatives caprylyl glycol and multiEx naturotics are reduced distinctly (-43.7 mV and -26.9 mV), most pronounced for multiEx naturotics, Table 9). This indicates that upon diluting the nanosuspension with water for the measurement, non-ionic preservative remained adsorbed, reducing the measured potentials. These data are an indication, that the two preservatives have a high affinity to the crystal surface. The presence of these preservatives, caprylyl glycol and multiEx naturotics, leads to the formation of a mixed film with the stabilizer Plantacare<sup>®</sup> 2000 UP, reducing the particle charge, distorting the film and finally reducing the stability (Cf. 4.1.2).

The group 1 preservatives with little effect on the stability all exhibited a zeta potential in the original dispersion medium of around 20 mV. In accordance with the theory, this nicely explains, the stability of the nanosuspensions (Cf. 4.1.2).

Zeta potential values of 10 mV and below, especially in the range 0-5 mV indicate highly instable suspensions. Caprylyl glycol exhibited a potential of -10.3 mV, the most destabilizing multiEx naturotics a potential as low as 3.1 mV. These data are an explanation for

the observed aggregation in the preserved nanosuspensions. Fig. 34 explains the differences in the potential courses in the model of the electrical double layer and related stability.

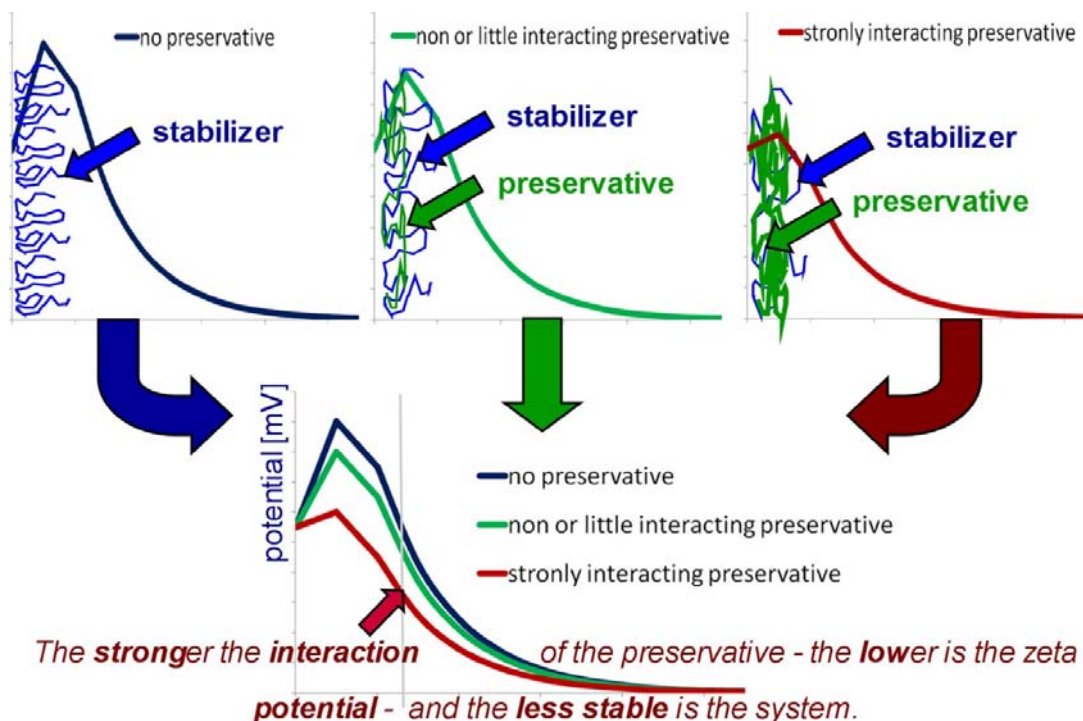


Fig. 34 Differences in potentials of preserved and non-preserved nanosuspensions [138]

Definitely the low zeta potential measured for the nanosuspension preserved with EUX9010 in the range of a few mV up to 10 mV is not sufficient for full electrostatic stabilization. The reason for the good physical stability of the nanosuspension being preserved with EUX9010 is likely due to ethylhexylglycerol. From all the preservatives investigated only EUX9010 contains ethylhexylglycerol [117]. Ethylhexylglycerol strongly reduces the interfacial tension. This leads to a lower energy within the nanosuspension and thus to a very low tendency of agglomeration and an increased physical stability therefore.

Non-ionic surfactants were chosen to avoid a zeta potential reduction due to electrolytes being present (e.g. avoiding the “compression” of diffuse layer). Preservatives need to act in the water phase, where the bacteria are present. Thus preservatives need to be water soluble. In addition, they also need to possess a certain lipophilicity to interact with the lipophilic membranes of bacteria and to inhibit their growth. Of course this lipophilicity leads also to adsorption on surfaces, especially onto hydrophobic ones. Hesperetin is a lipophilic, poorly soluble compound, therefore representing an ideal substrate for adsorption of lipophilic molecules.

Hydrolite<sup>®</sup>-5 is pentylene glycol, relatively hydrophilic and should possess the lowest affinity to the hesperetin surface. Therefore it showed least interaction with the surfactant and least impairment of the stability. EUX9010 consists of 90% of phenoxyethanol and 10% ethylhexylglycerol, due to the lipophilic benzene ring in phenoxyethanol the interaction with the hydrophobic crystal surface will be slightly stronger, placing the preservative as number 2. Ethylhexylglycerol is hydrophilic and should therefore adsorb only little onto the hydrophobic surface of the nanocrystals.

Rokonsal<sup>®</sup> PB-5 and PNP consist of phenoxyethanol (72% and 60-80%, respectively), but additionally contain parabens (28% and 40-20%), being even more hydrophobic in character. This might be a reason why these preservatives were placed in position 3 and 4.

Caprylyl glycol has a long hydrophobic carbon chain (as in SDS) which has surfactant character and promotes strong adsorption. multiEx naturotics contains various compounds, many of them being highly hydrophobic, the interaction of these hydrophobic molecules can be discussed referring to the basic hydrophobic molecular structure of Magnolol and Honokiol. These aspects might explain the strong destabilizing effect of these two preservatives.

#### *4.1.4.3 Optimised addition of preservatives*

By adding the preservatives before homogenization, the adsorption layer around the nanocrystals was not composed of stabilizer only, but of a mixture of stabilizer and adsorbed preservative. Of course, such mixed adsorbed layers can have different stabilizing properties compared to a pure stabilizer adsorption layer.

To examine the effect of type of addition the PCS diameters of both methods were compared. For the comparison the PCS diameters after 4 weeks were taken, not immediately after homogenisation/addition of the preservative. This makes sure that the systems are in equilibrium.

Fig. 35 shows that the PCS diameters are in most cases lower when the preservative is added after production. Obviously the preservatives present in the mixed adsorption layer had a negative effect on the stability, which means they led to aggregation.

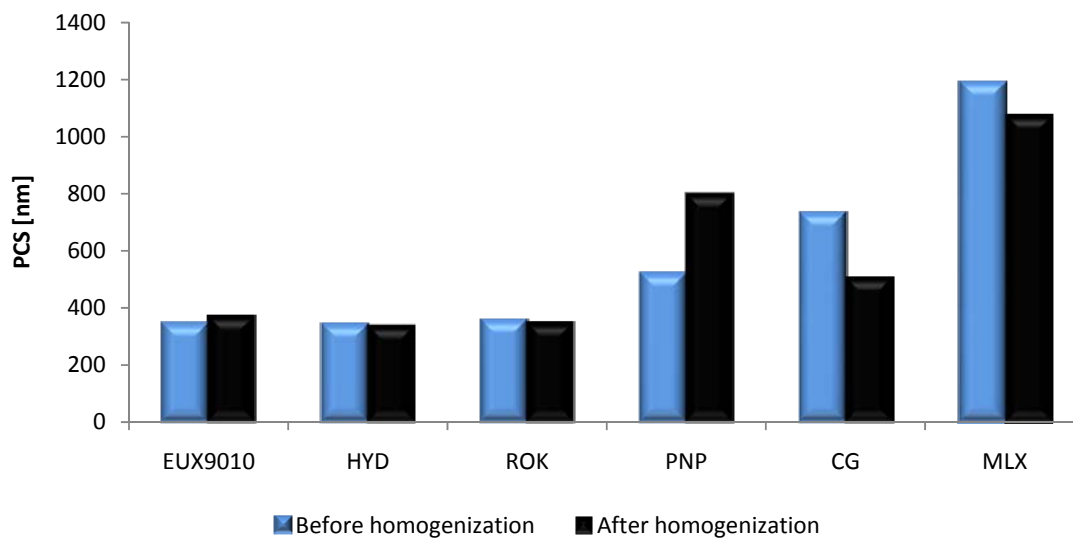


**Fig. 35 Comparison of PCS diameters of preserved hesperetin nanosuspensions using different preservatives (EUX9010= Euxyl<sup>®</sup> PE 9010, HYD= Hydrolite<sup>®</sup>-5, ROK= Rokonsal<sup>®</sup> PB-5, PNP= Phenonip<sup>®</sup>, CG= caprylyl glycol and MLX= multiEx naturotics) added before or after homogenization (after one month stability stored at room temperature)**

Logically no difference was found for the preservative least interacting with the nanocrystal surface, Hydrolite<sup>®</sup>-5. From this it can be concluded, that in case the nanosuspension is produced with a good stabilizer, the preservatives should be added after the production. In addition, the preservative should be added to the nanosuspension, not vice versa, to avoid that nanocrystals are added to a highly concentrated preservative solution.

#### 4.1.5 Antifoaming agents effect

Foams are dispersions of gases in liquid or solid matrices [135]. When a surface-active agent is added to water, it adsorbs on the surface and decreases the surface energy. This way the polar part of the surface-active molecules will be in contact with water and the hydrophobic parts will be in contact with air. When left in the open air, foams are destroyed because of liquid evaporation. The surface layers can affect evaporation rates. It is known that very compact monolayers, such as then one made from fatty alcohols, can significantly reduce water evaporation. Although the most important fact here is the degree of compaction of monolayers, a correlation with surface rheology is likely to exist, since the denser monolayers are also the more rigid ones. Ostwald ripening involves the transport of gas between bubbles of different sizes, which leads to the growth of average bubble sizes. The reduction or elimination of foam arising during pharmaceutical processing operations is often a critical factor for efficient operations [139]. The antifoaming mechanism of aqueous foams is quite established. Antifoaming agents are hydrophobic particles, liquid or solid, that can enter the



liquid/air interface. If the particle is liquid, it spreads at the interfacial and displaces the stabilizing surfactants. The spreading also leads to a drag of the continuous phase, which in turn can lead to film thinning [140].

As Plantacare<sup>®</sup> 2000 UP is a nonionic surfactant with an excellent foaming capacity; difficulties with production were encountered during the production. These difficulties were associated mostly with loss of samples. Antifoaming agent was used to alleviate the problem. However, a clear understanding of the effect of antifoaming agents on the highly dispersed systems such as nanosuspensions is still not available. Hence, different concentrations of antifoaming agent were employed in order to have an idea of its effect on the physical and chemical stability of the nanosuspensions.

Silicon antifoaming agents were used in this study as they are effective at concentrations considerably lower than those of known antifoaming agents such as organic and mineral oils, octanol, ether, etc. Two mechanisms are proposed for the ability of silicon formulations to perform as antifoaming agents:

- 1) Fine droplets of the antifoam enter into the liquid film and wet-out the bubbles. Hence, reduction in surface tension created by the spreading which in turn leads to film rupture.
- 2) A droplet of the antifoam agent enters the liquid film between bubbles, but instead of spreading around the foam particles, it produces a mixed monolayer on the surface of the bubbles. This monolayer, if of less coherence than the original film-stabilizing monolayer, will destabilize the film.

In addition, Silicon antifoaming agents can be used in oral and topical preparations.

Four different concentration (lower and above the stated concentration) of the antifoaming agent Dow Corning<sup>®</sup> Antifoam B emulsion (water, polydimethylsiloxane and methyl cellulose) were used. It was obtained from Dow Corning<sup>®</sup> Corporation (UK). Antifoaming agent was incorporated before homogenization and the results were compared with the same nanosuspension without the addition of the antifoaming agent.

PCS data showed a minor difference between the presence and absence of antifoaming agent. The particle size of formulations was smaller than that of the original nanosuspension with a better polydispersity index (Fig. 36). Surprisingly, LD data showed even further difference between them. Particle size distribution  $d(v)_{99\%}$  was about 3  $\mu\text{m}$  in comparison to that of formulations with Antifoam B emulsion with 2  $\mu\text{m}$ . No difference was noticed between formulations with variable concentrations of the antifoaming agent. Microscopic pictures showed no aggregation or growth in crystal sizes for all concentrations used (Fig. 37). This indicates that the Plantacare<sup>®</sup> 2000 UP as a stabilizer has more coherence to hesperetin

particles than that of the antifoaming agent which was sufficient to inhibit the destructive effect of the antifoaming agent on the film of the stabilizer.

However, the film around bubbles was destabilized due to the antifoaming effect. It is obvious that the incorporation of Antifoam B emulsion removed the undesired formed foam and not only facilitated the production process but also had a positive effect on the particle size and the efficacy of homogenization.

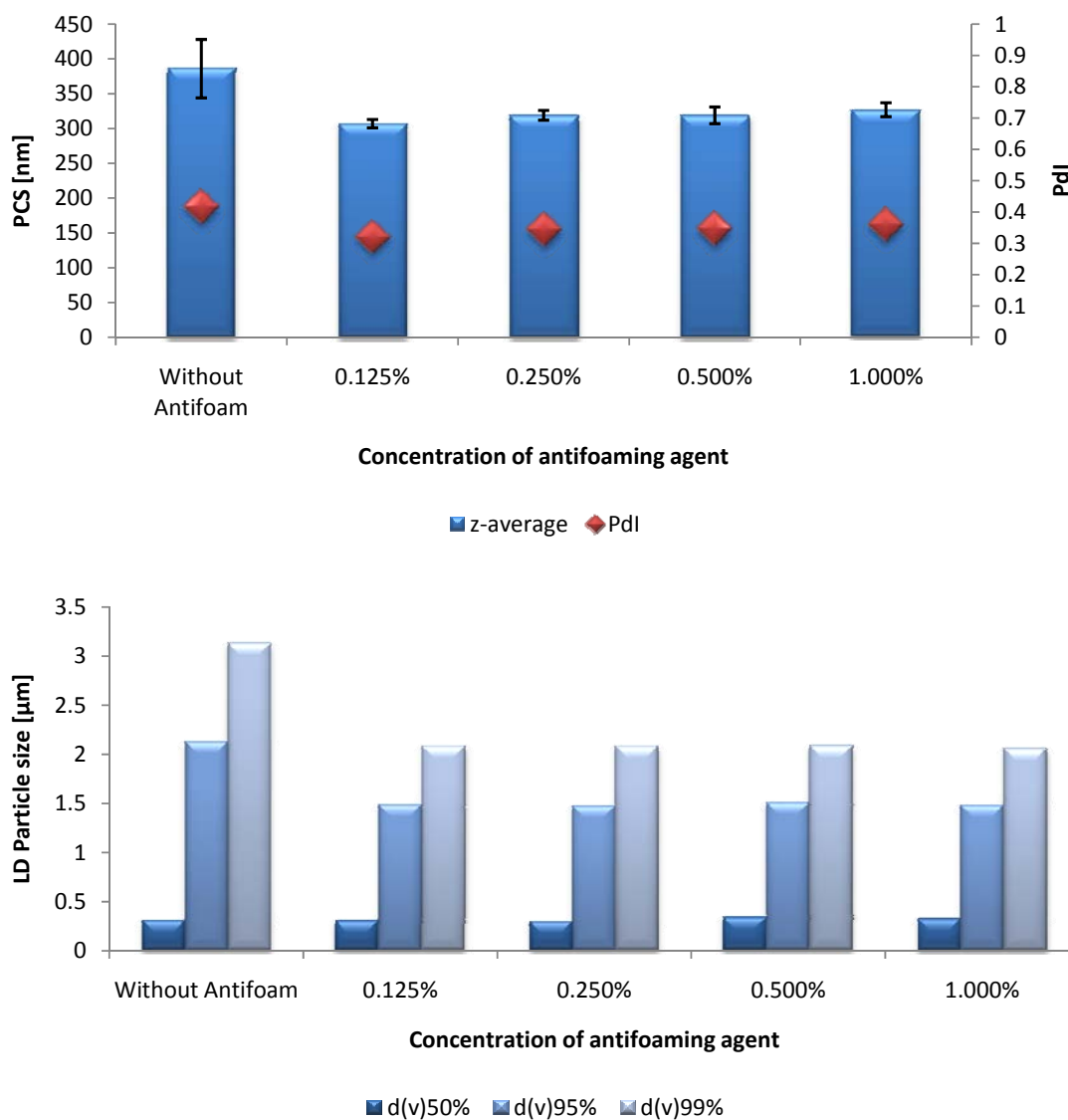
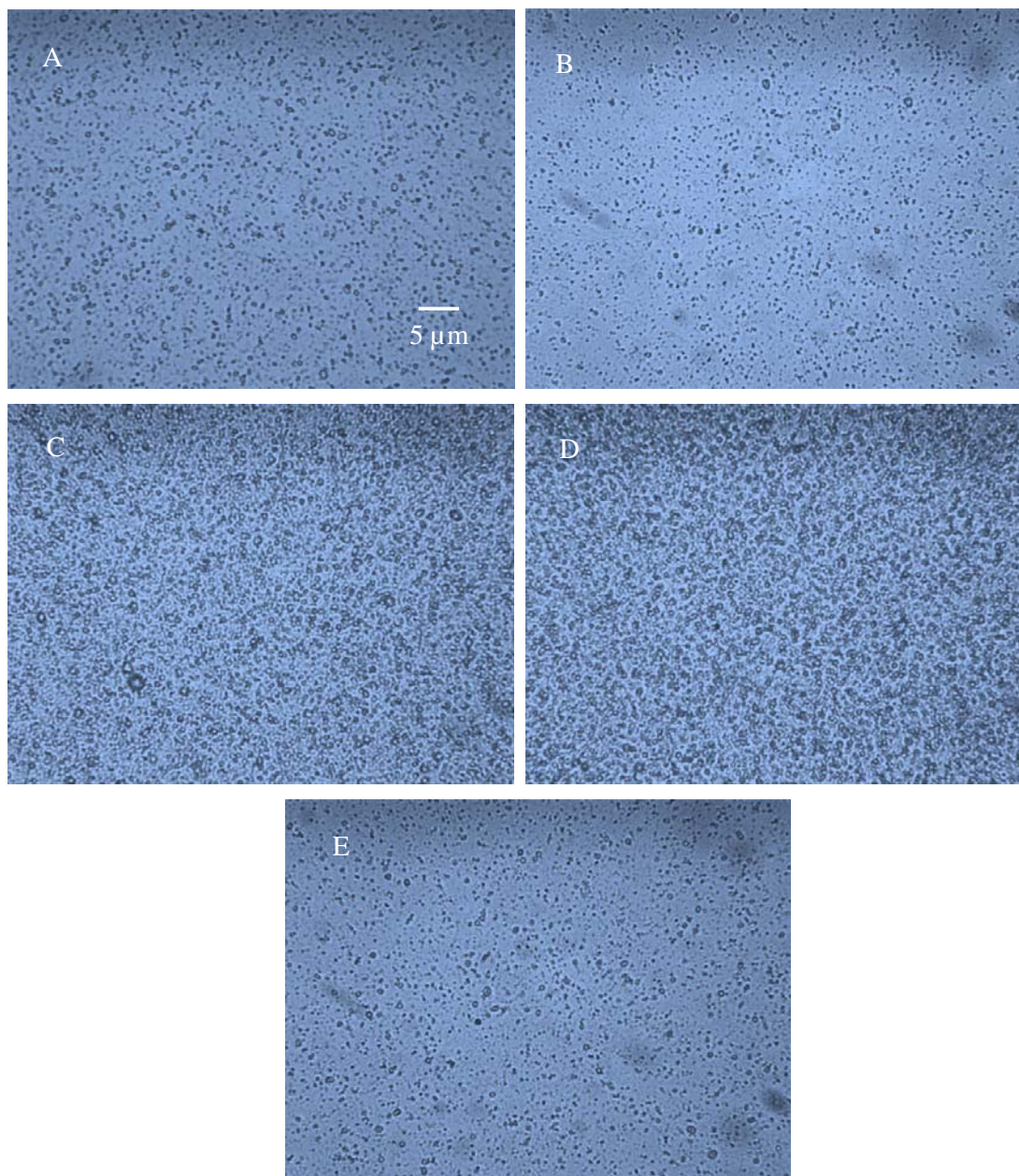


Fig. 36 Comparison of PCS diameters (up) and LD particle size (down) of preserved hesperetin nanosuspensions without or with the addition of antifoaming agent in different concentrations (% w/w)



**Fig. 37** Microscopic pictures of the nanosuspension with antifoaming agents according to the following concentrations: A) nanosuspension without antifoaming agent, B) 0.125% antifoaming agent, C) 0.25% antifoaming agent, D) 0.5% antifoaming agent, & E) 1.0% antifoaming agent. (magnification 1000 fold, bar = 5  $\mu\text{m}$ )

#### 4.1.6 Scale-up

Nanocrystals, generally produced on lab scale, were thoroughly studied for various administration routes. On the other hand, limited data about scaling-up of nanosuspensions is available [141]. The ability to scale-up from lab scale (20 g batch) to pilot scale of 3 kg batch was investigated, i.e. a scale factor of 150. Scaling-up the production of batch size was investigated using two different production methods. 1) Using Avestin Emulsiflex C50 (Avestin Europe GmbH, Germany), a normal pneumatic piston gap homogenizer, to produce

first generation nanocrystals. 2) Using the combination technology to produce smartCrystals<sup>®</sup> with the aid of the Bühler pearl mill PML-2 (Bühler AG, Switzerland) followed by homogenization with Avestin Emulsiflex C50 using low pressure of 300 bar.

#### 4.1.6.1 Batch production using Avestin C50

As a first step, scale-up was made using a piston-gap homogenizer with a larger capacity than that of Micron LAB 40. Avestin Emulsiflex C50 can produce continuously large amounts of nanosuspensions starting from 150 ml and reaching up to 50 liters and more.

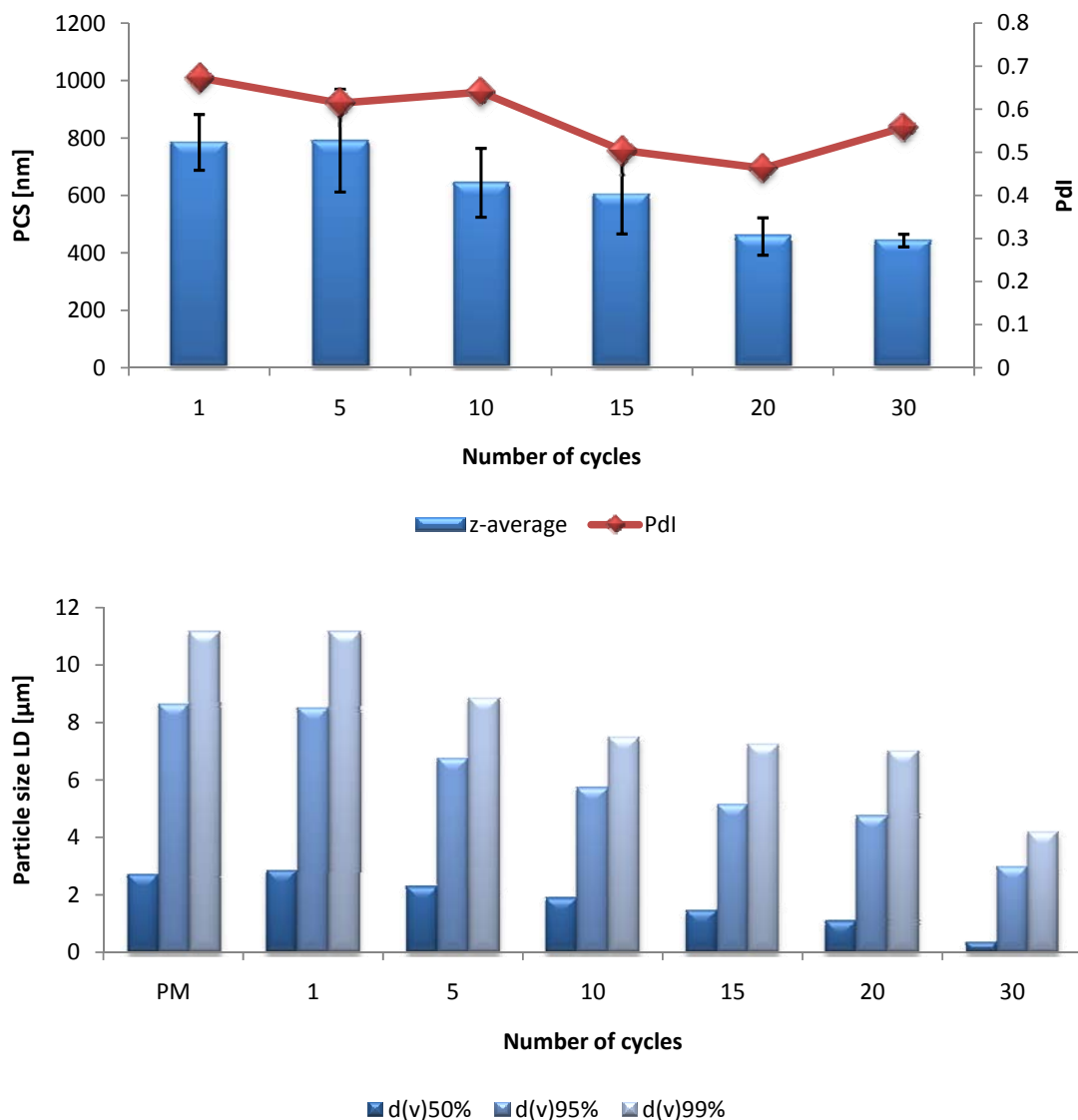
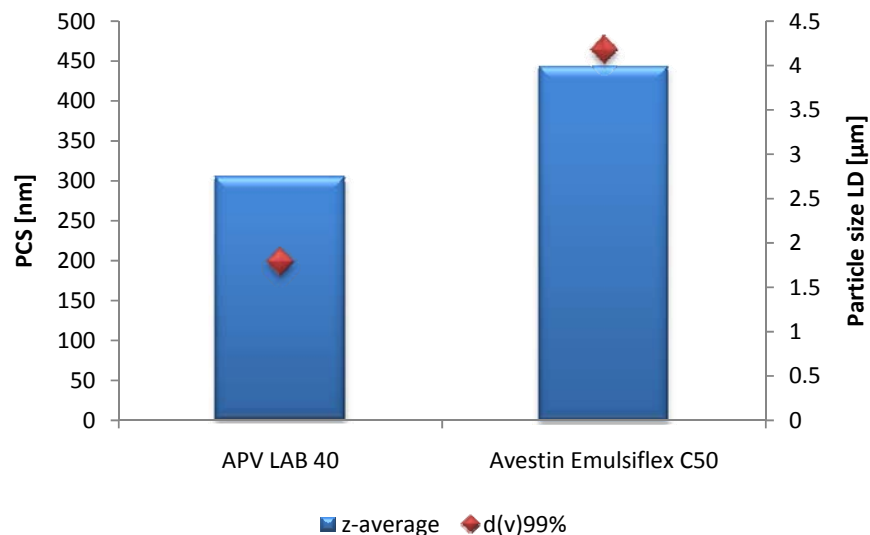


Fig. 38 Particle size reduction in nanosuspension during homogenization using PCS and LD

The same hesperetin formulation stabilized with Plantacare<sup>®</sup> 2000 UP that was used in Micron LAB 40 to produce 40 g was used also for Avestin C50 to produce 3 kg of the nanosuspension. In addition, the preservatives were added by simple admixing after producing the nanosuspension. Particle size determination was performed with PCS and LD between cycles and after adding the preservative. Fig. 38 depicts continuous reduction in particle size after passing the suspension in the homogenizer measured using PCS and LD. Size was observed by passing the suspension in the homogenizer.

PCS data shows constant reduction in the particle size starting from the 5<sup>th</sup> cycle, this is due to the fact that the particles were so large and were not in the measurable range of PCS. However, having a high PdI even after 30 cycles using 1,500 bar indicated a very wide distribution pattern with different particle sizes. This can be confirmed by the data obtained from LD, showing less reduction in d(v)99%. Which means that Avestin C50 was able to reduce particle size of generally small particles, but the nanosuspension needs further homogenization so the instrument can be able to crush the larger particles in order to get a more narrow distribution with lower PdI and lower d(v)99%.

Comparing the results obtained from PCS and LD between Micron LAB 40 (Cf. 4.1.3, pg. 39) and Avestin Emulsiflex C50 shows that Micron LAB 40 has better ability not only to obtain smaller particles in nanosuspensions but also a more confined distribution having better homogeneity as compared to nanosuspensions obtained from Emulsiflex C50 (Fig. 39).



**Fig. 39 Comparison between particle size (PCS & LD) after production of nanosuspensions using Micron LAB 40 & Avestin Emulsiflex C50**

Preservatives were then added to the nanosuspension after production and the effect of the preservatives was observed on the physical and chemical stability. A wider range of preservatives was screened in order to develop a stable system for topical application (Fig. 40).

The PCS and LD data shows that all preservatives except EUX702 and multiEx naturotics were of no destabilizing effect on the physical stability of the nanosuspensions. These results can be confirmed from the data obtained with LD instrument with an increase in  $d(v)50\%$ ,  $d(v)95\%$ , and  $d(v)99\%$ .

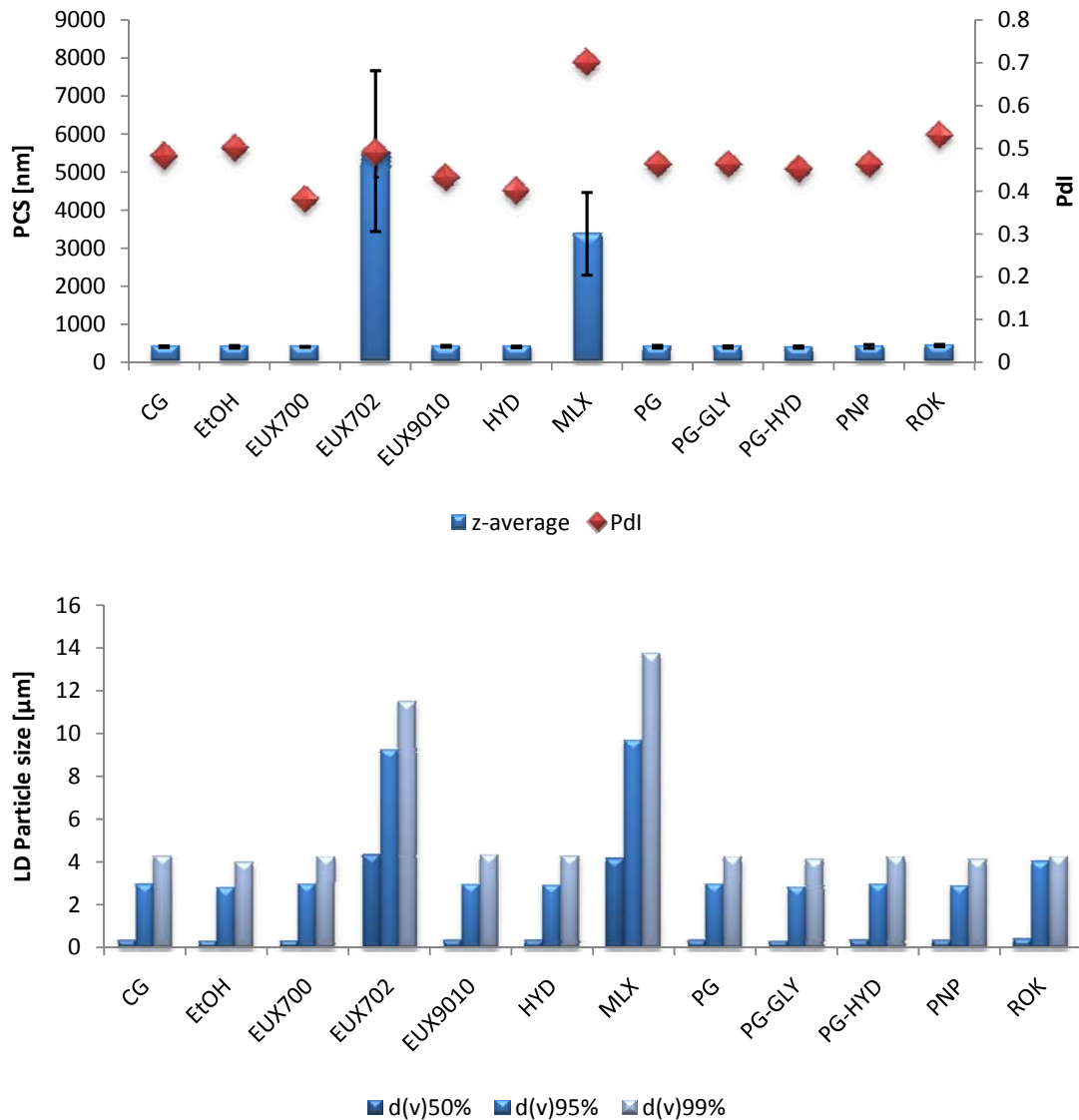
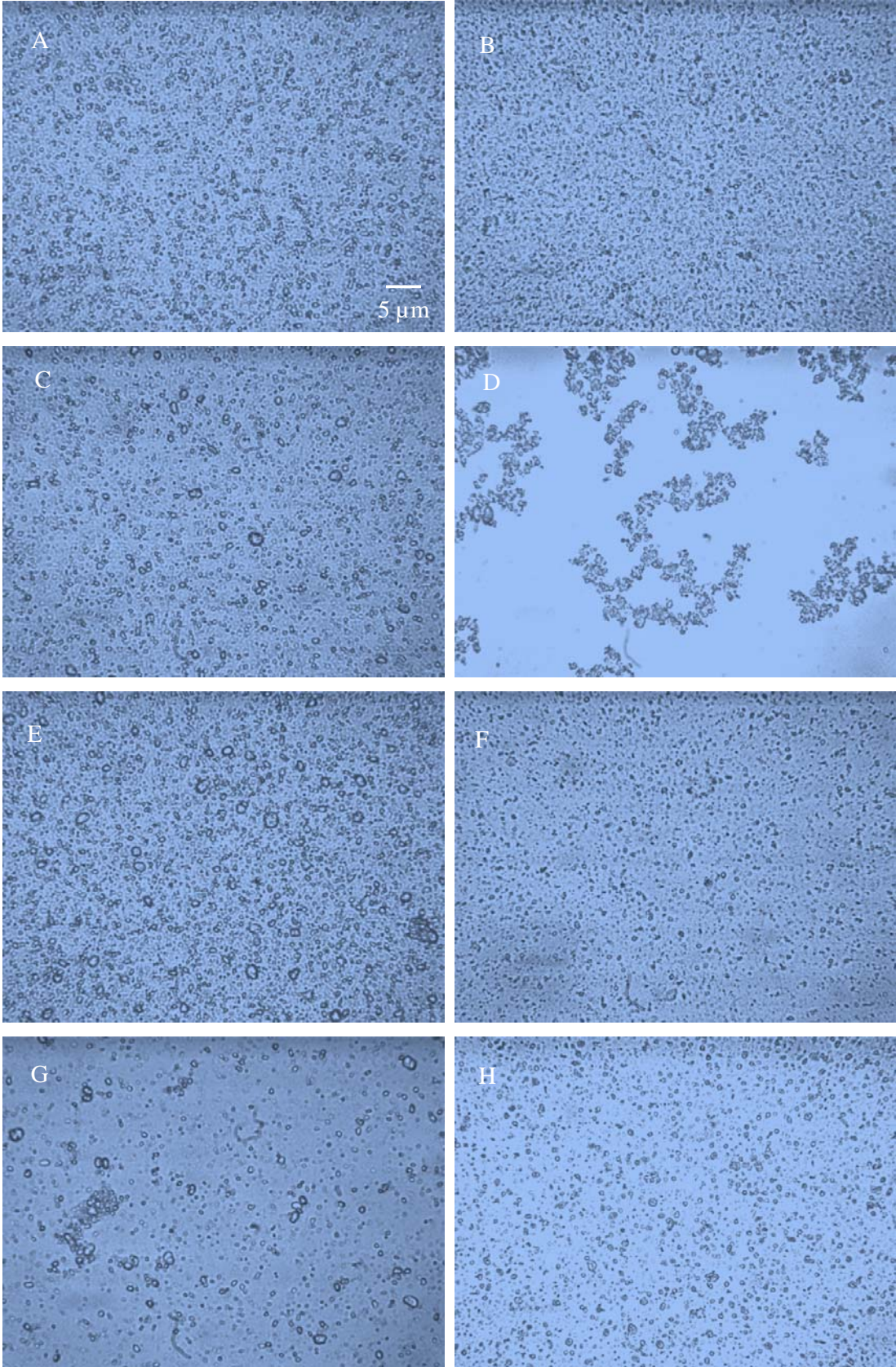
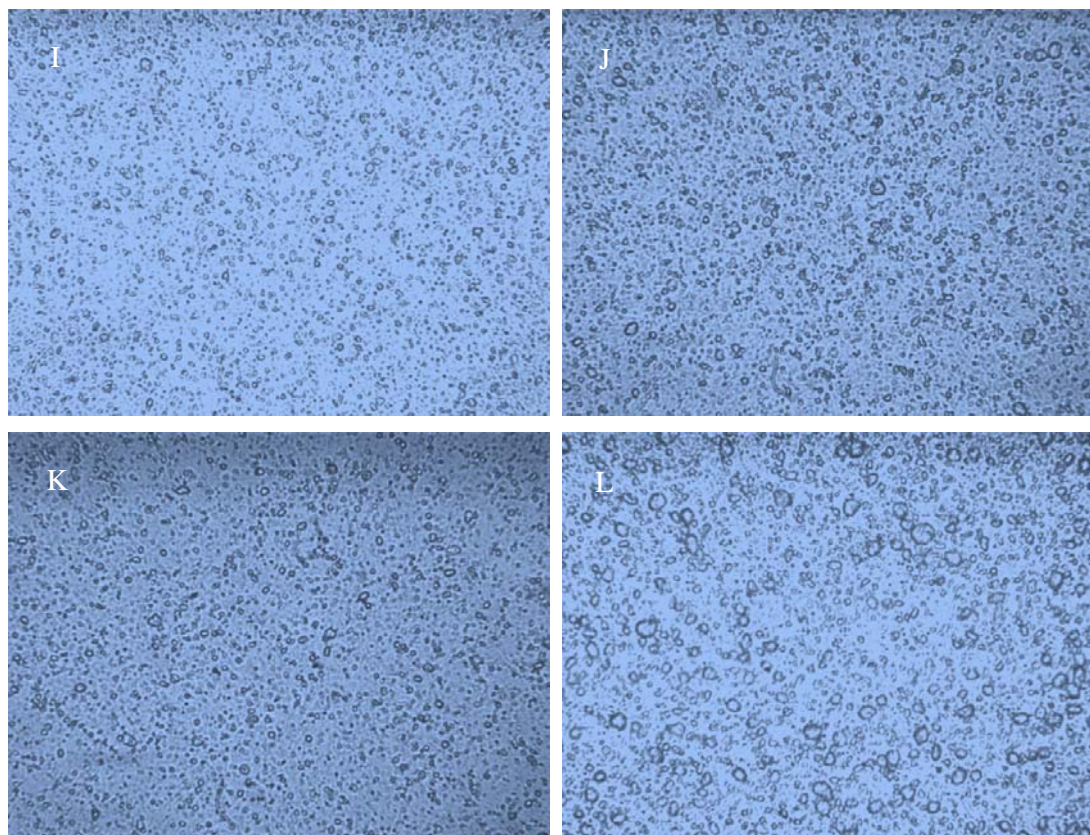


Fig. 40 Particle sizes measured using PCS (up) and LD (down) of preserved nanosuspensions produced using Avestin Emulsiflex C50 for 3 kg batch (CG= caprylyl glycol, EtOH= ethanol, EUX700= Euxyl<sup>®</sup> K700, EUX702= Euxyl<sup>®</sup> K702, EUX9010= Euxyl<sup>®</sup> PE 9010, HYD= Hydrolite<sup>®</sup>-5, MLX= multiEx naturotics, PG= propylene glycol, PG-GLY= propylene glycol & glycerol mixture 14% & 11%, PG-HYD= propylene glycol & Hydrolite<sup>®</sup>-5 mixture 5% & 3%, PNP= Phenonip<sup>®</sup>, ROK= Rokonsal<sup>®</sup> PB-5)





**Fig. 41** Light microscopy images of nanosuspensions preserved with: A) caprylyl glycol, B) ethanol, C) EUX700= Euxyl® K700, D) EUX702= Euxyl® K702, E) EUX9010= Euxyl® PE 9010, F) Hydrolite®-5, G) multiEx naturotics, H) propylene glycol, I) propylene glycol-glycerol 14% & 11%, J) propylene glycol-Hydrolite®-5 5% & 3%, K) Phenoniop®, L) Rokonsal® PB-5, (magnification 1000 fold, bar = 5  $\mu$ m)

Light microscopy (Fig. 41) showed aggregation for both EUX702 and multiEx naturotics preserved nanosuspensions, which was shown in PCS and LD measurements with a z-average reaching 6000 nm and  $d(v)99\%$  of 12  $\mu$ m. The z-average of 4,000 nm and  $d(v)99\%$  of 14  $\mu$ m was detected for multiEx naturotics preserved nanosuspension. Large crystals were noticed for Rokonsal® PB-5 preserved nanosuspensions in microscopic pictures. This was also detected with elevated  $d(v)90\%$  in LD data.

By measuring the Stern potentials (ZP in distilled water) of the preserved nanosuspensions, it was found that the zeta potential was around -50 mV for all preservatives except the ones preserved with EUX702 and multiEx naturotics (Table 10).

This supports that the preservatives, potentially adsorbed on the crystal surface (inner Helmholtz layer), are desorbed from the surface of the particles. However, the low ZP related to EUX702 & multiEx naturotics depicts a radical change on the particle surfaces and thus affects the physical stability of the nanosuspensions. This indicates that upon diluting the nanosuspension with water for the measurement, non-ionic preservative remained adsorbed, reducing the measured potentials. These data are an indication, that the two preservatives have



a high affinity to the crystal surface. The presence of these preservatives, EUX702 and multiEx naturotics, leads to the formation of a mixed film with the stabilizer Plantacare<sup>®</sup> 2000 UP, reducing the particle charge, distorting the film and finally reducing the stability (Cf. 4.1.8).

**Table 10 ZP values of the preserved nanosuspensions in distilled water and in original dispersion medium**

Preservative	Zeta potential (mV)	
	Water 50.0 $\mu$ S/cm and pH 5.8	Original dispersion medium
caprylyl glycol	-55.3	-10.0
ethanol	-58.6	-29.6
Euxyl <sup>®</sup> K700	-59.1	-31.4
Euxyl <sup>®</sup> K702	-21.3	-23.3
Euxyl <sup>®</sup> PE 9010	-58.8	-29.5
Hydrolite <sup>®</sup> -5	-59.3	-33.5
multiEx naturotics	-32.7	-29.7
propylene glycol	-56.3	-20.9
propylene glycol-glycerol (14:11)	-57.5	-33.7
propylene glycol-Hydrolite <sup>®</sup> -5 (5:3)	-57.6	-20.2
Phenonip <sup>®</sup>	-59.4	-32.1
Rokonsal <sup>®</sup> PB-5	-59.0	-33.1

By measuring the zeta potential in the original dispersion it was found that most of the preservatives have a ZP around -30 mV. Formulations containing caprylyl glycol, EUX702, propylene glycol, and propylene glycol-Hydrolite<sup>®</sup>-5 have a lower ZP of about -10, -23, -20, and -20 mV, respectively. The most de-stabilizing multiEx naturotics has a potential of -29 mV. PCS and LD data did not show any effect of the preservative on the stability of the nanosuspensions containing propylene glycol and propylene glycol-Hydrolite<sup>®</sup>-5. It can be explained that presence propylene glycol lead to mixed film as well but the produced film had the same stabilizing efficacy of the stabilizer alone. The destabilizing effect of EUX702 and multiEx naturotics was significantly noticed on the ZP for EUX702 but not for multiEx naturotics. On the other hand, caprylyl glycol preserved nanosuspensions were stable despite the low ZP value.

#### 4.1.6.2 Production of smartCrystals® (CT)

In smartCrystal® technology, the raw suspension undergoes first milling using the pearl mill till it reaches the nanorange and then passing the nanosuspension through high pressure homogenization [76]. This combined technology produces nanosuspensions with better physical characteristics and better stability than the first generation of nanosuspensions produced with high pressure homogenization alone.

After the first passage the PCS diameter was about 300 nm for hesperetin nanosuspensions. Applying a second passage led to a further reduction to about 256 nm, followed by a more slowly decrease until completion of passage 5. Further passages until the 7<sup>th</sup> have no significant effect on the size, and limited effect on the PdI. After 7 passages, the mean particle size was 195 nm with a narrow PdI of 0.180 (Fig. 42). The raw suspension was not measured using PCS because the particle size was outside the measurable particle size range for the instrument.

Subsequent homogenization step using lower pressures (e.g. 100-500 bar) yields smaller and more homogenous nanocrystal populations than applying 1,000-1,500 bar [73]. In addition, the size distribution gets narrower, hence the PdI decreases. Using 100 bar is difficult, because the pressure adjustment is not precisely possible. This is the reason, why 300 bar was applied. In some cases a further decrease in size is observed in the final HPH step, sometimes the size stays unchanged and only the PdI decreases. The mean PCS particle size stayed practically unchanged, but a further slight decrease in the polydispersity index was observed. LD data shows that the reduction of  $d(v)_{99\%}$  was constant till the 5<sup>th</sup> passage. Between the 5<sup>th</sup> and the 7<sup>th</sup> passage there was no significant decrease in particle size. This confirms the PCS data that maximum dispersitivity has been reached after 5 passages. The diameter 50% of the raw material was 9.029  $\mu\text{m}$ . It dropped sharply to 0.288  $\mu\text{m}$  after the 1<sup>st</sup> passage, and then decreased slowly till the 5<sup>th</sup> passage, with 0.173  $\mu\text{m}$ . After the 5<sup>th</sup> passage no significant decrease in size was noticed, i.e. 0.156  $\mu\text{m}$ . This is identical observation with that of  $d(v)_{50\%}$  value obtained using lab scale production.

In lab scale production, the z-average of 304 nm and a PdI of 0.33 after 30 cycles were noticed. The PCS diameter of 195 nm after 7 passages was almost as half as the z-average of the homogenized product at lab scale using the Micron LAB 40. Z-average remained unchanged after the subsequent passage through the Avestin C50 homogenizer. The PdI values were 0.18 and 0.16, indicating a narrowing of the size distribution and removal of larger particles in the final homogenization step in the pilot scale.

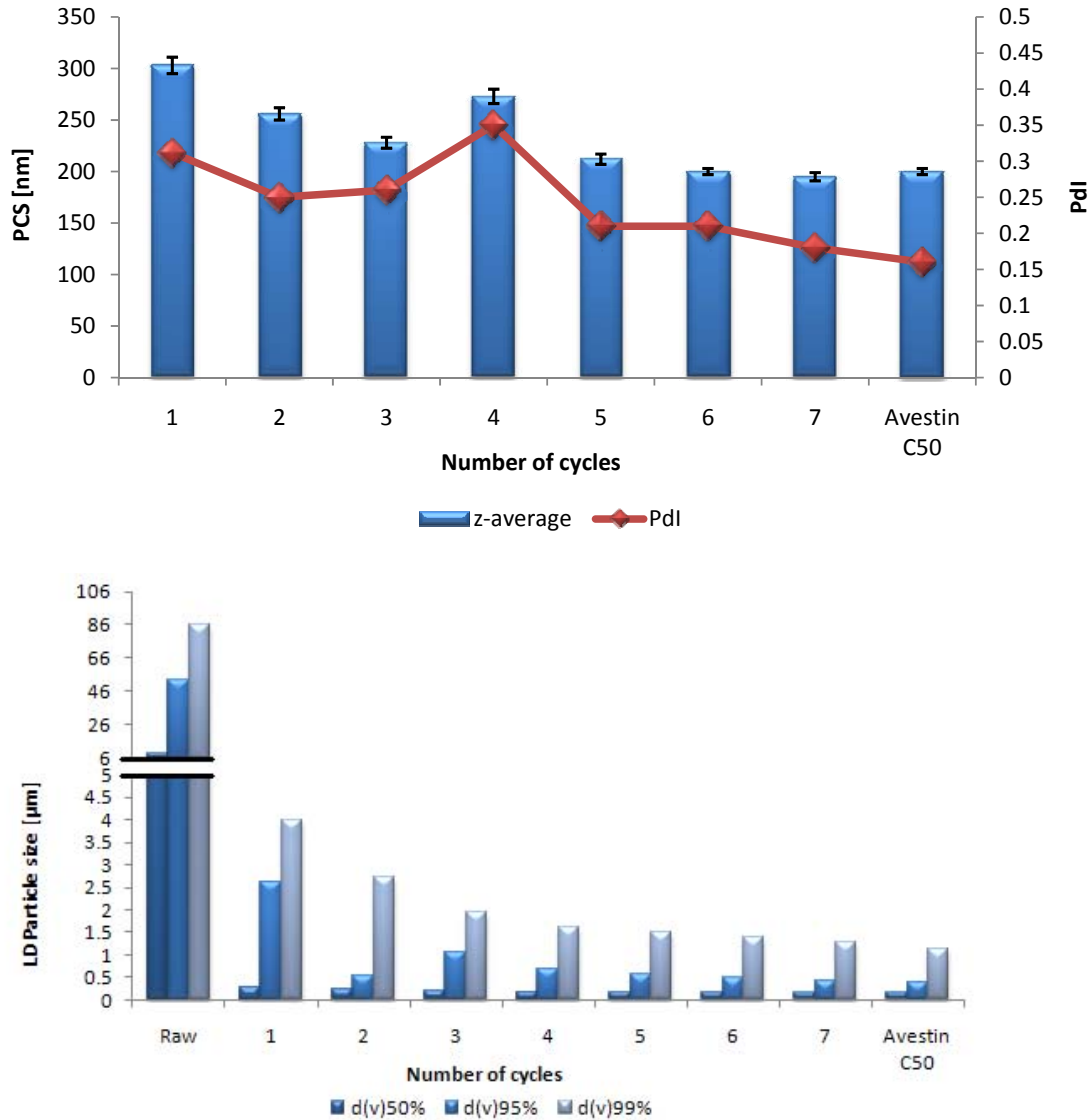


Fig. 42 Particle size reduction measured with PCS (upper) & LD (lower) according to number of passages (1 to 7) starting with the pearl mill and ending with Avestin C50 (Raw= raw material)

In lab scale production the LD diameter 50% was 0.303 μm after 30 homogenization cycles while in the pilot scale production smartCrystal<sup>®</sup> (CT process) it was 0.156 μm after passage 5 with the pearl mill, and 0.154 μm after the final homogenization step. This goes along with the data obtained from PCS.

Figure 43 shows the light microscopic pictures of the hesperetin nanocrystals from pilot scale using 160X magnification with non-polarized light according to the passages with the pearl mill and ending up with the homogenized smartCrystals<sup>®</sup>.

No clearly visible aggregation and no large crystals were seen for the formulations on the day of production.

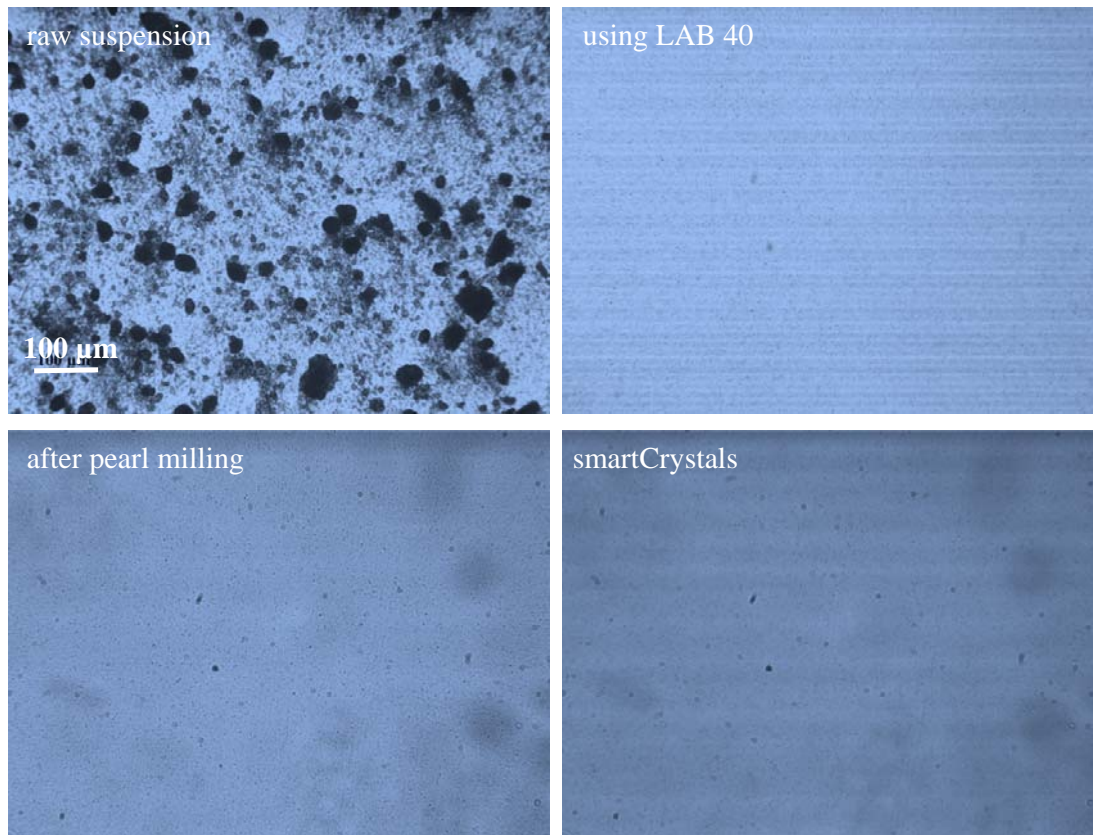
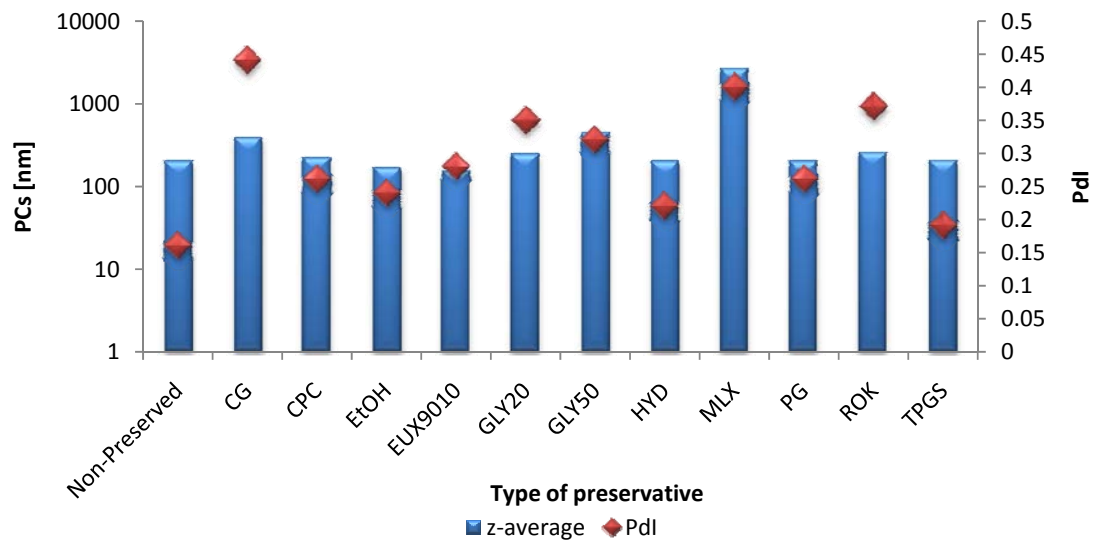
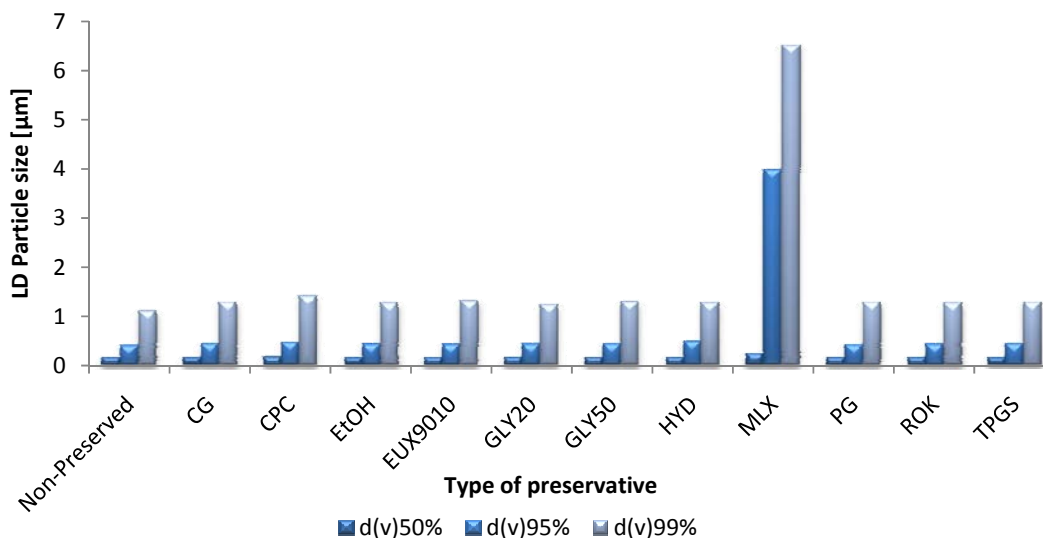


Fig. 43 Microscopic pictures of hesperetin nanosuspensions using LAB 40 and the combination technology (magnification 160 fold, bar = 100 µm)

Adding the preservatives to the produced smartCrystals<sup>®</sup> has an expected destabilizing as seen in lab scale and Avestin C50 produced nanocrystals. Figure 44 shows the destabilizing effect of preservatives on the smartCrystals<sup>®</sup> by measuring the particle size with PCS and LD.





**Fig. 44** Particle size using PCS (upper) and LD (lower) after the addition of different preservatives to the produced smartCrystals<sup>®</sup> (CG= caprylyl glycol, CPC= cetylpyridinium chloride, EtOH= ethanol, EUX9010= Euxyl<sup>®</sup> PE 9010, GLY20= glycerol 20%, GLY50= glycerol 50%, HYD= Hydrolite<sup>®</sup>-5, MLX= multiEx naturotics, PG= propylene glycol, PNP= Phenonip<sup>®</sup>, ROK= Rokonsal<sup>®</sup> PB-5 and TPGS= D-alpha tocopherol polyethylene glycol 1000 succinate )

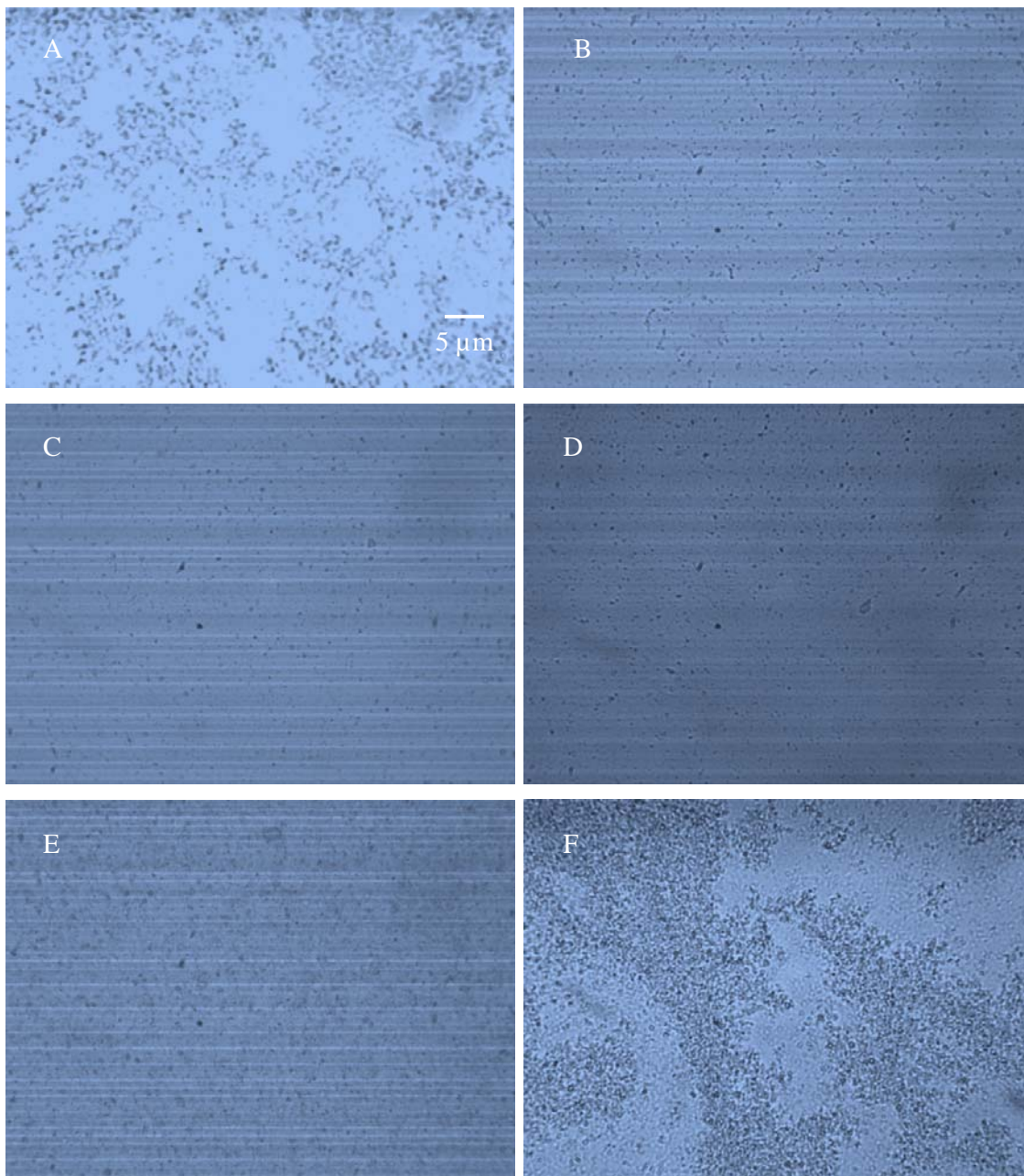
A minor increase in particle size, z-average and d(v)99% as well, was noticed with particle size of about 210 nm for most preservatives. Significant increase was observed for caprylyl glycol, glycerol 20%, glycerol 50%, & multiEx naturotics with PCS z-average of 388, 250, 450 & 2638 nm, respectively.

**Table 11** ZP values of the preserved and nonpreserved smartCrystals<sup>®</sup>

Preservative	Zeta potential (mV)	
	Water 50.0 µS/cm and pH 5.8	Original dispersion medium
Non-preserved	-41.6	-18.9
caprylyl glycol	-41.3	-2.94
cetylpyridinium chloride	58.9	19.6
ethanol	-40.4	-10.5
Euxyl <sup>®</sup> PE 9010	-36.8	-17.0
glycerol 20%	-39.9	-16.5
glycerol 50%	-38.9	-17.8
Hydrolite <sup>®</sup> -5	-44.1	-11.1
multiEx naturotics	-21.9	-19.1
propylene glycol	-43.3	-16.5
Rokonsal <sup>®</sup> PB-5	-42.1	-21.1
TPGS	-20.6	-11.0

The destabilizing effect can be seen in data obtained from LD by observing  $d(v)99\%$  but only with multiEx naturotics. Formulations containing caprylyl glycol, glycerol 20% & glycerol 50%  $d(v)99\%$  as the rest of preservatives have a diameter of about  $1.300\ \mu\text{m}$ , that indicate loose agglomerates that deaggregates with the stirring force from the built-in stirrer.

The ZP was measured in both media (adjusted conductivity water and original dispersion medium) to predict the stability of the nanosuspensions. Table 11 shows the ZP data for the smartCrystals with and without preservatives. Formulation containing Phenonip<sup>®</sup> as a preservative was discarded because after the addition of the preservative hugely large agglomeration was noticed, hence it was discarded from the list.



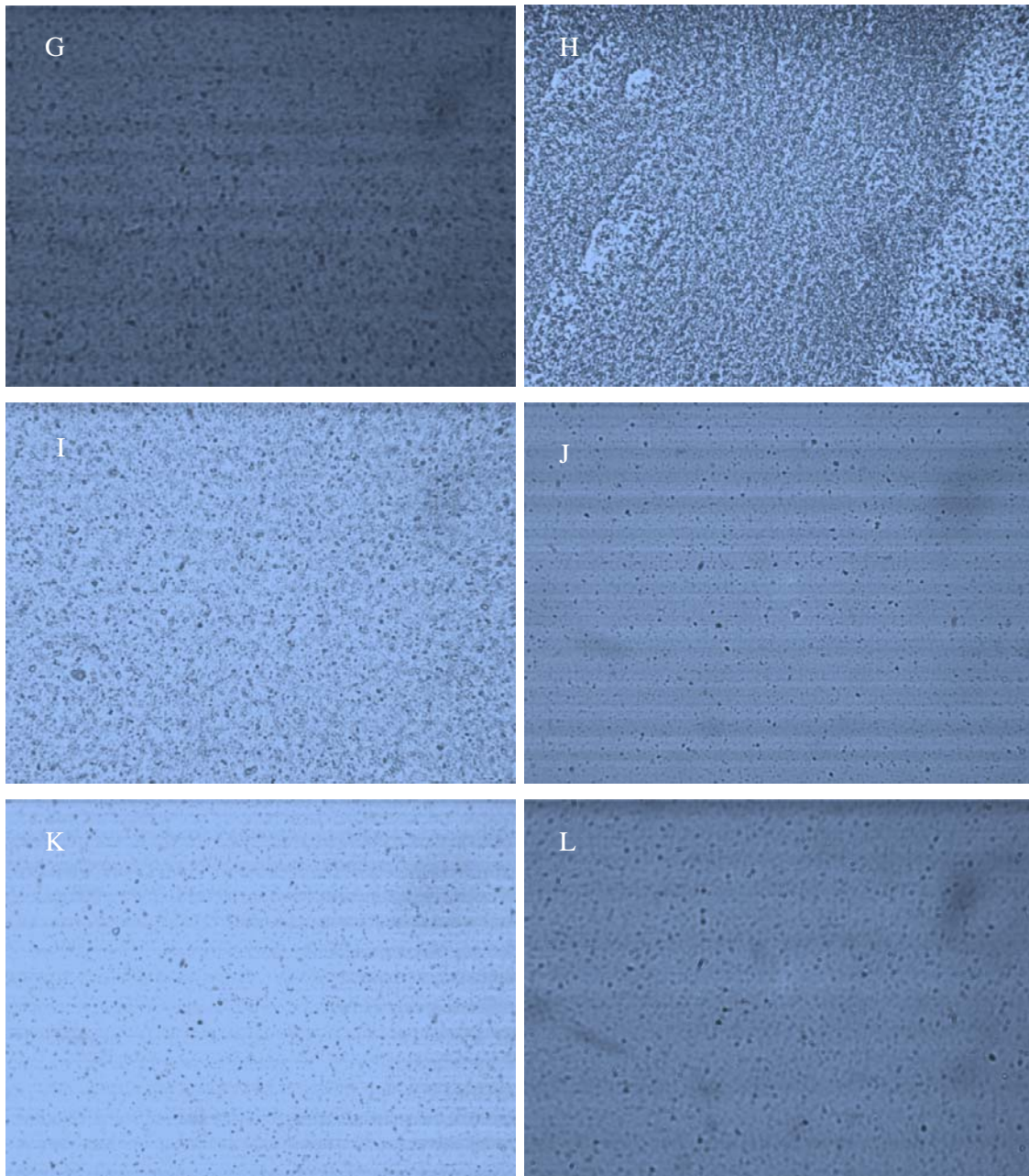


**Fig. 45** Light microscopy images of hesperetin smartCrystals<sup>®</sup> preserved with: A) caprylyl glycol, B) CPC= cetylpyridinium chloride, C) ethanol, D) EUX9010= Euxyl<sup>®</sup> PE 9010, E) glycerol 20%, F) glycerol 50%, G) Hydrolite<sup>®</sup>-5, H) multiEx naturotics, I) propylene glycol, J) Rokonsal<sup>®</sup> PB-5, K) TPGS, L) Non-preserved nanosuspension directly after admixing (magnification 1000 fold, bar = 5  $\mu$ m).

By investigating the hesperetin preserved smartCrystals<sup>®</sup> under light microscope, the results obtained from PCS and LD were confirmed (Fig. 45). Intense agglomerations has been found in hesperetin nanosuspensions preserved with multiEx naturotics, which confirms the high  $d(v)99\%$  obtained from LD data. In addition, caprylyl glycol and glycerol 50% showed as well significant aggregates under microscopic investigation proving that the normal  $d(v)90\%$  and  $d(v)99\%$  results obtained from LD measurements are due to the loose agglomerates.

#### 4.1.7 Screening of gelling agents

Different gelling agents were picked up to screen the suitability without affecting the physical stability of the smartCrystals<sup>®</sup>. As a first step an adequate amount of the gelling agent has to be verified before incorporating the nanosuspension in it.

Tylose<sup>®</sup> and CMC Na were dispersed in water and allowed to swell overnight. As for Carbopol<sup>®</sup> polymers they were dispersed in water and then the pH was adjusted to 7.0 – 7.5 by adding L-Arginine under stirring.

It was found that the topical application of nitric oxide precursor, L-Arginine, in its various forms can enhance the penetration of active ingredients [142].

An optimum concentration of gelling agents was obtained by preparing 8.0% gels from Tylose<sup>®</sup> H30000 and CMC Na and 10.0% gel from Tylose<sup>®</sup> H10000. On the other hand, a concentration of 1.0% Ultrez 10, 20 and 21 was sufficient to get a good texture gel. The prepared gels were mixed with the nanosuspensions 50 : 50 and left over night. After the gels were prepared, they were left for one year and the physical compatibility of the nanosuspensions with the added gelling agents was investigated.

#### 4.1.8 Long term physical Stability

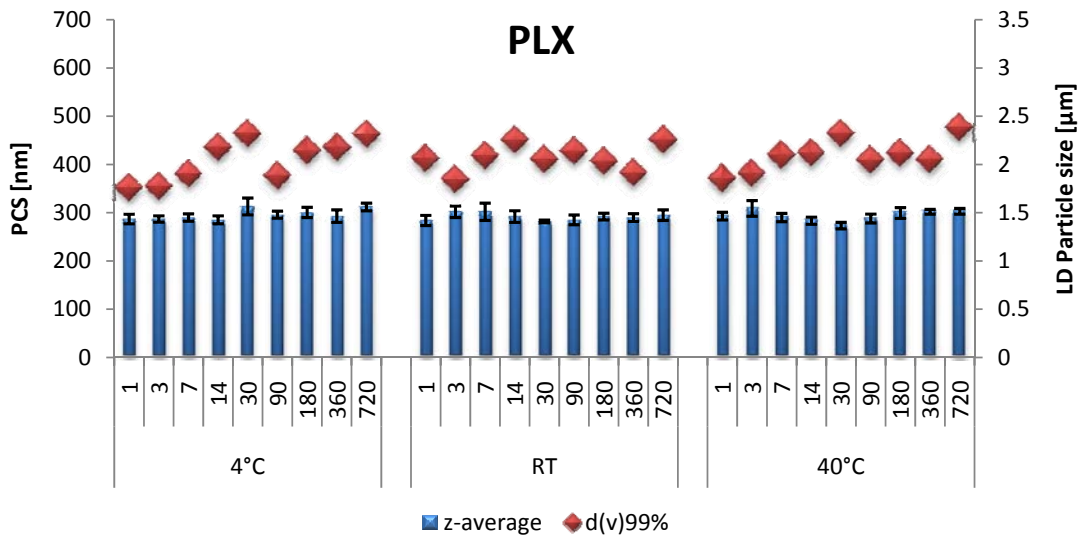
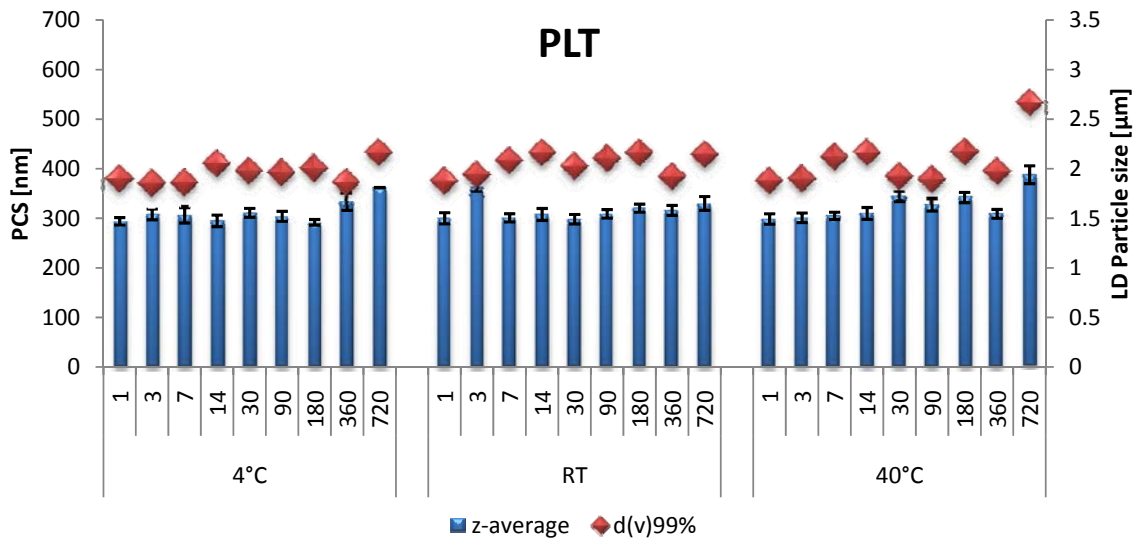
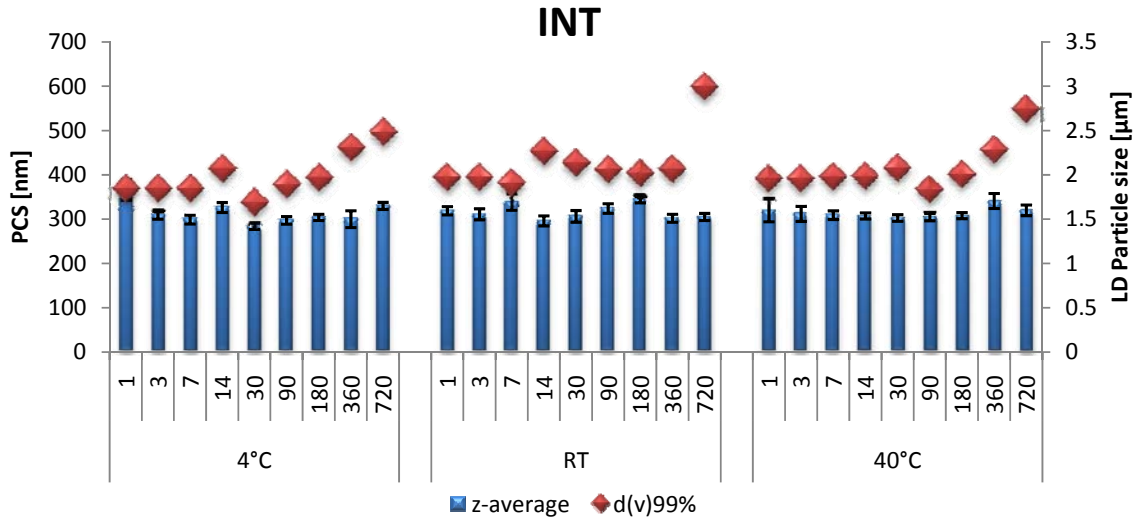
Stability was carried out for all prepared hesperetin nanosuspensions and smartCrystals in both preserved and nonpreserved forms. All samples were stored in 3 different temperatures 4°C, room temperature, and 40°C.

##### 4.1.8.1 Long term physical stability of hesperetin nanosuspensions in different stabilizers

Although Tween 80 was not efficient enough to completely stabilize the nanosuspension produced with Micron LAB40, the stability data of Tween 80 shows satisfying results. For the remaining three stabilizers, the good stability results were expected as predicted from the production data and the ZP results (Fig. 46).

The samples were stored at the refrigeration (4°C), room temperature and at 40°C conditions. From the previous experiences nanosuspensions exhibited best stability when stored at room temperature. As known, the nanosuspensions possess increased saturation solubility [143].





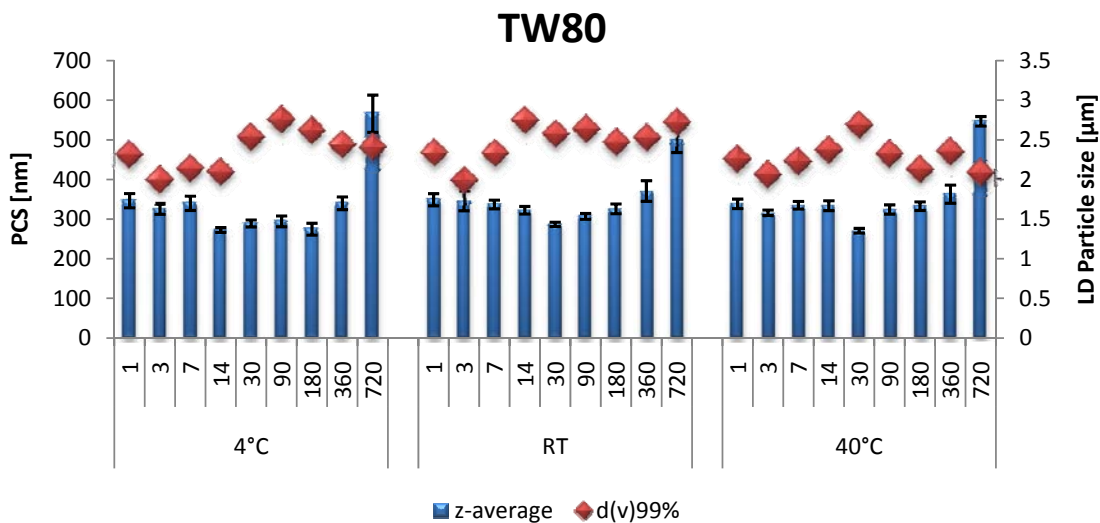


Fig. 46 The physical stability of nanosuspensions, stabilized with the four different stabilizers (INT= Inutec<sup>®</sup> SP1, PLT= Plantacare<sup>®</sup> 2000 UP, PLX= poloxamer 188 and TW80= Tween 80), measured by PCS (z-average) and LD [d(v)99%] in fridge (4°C), room temperature (RT), and in oven (40°C)

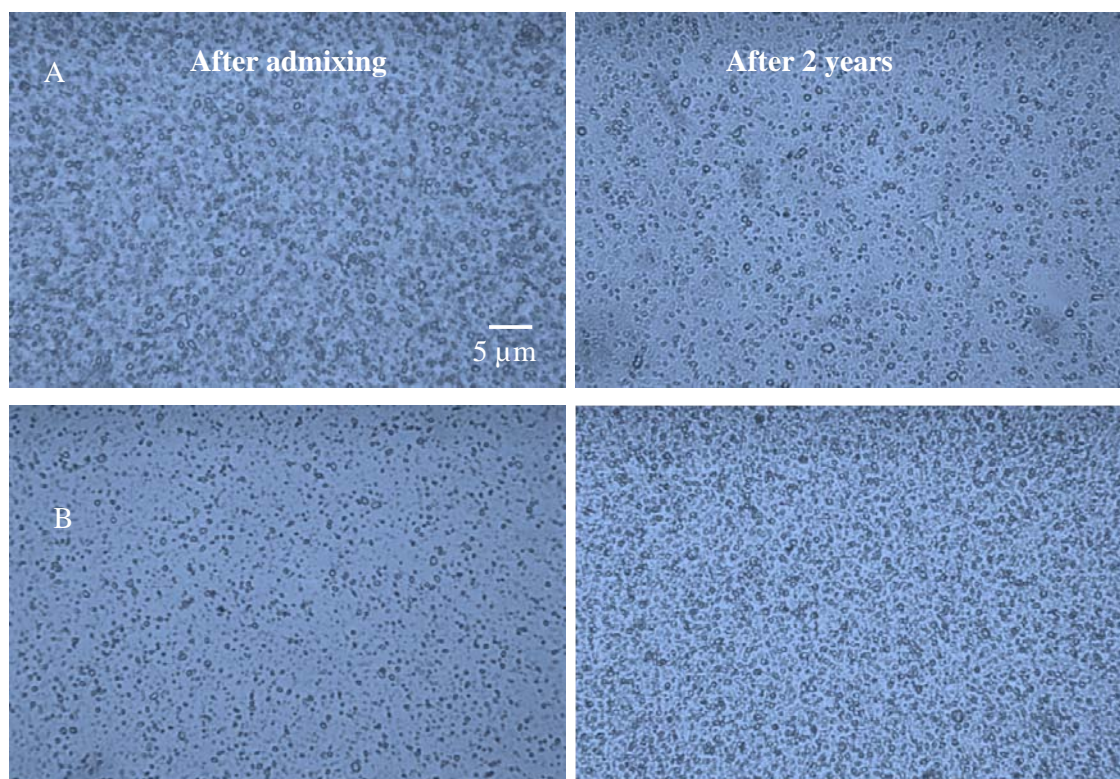
Storing them at the refrigeration temperature reduces the solubility for many actives, leading to re-crystallisation of the active in form of large crystals. Depending on the extent of solubility reduction, the size increase is not detectable, very limited or clearly detectable. Storage at 40°C increases for many actives the solubility; thus it can slightly reduce the nanocrystal size by dissolution of the drug nanocrystals. However, the smallest crystals dissolve best and disappear, larger ones remain which can also lead to an increase in the measured size [144].

Fig. 46 shows the PCS mean diameters and the LD diameters 99% of the four differently stabilized nanosuspensions at the three storage temperatures. The PCS diameter (z-average) shows very sensitive changes in the bulk population, the d(v)99% is highly sensitive towards the occurrence of larger sized particles. Therefore, both parameters are useful tools to follow the physical stability. At all three storage temperatures, Inutec<sup>®</sup> SP1, Plantacare<sup>®</sup> 2000 UP, and poloxamer 188 stabilized nanosuspensions show practically unchanged PCS and d(v)99% diameters. The PCS values slightly augment to around 350 nm, within the reproducibility of the PCS measurements. In general, the d(v)99% shows more fluctuations than, e.g. d(v)90% or d(v)50% in the measurements. Increase in d(v)99% after 2 years was detected for both Inutec<sup>®</sup> SP1 and Plantacare<sup>®</sup> 2000 UP stabilized nanosuspensions, where slighter increase was seen for poloxamer 188 stabilized nanosuspension. However, slight increase in particle size is always predicted for nanosuspensions after this long period of storage.

This slight increase is not limiting the use of these nanocrystals in dermal formulations. In addition, it needs to be considered that in creams and gels the viscosity  $\eta$  is higher. Thus, the diffusion velocity – quantified by the diffusion coefficient  $D$  – is, according to the Einstein equation, lower ( $D$  reverse proportional to  $\eta$ ) and thus also the related kinetic energy of the particles. Therefore, the nanocrystals will be a priori more stable in these dermal formulations. Based on these considerations, adding the nanocrystals to the dermal formulation immediately after production might potentially avoid any change in size of the poloxamer 188 stabilized nanocrystals.

The Tween 80 stabilized nanosuspensions showed a slight increase of  $d(v)_{99\%}$  at all three storage temperatures. From these data, the Tween 80 stabilized nanosuspensions were classified as the least stable ones. However, the considerations made for incorporation in more viscous dermal formulations are also valid for the Tween 80 stabilized nanosuspensions.

With microscopic investigation (Fig. 47), it can be seen that hesperetin nanosuspensions stabilized with Inutec<sup>®</sup> SP1, Plantacare<sup>®</sup> 2000 UP and poloxamer 188 showed no difference after 2 years storage. However, large aggregates were seen for hesperetin nanosuspensions stabilized with Tween 80. These aggregates were detected with PCS but not with LD measurements, proving that these aggregates were loose ones.



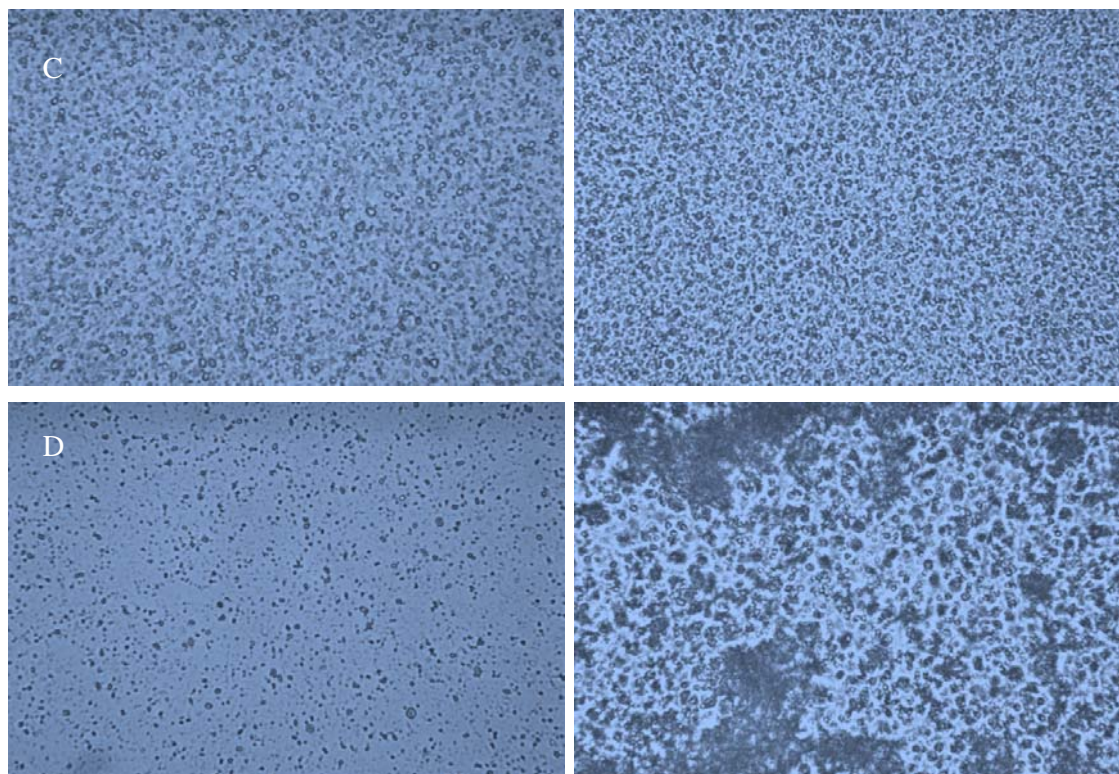


**Fig. 47** Microscopic pictures of hesperetin nanosuspensions with the four stabilizers: (A) Inutec<sup>®</sup> SP1, (B) Plantacare<sup>®</sup> 2000 UP, (C) poloxamer 188 and (D) Tween 80 (magnification 1000 fold, bar = 5  $\mu$ m). The right side is directly after production and the right side is after 2 years storage at room temperature

#### **4.1.8.2 Long term physical stability of lab scale preserved batches**

##### **a) Preservatives added after homogenization**

Preserved hesperetin batches, where the preservatives were added after the homogenization, were kept for stability study under 3 different temperatures as well as discussed previously (Cf. 4.1.8.1).

Caprylyl glycol had a slight destabilizing effect at 40°C which was augmenting over the time. Increasing the particle size was obviously seen in the one year stability data and the year after it. PCS data, except for 40°C, showed slight change through the whole period (Fig. 48). The destabilizing effect was seen earlier at 40°C as the product undergoes stress condition. LD data presented by d(v)99% showed a huge increase in the last two results for all three temperatures which indicates that the stirrer effect in deaggregating the particles was not more sufficient (Fig. 48).

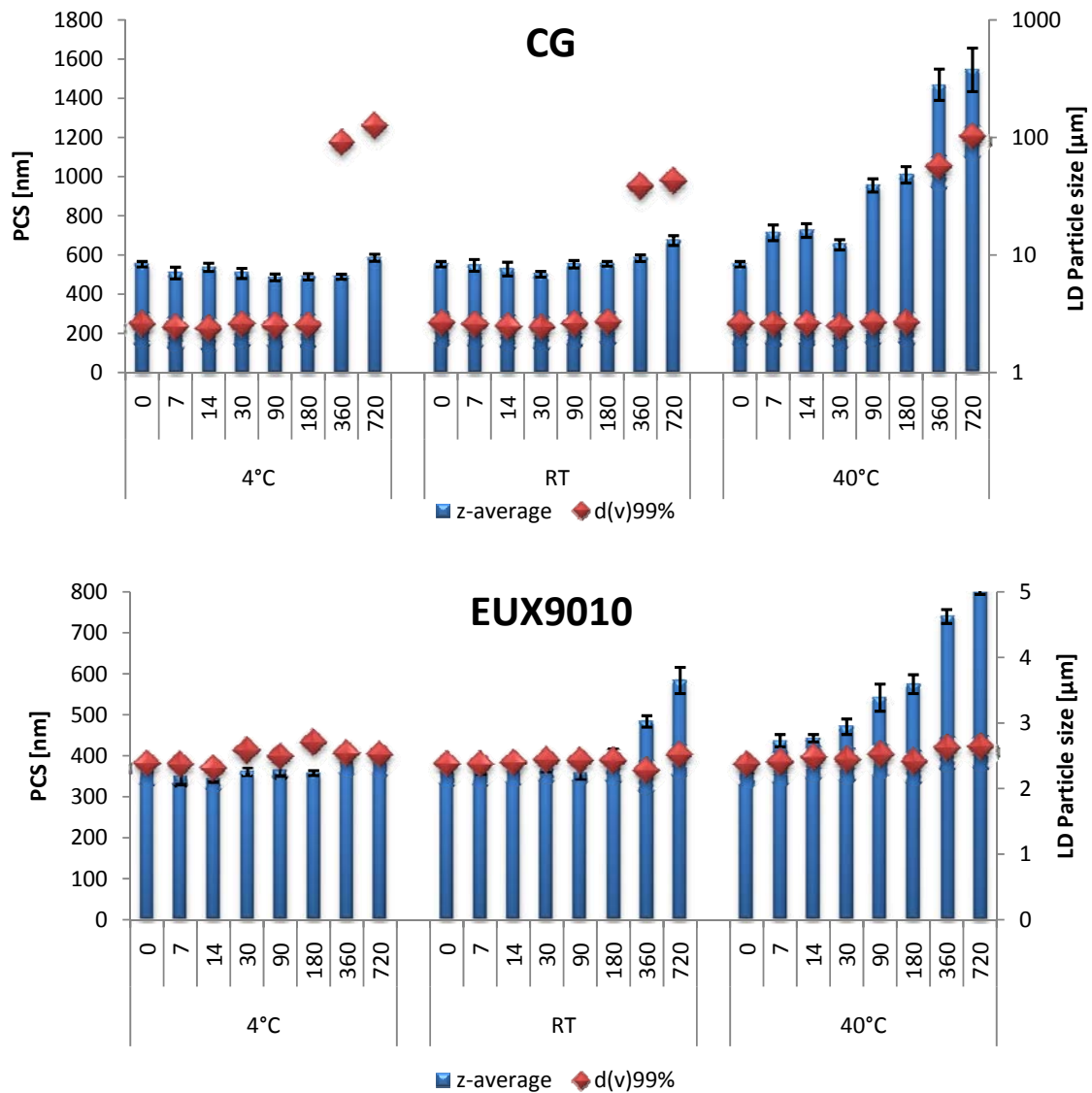


**Fig. 48** Particle size of hesperetin nanosuspensions preserved with CG= caprylyl glycol and EUX9010= euxyl PE 9010 stored at three different temperatures (4°C, RT & 40°C) as a function of time (days)

Investigation hesperetin nanosuspensions preserved with caprylyl glycol using microscope (Fig. 49A) showed the oversized aggregates confirming the data obtained from LD.

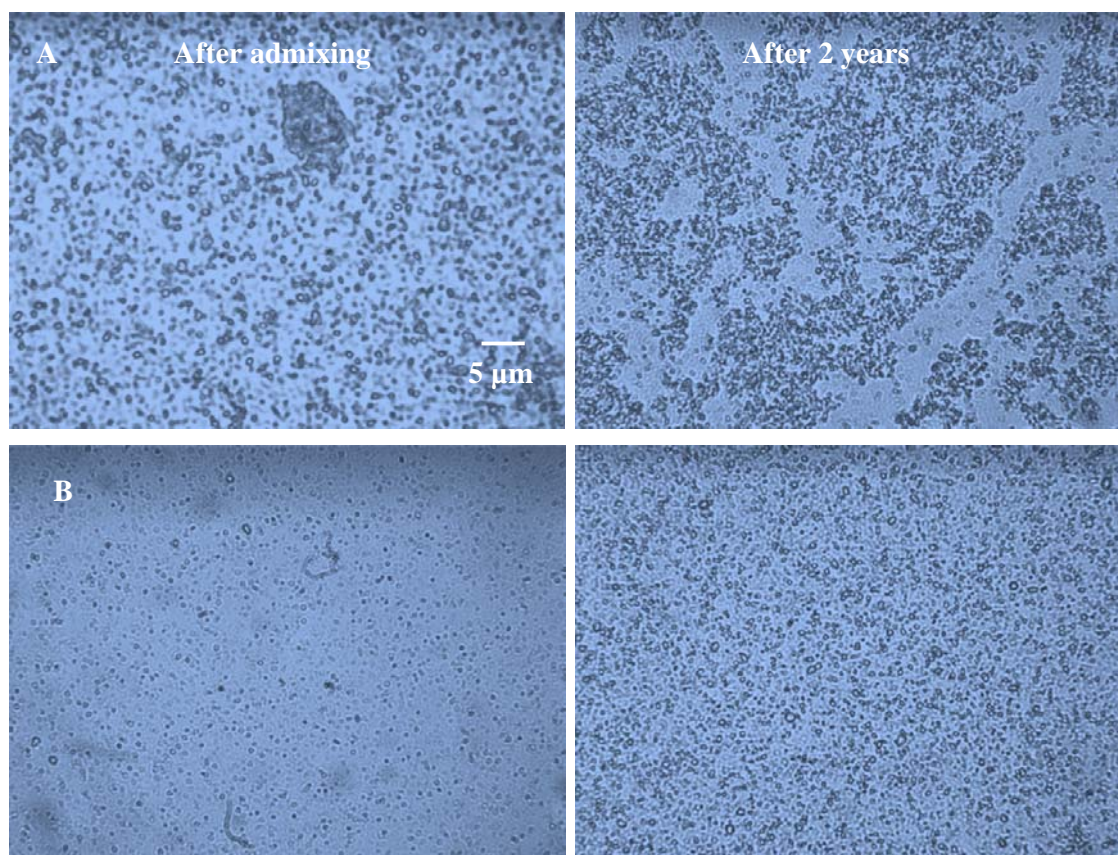


**Fig. 49** Light microscopy images of nanosuspensions preserved with: (A) caprylyl glycol, (B) EUX9010. (magnification 1000 fold, bar = 5  $\mu\text{m}$ ). The right side is directly after production and the right side is after 2 years storage at room temperature

EUX9010 stability profile was stable for samples kept in 4°C. Instability was significantly seen at 40°C but only from PCS data which can be interpreted as loose aggregates (Fig. 48, 49B).

Hydrolite<sup>®</sup>-5 is, according to the data obtained, the most suitable preservative for hesperetin nanosuspension prepared with the least effect on the physical stability. No changes were noticed for all samples stored at the three different temperatures. A very slight increase was observed for the samples stored at 40°C sample after 2 years (Fig. 50). No agglomerates were detected upon investigating the nanosuspensions using microscope (Fig. 51C).

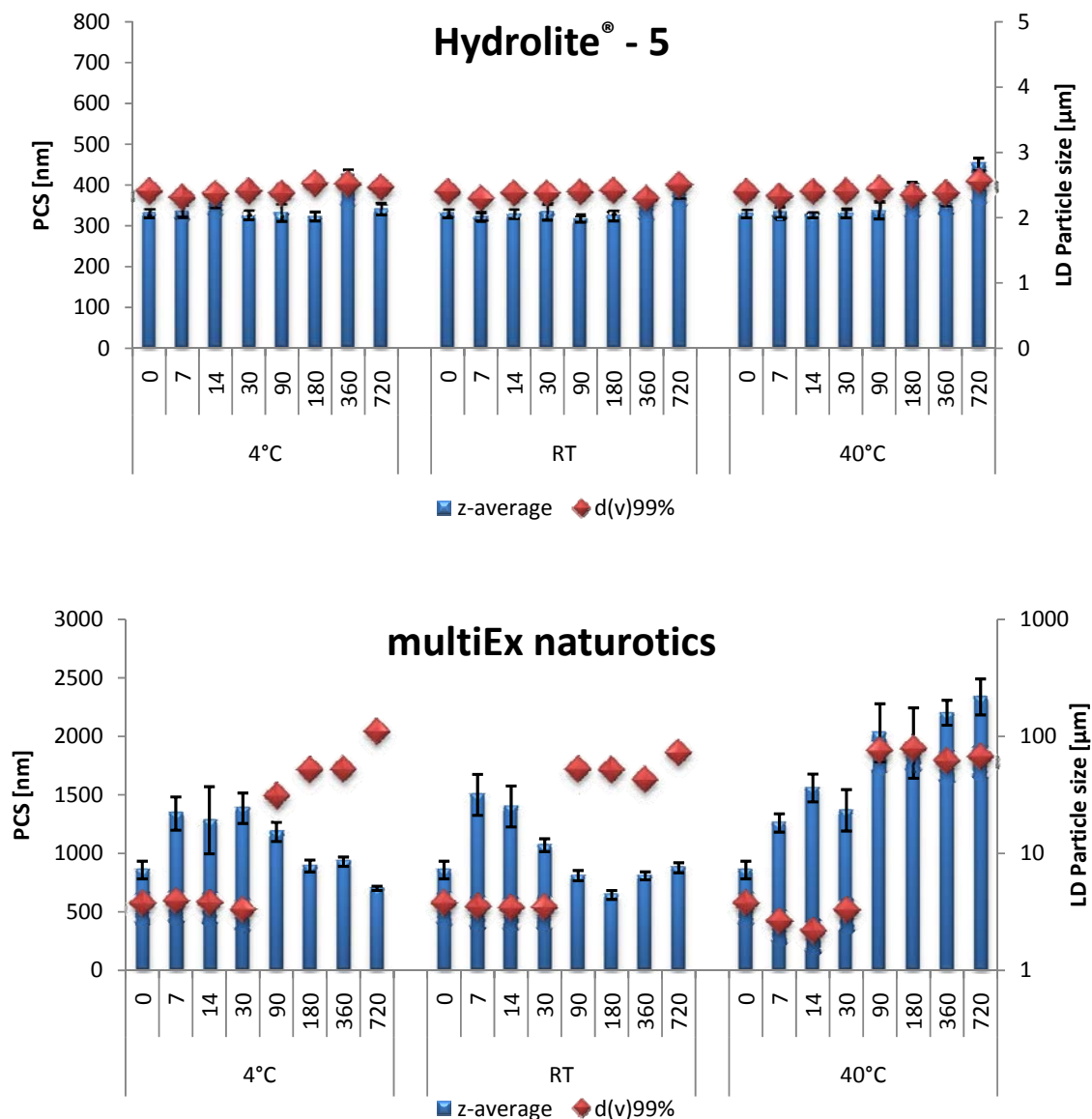


**Fig. 50 Particle size of hesperetin nanosuspensions preserved with Hydrolite®-5 and multiEx naturotics stored at three different temperatures (4°C, RT & 40°C) as a function of time (days)**

On the other hand, nanosuspensions preserved with multiEx naturotics were the most instable ones. The PCS data varied between 700 – 2,400 nm. Different particle size can be seen in Fig. 50 due to the different agglomerate sizes with a wide distribution (higher PdI) and how much they are intense. LD stirrer was able to deaggregate the agglomeration till the 30<sup>th</sup> day. The d(v)99% data measured after 3 months were higher showing high agglomeration rate and strong glumps. These oversized agglomerates were obviously seen using microscope (Fig. 51D)

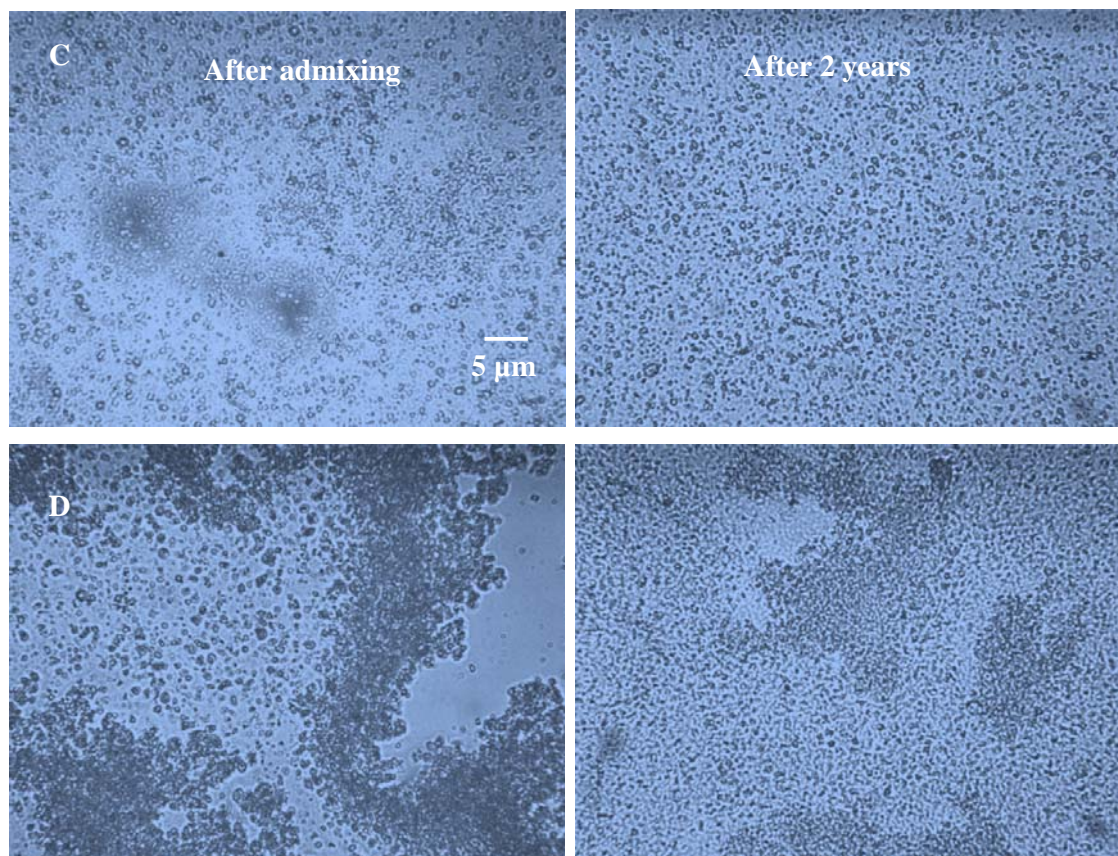


**Fig. 51** Light microscopy images of nanosuspensions preserved with: (C) Hydrolite®-5, (D) multiEx naturotics. (magnification 1000 fold, bar = 5 µm). The right side is directly after production and the right side is after 2 years storage at room temperature

Fig. 52 shows the stability data presented as well from PCS and LD as z-average and d(v)99% of Phenonip® and Rokonsal® PB-5 as both are similar to each other.

Hesperetin nanosuspension preserved with Phenonip® was less stable than that of hesperetin nanosuspension preserved with Rokonsal® PB-5, due to the higher percentage of longer carbon chains parabens in Phenonip®.

Instability for Phenonip® preserved nanosuspensions can be seen as increased particle size for z-average of around 950 nm from the day of production. As expected, the z-average of the sample stored at 40°C got quickly high than other samples due to stress conditions. LD data were low at the beginning due to the loose aggregates and they augmented after one year storing period proving the maximization of instability in the nanosuspension. These aggregates can be easily seen using the microscope (Fig. 53E)



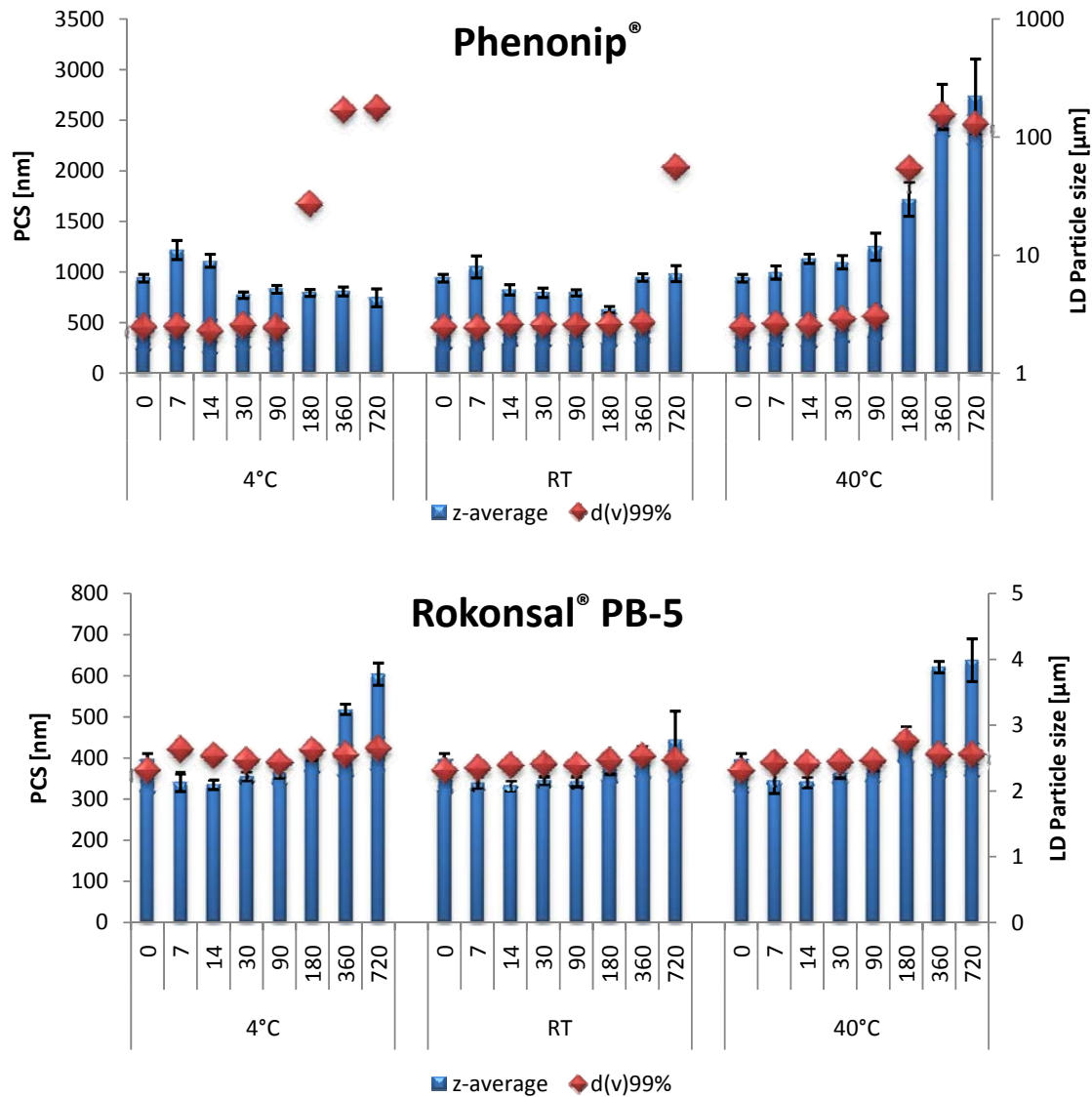
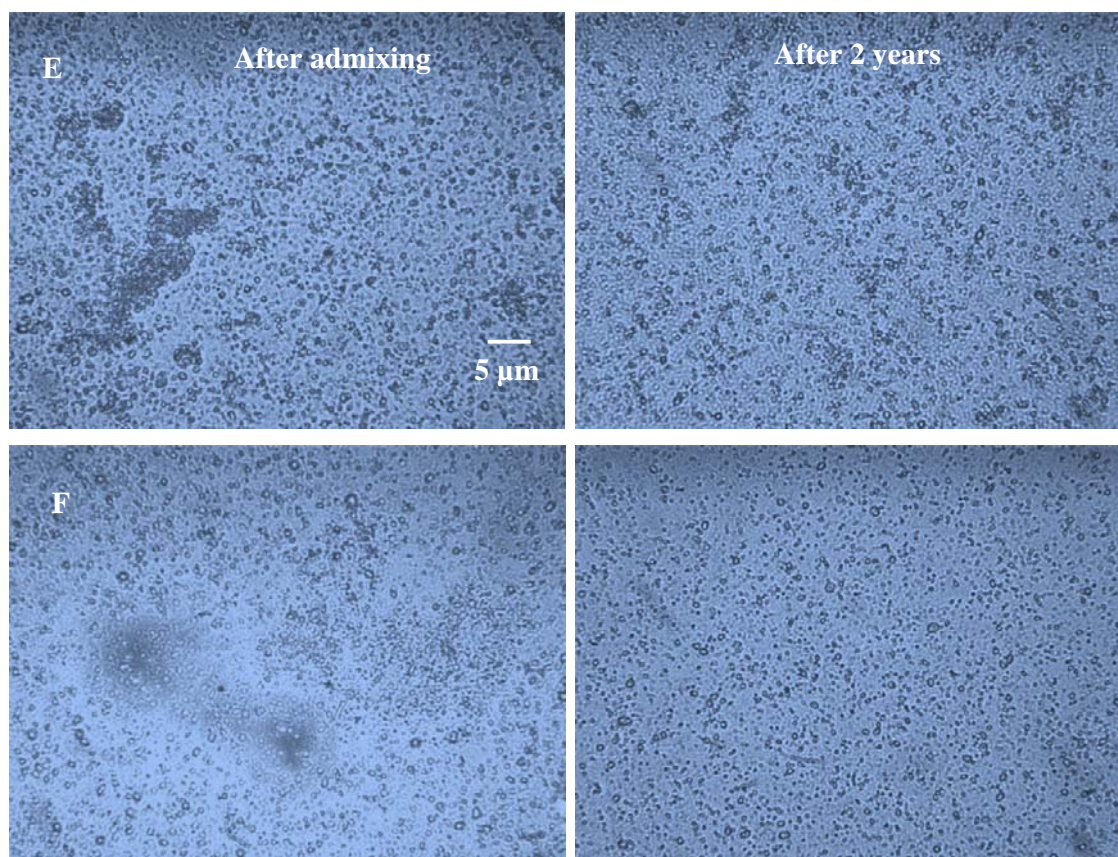


Fig. 52 Particle size of hesperetin nanosuspensions preserved with Phenonip® and Rokonsal® PB-5 stored at three different temperatures (4°C, RT & 40°C) as a function of time (days)

Nanosuspensions with Rokonsal® PB-5 as a preservative were more stable than the Phenonip® ones but not as stable as nanosuspensions preserved with Hydrolite®-5. The Rokonsal® PB-5 instability can be seen mainly at 4°C and 40°C stored samples and that to only for z-average after 1 year stability. LD data does not show any instability mentioned by PCS which indicates a loose aggregates (Fig. 52, 53F).



**Fig. 53** Light microscopy images of nanosuspensions preserved with: (E) Phenonip<sup>®</sup>, (F) Rokonsal<sup>®</sup> PB-5. (magnification 1000 fold, bar = 5  $\mu\text{m}$ ). The right side is directly after production and the right side is after 2 years storage at room temperature

#### b) Preservatives added before homogenizations

Adding caprylyl glycol to hesperetin nanosuspension before homogenization has a direct effect on the physical stability of it. By measuring the z-average for hesperetin nanosuspensions preserved with caprylyl glycol, it can be seen that the mean particle size declined with time for both samples (4°C & RT) while it decreased firstly in 40°C then it increased after 1 month storage. The dropping phase can be explained by shifting the distribution to a larger range than the PCS can detect. Hence, it can only measure the remaining smaller particles because the larger particles tend to agglomerates. On the other hand, the ascending phase can be due to the increase in the mean particle size of the rest small particles (Fig. 54, 55A). LD data showed no changes for  $d(v)99\%$  for the whole period of storage despite the large aggregates. This can be only explained by the presence of loose aggregates. These aggregates can be obviously seen in the microscopic pictures (Fig. 55A).

EUX9010 did not cause any pronounced instability in hesperetin nanosuspensions. All hesperetin nanosuspensions preserved with EUX9010 were stable without big changes for 4°C & RT samples. Small increase in the z-average was noticed after 6 months for 40°C

sample which is predicted due to the stress conditions and the increase solubility of the smaller particles (Fig. 54, 55B).

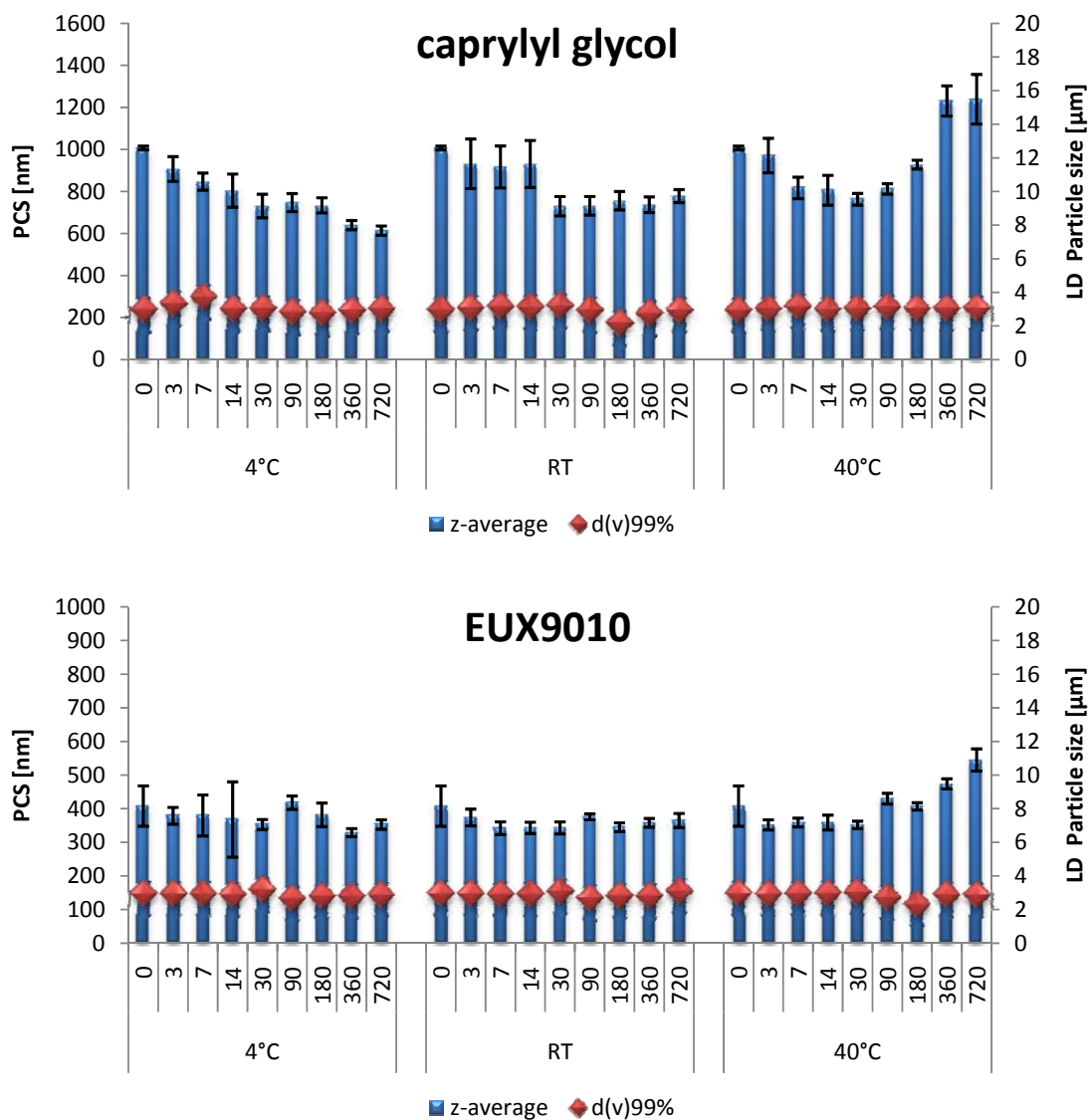


**Fig. 54** Particle size of hesperetin nanosuspensions preserved with caprylyl glycol and EUX9010= Euxyl® PE 9010 stored at three different temperatures (4°C, RT & 40°C) as a function of time (days)

Although Hydrolite®-5 was added in this trial prior homogenization but the destabilizing effect was also not pronounced. PCS data as well as LD data showed no changes in the particle size and d(v)99%, respectively. Hence, the high hydrophilicity of Hydrolite®-5 enables it to be incorporated in many highly dispersed systems with less effect on the physical stability (Fig. 56, 57C).

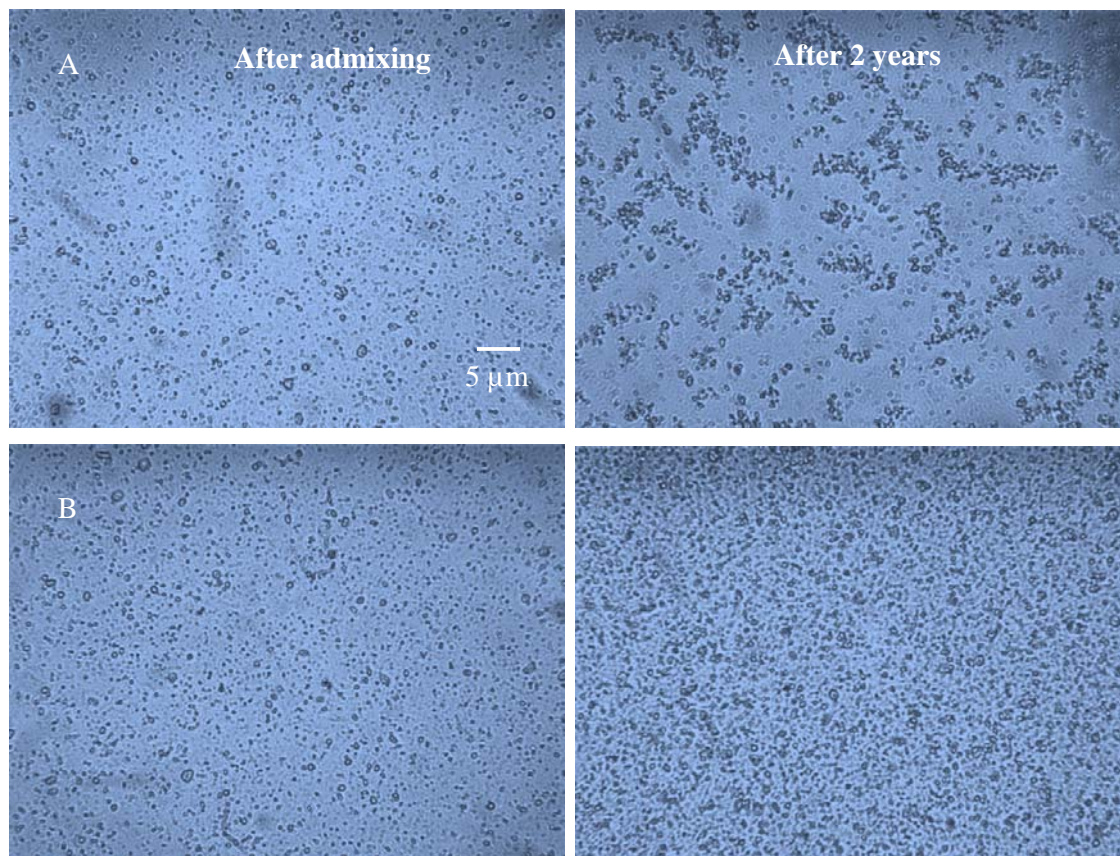


**Fig. 55** Light microscopy images of nanosuspensions preserved with: (A) caprylyl glycol, (B) EUX9010. (magnification 1000 fold, bar = 5  $\mu\text{m}$ ). The right side is directly after production and the right side is after 2 years storage at room temperature

Due to multiEx naturotics lipophilicity, the preserved nanosuspensions were highly aggregating with unstable particle size during the whole storing period. The instability profile of multiEx naturotics imitates the instability profile of caprylyl glycol, with only decreasing phase for 4°C & RT samples and declining phase followed by increasing phase for 40°C (Fig. 56, 57D). The aggregates in these nanocrystals can be clearly seen under microscope directly after admixing and after 2 years of storage (Fig. 57D).

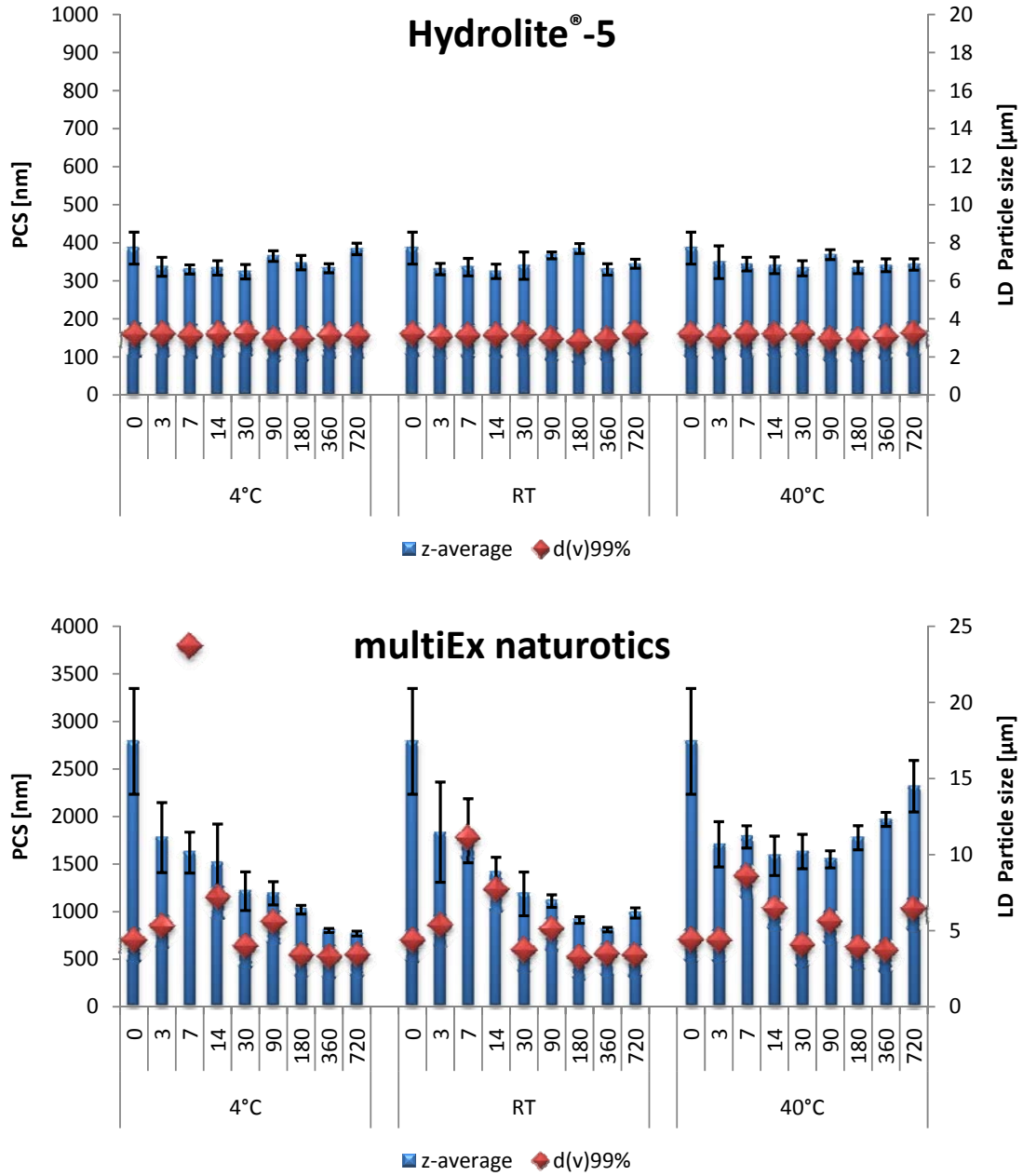
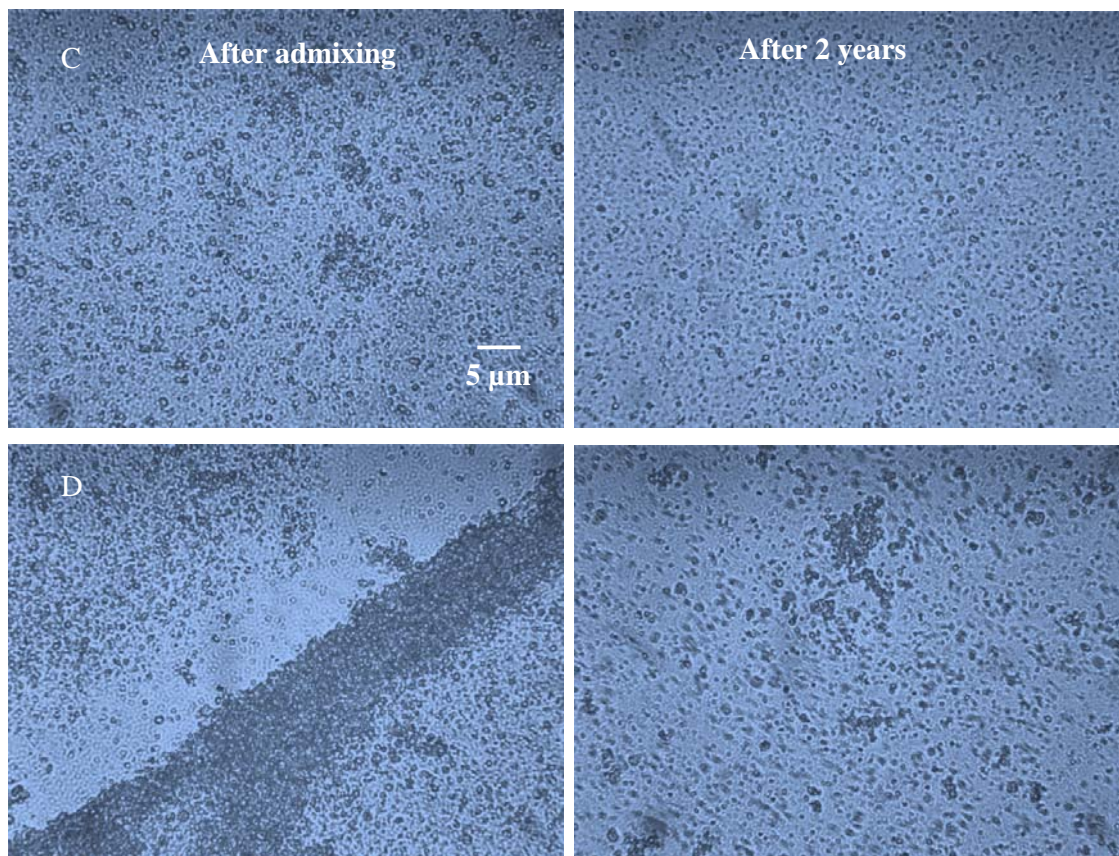
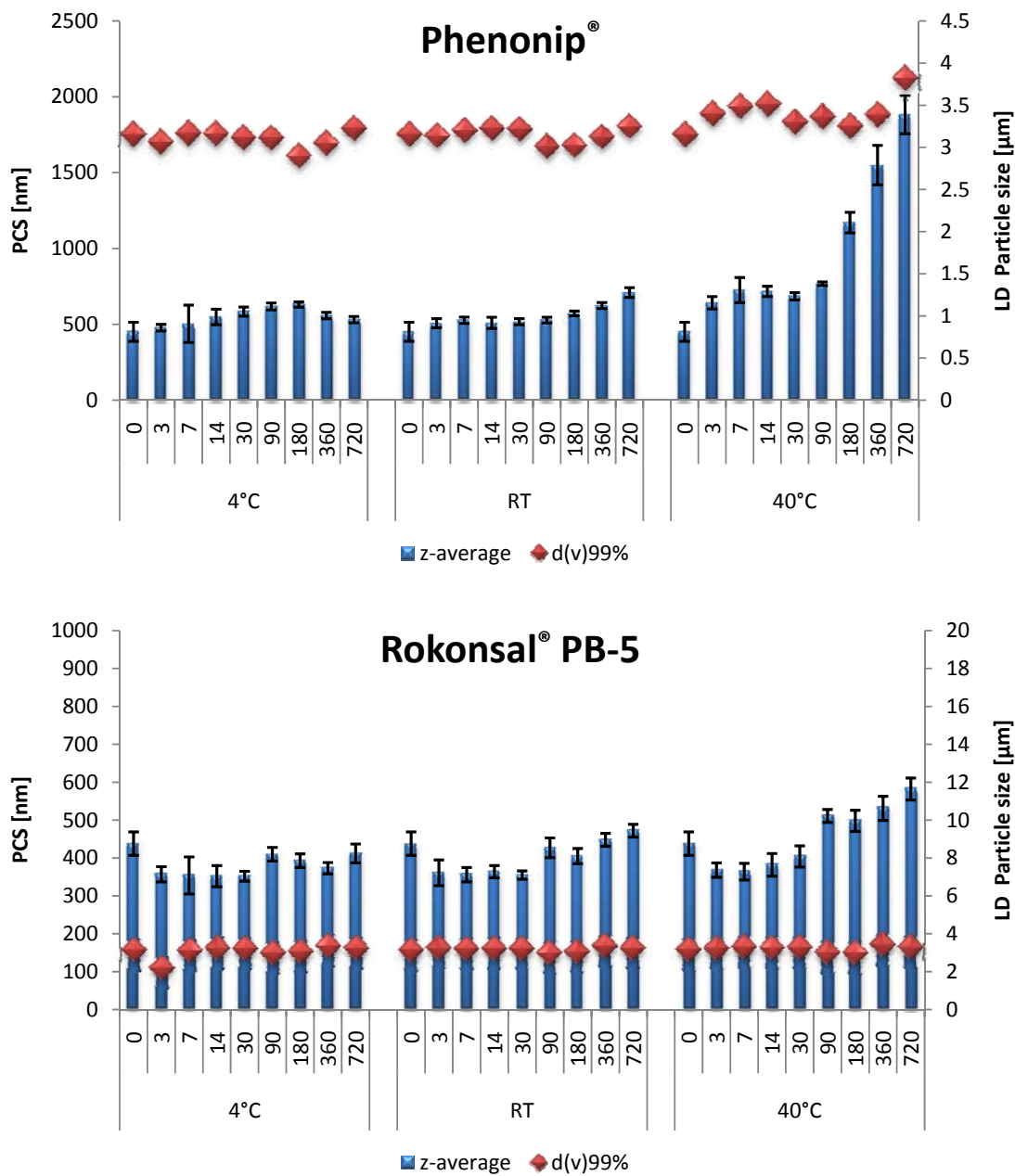


Fig. 56 Particle size of hesperetin nanosuspensions preserved with Hydrolite®-5 and multiEx naturotics stored at three different temperatures (4°C, RT & 40°C) as a function of time (days)



**Fig. 57** Light microscopy images of nanosuspensions preserved with: (C) Hydrolite<sup>®</sup>-5, (D) multiEx naturotics. (magnification 1000 fold, bar = 5 µm). The right side is directly after production and the right side is after 2 years storage at room temperature

PCS data of hesperetin preserved nanosuspensions with Phenonip<sup>®</sup> for samples stored at 4°C were almost stable till 2 years. Samples stored at RT showed a continuous increase in particle size after 6 months. Samples stored at 40°C showed a quite high growth in particle size compared to that of 4°C & RT samples, which indicates, besides being in stress conditions, that the parabens can cause more instability in 40°C than that of 4°C and RT. This could be due to the enhanced solubility of parabens in higher temperatures. However, LD data did not show large increase which can be due to lose aggregates (Fig. 58,59E).



**Fig. 58** Particle size of hesperetin nanosuspensions preserved with Phenonip® and Rokonsal® PB-5 stored at three different temperatures (4°C, RT & 40°C) as a function of time (days)

hesperetin nanosuspensions preserved with Rokonsal® PB-5 showed better stability profile than that of Phenonip® as previously explained, Cf. 4.1.8.2.1 (Fig. 58, 59F)

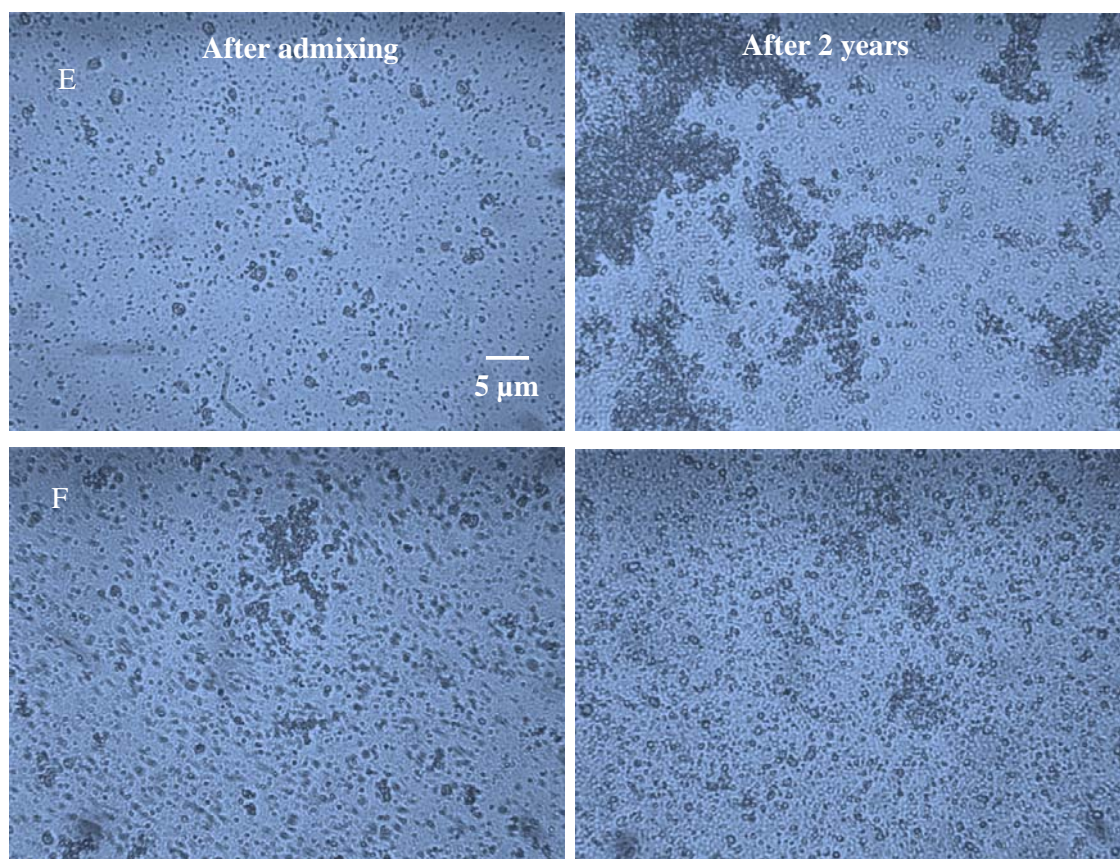
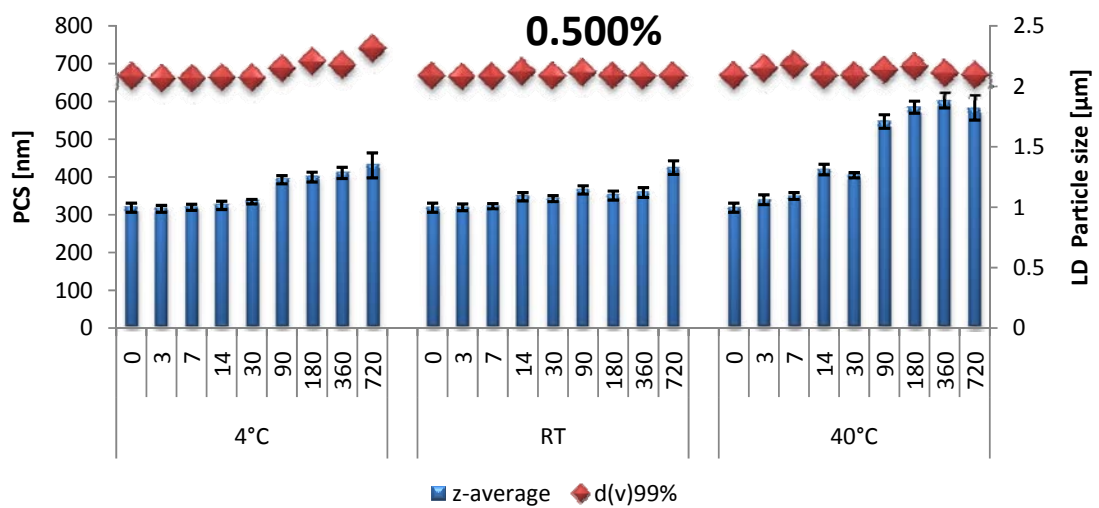
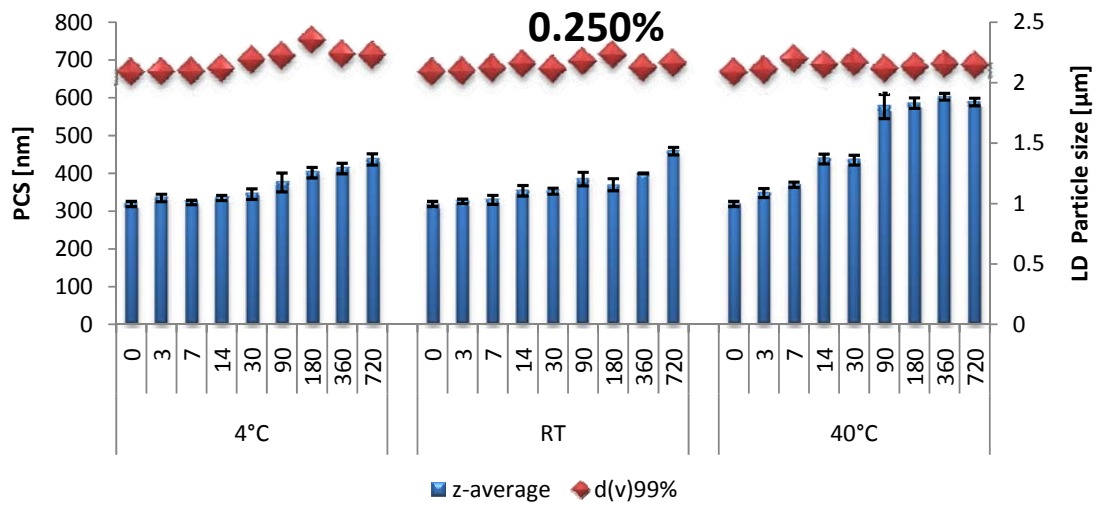
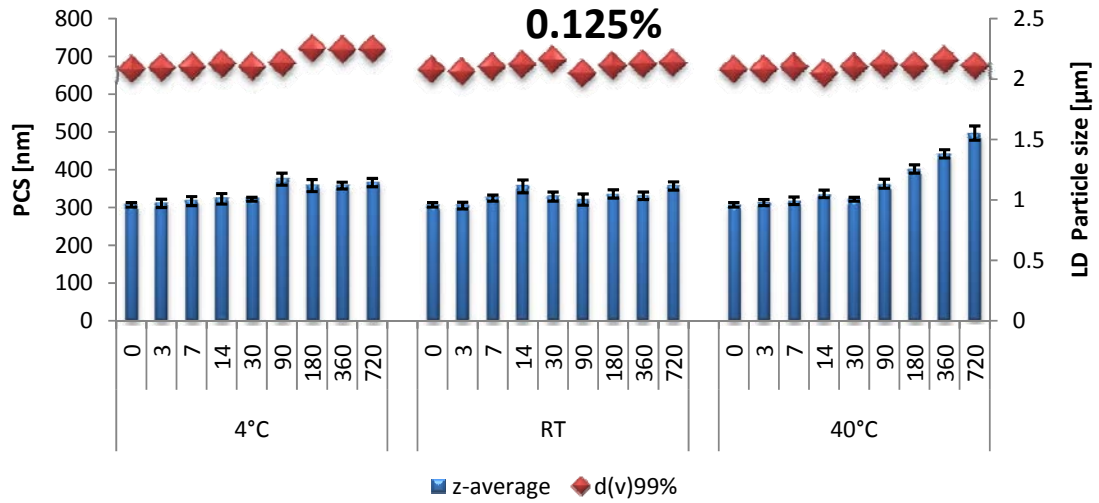


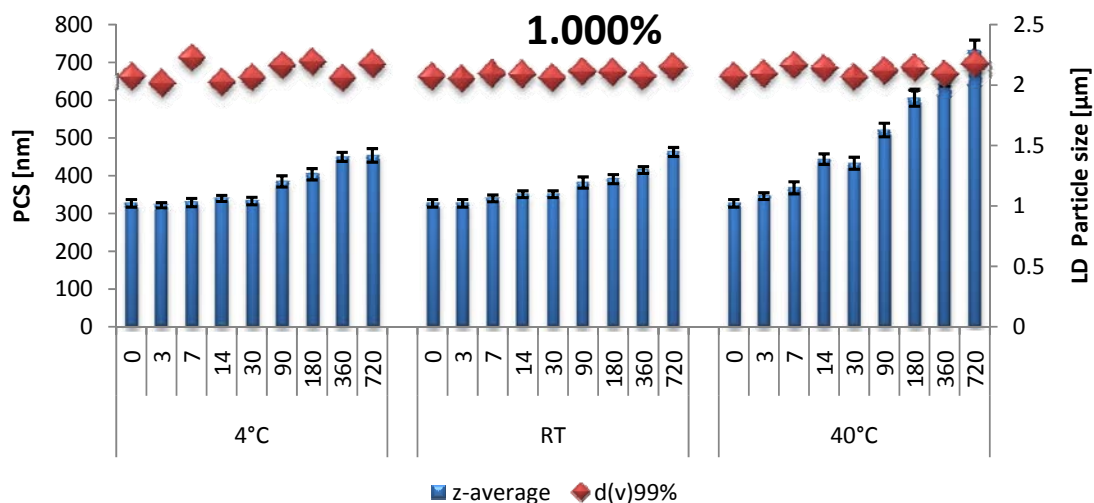
**Fig. 59** Light microscopy images of nanosuspensions preserved with: (E) Phenonip<sup>®</sup>, (F) Rokonsal<sup>®</sup> PB-5. (magnification 1000 fold, bar = 5  $\mu\text{m}$ ). The right side is directly after production and the right side is after 2 years storage at room temperature

#### ***4.1.8.3 Long term physical stability of hesperetin nanosuspensions in presence of antifoaming agent***

Adding high concentration of an antifoaming agent in this study was to investigate how the physical stability of the nanosuspension may be affected by its presence. Keeping in mind that normal usage concentration of an antifoaming agent can reach only up to 50 PPM (0.005% w/w). By comparing the four different concentrations of an antifoaming agent in the nanosuspension showed that there is no difference between using a concentration of 0.250% (w/w) or 1.000% (w/w). PCS data showed an increase in z-average from 300 nm directly after production up to 400 nm for both 4°C and RT samples (Fig. 60). These data correlate to the data obtained from the stability study of hesperetin nanosuspensions preserved with Hydrolite<sup>®</sup>-5 before homogenization (Blank, without antifoaming agent) Cf. 4.1.8.2.2. However, using a concentration of 0.125% (w/w) did not show an increase in z-average. As for LD data, it can be seen from Fig. 60 that the LD data remained unchanged all the storing period. The obtained results from the four concentration shows that the instability of the nanosuspension is not related to the concentration of the antifoaming agent.



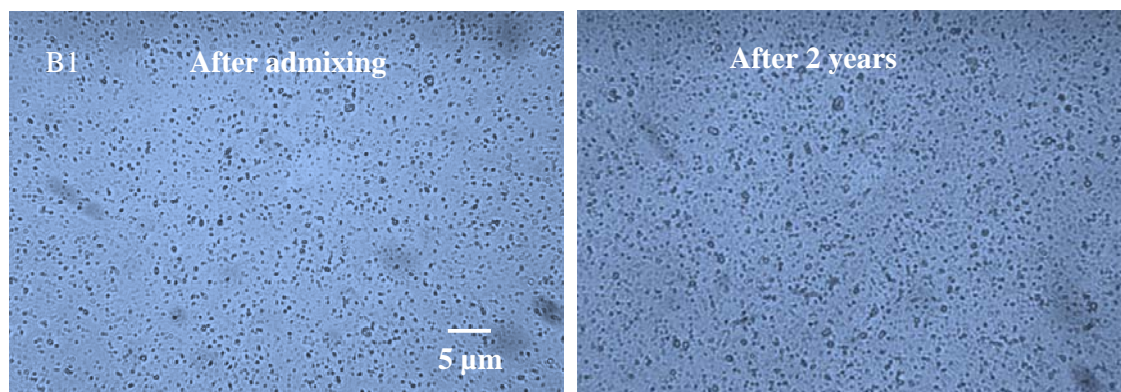




**Fig. 60** Particle size of hesperetin nanosuspensions preserved with hydrolite-5 with the addition of different concentration of antifoaming agent (Antifoam B Emulsion). 0.125% w/w, 0.250%, 0.500%, 1.000% stored at three different temperatures (4°C, RT & 40°C) as a function of time (days)

On the contrary, as seen in B1 (containing 0.125% Antifoam B Emulsion) sample a similar concentration can be obtained by adding sufficient quantity of the antifoaming agent without affecting the stability of the nanosuspension. Increasing the particle size for all batches at 40°C samples is due to a natural particle augmentation caused by the stress conditions. Hence, adding an antifoaming agent has more advantages in depressing foam formation, accordingly easier production with less product loss, than its disadvantage in possible increase of particle size even when used in unusual quantities.

By comparing the microscopic pictures for the produced nanocrystals directly after production and after two years storing period, it can be clearly seen that there were no apparent aggregates or large increase in the nanocrystals in the presence of an antifoaming agent (Fig. 61). This confirms the results obtained from PCS and LD, that adding an antifoaming agent may hinder the foam formation without affecting the particle size.



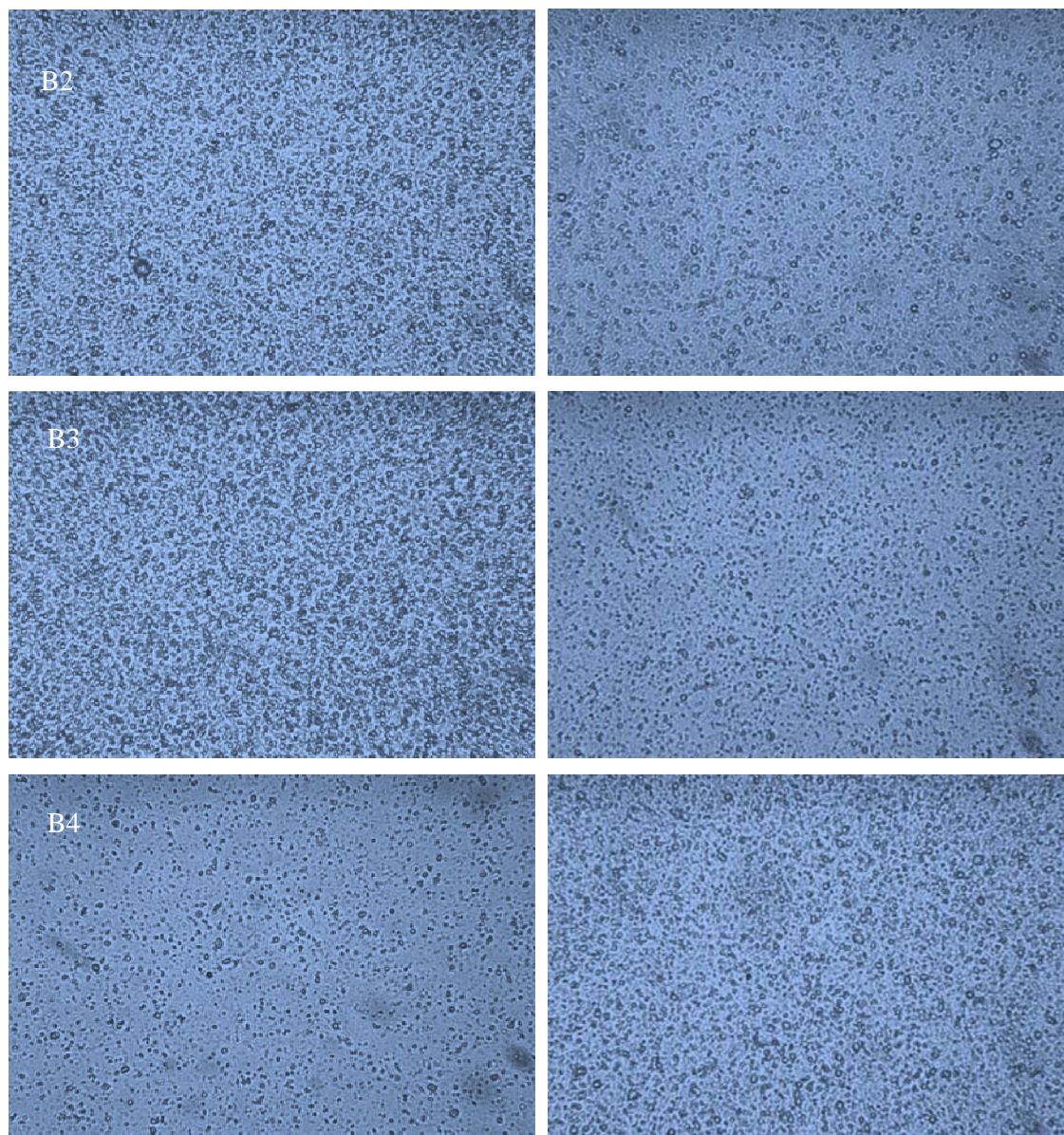


**Fig. 61** Light microscopy images of nanosuspensions preserved with Hydrolite<sup>®</sup>-5 with the addition of different concentration of antifoaming agent (Antifoam B Emulsion). B1 (0.125% w/w), B2 (0.250%), B3 (0.500%), B4 (1.000%) (magnification 1000 fold, bar = 5  $\mu$ m). The right side is directly after production and the right side is after 2 years storage at room temperature

#### ***4.1.8.4 Long term physical stability of hesperetin nanosuspensions incorporated in different gels***

As a next step for rendering the nanosuspensions in applicable dosage forms, the nanosuspensions were incorporated in gels for the aim of topical application.

Particle size distribution was measured after the prepared gels were admixed with water and left to swell further. The gels were investigated after the addition of the nanosuspension in one week and after one year.

Hesperetin nanosuspension incorporated in Tylose<sup>®</sup> 10000 and Tylose<sup>®</sup> 30000 gels tended to agglomerate after admixing and after storing the samples at RT for one year. As for hesperetin gels with CMCNa, the particle size distribution remained exactly the same like from the nanosuspension itself after one month and even after 1 year. On the other hand, measuring the mentioned gels in PCS showed an increase in z-average compared to the original nanosuspensions. Using Carbomer<sup>®</sup> derivatives such as Ultrez 10, Ultrez 20 or even Ultrez 21 had no effect on the particle size distribution for the whole period of storage (Table 12).

**Table 12 LD diameter for hesperetin nanosuspensions incorporated in different gels after 1 month and 1 year**

Gelling agent used	Size after 1 month [ $\mu\text{m}$ ]			Size after 1 year [ $\mu\text{m}$ ]		
	z-average	d(v)50%	d(v)99%	z-average	d(v)50%	d(v)99%
Tylose <sup>®</sup> 10000	1.938	11.232	511.186	3.271	28.548	400.442
Tylose <sup>®</sup> 30000	5.210	34.278	324.712	7.205	12.362	163.765
CMCNa	1.588	0.186	0.558	1.859	0.234	0.614
Ultrez 10	0.502	0.178	0.519	0.584	0.181	0.504
Ultrez 20	0.619	0.210	0.522	0.632	0.257	0.617
Ultrez 21	0.466	0.222	0.540	0.517	0.168	0.484

#### 4.1.8.5 Long term physical stability of scaled up nanosuspensions

##### a) Using avestin C50

Instability of hesperetin preserved nanosuspension with caprylyl glycol using Avestin C50 went as well in two phases as in LAB40 a declining phase at the beginning followed by an ascending phase Cf. 4.1.8.2 (Fig. 62). Fig. 63A shows the formation of small aggregates after two years storage.

Ethanol as a preservative did not affect the stability of hesperetin nanosuspension (Fig. 62). However, a slight decrease was noticed. This small phase can be seen in most of the formulations as the nanosuspensions tend to aggregate, to a small extent, directly after production due to the high energy given during production. The reduction in particle size stops normally after a period of 7 to 14 days after production. Slight increase in particle size was then detected in the last year of storage which can be explained by the increased solubility of hesperetin in water.

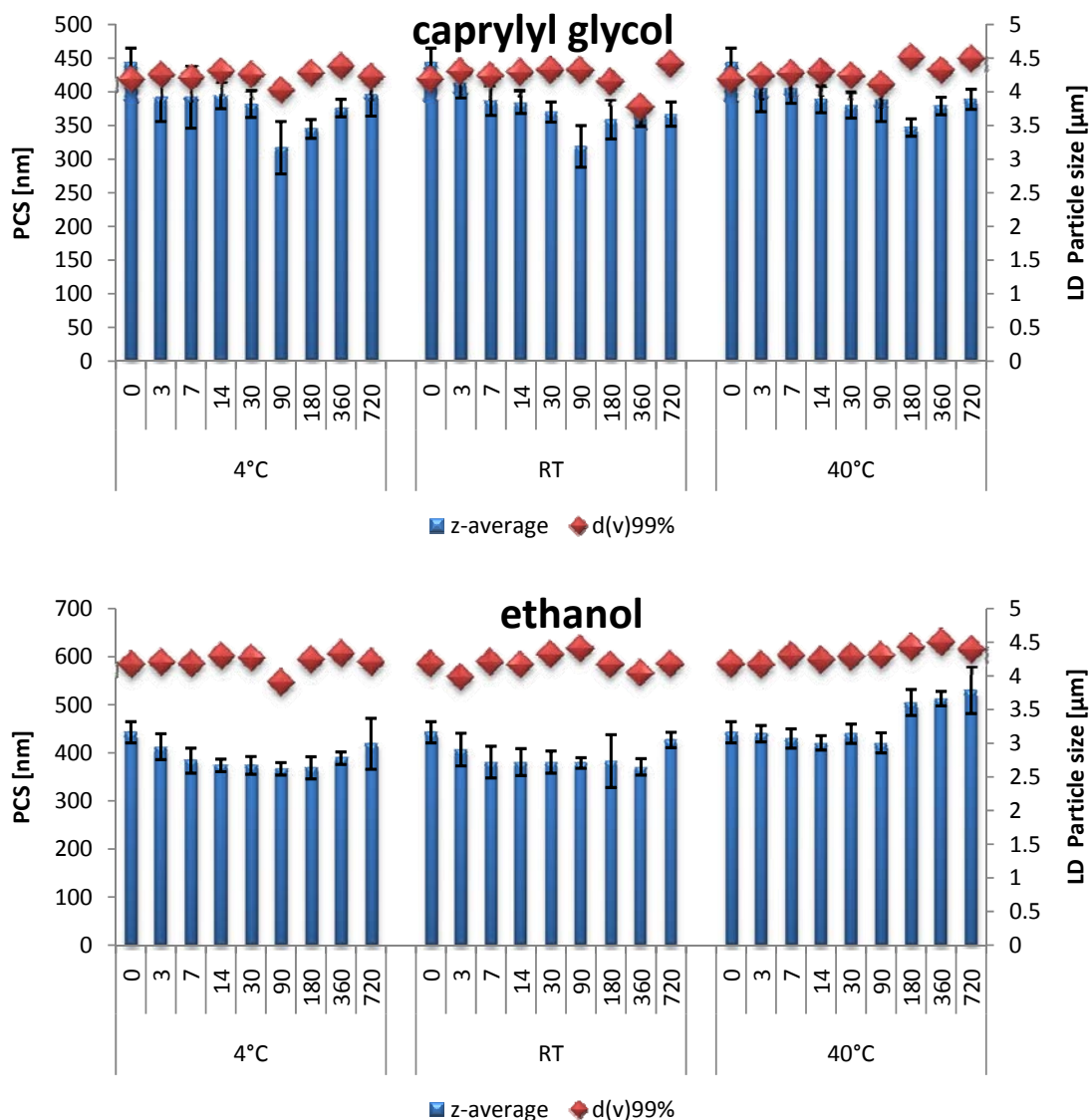


**Fig. 62** Particle size of hesperetin nanosuspensions preserved with caprylyl glycol and ethanol stored at three different temperatures (4°C, RT & 40°C) as a function of time (days)

Ethanol did not only serve as a preservative but also as a co-solvent [145]. This caused the small particles to dissolve, thus shifting the distribution to a larger mean particle size. Light microscopy did not show any formation of aggregates for the two years storing period (Fig. 63B).

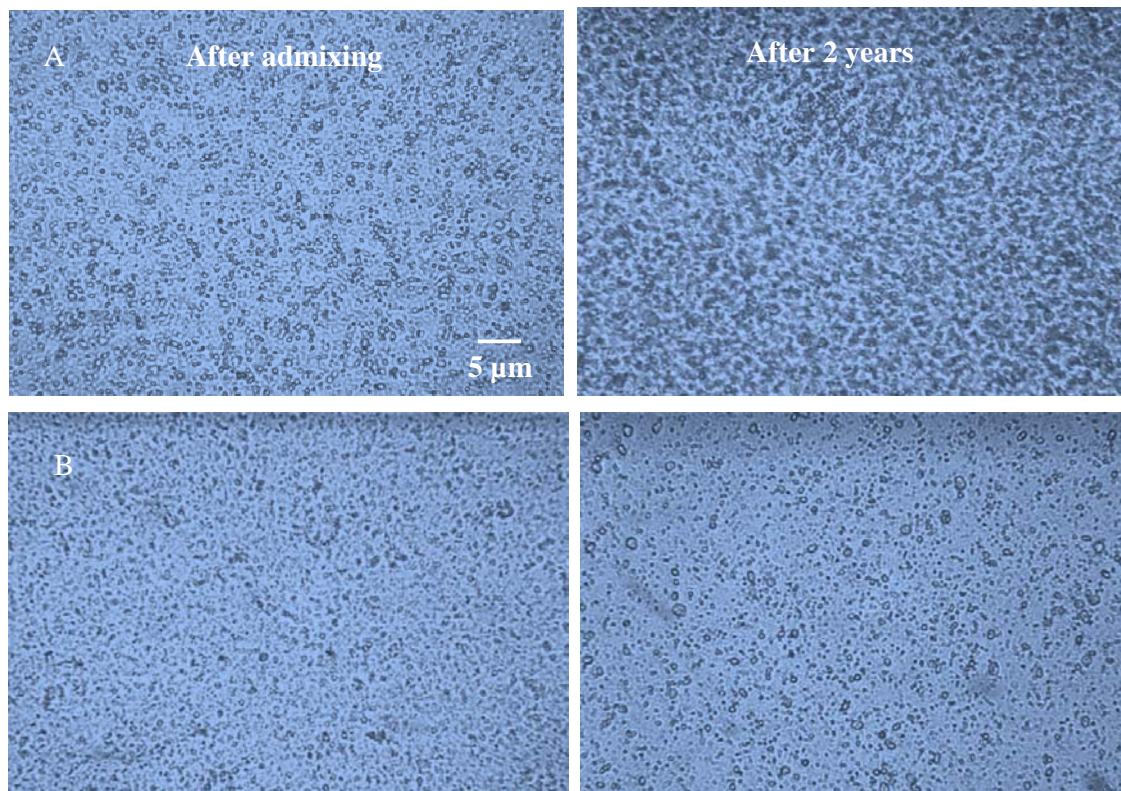


**Fig. 63** Light microscopy images of nanosuspensions preserved with: (A) caprylyl glycol, (B) ethanol (magnification 1000 fold, bar = 5  $\mu\text{m}$ ). The right side is directly after production and the right side is after 2 years storage at room temperature

Although using EUX700 & EUX702 shifts the pH of the nanosuspensions to 5.0 (preferably effective pH range), which may affect the stability of hesperetin nanosuspension, a trial was worth to be done to check the stability of the nanosuspension after the addition of these preservatives. EUX700 did not have a significant effect on the stability of the nanosuspension although the pH of the nanosuspension was shifted to around 5.0.

LD measurement expressed by  $d(v)99\%$  did not even show considerable change (Fig. 64). However, by investigating the nanosuspension using the microscope, agglomerates were found after two years storing period (Fig. 65C).

On the other hand, EUX702 did affect the mean particle size (PCS) and LD diameter by seeing fluctuation in z-average and  $d(v)99\%$  (Fig. 64). Oversized aggregates were detected in microscopic pictures for the hesperetin nanosuspensions preserved with EUX702 after admixing and after 2 years storage (Fig. 65D).

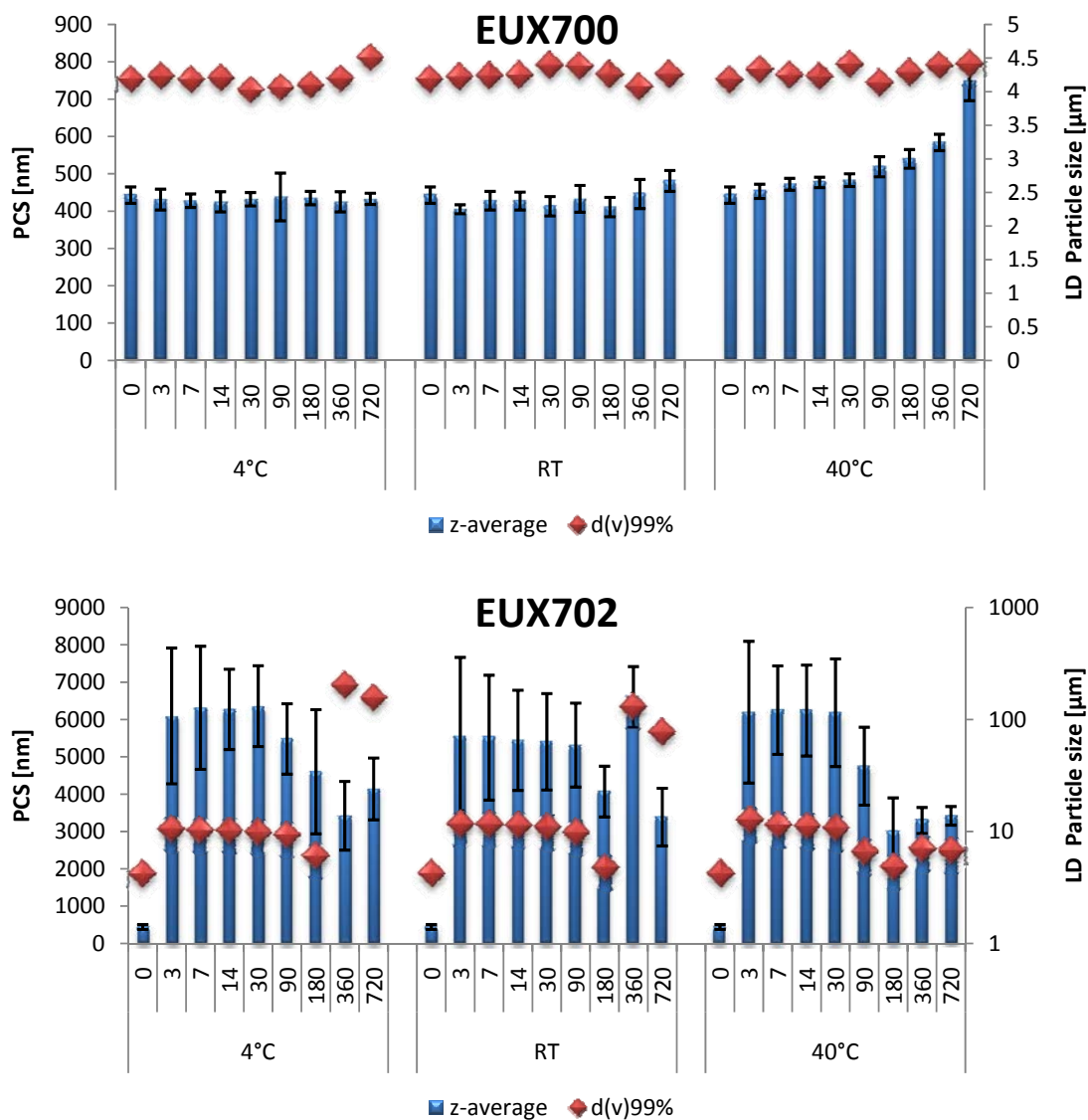


**Fig. 64** Particle size of hesperetin nanosuspensions preserved with EUX700= Euxyl® K700 and EUX702= Euxyl® K702 stored at three different temperatures (4°C, RT & 40°C) as a function of time (days)

This could be to the highly acidic content in EUX702 (e.g. benzoic acid and dehydroacetic acid), where these acidic compounds were substituted with alcohol derivatives in EUX700.

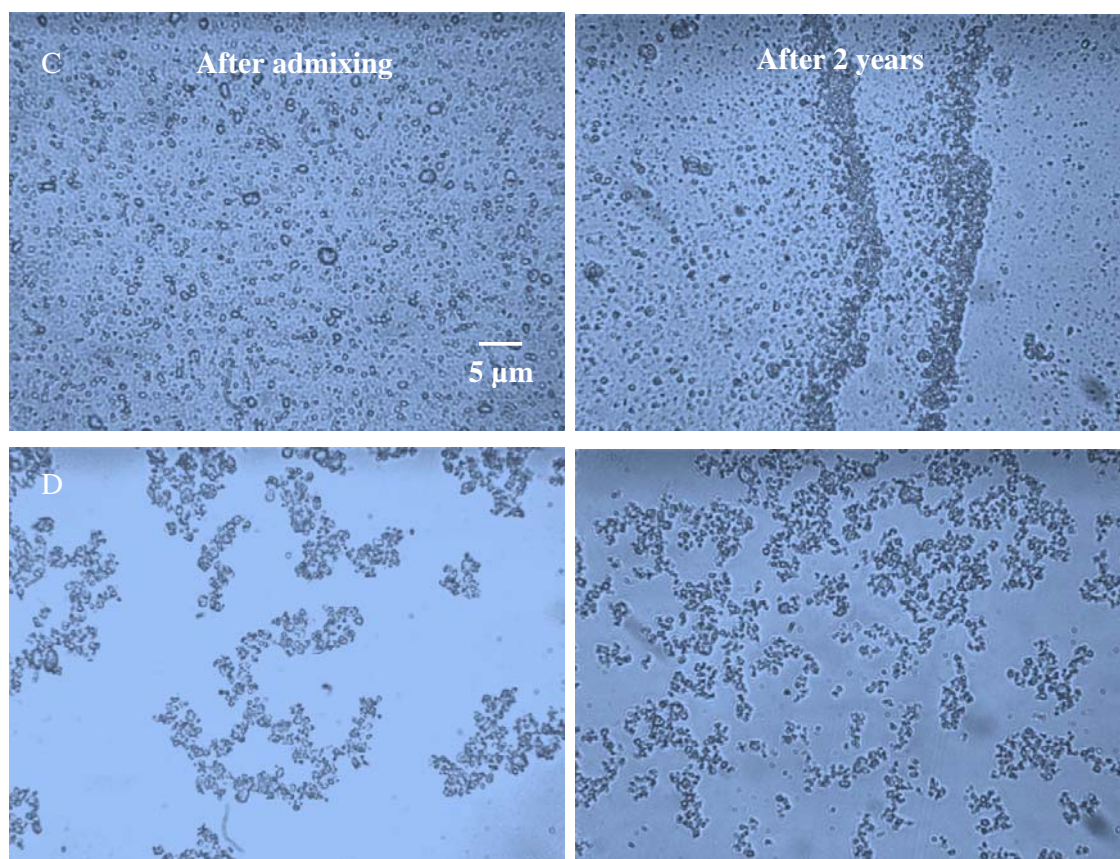


**Fig. 65** Light microscopy images of nanosuspensions preserved with: (C) EUX700= Euxyl® K700 and (D) EUX702= Euxyl® K702. (magnification 1000 fold, bar = 5 µm). The right side is directly after production and the right side is after 2 years storage at room temperature

EUX9010 samples at 4°C did not show any changes in z-average nor in  $d(v)99\%$ . 40°C sample showed increase in z-average after 180 days storage period without any increase in  $d(v)99\%$  (Fig. 66), which can be explained as loose aggregates that appear in the last year (Fig 67E).



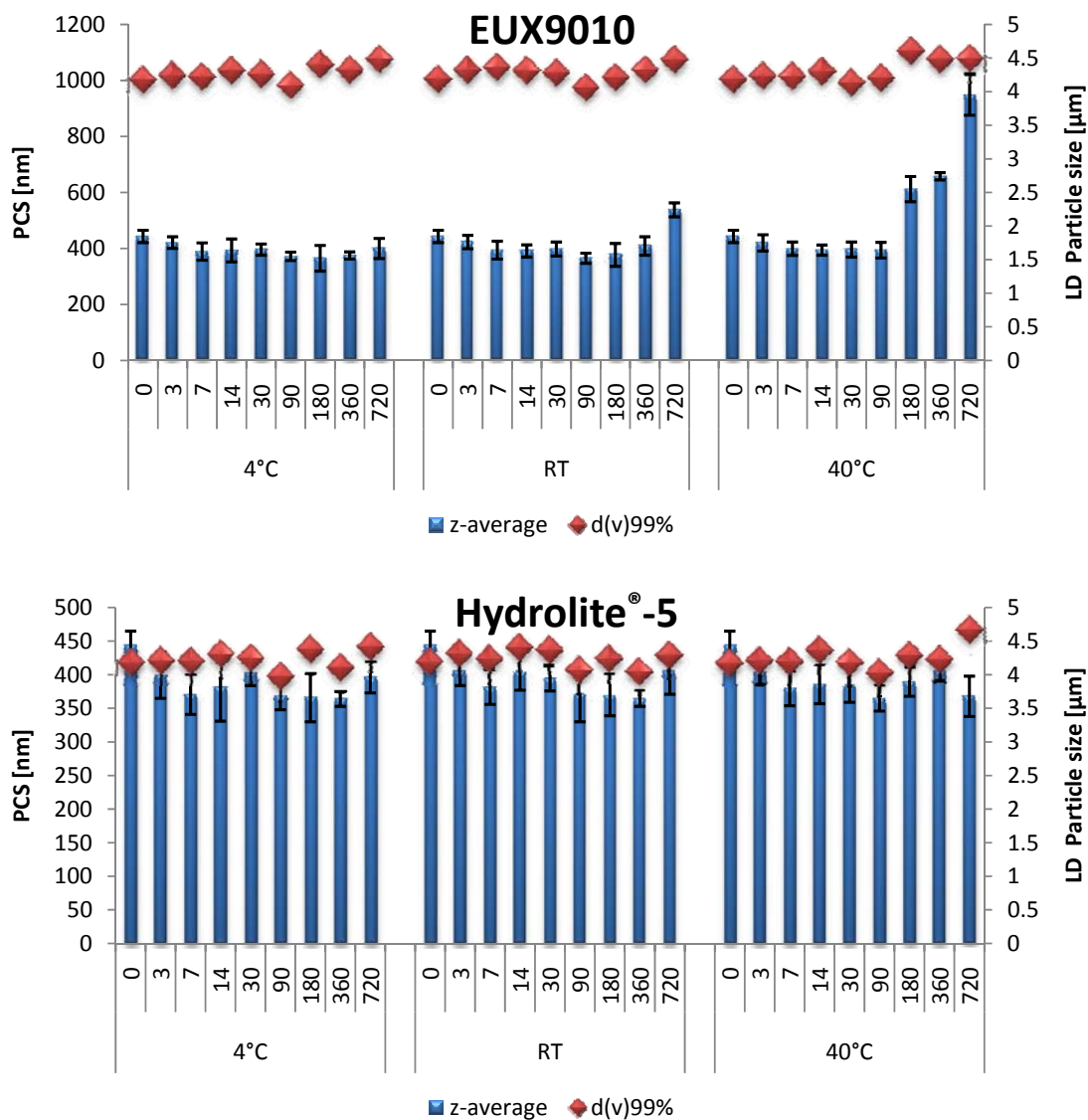
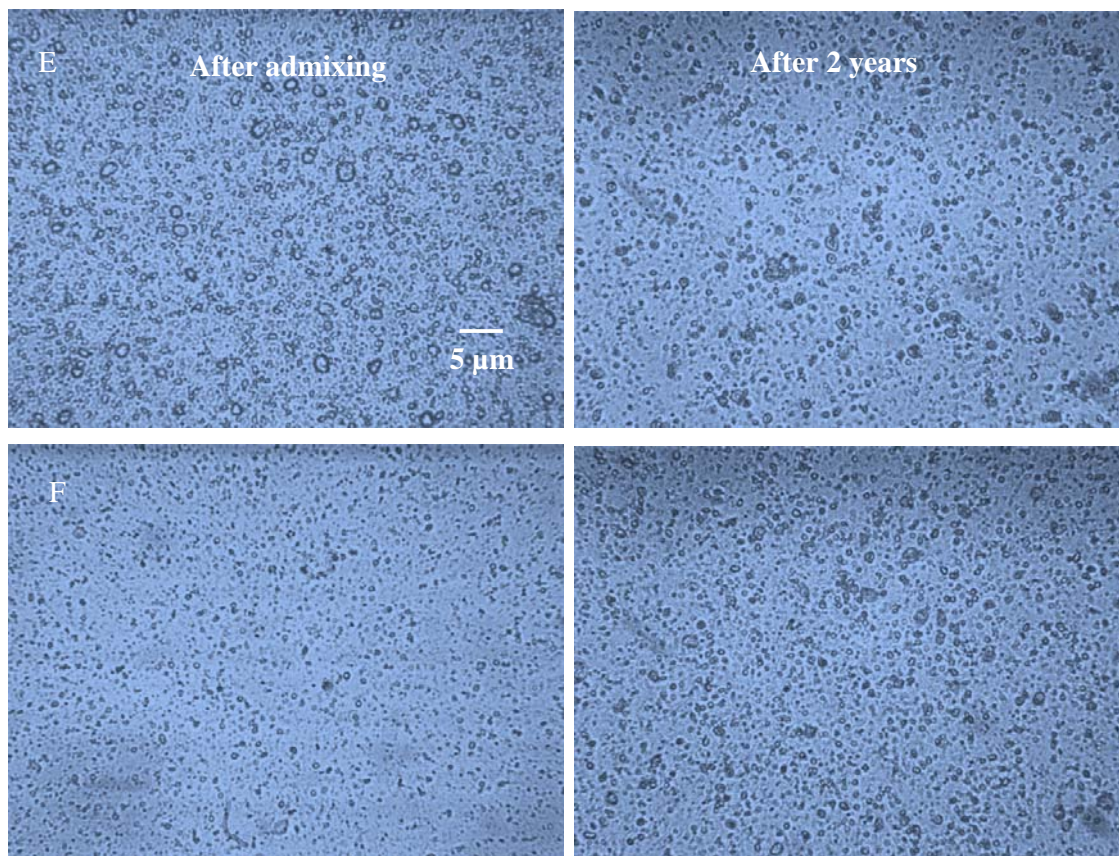


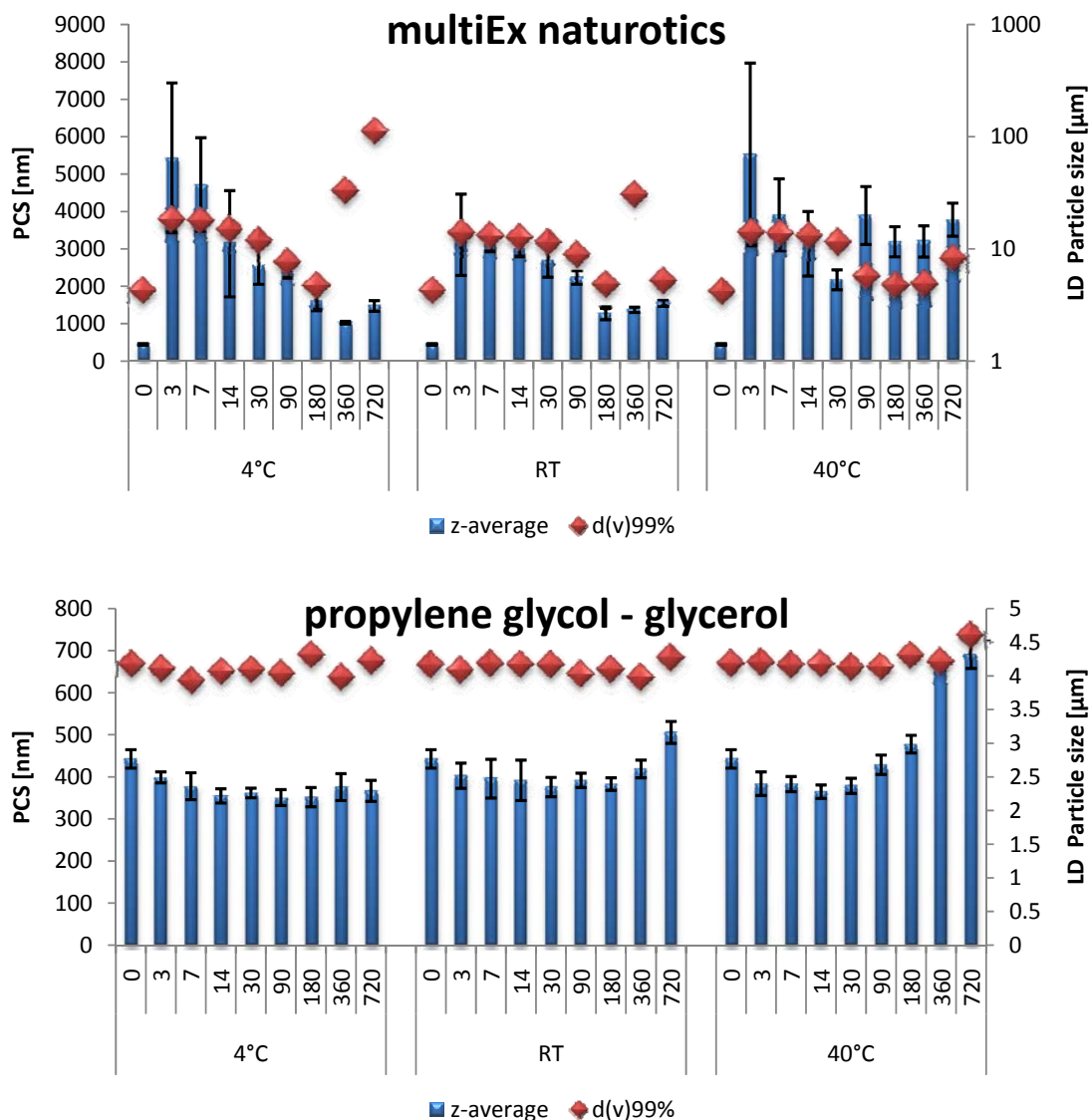
Fig. 66 Particle size of hesperetin nanosuspensions preserved with EUX9010= Euxyl® PE 9010 and Hydrolite®-5 stored at three different temperatures (4°C, RT & 40°C) as a function of time (days)

Hydrolite®-5, on the other hand, had almost a stable profile during the whole period of storage for both z-average and d(v)99% (Fig. 66). Microscopic pictures showed also no aggregates after 2 years of storage (Fig. 67F).



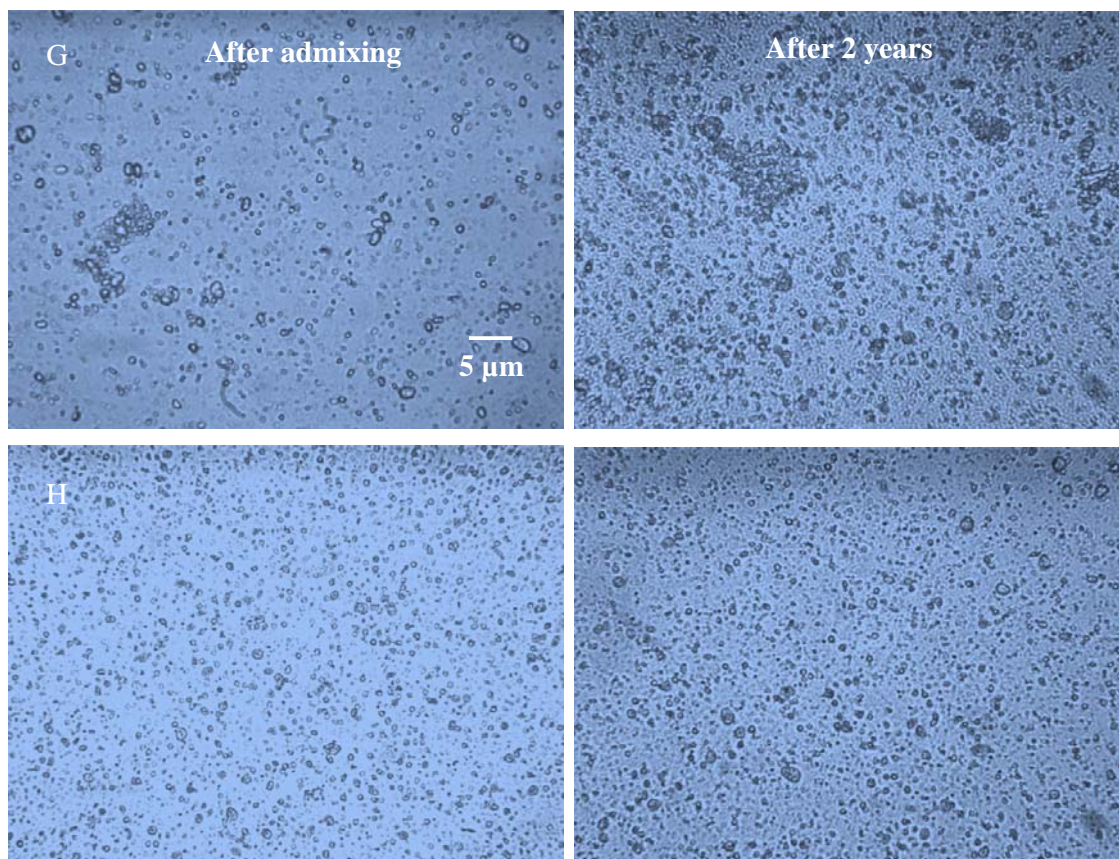
**Fig. 67** Light microscopy images of nanosuspensions preserved with: (E) EUX9010= Euxyl® PE 9010 and (F) Hydrolite® -5. (magnification 1000 fold, bar = 5  $\mu\text{m}$ ). The right side is directly after production and the right side is after 2 years storage at room temperature

Fig. 68 shows the z-average and  $d(v)99\%$  of hesperetin nanosuspensions preserved with multiEx naturotics. Apparently, multiEx naturotics affected the stability of the nanosuspension prepared with Avestin C50 even worse than it affected the one prepared with Micron LAB40, due to the diversity in particle size and ununiformity of particle size distribution. The possible solubilizing effect of multiEx naturotics, due to the abundant alcohol groups, can be seen with stropy declining phase of both PCS and LD data (Fig. 68). The increase in particle size afterwards for 360 days and 720 days at  $4^{\circ}\text{C}$  can be explained by recrystallization of dissolved hesperetin particles (Fig. 68). The microscopic pictures of hesperetin nanosuspensions preserved with multiEx naturotics can show the tendency to agglomerate after admixing and after 2 years storage (Fig. 69G).



**Fig. 68** Particle size of hesperetin nanosuspensions preserved with multiEx naturotics and propylene glycol - glycerol mixture (14% & 11%) stored at three different temperatures (4°C, RT & 40°C) as a function of time (days)

PG-GLY mixture showed a good stability profile for 4°C sample with a small continuous reduction in particle size during the first months due to the enhanced solubility in water [145]. However, in RT sample a small, and to a larger extent in 40°C sample, increase in particle size was detected in the last measurement which can be an indicator of possible recrystallization or beginning of aggregation (Fig. 68). The microscopic pictures showed some larger particles of hesperetin which confirms the results obtained from PCS and LD (Fig. 69H)



**Fig. 69** Light microscopy images of nanosuspensions preserved with: (G) multiEx naturotics and (H) propylene glycol - glycerol mixture (14% & 11%). (magnification 1000 fold, bar = 5  $\mu\text{m}$ ). The right side is directly after production and the right side is after 2 years storage at room temperature

PCS data for PG samples showed no significant changes for z-average. The slight decrease in particle size is a normal behavior after production. LD data did not change significantly during storage period (Fig. 70). Microscopic pictures showed no formation of aggregates after 2 years storage confirming PCS and LD results (Fig. 71I).

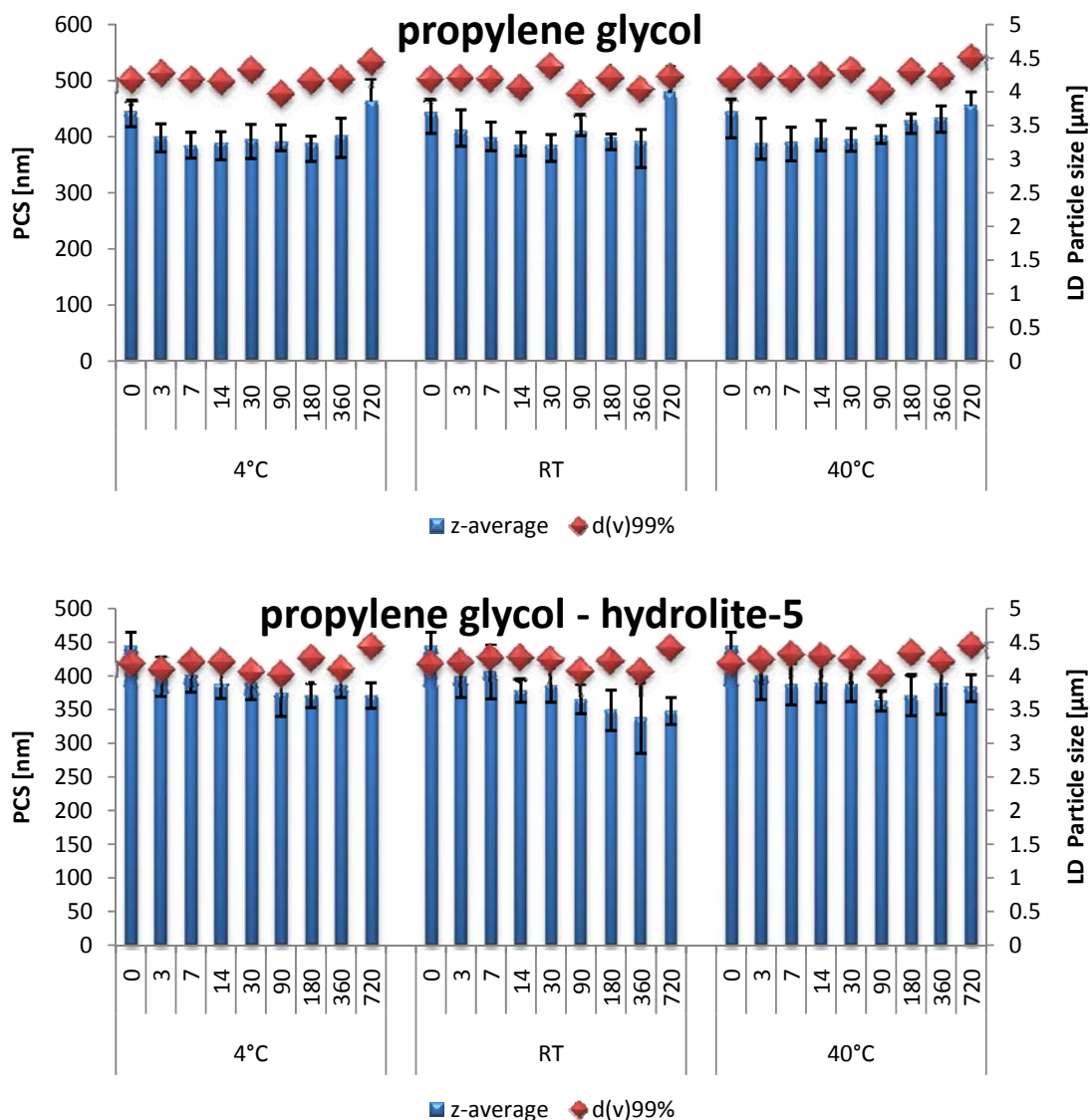


**Fig. 70** Particle size of hesperetin nanosuspensions preserved with PG (G) and PG-Hydrolite<sup>®</sup>-5 (5% & 3%) (H) stored at three different temperatures (4°C, RT & 40°C) as a function of time (days)

Propylene glycol – Hydrolite<sup>®</sup>-5 mixture had a decreasing profile for z-average during the whole period of storage for all temperature followed by stable readings. LD data had stable profile through storing period confirming the data obtained from PCS (Fig. 70). Microscopic pictures proved the PCS and LD data showing no aggregations or particle growth after 2 years storage (Fig. 71J).

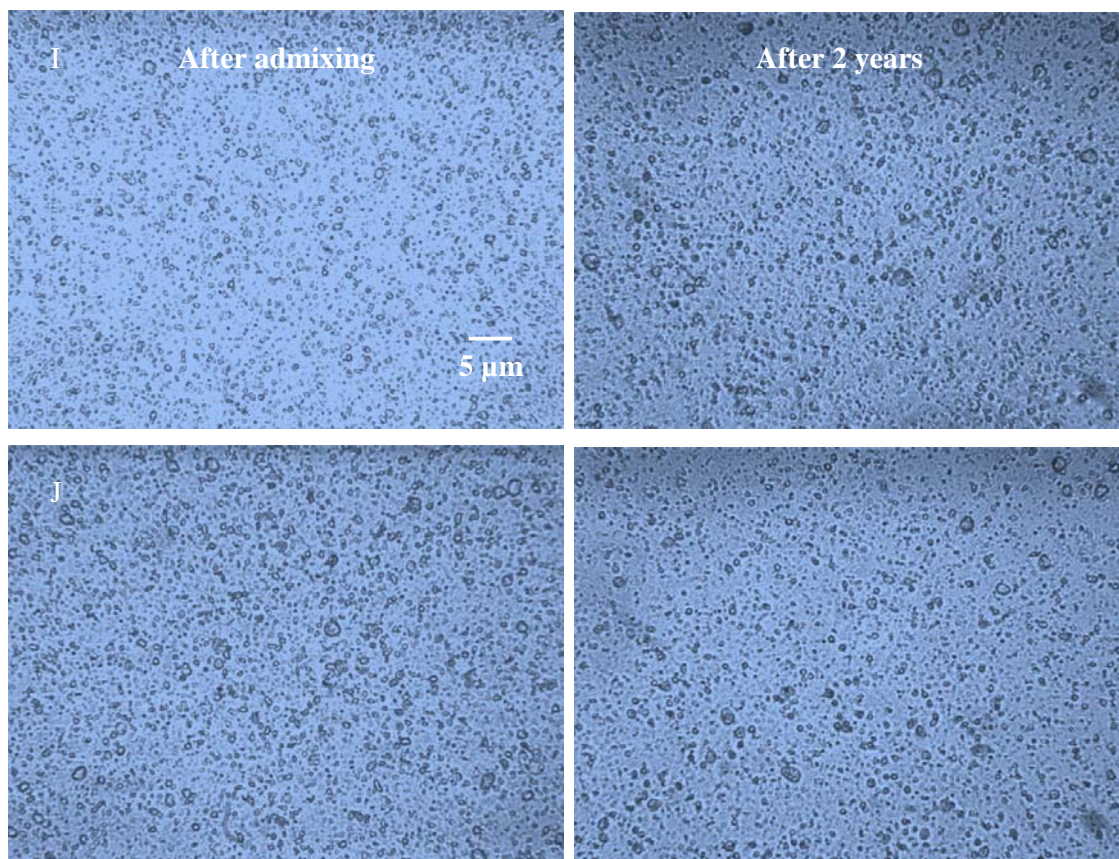


**Fig. 71** Light microscopy images of nanosuspensions preserved with: (I) propylene glycol, (H) propylene glycol – Hydrolite®-5 mixture (5% & 3%). (magnification 1000 fold, bar = 5  $\mu\text{m}$ ). The right side is directly after production and the right side is after 2 years storage at room temperature

Phenonip® did not have a huge destabilizing effect as it was seen in hesperetin nanosuspensions produced using Micron LAB40. This could be largely due to the insufficient reduction of particle size from Avestin C50. However, in 40°C sample gradual increase in z-average was observed reaching around 2,500 nm and 100  $\mu\text{m}$  for PCS and d(v)99%, respectively (Fig. 72). This increase in particle size was confirmed as large agglomerates by investigation under microscope (Fig. 73K).

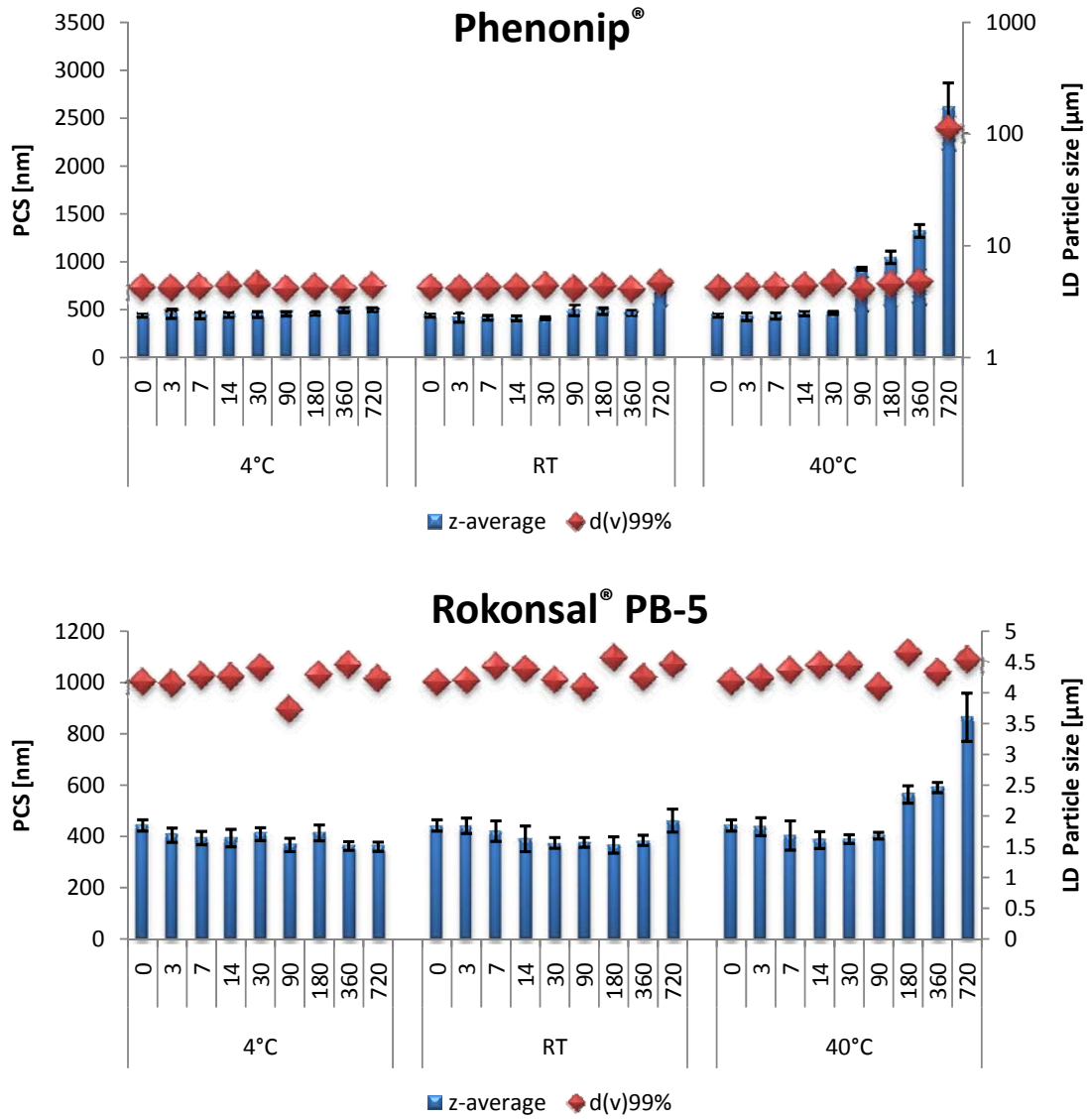
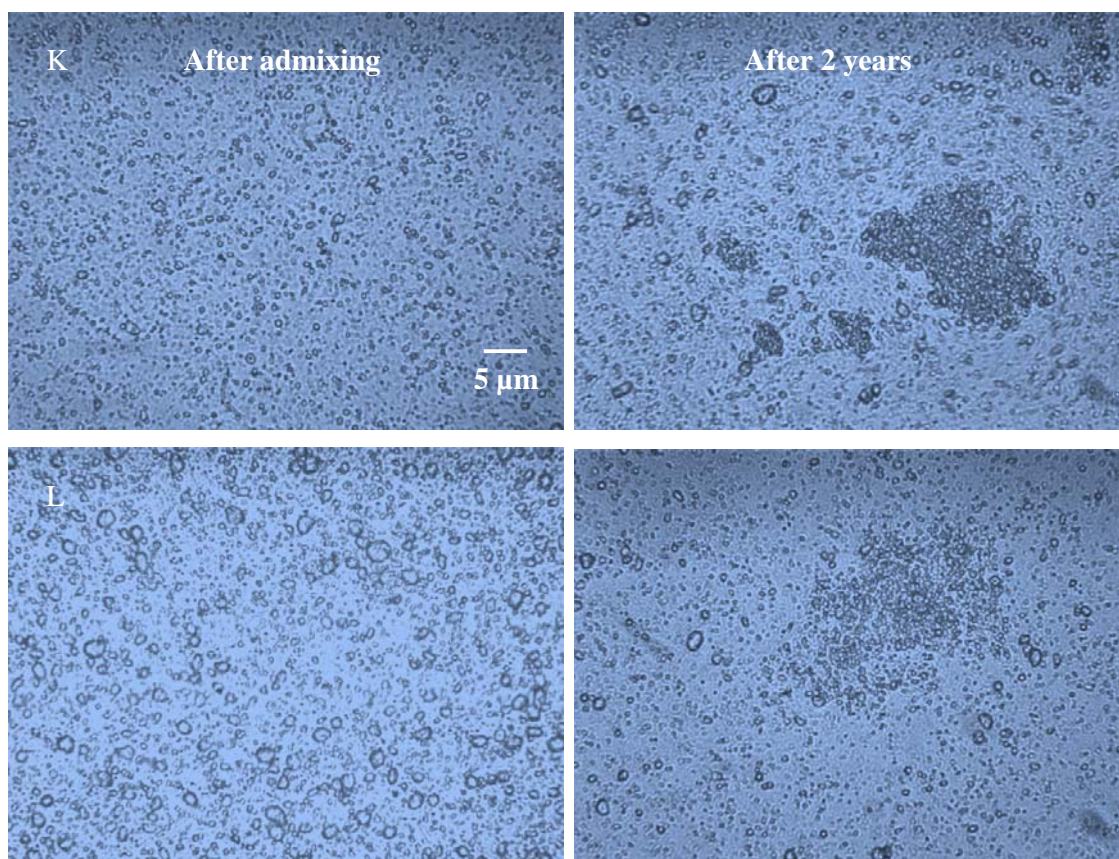


Fig. 72 Particle size of hesperetin nanosuspensions preserved with Phenonip® and Rokonsal® PB-5 stored at three different temperatures (4°C, RT & 40°C) as a function of time (days)

Rokonsal® PB-5 had the same destabilizing effect as of Phenonip® (as predicted) but to a lesser extent (Fig. 72, 73L).



**Fig. 73** Light microscopy images of nanosuspensions preserved with: Phenonip® and Rokonsal® PB-5. (magnification 1000 fold, bar = 5 μm). The right side is directly after production and the right side is after 2 years storage at room temperature

#### b) SmartCrystal®

SmartCrystals® may act differently in the presence of preservatives than other nanosuspensions. This could be due to the small particle size obtained without giving a high amount of energy as in the case of Micron LAB40 or Avestin C50.

Caprylyl glycol preserved smartCrystals® behaved in three different ways depending on the temperature of storage. The sample stored at 4°C was almost stable during the entire period of storage with little fluctuation that can be caused by some loose aggregates. No big changes were detected in LD data. RT sample behaved differently with two distinctive phases, a declined and an ascending phase, Cf. 4.1.8.2. On the other hand, 40°C samples undergo a continuous augmentation in particle size (z-average), which is highly due to aggregates. These aggregates tend to be loose as the LD data showed no significant increase in LD diameter expressed as  $d(v)99\%$  (Fig. 74). Light microscopy showed the oversized agglomerations in hesperetin smartCrystals® preserved with caprylyl glycol after 2 years storage (Fig. 75A).



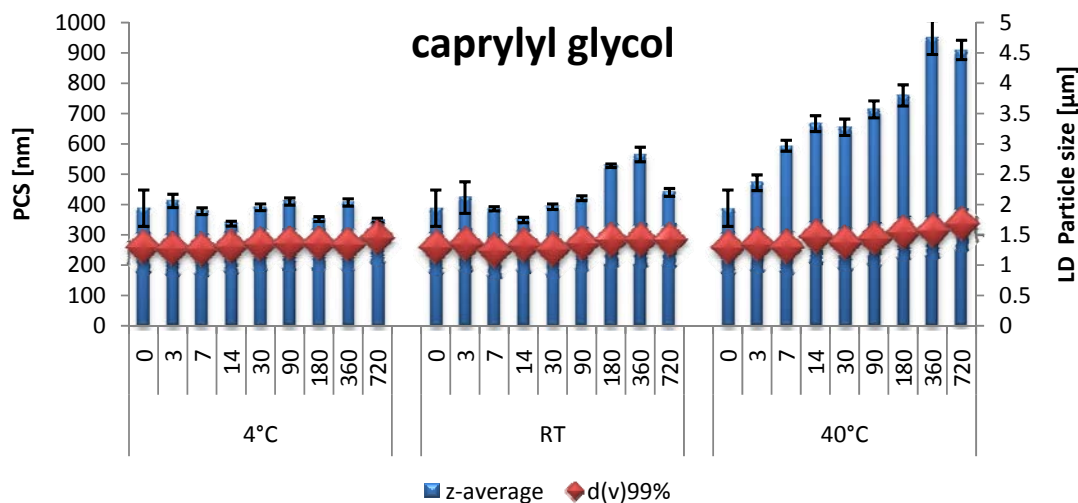


Fig. 74 Particle size of hesperetin nanosuspensions preserved with caprylyl glycol stored at three different temperatures (4°C, RT & 40°C) as a function of time (days)

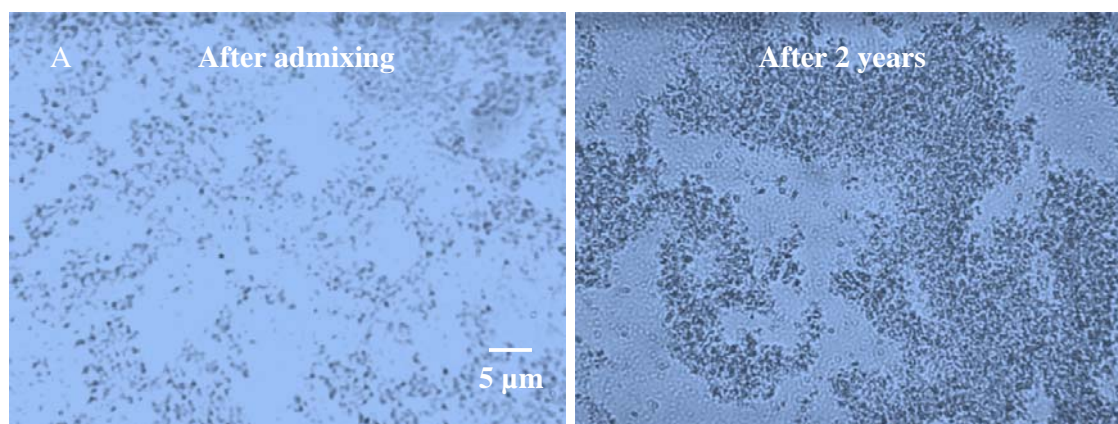


Fig. 75 Light microscopy images of nanosuspensions preserved with (A) caprylyl glycol (magnification 1000 fold, bar = 5 μm). The right side is directly after production and the right side is after 2 years storage at room temperature

CPC, ethanol and Euxyl® PE 9010 did not show any significant changes in the PCS data (z-average) nor in LD results d(v)99% which confirms that these preservatives did not have any effect on the physical stability of the particles (Fig. 76).

The small changes that were observed for the preserved nanosuspensions produced with Avestin C50 were mostly due to the high energy input for the particles.

No aggregates were detected in the three formulations by investigation them under light microscope (Fig. 77).

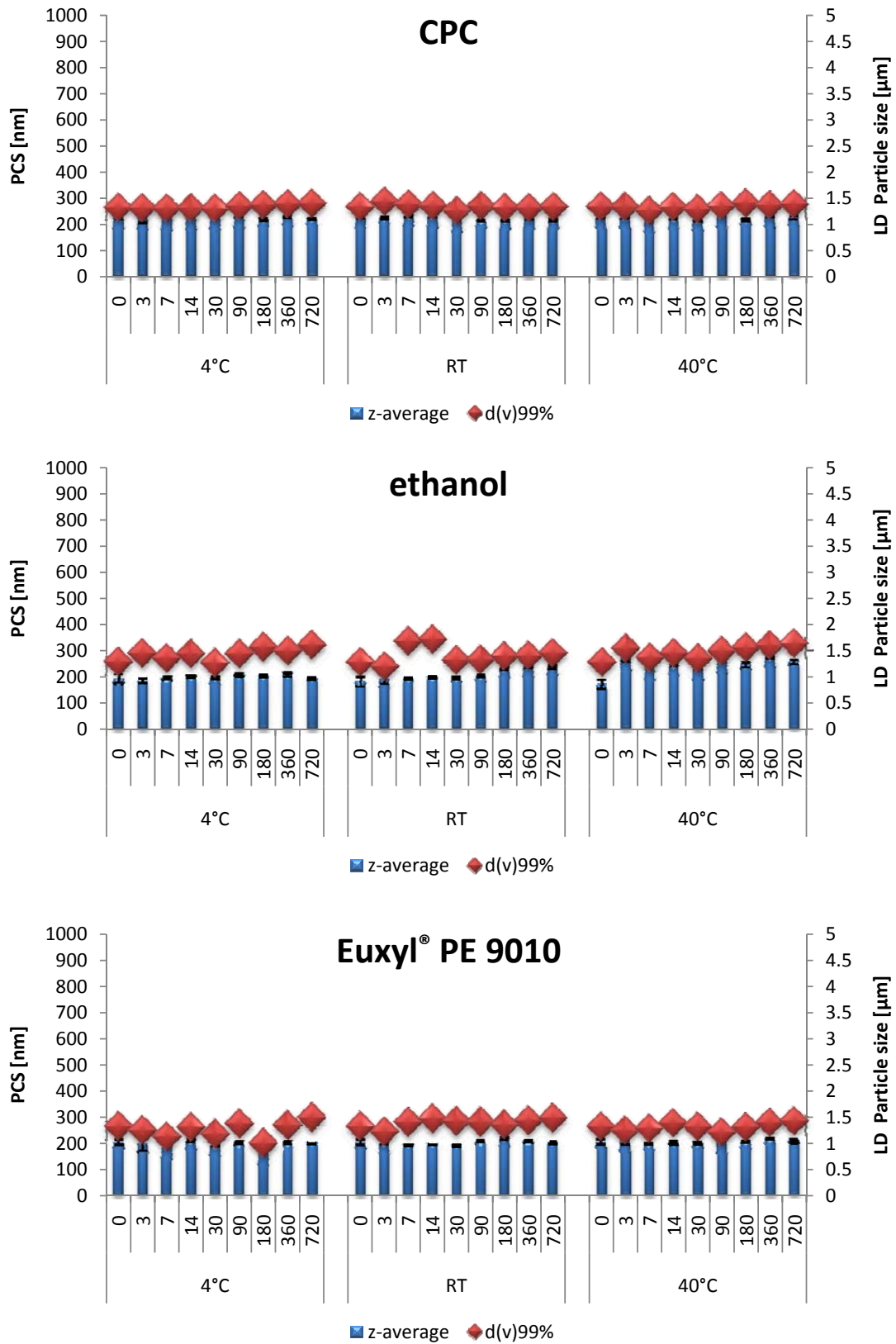
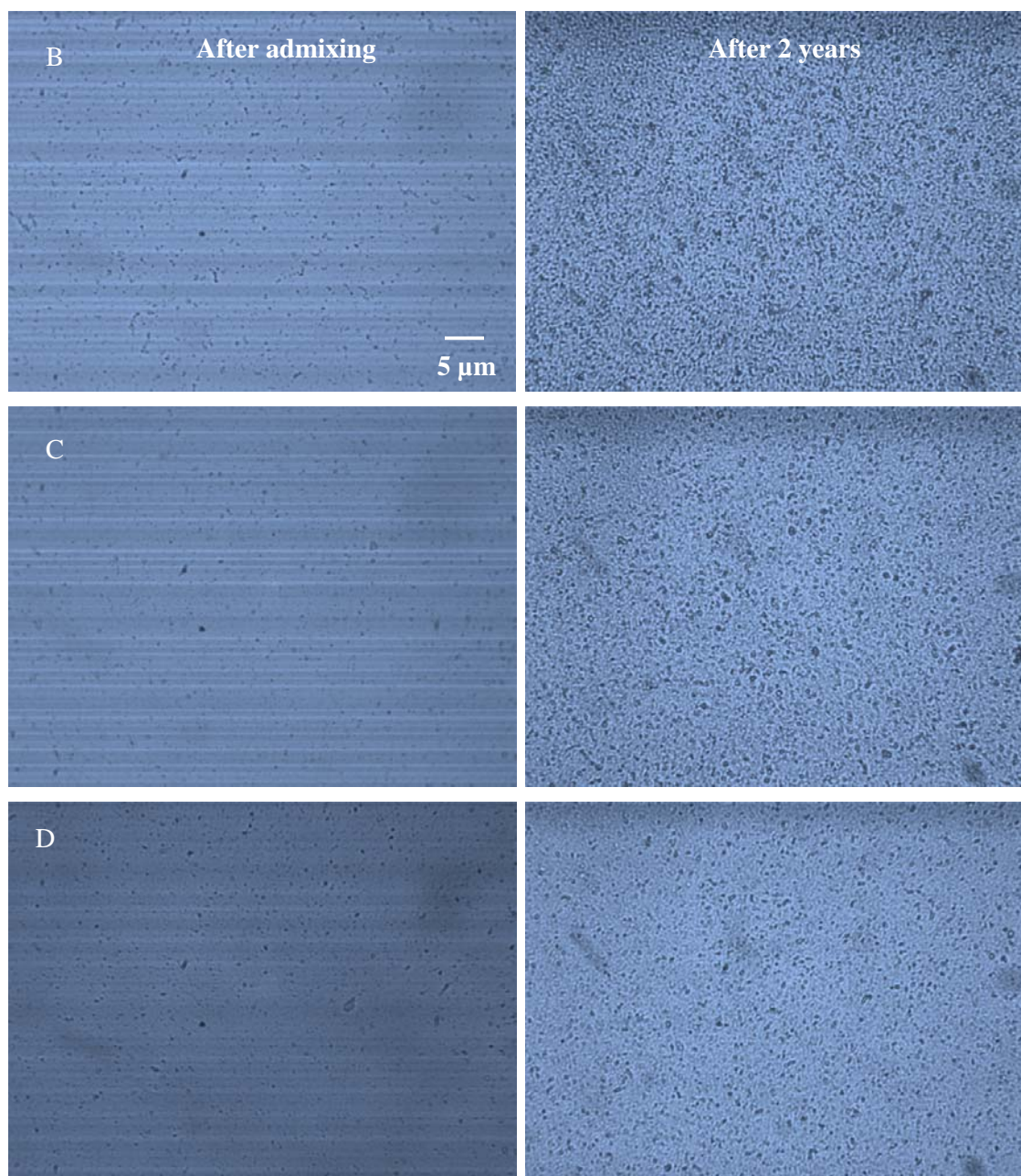


Fig. 76 Particle size of hesperetin nanosuspensions preserved with CPC= cetylpyridinium chloride, ethanol and EUX9010= Euxyl® PE 9010 stored at three different temperatures (4°C, RT & 40°C) as a function of time (days)



**Fig. 77** Light microscopy images of nanosuspensions preserved with: (B) CPC= cetylpyridinium chloride, (C) ethanol and (D) EUX9010= Euxyl® PE 9010. (magnification 1000 fold, bar = 5  $\mu\text{m}$ ). The right side is directly after production and the right side is after 2 years storage at room temperature

Hesperetin smartCrystals® preserved with glycerol 20% and glycerol 50% had 2 different stability profiles. Glycerol 20% did not affect the physical stability for the sample in 4°C, but an increase in z-average was seen in both RT and 40°C samples. LD data did not show any increase in  $d(v)_{99\%}$  which indicate loose agglomerates (Fig. 78).

Glycerol 50% had more destabilizing effect on the nanosuspensions (Fig. 78). This indicates that the destabilizing effect is related directly to the concentration of the glycerol used in the formulation. Even a huge increase can be seen in z-average for the 40°C sample, but no large increase in LD data was detected.

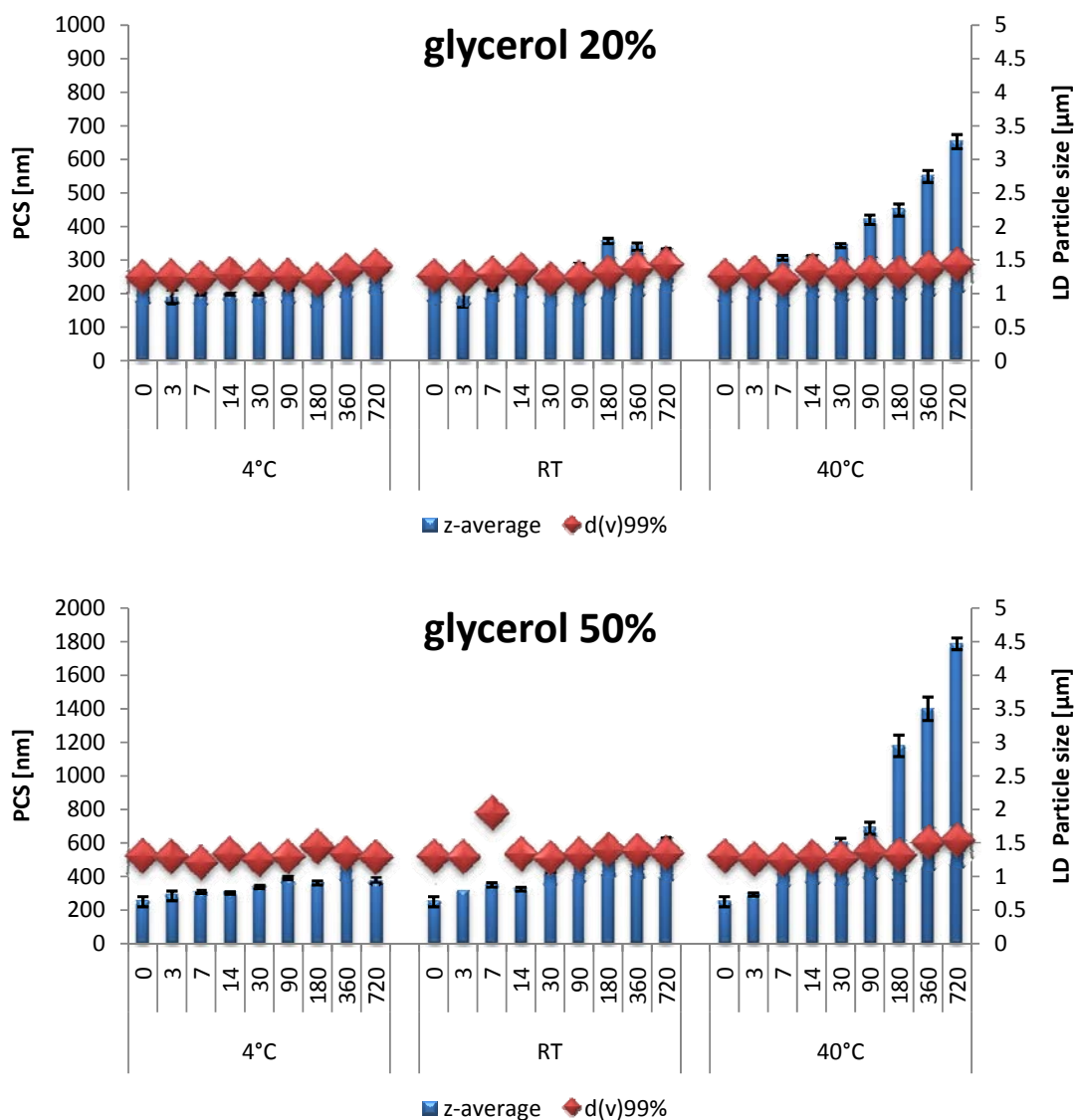


**Fig. 78** Particle size of hesperetin nanosuspensions preserved with glycerol 20% and glycerol 50% stored at three different temperatures (4°C, RT & 40°C) as a function of time (days)

Oversized agglomerates were detected using microscope by comparing hesperetin smartCrystals<sup>®</sup> preserved with glycerol 50% with the one preserved with glycerol 20% (Fig. 79).

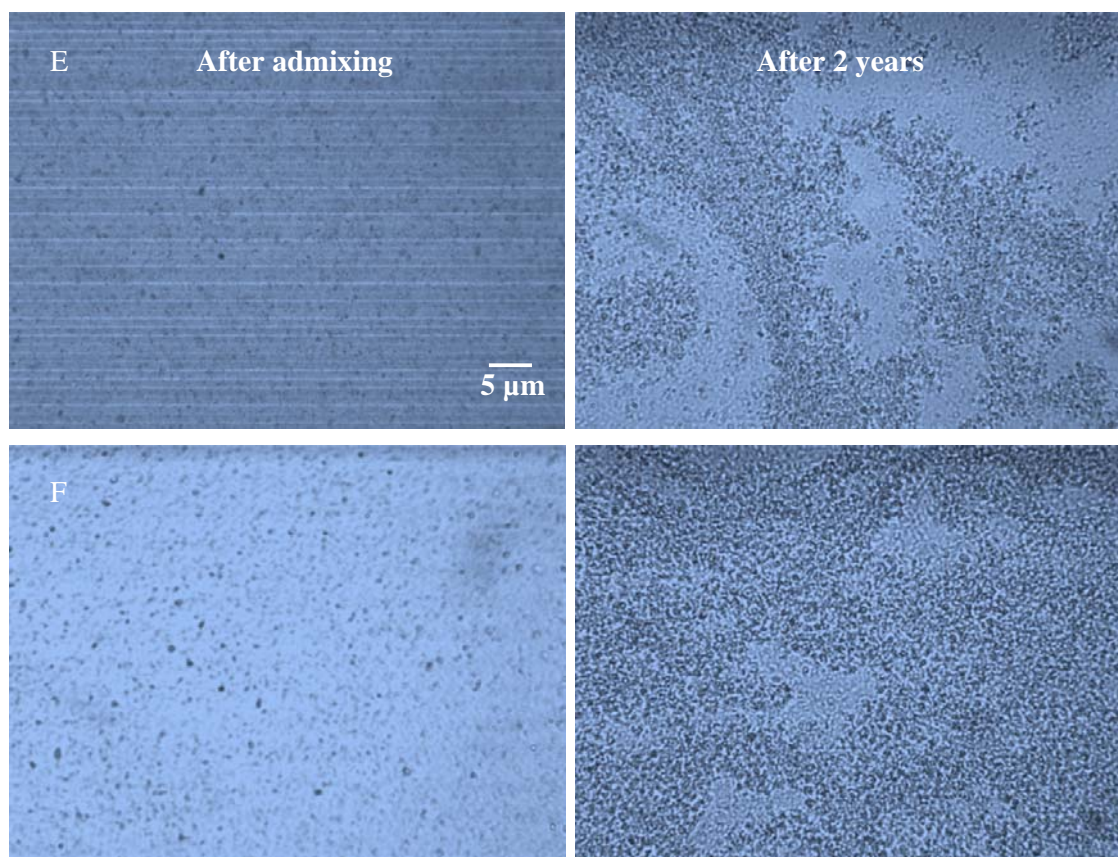


**Fig. 79** Light microscopy images of nanosuspensions preserved with: (E) glycerol 20% and (F) glycerol 50% (magnification 1000 fold, bar = 5  $\mu\text{m}$ ). The right side is directly after production and the right side is after 2 years storage at 40°C

As expected, Hydrolite<sup>®</sup>-5 did not affect the physical stability of the nanosuspension over the time as it can be seen from the z-average and LD diameter (Fig. 80). In addition, no agglomerates were detected with microscopic investigation (Fig. 81G)

MultiEx naturotics had a quite fast destabilizing effect on the nanosuspensions. This stabilizing effect was presented as a solubilizing impact in the hesperetin nanosuspensions. An increase in  $d(v)_{99\%}$  for 40°C samples which indicates a start of recrystallization of the dissolved small particles on the bigger crystals (Fig. 80).

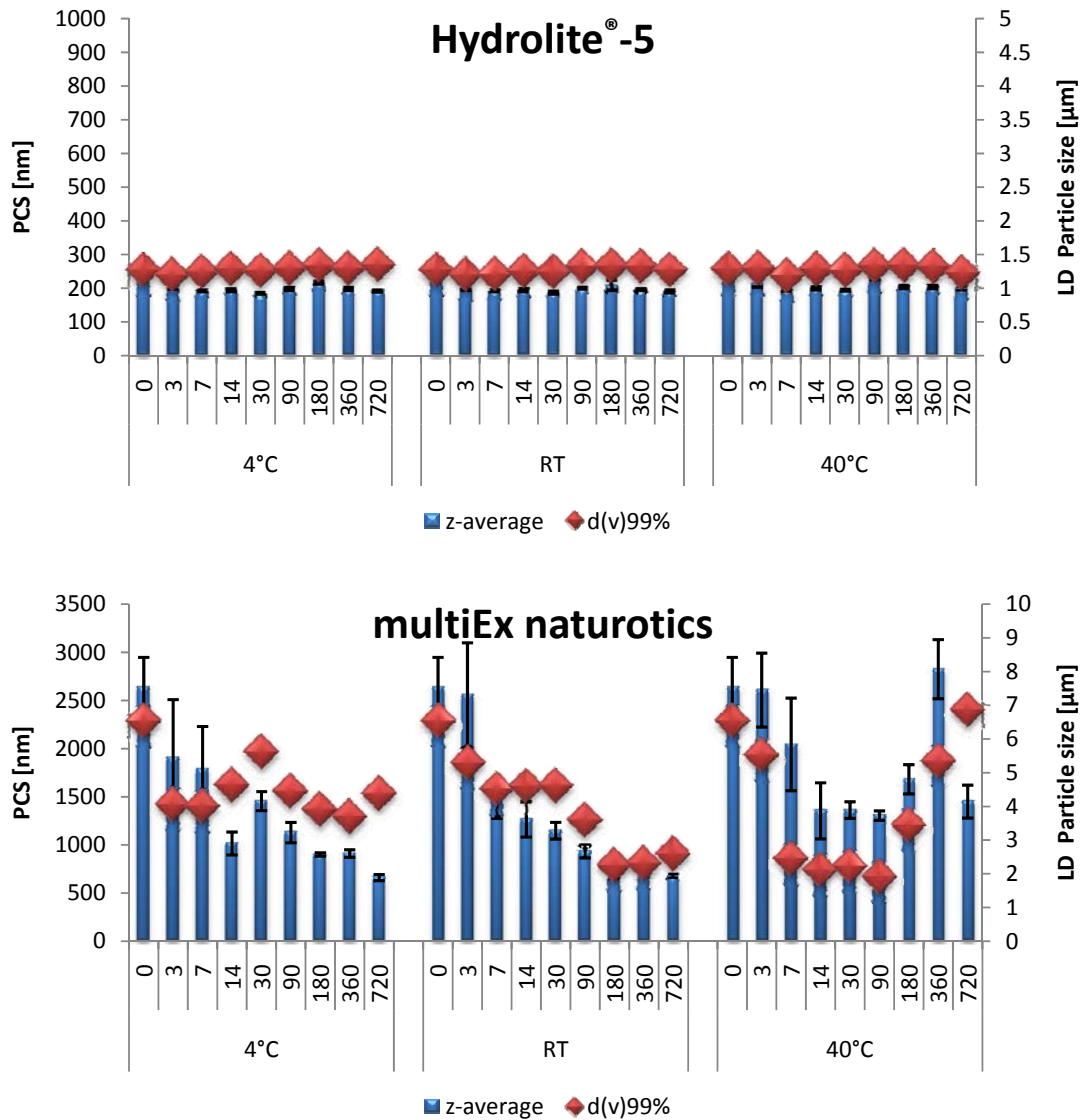


**Fig. 80** Particle size of hesperetin nanosuspensions preserved with Hydrolite®-5 and multiEx naturotics stored at three different temperatures (4°C, RT & 40°C) as a function of time (days)

Microscopic pictures proved the results obtained from PCS and LD for multiEx naturotics preserved hesperetin smartCrystals (Fig. 81H).

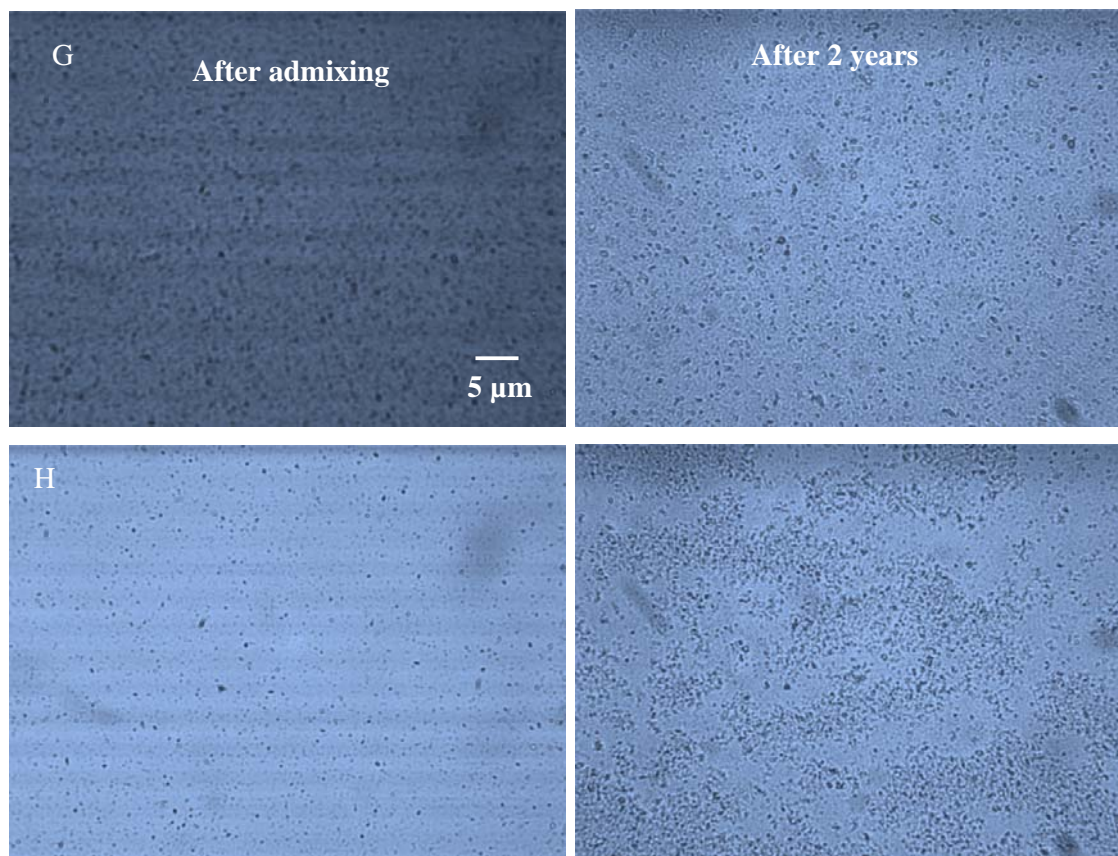


**Fig. 81** Light microscopy images of nanosuspensions preserved with: (G) Hydrolite<sup>®</sup>-5 and (H) multiEx naturotics. (magnification 1000 fold, bar = 5  $\mu\text{m}$ ). The right side is directly after production and the right side is after 2 years storage at room temperature

Hesperetin nanosuspensions preserved with propylene glycol showed neither significant change in z-average nor in  $d(v)99\%$  for the whole storage period (Fig 82). The microscopic pictures showed no aggregates for these smartCrystals<sup>®</sup> (Fig. 83I)

On the other hand, Rokonsal<sup>®</sup> PB-5 showed as for caprylyl glycol two different phases for the particle size, a descending phase for nanosuspension resting after the production and an ascending phase for loose agglomerations. These agglomerates were growing and getting more stable to a stage where the stirrer was not able any more to deaggregate them from each other (Fig. 82).

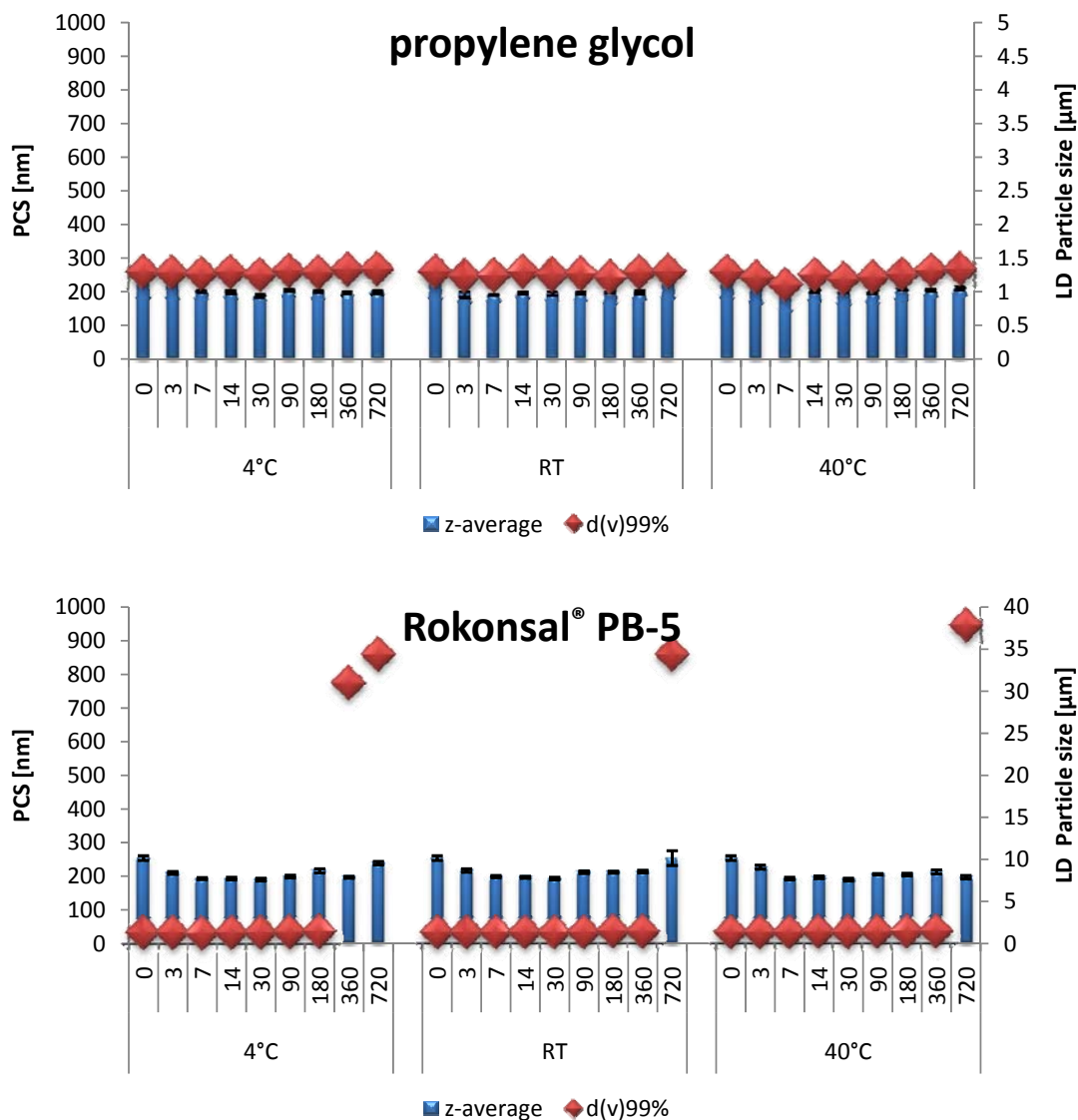
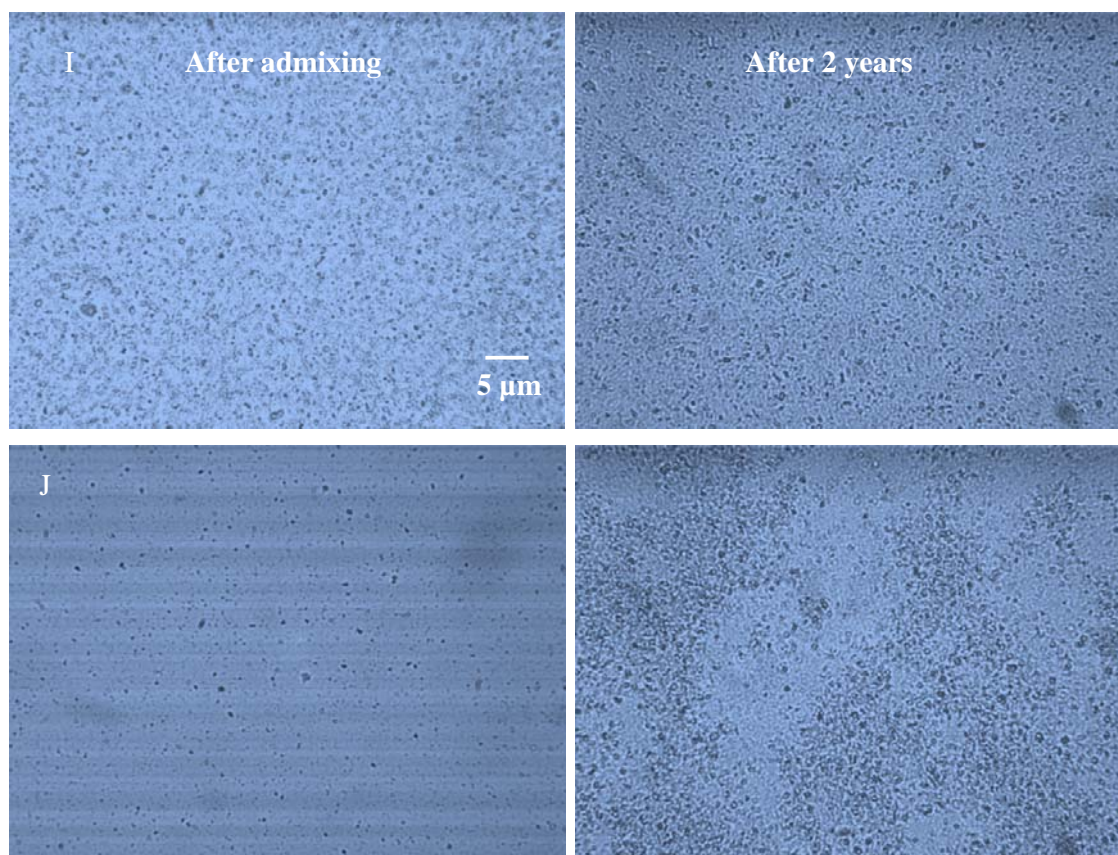


Fig. 82 Particle size of hesperetin nanosuspensions preserved with propylene glycol and Rokonsal® PB-5 stored at three different temperatures (4°C, RT & 40°C) as a function of time (days)

Distinctive agglomerates were detected for hesperetin smartCrystals® preserved with Rokonsal® PB-5 after 2 years storage that affirm the data obtained from LD (Fig. 83J).





**Fig. 83** Light microscopy images of nanosuspensions preserved with: (I) propylene glycol and (J) Rokonsal® PB-5. (magnification 1000 fold, bar = 5  $\mu\text{m}$ ). The right side is directly after production and the right side is after 2 years storage at room temperature

TPGS is not a classical preservative, but as surface active agents they have negative, damaging effects on bacterial membranes – especially at higher concentrations, which are typically not used for physical stabilization of dispersions. In general stabilizer concentrations are used as low as possible; to minimize side effects (e.g. cell membrane damage). The classical example for such damaging effects is the topical microemulsions, containing high concentrations of surfactants [112]. However in concentrated nanosuspensions such higher surfactant concentrations can be used, because for the final formulation these concentrates (and consequently the contained surfactants) are diluted by a factor 10-50. TPGS is of interest, because as additional desired effect it promotes oral absorption of many compounds from the gut [146]. Unaffected z-average and stable  $d(v)99\%$  were obtained the period of storage (Fig. 84).

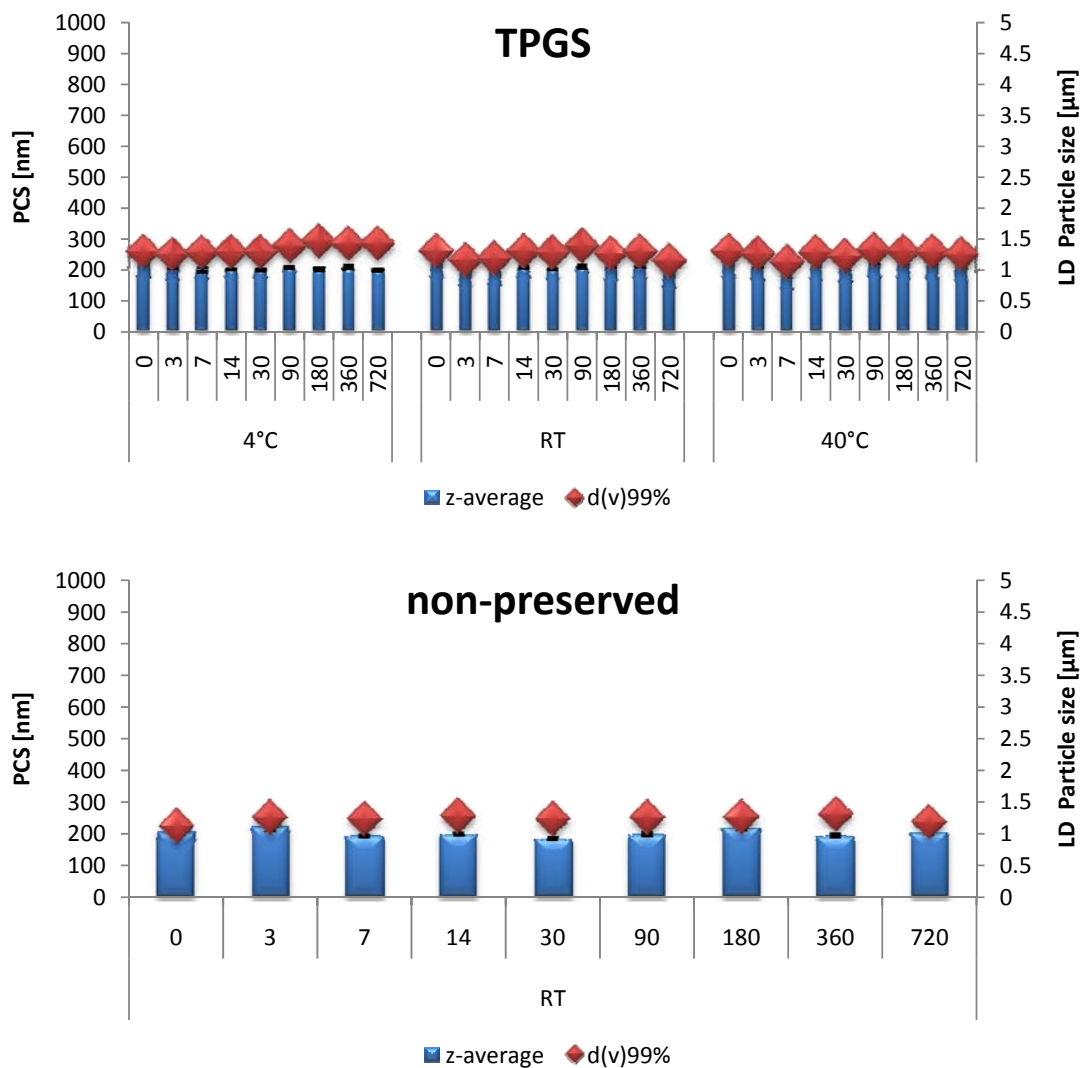


**Fig. 84** Particle size of hesperetin nanosuspensions preserved with TPGS= D-alpha tocopherol polyethylene glycol 1000 succinate and non-preserved stored at three different temperatures (4°C, RT & 40°C) as a function of time (days)

Investigating the hesperetin smartCrystals<sup>®</sup> preserved with TPGS using microscope, no agglomerates were found after 2 years storage (Fig. 85K).

All preserved nanosuspensions were compared to non-preserved hesperetin smartCrystals<sup>®</sup> which was stable the period of storage and showed no change in particle size or LD diameter (Fig. 84). Non-preserved hesperetin smartCrystals<sup>®</sup> did not show any agglomeration when investigated under microscope after 2 years storage (Fig. 85L).

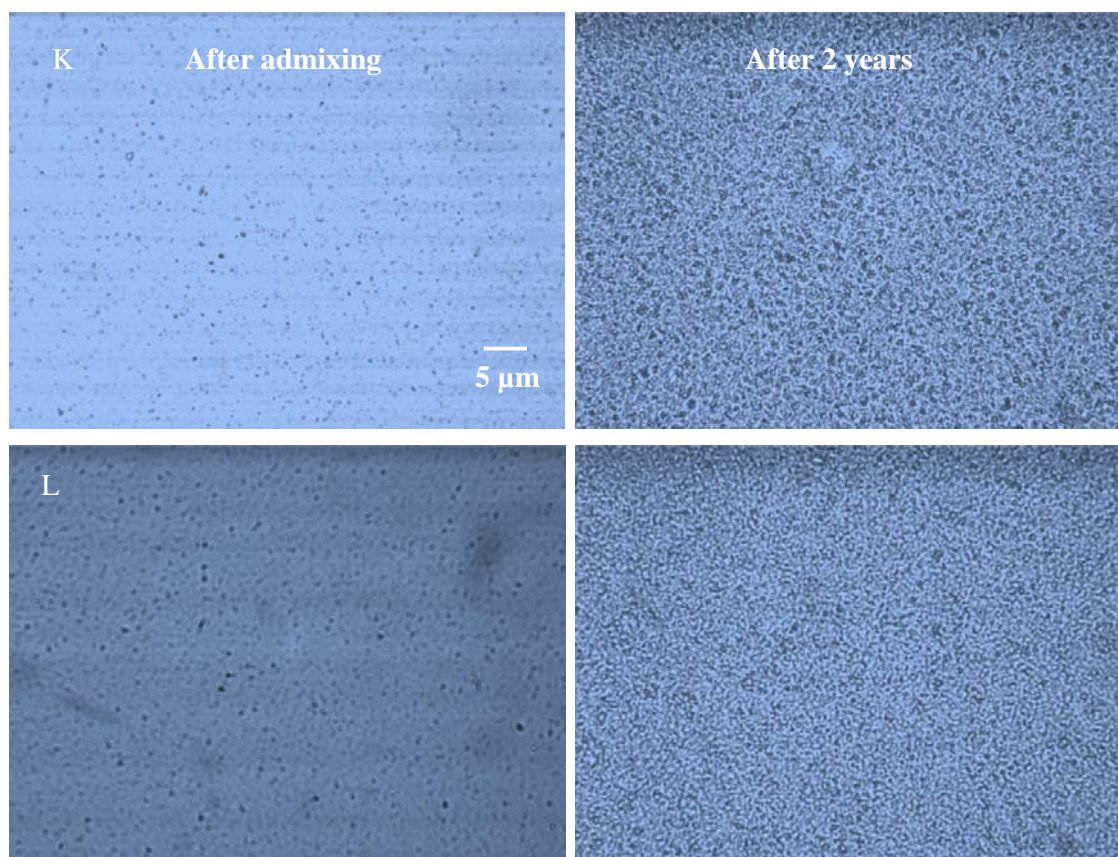


Fig. 85 Light microscopy images of nanosuspensions preserved with: (K) TPGS= D-alpha tocopherol polyethylene glycol 1000 succinate and (L) Non-preserved. (magnification 1000 fold, bar = 5  $\mu\text{m}$ ). The right side is directly after production and the right side is after 2 years storage at room temperature

#### 4.1.9 Saturation solubility

The saturation solubility of hesperetin smartCrystals<sup>®</sup>, hesperetin macrosuspension (hesperetin powder suspended in Plantacare<sup>®</sup> 2000 UP aqueous solution) as well as hesperetin powder was determined at 25°C in water. Fig. 86 shows the saturation solubility of the three mentioned suspensions. In order to discard the effect of the stabilizer in solubilizing or wetting the hesperetin, the nanosuspension was compared also to a macrosuspension containing the same amount of stabilizer. In addition, the saturation solubility was determined in surfactant solutions and in the presence of penetration enhancers to compare them as well to the saturation solubility of the hesperetin rendered as smartCrystals<sup>®</sup>. The smartcrystals<sup>®</sup> provide increased saturation solubility by 290% than that of macrosuspension by just decreasing the particle size from the micrometer [ $d(v)_{99\%} = 85.616 \mu\text{m}$ ] to the nanometer [ $d(v)_{99\%} = 1.114 \mu\text{m}$ ] in hesperetin smartCrystals<sup>®</sup>. In addition, a significant increase was observed by comparing the saturation solubilities of the nanosuspensions with that of powder mixed with different solubilizing aqueous solutions. Even when using 20% of Tween 80 and

reaching a concentration around 80  $\mu\text{g/ml}$  was less than the saturation solubility of the produced smartCrystals<sup>®</sup>.

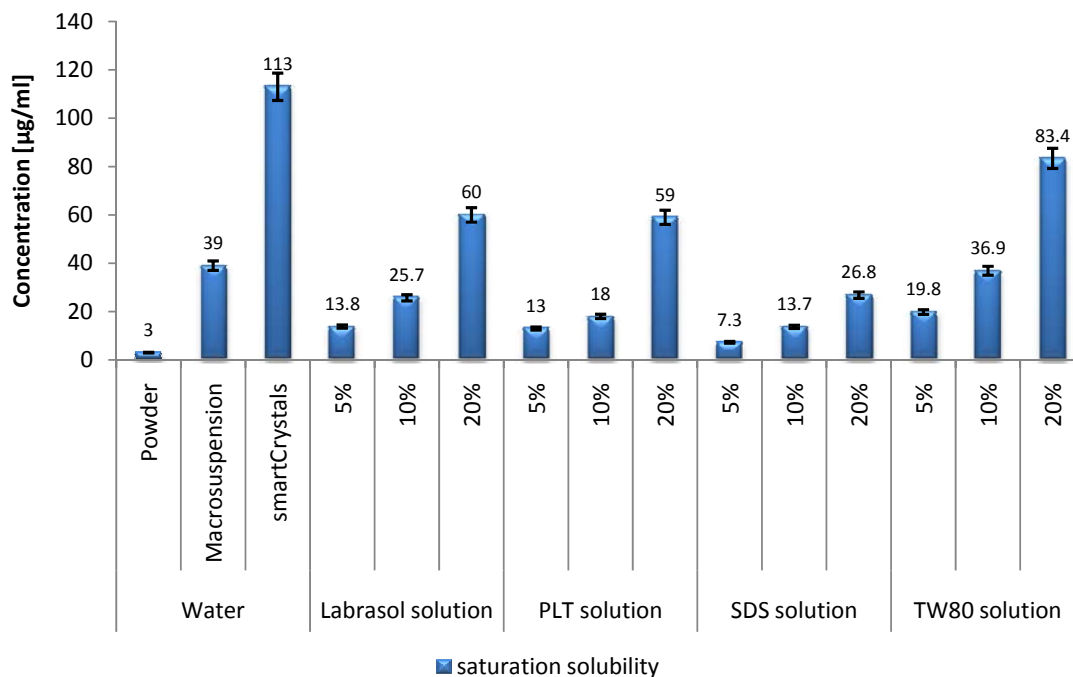


Fig. 86 Saturation solubility of hesperetin powder, macrosuspension, smartCrystals<sup>®</sup> and hesperetin powder with different solubilizing agents and different concentration.

#### 4.1.10 Antioxidant activity

The DPPH<sup>•</sup> radical scavenging test is a well reported in literature as a very convenient method for screening antioxidant molecules because one can see the reaction visually. The detection can be simply carried out using UV-Vis spectrophotometer (Fig. 87). The DPPH<sup>•</sup> radical is scavenged by the antioxidants through the donation of hydrogen to form the stable reduced DPPH-H molecule. The antiradical activity can be analyzed by plotting the residual percentage of DPPH<sup>•</sup>, after reaching the steady state, was plotted against the molar ratios of the antioxidant used to DPPH<sup>•</sup>.

Antioxidant activity depends generally on structural features such as O-H bond dissociation energy, resonance delocalization of phenol radicals and steric hindrance derived from bulky groups substituting hydrogen in the aromatic ring (Fig. 87) [147]. The concentration and the structure of the antioxidant play a crucial role in the residual amount of DPPH<sup>•</sup>.

DPPH<sup>•</sup> standard curve in Methanol was constructed in concentrations ranging between 10  $\mu\text{M}$  to 300  $\mu\text{M}$ . Maximum absorbance was noted at 515 nm. In further experiment concentrations were determined using the following calibration curve equation

$$y = 12.612 x \text{ (g/l)} \dots\dots\dots \text{correlation coefficient } r^2 = 0.9997$$

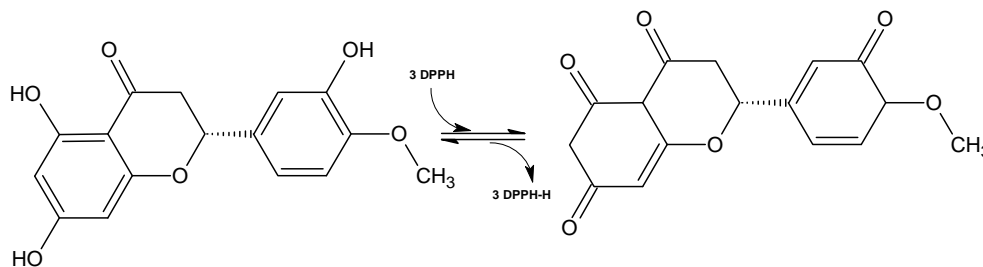


Fig. 87 Reaction kinetics of DPPH<sup>•</sup> and hesperetin

Steady state time ( $T_{\text{steadystate}}$ ) was determined in order to ensure the endpoint of reaction. hesperetin reacted quite rapidly with DPPH<sup>•</sup> free radicals and reached the steady state after 120 minutes (Fig. 88). This can be due to the higher solubility of hesperetin in the methanol solution of DPPH<sup>•</sup> [87], which lead to fast reaction between the hesperetin molecules and DPPH<sup>•</sup>.

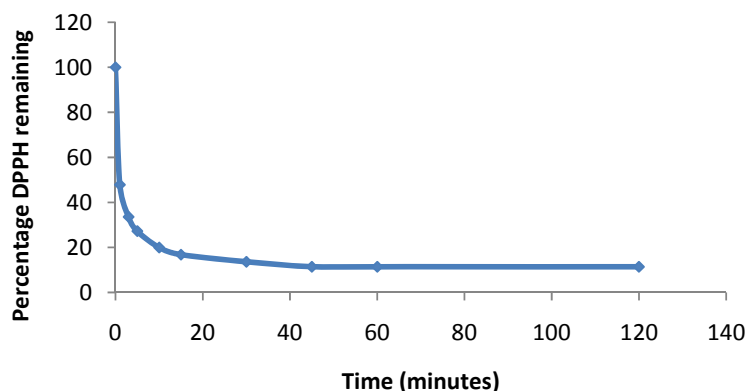
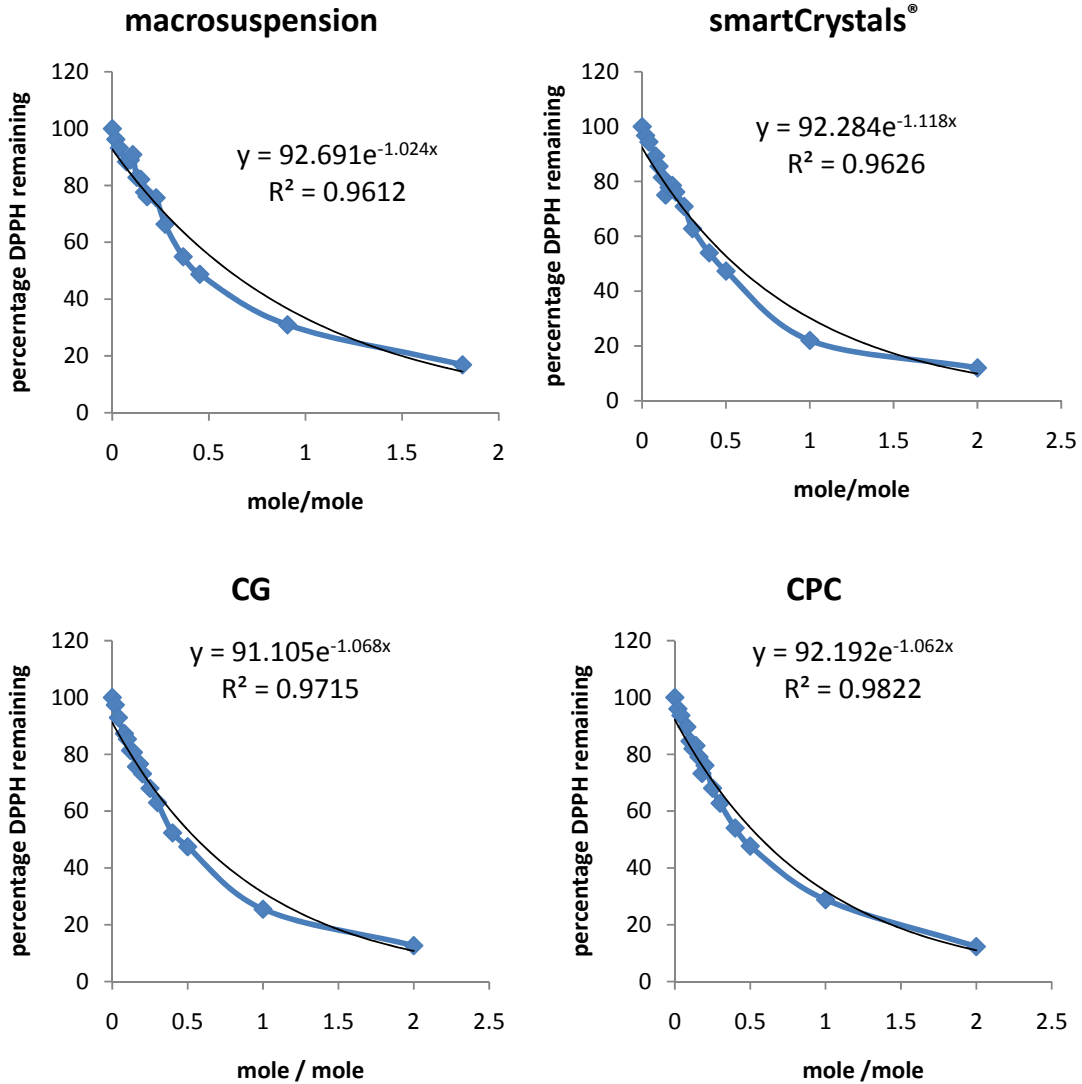


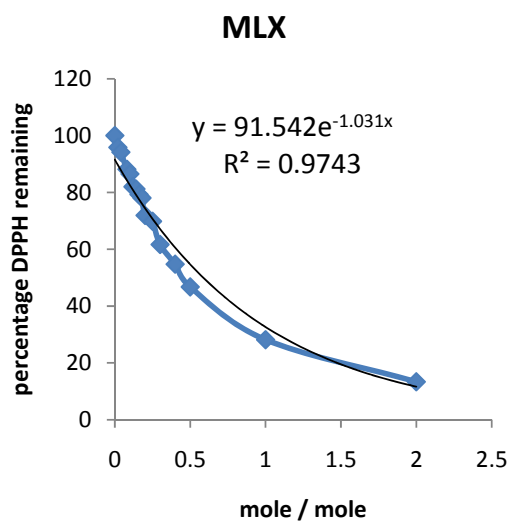
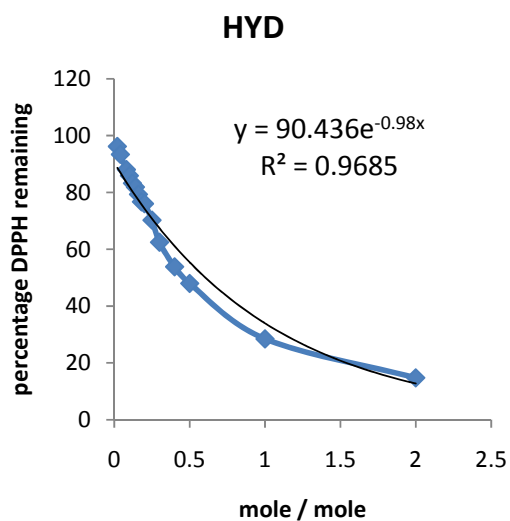
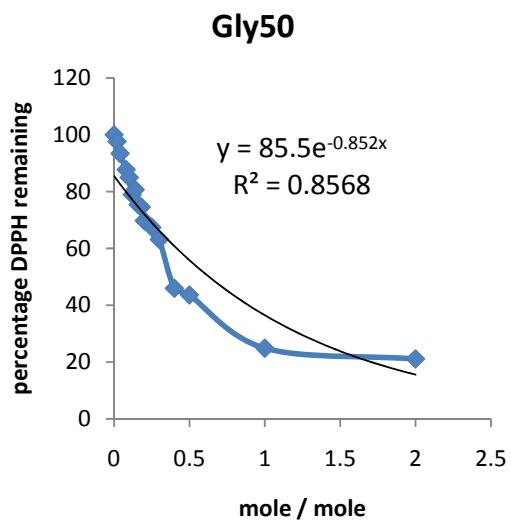
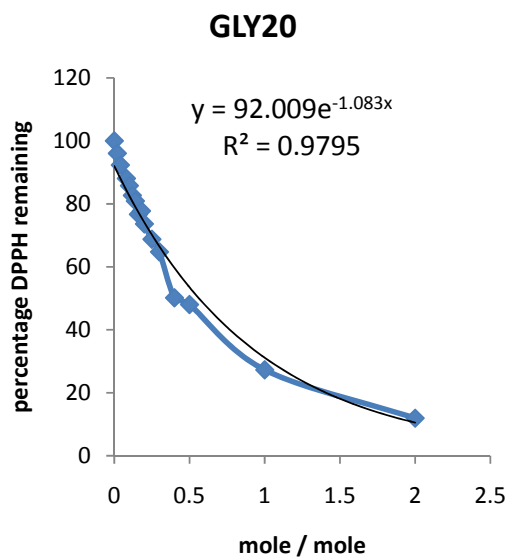
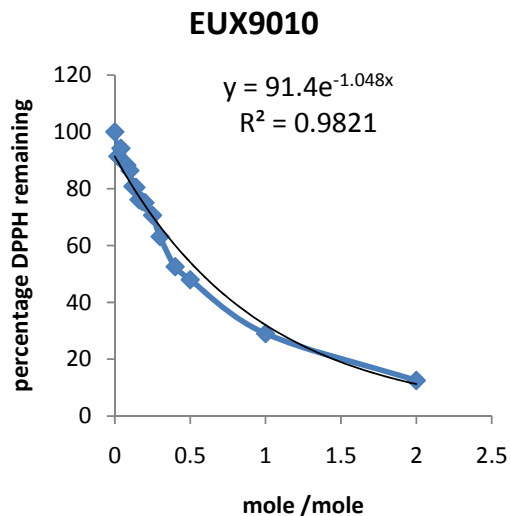
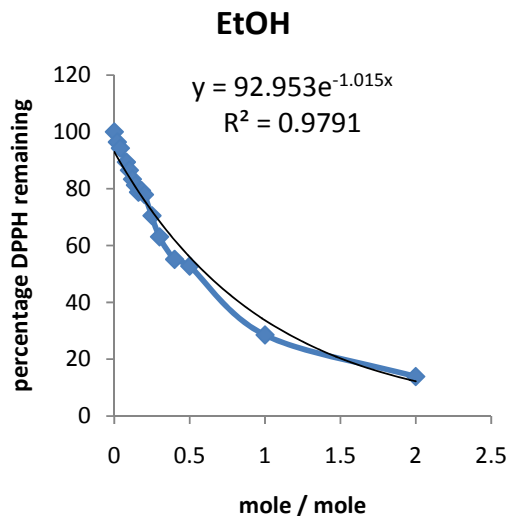
Fig. 88 The steady state for the antioxidant reaction of hesperetin nanosuspension and DPPH<sup>•</sup>

$EC_{50}$  (Efficient Concentration required to decrease the DPPH<sup>•</sup> concentration by 50%) of both hesperetin macro- and nano-suspensions was calculated by plotting the residual percentage of DPPH<sup>•</sup> against the molar ratios of the antioxidant to DPPH<sup>•</sup>. The lower the  $EC_{50}$ , the higher is the antioxidant activity of a compound. Hesperetin macrosuspension showed an  $EC_{50}$  value of 0.603, which was a little bit less than the  $EC_{50}$  of hesperetin nanosuspension about 0.548.

The effect of nanonization cannot be clearly seen in the case of hesperetin macro- and nanosuspension due to the high solubility of hesperetin in methanol [87] and hence the effect of surface area augmentation on the antioxidant activity was insignificant.

The destabilizing effect of preservatives on the physical stability of hesperetin nanosuspensions may negatively affect the antioxidant activity of the active ingredient due to the formation of agglomerations. Antioxidant activity was further studied of hesperetin smartCrystals after the incorporation of the preservatives in the formulation Fig. 89.





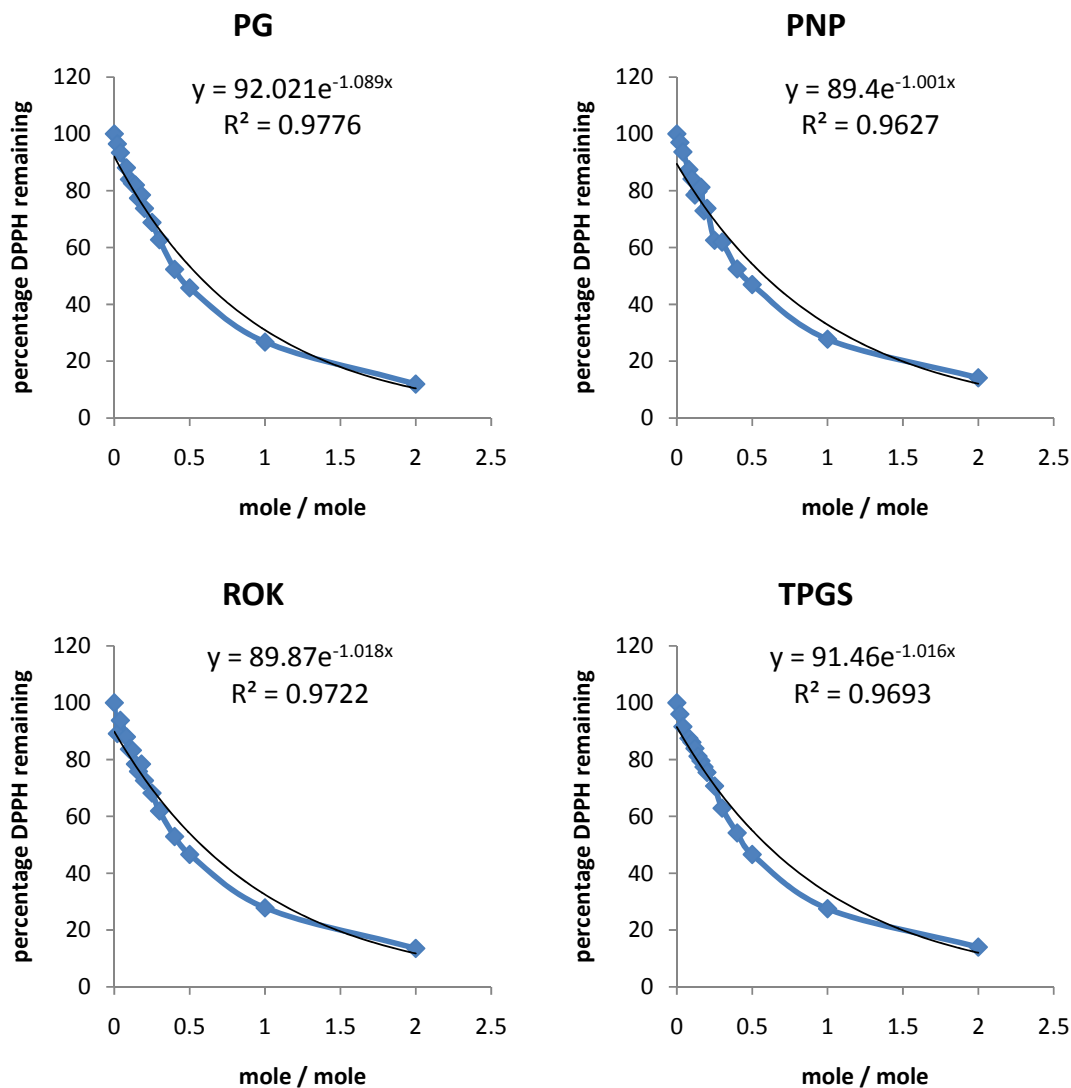


Fig. 89 The declining in DPPH<sup>•</sup> concentration as a function of the number of moles of hesperetin / moles of DPPH<sup>•</sup> for hesperetin macrosuspension, Non-preserved hesperetin smartCrystals<sup>®</sup> and preserved hesperetin smartCrystals<sup>®</sup> with (CG= caprylyl glycol, CPC= cetyl pyridinium chloride, EtOH= ethanol, EUX9010= Euxyl<sup>®</sup> PE 9010, GLY20= glycerol 20%, GLY50= glycerol 50%, HYD= Hydrolite<sup>®</sup>-5, MLX= multiEx naturotics, PG= propylene glycol, PNP= Phenonip<sup>®</sup>, ROK= Rokonsal<sup>®</sup> PB-5 and TPGS= D-alpha tocopherol polyethylene glycol 1000 succinate)

Table 13 shows the EC<sub>50</sub> values of hesperetin macrosuspension, smartCrystals<sup>®</sup> and preserved smartCrystals<sup>®</sup>.

Although The EC<sub>50</sub> increased to a small extent after the addition of the preservatives, but the impact of the preservatives was so low that it cannot be taken into account. The EC<sub>50</sub> values of hesperetin macro- and nano-suspension with or without the addition of preservatives were almost same and ranging from 0.548 for hesperetin non-preserved smartCrystals<sup>®</sup> to 0.630 for hesperetin smartCrystals<sup>®</sup> preserved with GLY50.



**Table 13** EC<sub>50</sub> values of hesperetin macrosuspension, smartCrystals<sup>®</sup> and preserved hesperetin smartCrystals (CG= caprylyl glycol, CPC= cetyl pyridinium chloride, EtOH= ethanol, EUX9010= Euxyl<sup>®</sup> PE 9010, GLY20= glycerol 20%, GLY50= glycerol 50%, HYD= Hydrolite<sup>®</sup>-5, MLX= multiEx naturotics, PG= propylene glycol, PNP= Phenonip<sup>®</sup>, ROK= Rokonsal<sup>®</sup> PB-5 and TPGS= D-alpha tocopherol polyethylene glycol 1000 succinate)

Type of hesperetin suspension	EC <sub>50</sub> values
<b>Macrosuspension</b>	0.603
<b>smartCrystals</b>	0.548
<b>CG</b>	0.562
<b>CPC</b>	0.576
<b>EtOH</b>	0.611
<b>EUX9010</b>	0.575
<b>GLY20</b>	0.563
<b>GLY50</b>	0.630
<b>HYD</b>	0.605
<b>MLX</b>	0.587
<b>PG</b>	0.560
<b>PNP</b>	0.580
<b>ROK</b>	0.576
<b>TPGS</b>	0.594

#### 4.1.11 X-ray diffraction (XRD)

XRD is normally used to examine the crystalline status of the materials on an atomic and on molecular levels. The sample is exposed to x-rays at different angles and the diffracted light is afterwards compared with reference standards. The results obtained from the measurements verify whether the sample is amorphous, partially amorphous or crystalline. Four samples were used to check their crystalline status after drying them: hesperetin powder dispersed in water, hesperetin powder dispersed in a Plantacare<sup>®</sup> 2000 UP aqueous solution, hesperetin nanosuspension produced with Micron LAB40 (lab-scale batch) and hesperetin smartCrystals<sup>®</sup> (scaled-up batch).

Hesperetin diffractions patterns were depicted in the X-ray diffractogram shown in Fig. 90. By comparing the 4 different samples it can be obviously seen that no different peaks appeared when the Plantacare<sup>®</sup> 2000 UP was added to the formulation. In addition, the diffractogram showed identical peak shapes for both samples of hesperetin nanosuspension and hesperetin smartCrystals<sup>®</sup> compared to the macrosuspension. According to these findings, all produced nanosuspensions on lab and large scale have the same crystallinity as the raw material. Applying very high energy to obtain smaller particles such as the case in Micron LAB40 produced nanosuspension or less energy such as the case in smartCrystals<sup>®</sup> did not

affect the crystalline status of the formulation. Staying in the crystalline status assure the stability of the product, as crystalline substances are physically more stable than amorphous ones [139].

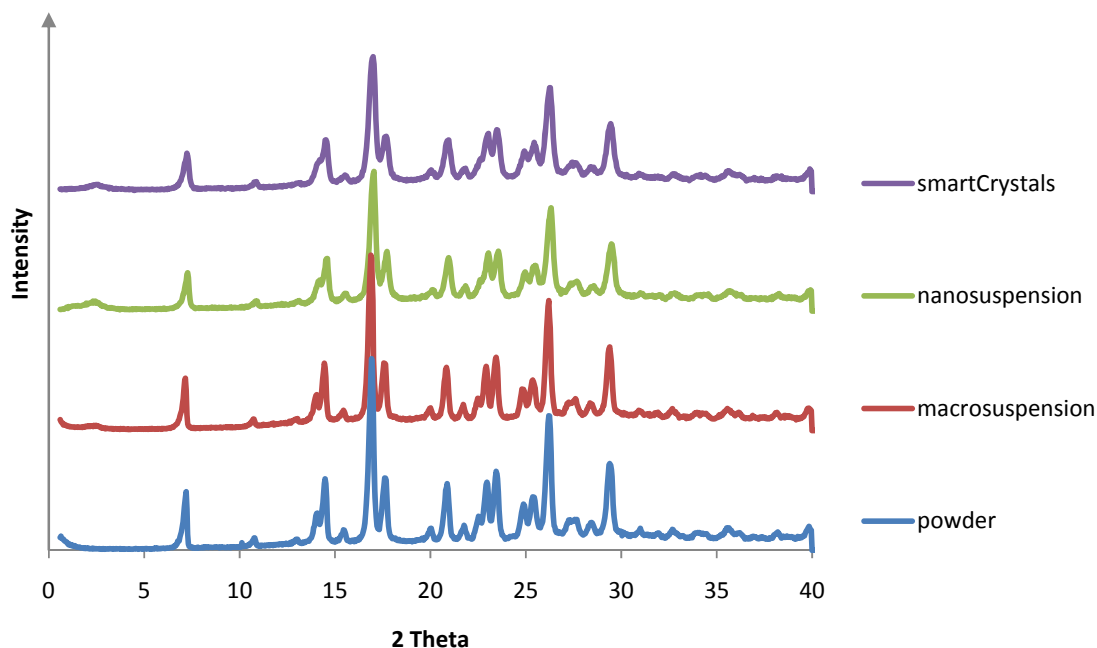


Fig. 90 X-ray diffractogram of dried hesperetin coarse suspension, dried hesperetin suspension in Plantacare® 2000 UP aqueous solution (macrosuspension), dried hesperetin nanosuspension produced with Micron LAB40 and dried hesperetin smartCrystals®

#### 4.1.12 *In vitro* release

##### 4.1.12.1 Cellulose acetate membranes

Franz diffusion cells were used to evaluate the permeation rate of hesperetin. For this purpose, two different receptor media were used. Fig. 91A shows the cumulative amount of hesperetin dissolved in the PBS medium for 24 hours. Three different formulations were tested: hesperetin powder dispersed in water, hesperetin macrosuspension and hesperetin smartCrystals® (Fig. 91).

The penetrated amount of hesperetin from the smartCrystals® was almost double the amount of hesperetin penetrated from the macrosuspensions and the powder dispersed in water. However, the difference in solubility was not big during the first 6 hours.

On the other hand, using a receptor medium containing PEG 400 and ethanol increased the solubility quite well for all of the studied samples and showed a real difference between them. The solubility of hesperetin samples from macrosuspensions and powder were very less compared to that of smartCrystals®. The maximum amount of hesperetin diffused for both of

them reached to 10% after 24 hours, due to the low saturation solubility and dissolution velocity of hesperetin in water [67, 87], while it was extremely higher for hesperetin smartCrystals<sup>®</sup> reaching 100±10%.

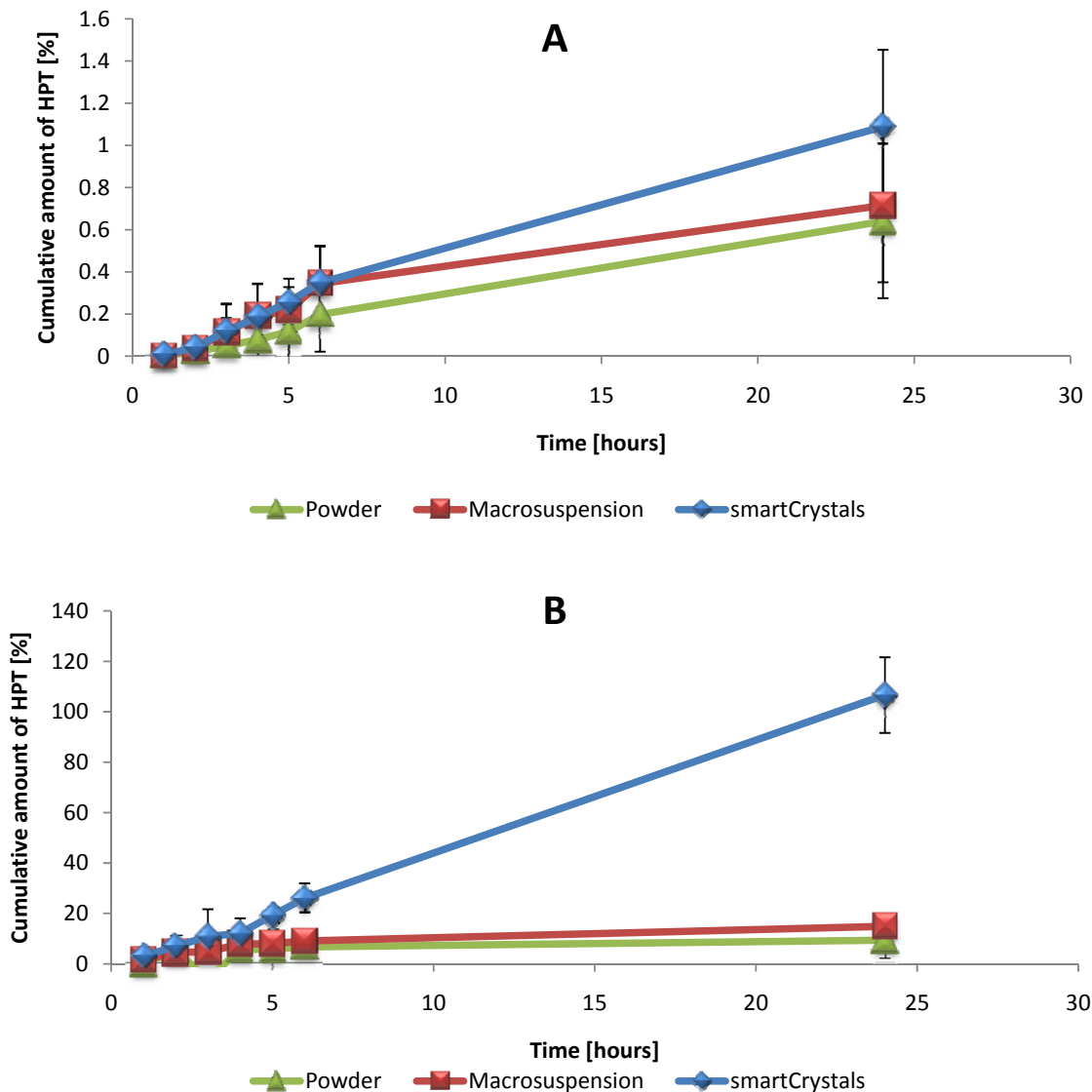


Fig. 91 The cumulative amount of hesperetin dissolved from the smartCrystals<sup>®</sup>, macrosuspensions and dispersed powder in water in (A) PBS as a receptor medium or (B) a mixture of PBS : ethanol : PEG 400 (40:20:40)

These results confirm that the smartCrystals<sup>®</sup> does not only have higher saturation solubility but also a better and faster dissolution velocity [143].

#### 4.1.13 Chemical stability

The chemical stability is a very important indicator beside the physical stability to evaluate the compatibility of the active ingredient with the additives.

As a start, the compatibility of the stabilizers were screened. Hesperetin quantification was performed after the production and after 1 year and after 2 years. In general, it can be seen from Fig. 92 that the reduction in concentration for the 2 years was around 10% of the original dose.

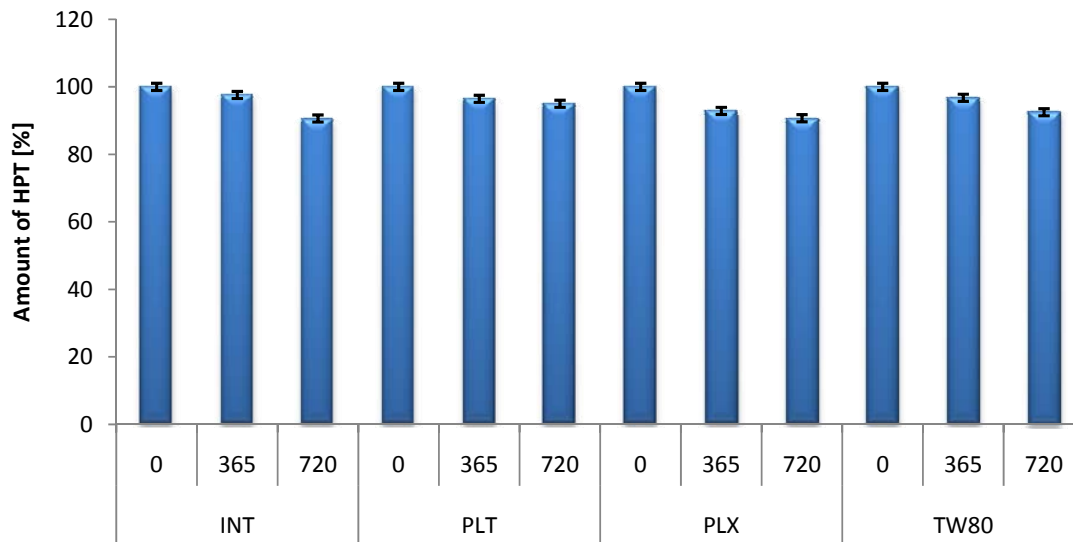


**Fig. 92** Amount of hesperetin [%] in the produced nanosuspension produced with Micron LAB40 using different stabilizers (INT= Inutec<sup>®</sup> SP1, PLT= Plantacare<sup>®</sup> 2000 UP, PLX= poloxamer 188 and TW80= Tween 80) as a function of time (days)

As well, the quantification of hesperetin was done for samples preserved with different preservatives added either before or after the homogenization using Micron LAB40. All samples did not show more than 10% decrease of the original concentration of hesperetin after 2 years stability (Fig. 93).

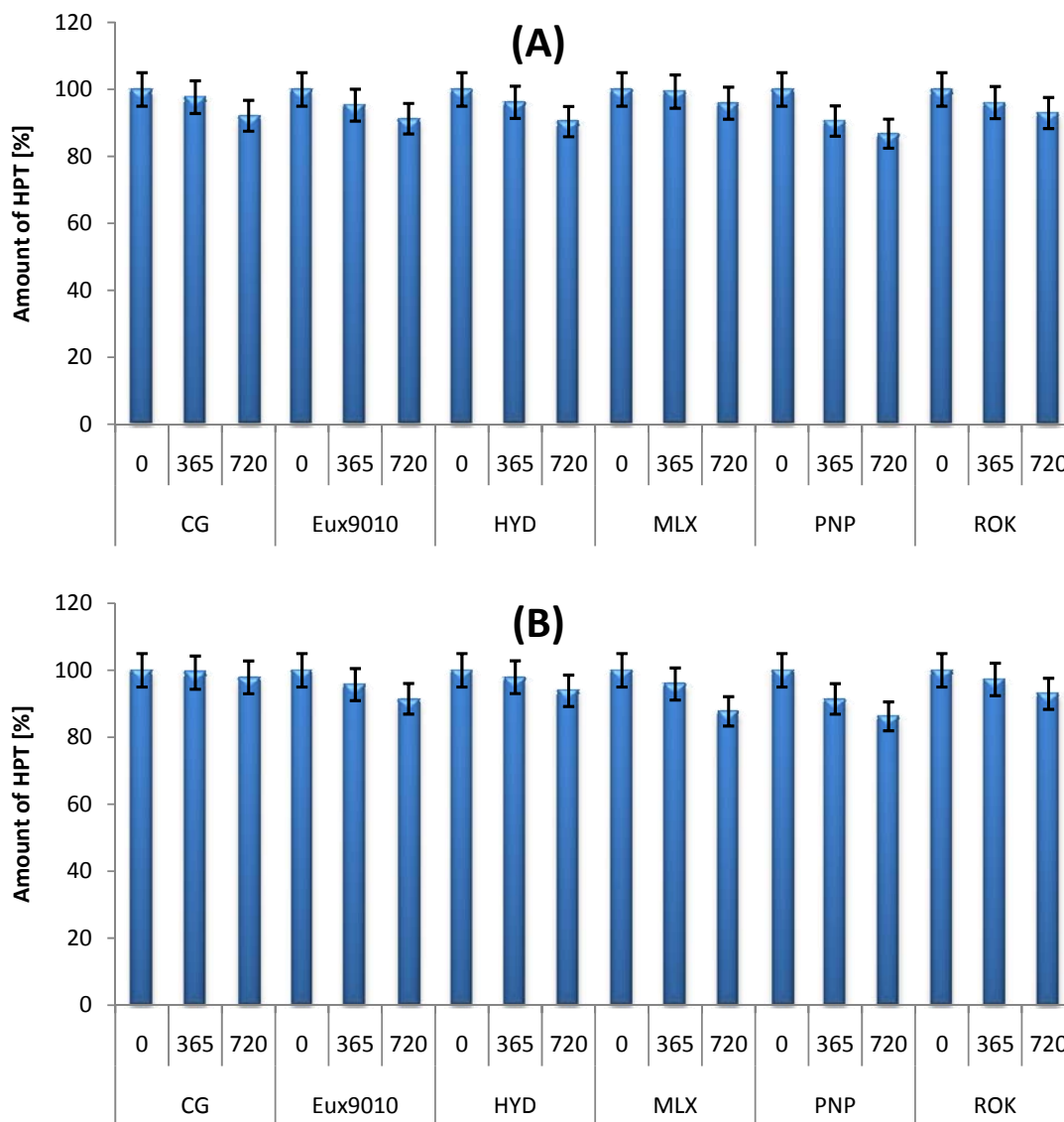


**Fig. 93** Amount of hesperetin [%] in the preserved hesperetin nanosuspension produced with Micron LAB40 using different preservatives (CG= caprylyl glycol, EUX9010= Euxyl<sup>®</sup> PE 9010, HYD= Hydrolite<sup>®</sup>-5, MLX= multiEx naturotics, PNP= Phenonip<sup>®</sup> and ROK= Rokonsal<sup>®</sup> PB-5) as a function of time (days) either added before (A) or after (B) homogenization

In order to check the effect of the antifoaming agent on the chemical stability of hesperetin, the study was also performed on the samples where different concentrations of antifoaming agent were added. From Fig. 94, it can be seen that all concentrations of the antifoaming agents had no effect on the chemical stability of hesperetin.

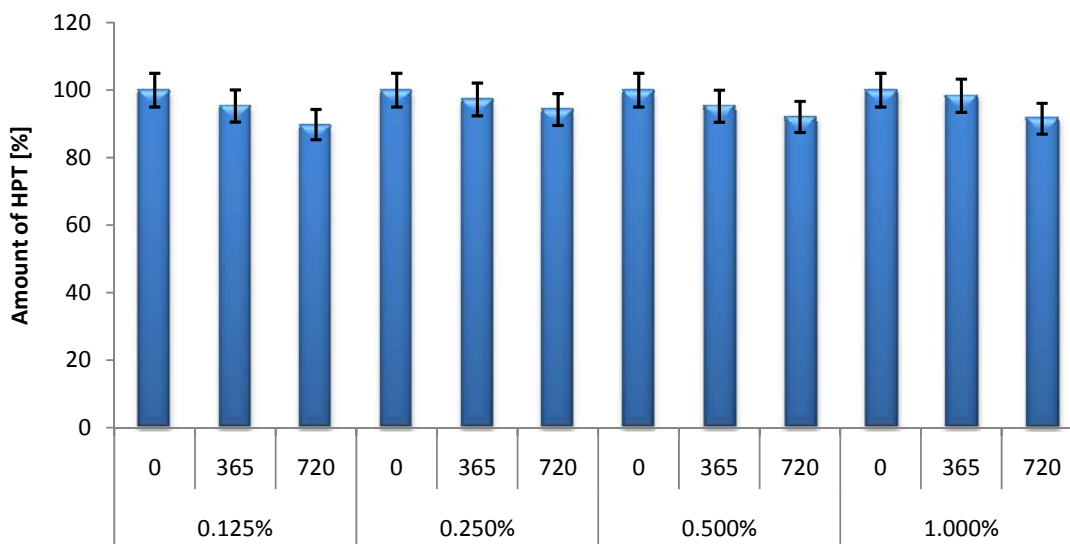


**Fig. 94** Amount of hesperetin [%] in the hesperetin nanosuspension produced with Micron LAB40 with the addition of an antifoaming agent as a function of time (days)

For scaled up samples using Avestin C50 (Fig. 95) or the smartCrystal<sup>®</sup> technology (Fig. 96) it was also found that the effect of the preservatives on the nanocrystals is really limited, hence they are considered all of no chemical incompatibility to hesperetin nanosuspensions.

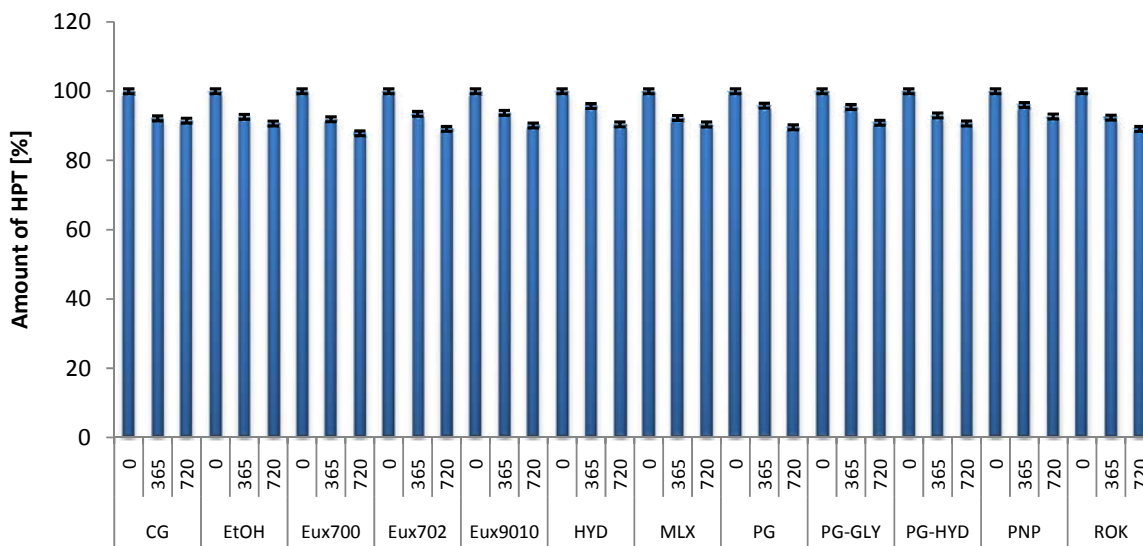


**Fig. 95** Amount of hesperetin [%] in the hesperetin nanosuspension produced with Avestin C50 as a function of time (days) after mixing the nanosuspension with different preservatives (CG= caprylyl glycol, EtOH= ethanol, EUX700= Euxyl<sup>®</sup> K700, EUX702= Euxyl<sup>®</sup> K702, EUX9010= Euxyl<sup>®</sup> PE 9010, HYD= Hydrolite<sup>®</sup>-5, MLX= multiEx naturotics, PG= propylene glycol, PG-GLY= propylene glycol - glycerin mixture, PG-HYD= propylene glycol - Hydrolite<sup>®</sup>-5 mixture, PNP= Phenonip<sup>®</sup>, ROK= Rokonsal<sup>®</sup> PB-5)

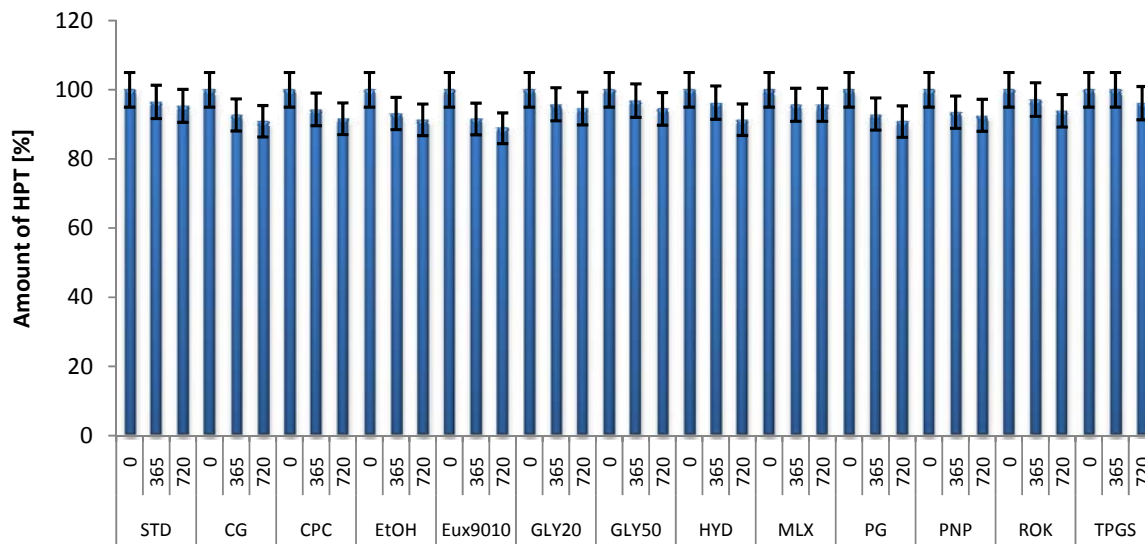


**Fig. 96** Amount of hesperetin [%] in the hesperetin nanosuspension produced with the smartCrystals technology preserved with different preservatives (CG= caprylyl glycol, CPC= cetylpyridinium chloride, EtOH= ethanol, EUX9010= Euxyl<sup>®</sup> PE 9010, GLY20= glycerol 20%, GLY50= glycerol 50%, HYD= Hydrolite<sup>®</sup>-5, MLX= multiEx naturotics, PG= propylene glycol, PNP= Phenonip<sup>®</sup>, ROK= Rokonsal<sup>®</sup> PB-5 and TPGS= D-alpha tocopherol polyethylene glycol 1000 succinate) as a function of time (days)

## 4.2 Apigenin

### 4.2.1 Refractive index

For apigenin, acetone and DMSO were used as solvents. Table 4.2.1-1 shows the results obtained from the Saveyn et al. method as well as RI data calculated using the Clausius-Mossotti-equation.

**Table 14** calculated and measured RI for apigenin. For the standard curve [ $y = \text{RI}$  related to the concentration of the substance,  $c = \text{concentration of the material in the defined solvent (mg/100 mL)}$ ].

	Method	Solvent	Standard curve equation	RI
Apigenin	Saveyn et al.	Acetone	$y = 0.0038c + 1.3562$	1.736
		DMSO	$y = 0.0041c + 1.3336$	1.743
	Clausius-Mossotti-equation			$1.732 \pm 0.02$

As a result, the RI of apigenin is 1.736.

### 4.2.2 Screening of stabilizers

The stabilizer screening was done in a previous work and the best stabilizer was found to be Plantacare® 2000 UP [148].

### 4.2.3 Reproducibility

The reproducibility of producing apigenin nanosuspensions using APV LAB 40 was investigated by producing 3 different batches [5% (w/w) apigenin, 1% (w/w) Plantacare® 2000 UP and 94% (w/w) purified water] and the particle size characterization was performed using PCS and LD.

Three different batches were produced with Micron LAB 40 (Fig. 97, Fig. 98) and the physical characteristics were measured with PCS and LD. As seen also in hesperetin batches, no big difference was detected between the produced batches.



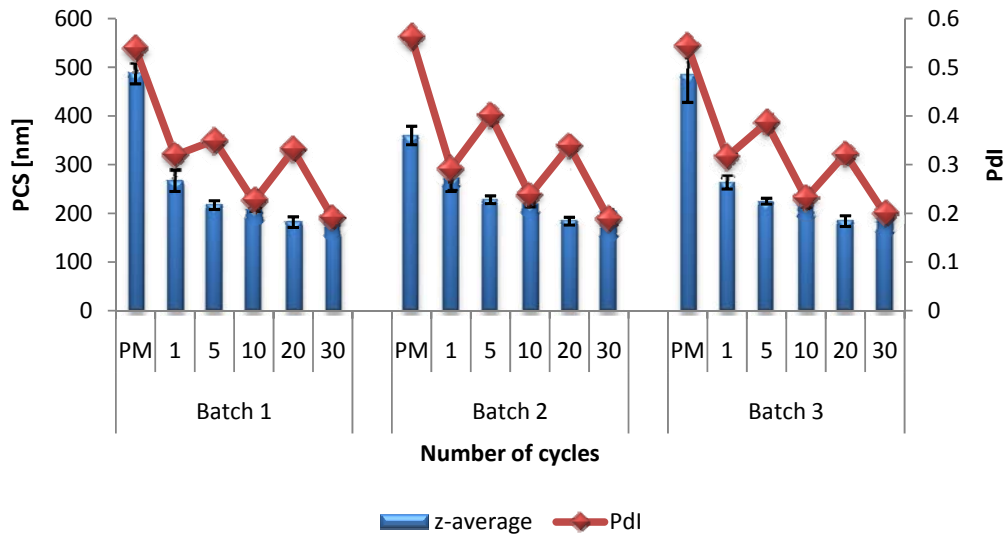


Fig. 97 PCS particle size (z-average) and polydispersity index (PDI) of three different batches of apigenin nanosuspensions

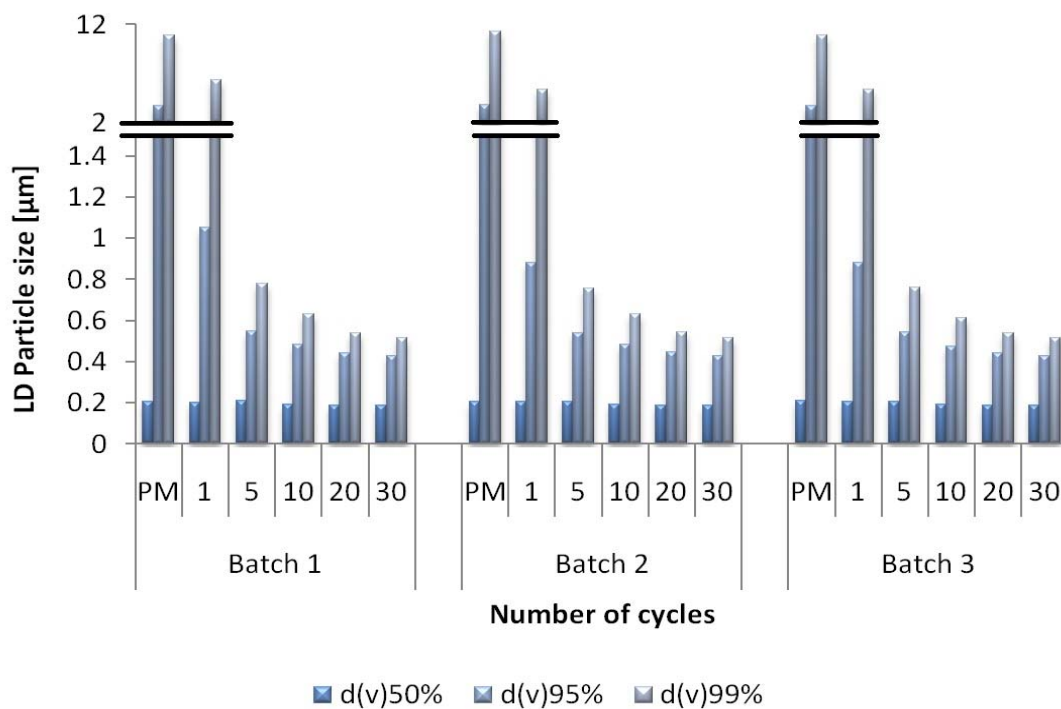


Fig. 98 LD particle size of three different batches of apigenin nanosuspensions

#### 4.2.4 Preservative screening

From the hesperetin results and the experienced gained by scanning the hesperetin preserved nanosuspension, the scanning of the preservatives with apigenin was investigated after admixing the preservatives with the produced nanosuspensions. Particle size was then examined using PCS and LD.

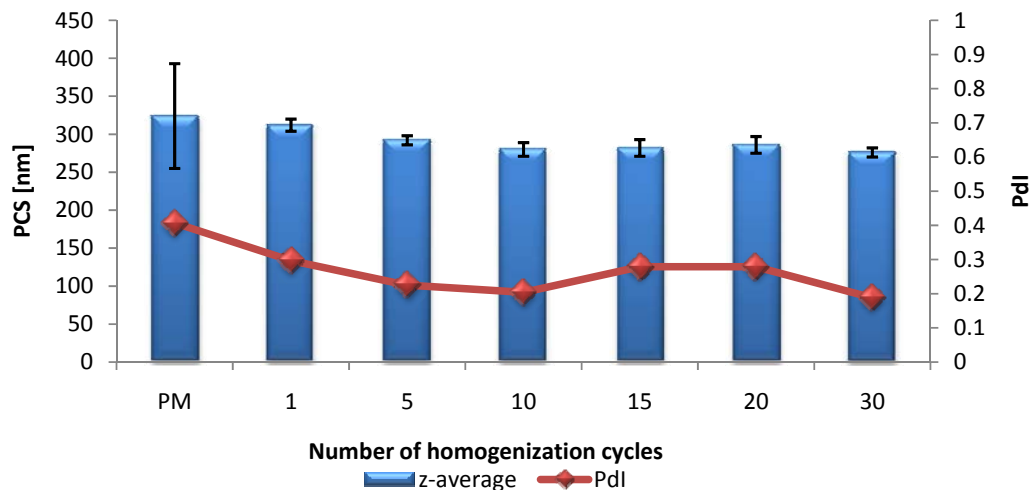


Fig. 99 Reduction in particle size (PCS) along with the decrease in polydispersity index (PDI) as a function of homogenization cycles (PM = pre-milling).

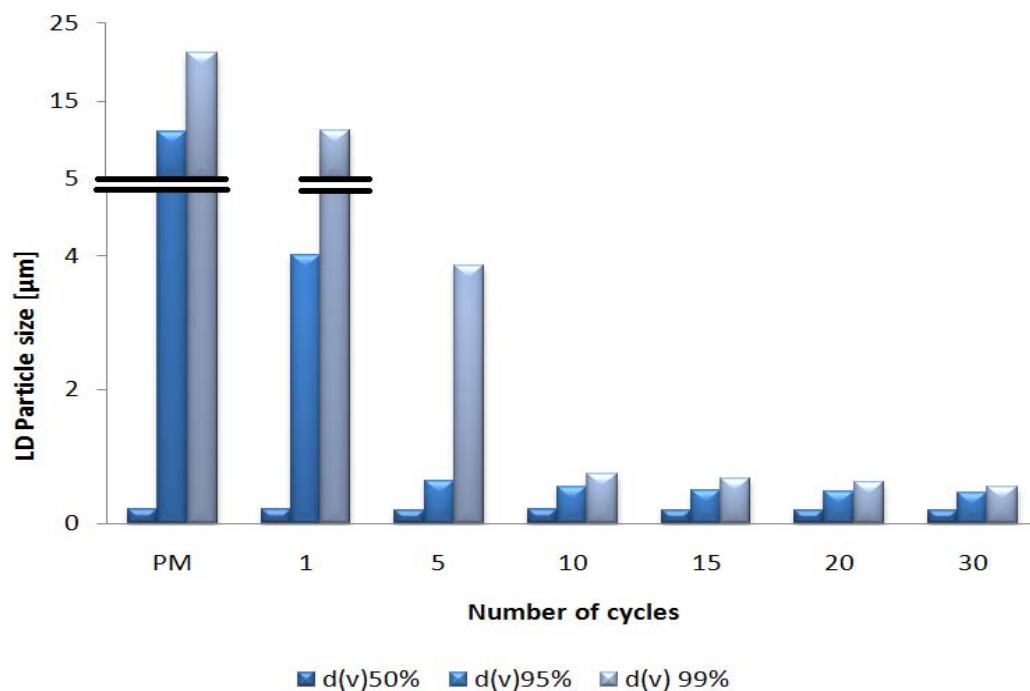


Fig. 100 Reduction in LD diameter as function of homogenization cycles (PM = pre-milling).

In the lab scale production using HPH, the PCS diameter decreased until cycle 10 (280 nm). Further increase in cycle number did not further decrease the size, which means that the maximum dispersivity was reached at 10 cycles. In parallel, the polydispersity index decreased indicating removal of particles larger than the bulk population and a narrowing of the size distribution. Apigenin nanosuspension showed a mean particle size of  $276 \pm 5$  nm

after 30 cycles with narrow polydispersity index of  $0.136 \pm 0.05$  (Fig. 99). The results were reproducible ( $n=3$ , the diameters for the other 2 productions were 247 nm and 255 nm after 30 cycles).

For a pharmaceutical or cosmetic product, one does not have necessarily the smallest achievable nanocrystal size. A size of apigenin of about 300 nm after pre-milling and 1 production cycle at 1,500 bar might be sufficient. Of course this would reduce clearly the production costs. In case maximum solubility enhancement is required, the smallest achievable size should be chosen. In addition, when the final product is liquid (e.g. oral suspension), the PdI should be as low as possible, to minimize content of remaining larger crystals which can cause Ostwald ripening. This requires 20-30 homogenization cycles.

The laser diffractometry results of the lab scale nanosuspensions produced by HPH were well in agreement with the results obtained by PCS. The LD diameters  $d(v)90\%$  to  $d(v)99\%$  decreased continuously until cycle 20, at which maximum dispersitivity was found based on the PCS data. The most pronounced decrease took place between pre-milling and cycle 10, little decrease up to cycle 30. These diameters are a measure for larger remaining particles in the population. Their decrease is in parallel to the decrease in PdI in the PCS measurements. In contrast the diameter 50%, representing the bulk population, should little decrease (Fig. 100). This is also in agreement with the PCS data, all PCS diameters were in the range of about 350 nm (after pre-milling) to 265 nm (after 30 cycles), a difference.

By adding the preservatives to prepared nanosuspension the physical characteristics will be altered as a consequence to changes on the particle surfaces. Particle size was also characterized after the addition of the preservatives using PCS and LD.

In general, by interpreting the data obtained from PCS (Fig. 101), preservatives which are more hydrophilic such as cetylpyridinium chloride, ethanol, Euxyl<sup>®</sup> PE 9010, glycerol 20%, Hydrolite<sup>®</sup>-5, propylene glycol and TPGS had no significant effect on the particle size. Investigating these preserved nanosuspensions under microscope confirmed the data obtained from PCS (Fig. 103). Less hydrophilic preservatives such as caprylyl glycol, Phenonip<sup>®</sup> and Rokonsal<sup>®</sup> PB-5 had more effect on the stabilization effect of Plantacare<sup>®</sup> 2000 UP and therefore cause partial agglomeration in the produced nanosuspensions (Fig. 103). MultiEx naturotics as a hydrophobic preservative had a significant effect on the particle size which can be seen as oversized agglomerates by investigating the nanosuspensions with microscope (Fig. 103). Glycerol 50% had as well a negative effect on the physical characteristics of the nanosuspension although they are hydrophilic (Fig. 103). This can be due to the very high

hygroscopicity of glycerol, which probably played a role in dehydrating the stabilizing film from the particle surfaces due to its hygroscopic characteristics (Fig. 101).

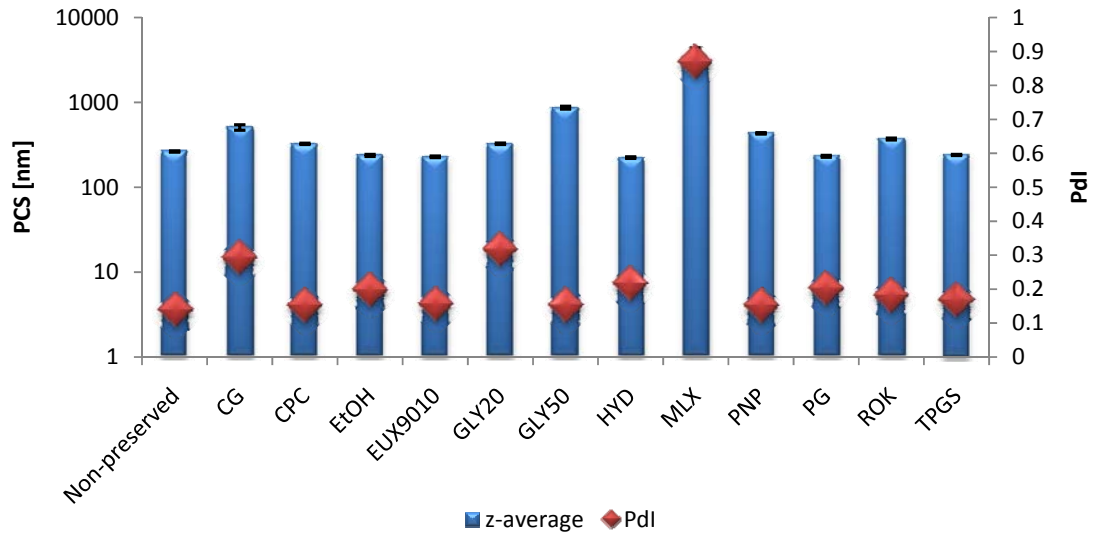


Fig. 101 Particle size (z-average) and PDI after addition of various preservatives (CG= caprylyl glycol, CPC= cetylpyridinium chloride, EtOH= ethanol, EUX9010= Euxyl® PE 9010, GLY20= glycerol 20%, GLY50= glycerol 50%, HYD= Hydrolite®-5, MLX= multiEx naturotics, PNP= Phenonip®, PG= propylene glycol, ROK= Rokonsal® PB-5 and TPGS= D-alpha tocopherol polyethylene glycol 1000 succinate)

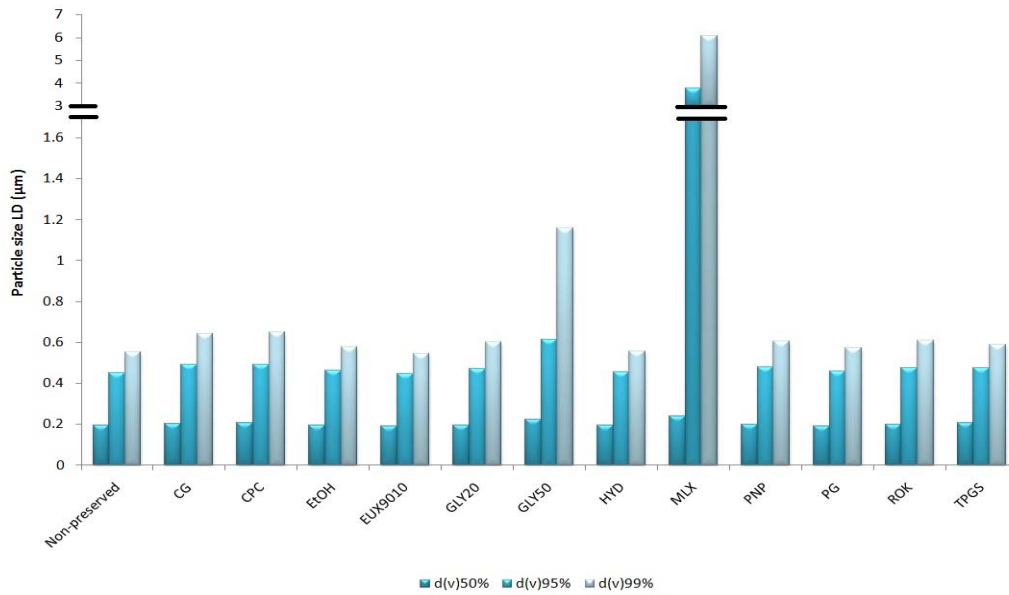
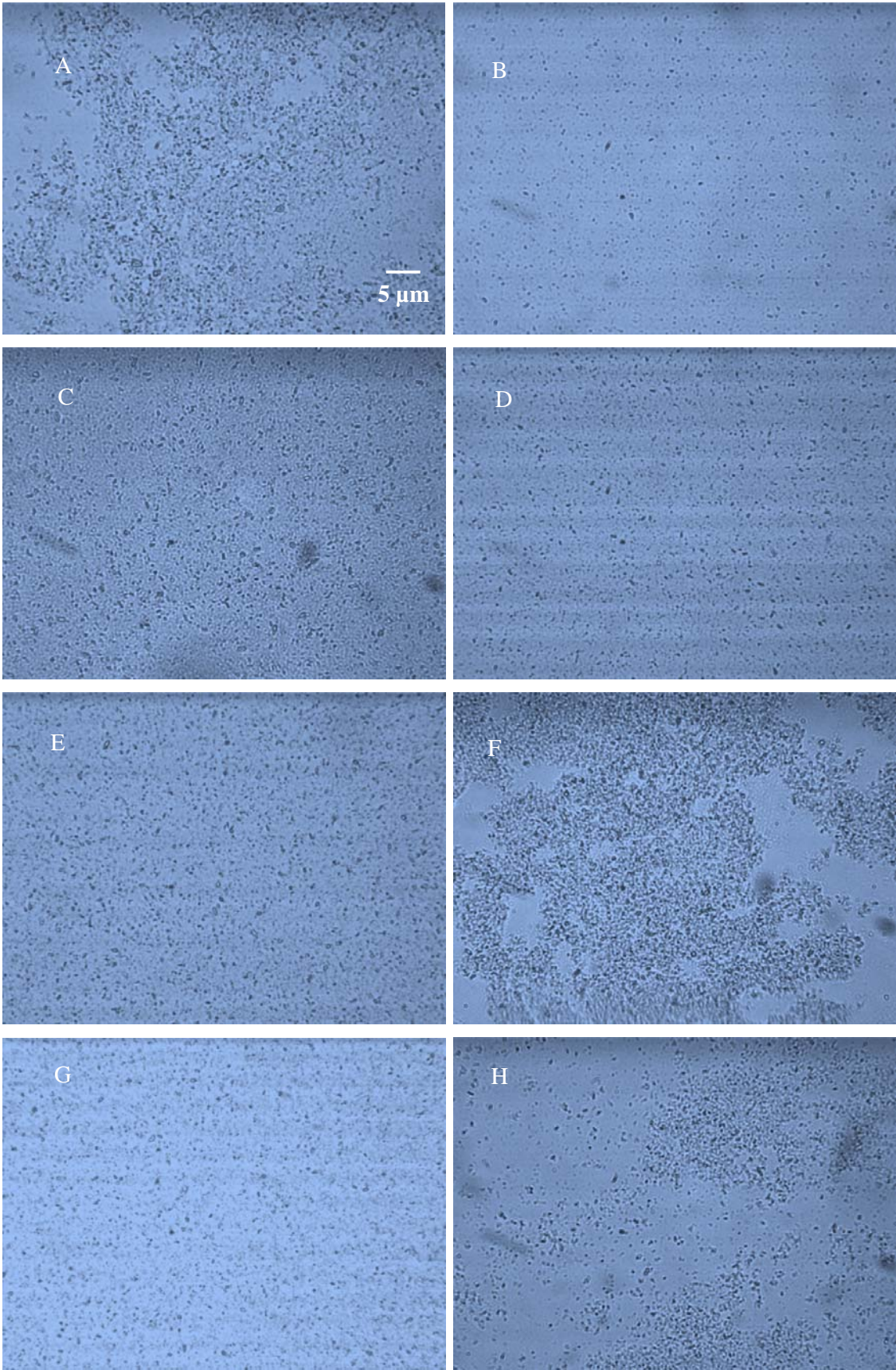
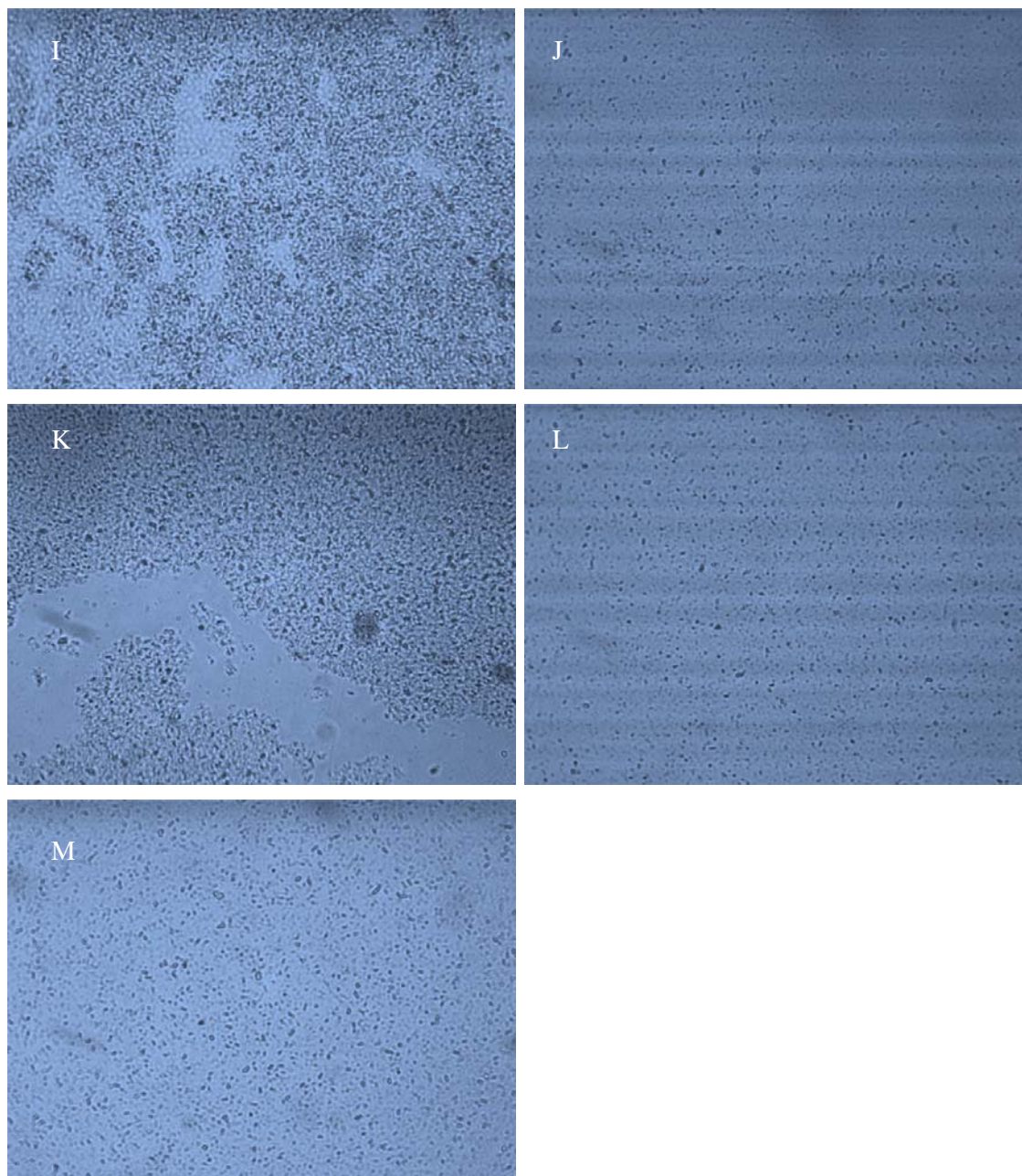


Fig. 102 LD diameter [µm] after addition of various preservatives (CG= caprylyl glycol, CPC= cetylpyridinium chloride, EtOH= ethanol, EUX9010= Euxyl® PE 9010, GLY20= glycerol 20%, GLY50= glycerol 50%, HYD= Hydrolite®-5, MLX= multiEx naturotics, PNP= Phenonip®, PG= propylene glycol, ROK= Rokonsal® PB-5 and TPGS= D-alpha tocopherol polyethylene glycol 1000 succinate)





**Fig. 103** Light microscopy images of apigenin nanosuspensions preserved with: (A) caprylyl glycol, (B) CPC, (C) ethanol, (D) Euxyl® PE 9010, (E) glycerol 20%, (F) glycerol 50%, (G) Hydrolite®-5, (H) multiEx naturotics, (I) Phenonip®, (J) propylene glycol, (K) Rokonsal® PB-5, (L) TPGS= D-alpha tocopherol polyethylene glycol 1000, (M) Non-preserved nanosuspension directly after admixing (magnification 1000 fold, bar = 5 µm)

The same conclusion was obtained by measuring the nanosuspensions with LD (Fig. 102). Even the nanosuspensions preserved with hydrophilic preservatives and the preservatives less hydrophilic had a good LD results as the one obtained from the non-preserved nanosuspension. This indicates loose agglomerates for the nanosuspensions preserved with the less hydrophilic preservatives. As for glycerol 50% and multiEx naturotics the agglomerates were so strong that the built-in stirrer was unable to disperse them (Fig. 102).

#### 4.2.5 Scale-up (smartCrystals®)

In order to produce smartCrystals® by the CT process, the pearl milling was employed as the first step followed by homogenizing using an Avestin C50. After the first passage the PCS diameter is about 1,550 nm, compared to about 350 nm after pre-milling in the HPH process. Applying a second passage led to a very distinct decrease to about 800 nm then followed by a slower decrease until completion of passage 5. This is the smallest size obtained; further passages until 7 have practically no effect on the size, and little effect on the PDI. After 7 passages, the mean particle size was 440 nm with a narrow polydispersity index of 0.265 (Fig. 104). A sharp decline in polydispersity index was observed from 0.588 to 0.265 from the 1<sup>st</sup> passage to the 7<sup>th</sup> passage.

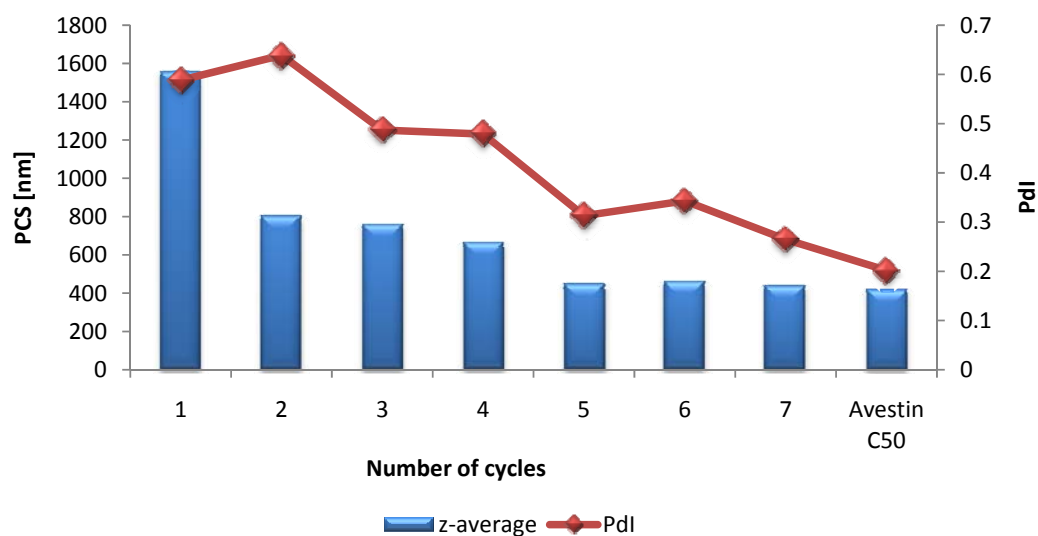


**Fig. 104 Particle size reduction measured with PCS (z-average) along with PDI reduction by producing using the pearl mill and followed with Avestin C50**

In some cases, a further decrease in size was observed in the final HPH step, sometimes the size stayed unchanged and only the PDI decreased. The latter was the case with the apigenin nanocrystals. With apigenin, the mean PCS particle size stayed practically unchanged, but further slight decrease in polydispersity index was observed. In the pearl mill process, the  $d(v)99\%$  decreased constantly till the 5<sup>th</sup> passage. Between the 5<sup>th</sup> and the 7<sup>th</sup> passage there was no change (Fig. 105). This confirms the PCS data that maximum dispersitivity has been reached after 5 passages. The diameter 50% of the raw material was 9.297  $\mu\text{m}$ . It dropped sharply to 0.223  $\mu\text{m}$  after the 1<sup>st</sup> passage, and then remained unchanged till the 7<sup>th</sup> passage, i.e. 0.231  $\mu\text{m}$ . This is identical to the observation with  $d(v)50\%$  in the lab scale production. However, a further reduction in  $d(v)50\%$  to 0.165  $\mu\text{m}$  was obtained after homogenizing the pearl milled nanosuspension with the Avestin C50, which is according to theory [73].

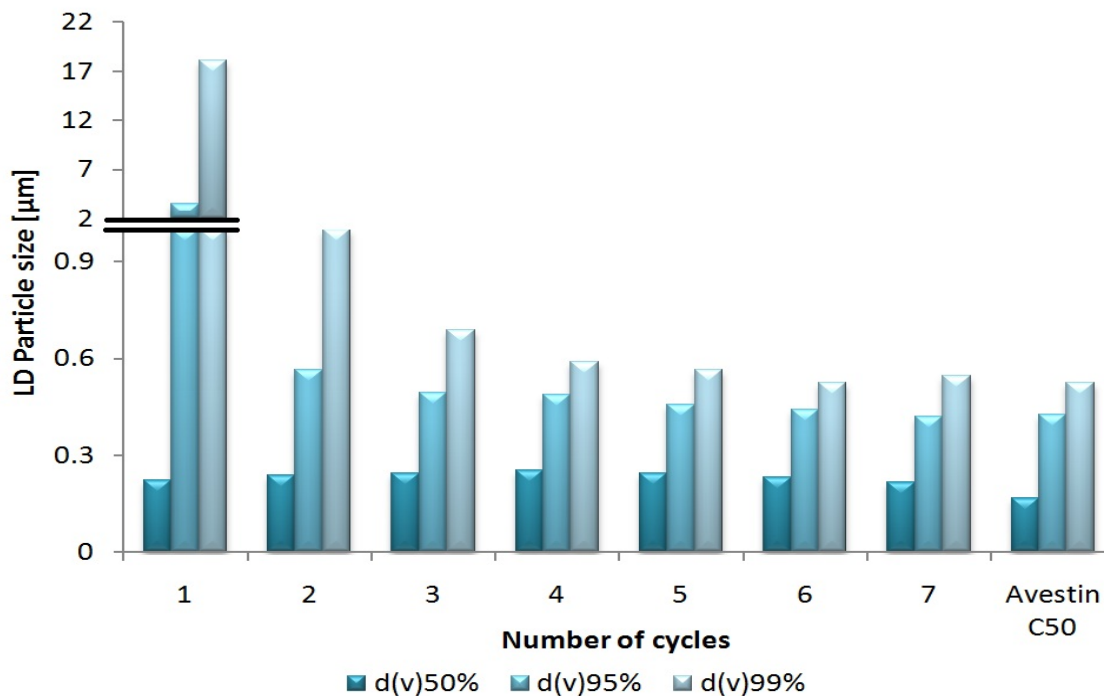


**Fig. 105 Particle size reduction measured with PCS (z-average) along with PdI reduction by producing using the pearl mill and followed with Avestin C50**

Commercial nanocrystals are produced and sold as aqueous concentrates, which are further processed into finished products for oral or dermal application. For reasons of safety against microbial contamination, preservation of the concentrates is essential. In addition, certain final formulations, e.g. multi-dose oral nanosuspensions, also need to be preserved. However, many preservatives can negatively affect the suspension stability, particularly in case of highly dispersed colloidal systems such as nanosuspensions. Hence, a systematic screening of preservatives is essential to identify preservatives having no destabilizing effect.

Till date many different preservatives from natural and synthetic origin are being used for preservation of different dosage forms. A total of 12 preservatives including mixtures were screened for their potential non-destabilizing effect on apigenin nanocrystals. Selection was performed on experiences with preserved hesperetin nanosuspensions [138], but also using some different, previously not yet investigated preservatives. The measurements were performed immediately after addition of the preservatives and after 1 month of storage, and the data compared with the non-preserved nanosuspension. In addition HPLC analysis was performed to confirm unaffected chemical stability of the nanosuspensions.



#### 4.2.5.1 Ethanol and glycols

Ethanol is approved GRAS status in the US as direct human food ingredient [107]. Ethanol has amphiphilic properties because of hydrophobic alkane ethane and a polar hydroxyl group. It has been used for centuries as disinfectant or antiseptic. The antimicrobial activity of alcohols is due to their ability to disorganize lipid membranes by penetration into the hydrocarbon microbial membrane region, thereby disrupting hydrophobic interactions of cytoplasm and proteins. Also the cell metabolism is affected because of distorted distribution of metabolites within the cell. This phenomenon can be compared to heat shock proteins in bacteria and yeast [149]. In general, short chain alcohols greater changes in membrane disorganization than the higher homologues. A patent by Kuchen (1963) describes preservative action of ethanol for food products. Spirits are self-preserving above about 20% alcohol concentration. The effect of ethanol and other alcohols on microorganisms have been reviewed by Ingram and Buttke [150, 151].

Based on these considerations, the effect of ethanol was investigated at 20% w/w of added 97% ethanol. The ethanol preserved nanosuspensions showed mean particle size of 329 nm, even below the 400 nm in the non-preserved nanosuspension. This is only explainable by dissolving of nanocrystals, because of the solubility of apigenin in ethanol. The polydispersity index remained low with a value of 0.180. The laser diffractometry data confirmed that the physical stability was not affected, 99% particles were below about 500 nm (practically identical to non-preserved nanosuspension, (Fig. 106)). From this 20% ethanol appears as suitable preservative. These results were proved by light microscopy (Fig. 107).

Glycerol at certain concentration levels are known for their antimicrobial activity [107] and can be used as sole preservatives. Most of the glycols are used as humectants; however they can be used as preservatives at concentration higher than 18%. It was found that the antibacterial effect of short chain glycols depends on the number of carbon atoms and on the position of the hydroxyl moiety within the molecule. Bar and Thice (1957) suggested that the antimicrobial activity of propylene glycol is related to the presence of a free methyl group. Caprylyl glycol shows antimicrobial efficacy against gram positive and gram negative bacteria. Glycerol is also an excellent preservative (bacteriostatic) [152]. FDA circular 21 CFR 610.15 suggest products in multiple dose containers should contain a preservative, except that a preservative does need not be added to products containing 50 percent or more (v/v) glycerol. On the other side, the hand book of pharmaceutical excipients defines the preservation limits of glycerol in concentrations of 20% [107]. The investigated concentrations of the glycols are based on the above outlined considerations.

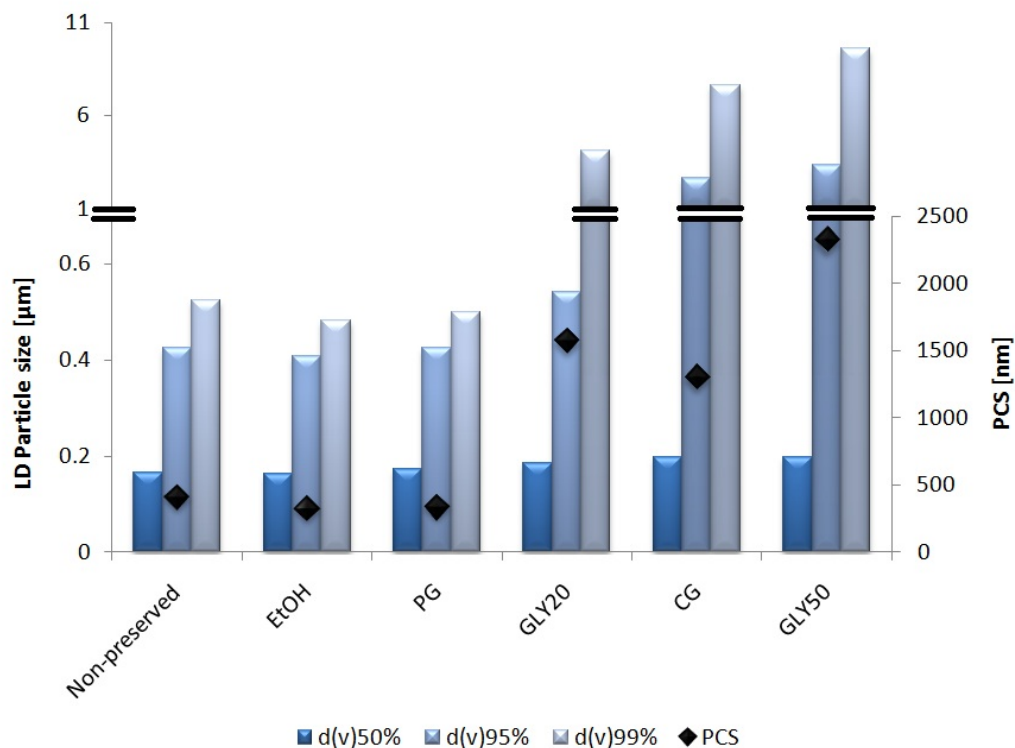


**Fig. 106 Comparative effect of alcohol and glycol preservatives (EtOH= ethanol, PG= propylene glycol, GLY20= glycerol 20%, CG= caprylyl glycol and GLY50= glycerol 50%) on mean particle size (PCS diameter) and LD diameter i.e. d(v)50%, d(v)95% and d(v)99% of apigenin nanosuspension on the day of production**

The glycols showed different effects on the stability of the nanosuspension. Glycerol at 50% (w/w) concentration showed a dramatic increase in the mean PCS particle size to 2,323 nm and in the d(v)50% to >1 µm. Reduction in the glycerol concentration to 20% (w/w) resulted in less destabilization. The mean PCS particle size obtained was 1,574 nm which was still almost 4 times higher than that of original nanosuspensions. These aggregates were detected as well by light microscopy (Fig. 107). Below the concentration of 20% one does not get a sufficient preservative effect in many products. Therefore glycerol as a single preservative was not considered as suitable (Fig. 106).

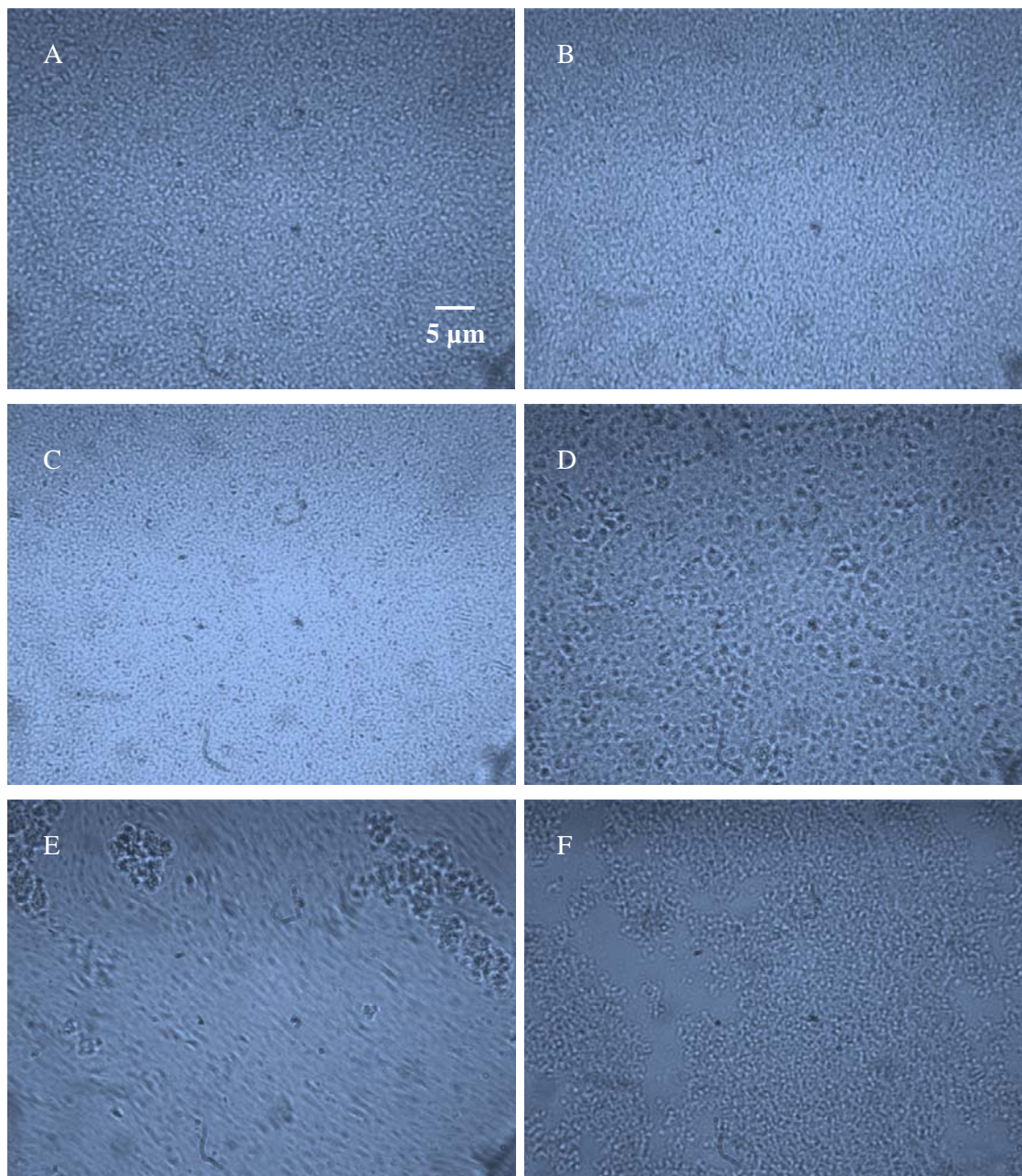


**Fig. 107** Light microscopy images of apigenin smartCrystals® (A) non-preserved and preserved with: (B) ethanol, (C) propylene glycol, (D) glycerol 20%, (E) caprylyl glycol and (F) glycerol 50% directly after admixing (magnification 1000 fold, bar = 5 µm)

Caprylyl glycol behaved similar to glycerol giving a distinctly higher mean PCS particle size (1,304 nm). The  $d(v)99\%$  was 7.629 µm which confirmed the presence of crystal aggregates about and more than 3.00 µm. Therefore caprylyl glycol is not suitable (Fig. 107). In contrast to this propylene glycol acted as good, non-destabilizing preservative not affecting the physical and chemical stability at a concentration of 20% (w/w). The mean particle size of propylene glycol stabilized nanosuspensions was about 345 nm, the  $d(v)50\%$  and  $d(v)99\%$  were 0.172 µm and 0.500 µm, respectively. The particle sizes were comparable to those of the

non-preserved nanosuspension, propylene glycol being therefore a suitable stabilizer (Fig. 107).

#### 4.2.5.2 Synthetic established single preservatives

Hydrolite<sup>®</sup>-5 (1,3 pentandiol) and triclosan are well known preservatives with proven antibacterial activity. Both exhibit strong antibacterial, antifungal and antiviral properties. Triclosan has been used for over 30 years and first been introduced in the health care industry in a surgical scrub in 1972.

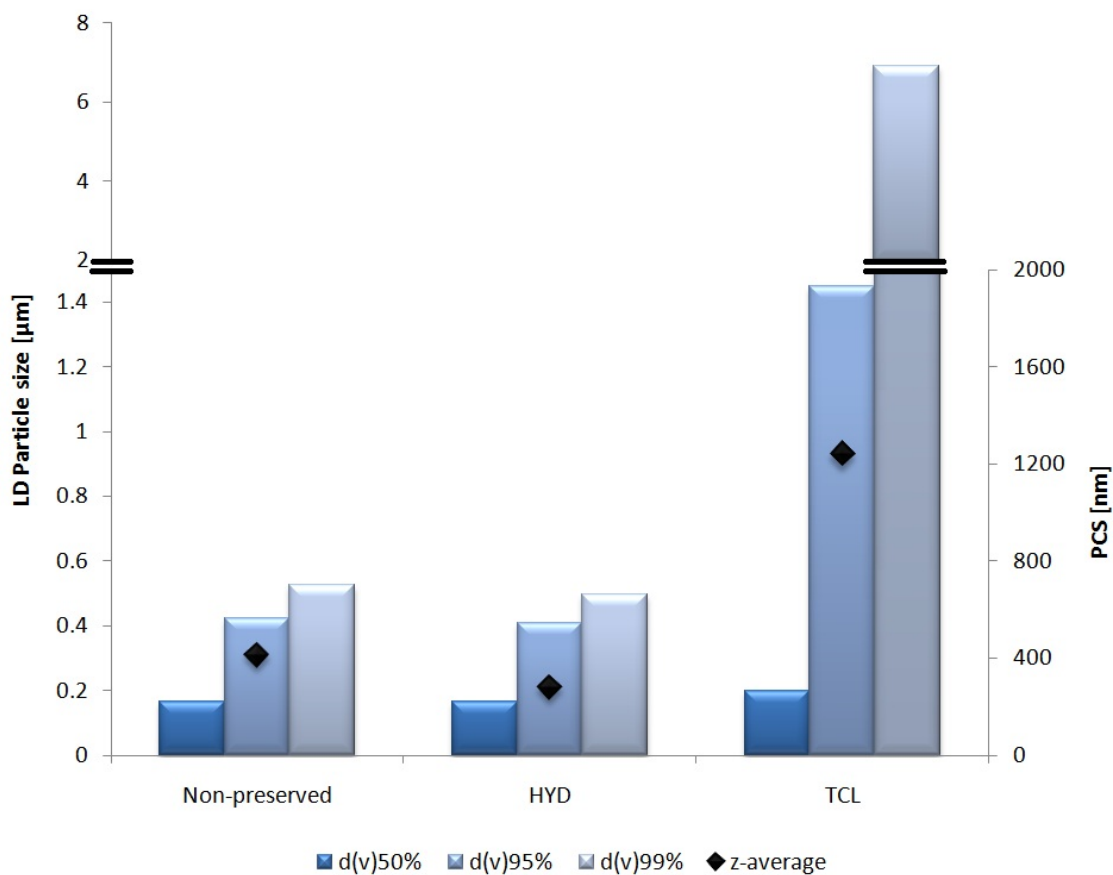


**Fig. 108 Comparative effect of synthetic established preservatives (HYD= Hydrolite<sup>®</sup>-5 and TCL= triclosan) on mean particle size (PCS diameter) and LD diameters i.e. d(v)50%, d(v)95% and d(v)99% of apigenin nanosuspension on the day of production**

Triclosan works by blocking the active site of the enoyl-acyl carrier protein reductase enzyme (ENR), which is an essential enzyme in the fatty acid synthesis in bacteria. By blocking the active site, triclosan inhibits the enzyme, and therefore prevents the bacteria from synthesizing fatty acids, necessary for building cell membranes and for reproduction. Since human do not have this ENR enzyme, triclosan has long been thought to be harmless to them.

Triclosan is a very potent inhibitor, therefore only a small amount is needed for powerful antibiotic action (applied concentration range 0.06-0.60%) [153].

At 5% concentration Hydrolite<sup>®</sup>-5 produced very stable nanosuspensions of apigenin with mean particle size of 280 nm and d(v)99% below 500 nm (Fig. 108). The preservative triclosan resulted in dramatic increase in particle size starting from the first day of production (Fig. 108). The mean particle size was much (3 fold) higher than that of standard suspension i.e unpreserved nanosuspensions. This may be due to interaction of active groups of triclosan and apigenin moiety. Immediately after addition of triclosan the changes were observed in particle aggregation. Fig. 109 shows the photomicrograph of apigenin smartCrystals<sup>®</sup> preserved with either Hydrolite<sup>®</sup>-5 or triclosan with comparison to non-preserved apigenin smartCrystals<sup>®</sup> on the day of production.

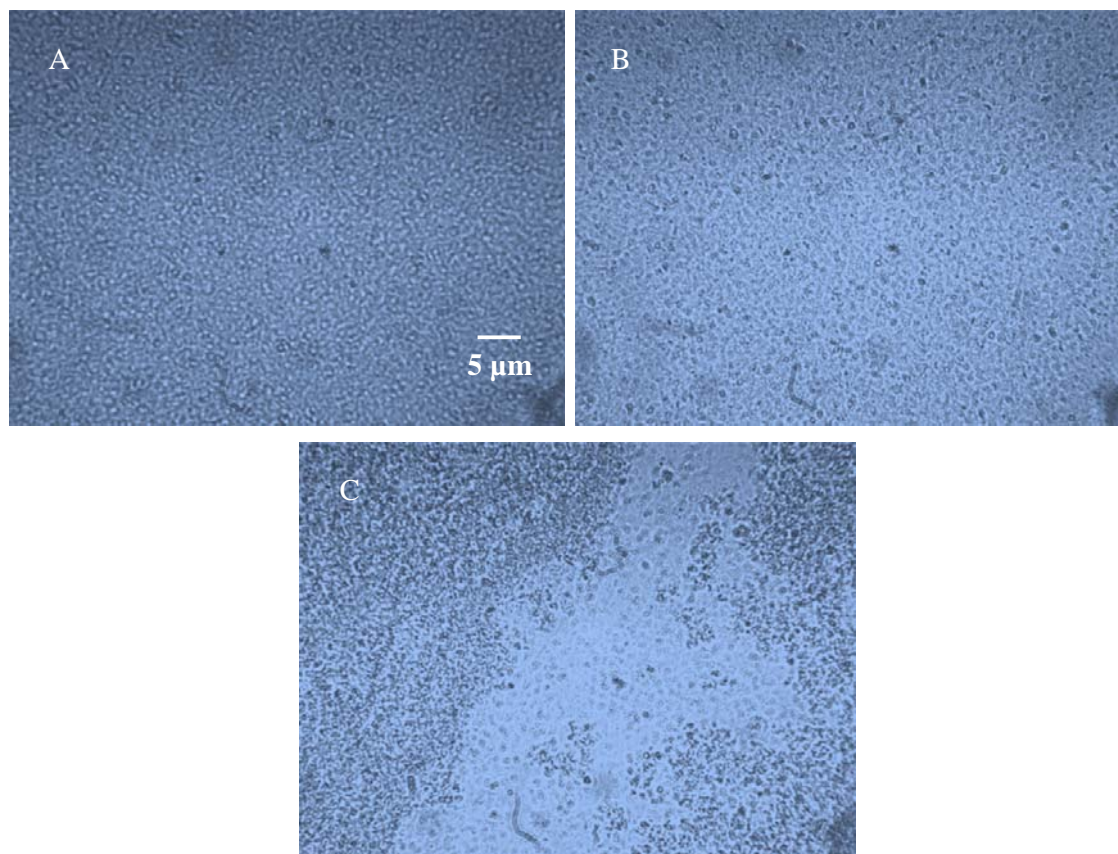


**Fig. 109** Light microscopy images of apigenin smartCrystals<sup>®</sup> (A) non-preserved and preserved with: (B) Hydrolite<sup>®</sup>-5, (C) triclosan directly after admixing (magnification 1000 fold, bar = 5 μm)

#### 4.2.5.3 Combinations of preservatives

Combinations of preservatives are often synergistic [154]. Euxyl<sup>®</sup> PE 9010 is the combination of phenoxyethanol and ethylhexylglycerin. Ethylhexylglycerin affects the interfacial tension at the cell membrane of microorganisms, in combination it improves the preservative activity

of phenoxyethanol [155]. Addition of Euxyl® PE 9010 to the nanosuspension did not affect PCS and LD diameters (Fig. 110). The PCS diameters were 413 nm and 375 nm, the LD diameters  $d(v)99\%$  - as very sensitive parameter towards the formation of aggregates - were  $0.525\ \mu\text{m}$  and  $0.500\ \mu\text{m}$  for the non-preserved and the Euxyl® PE 9010 preserved nanosuspensions, respectively. Based on this preservative is suitable for preservation.

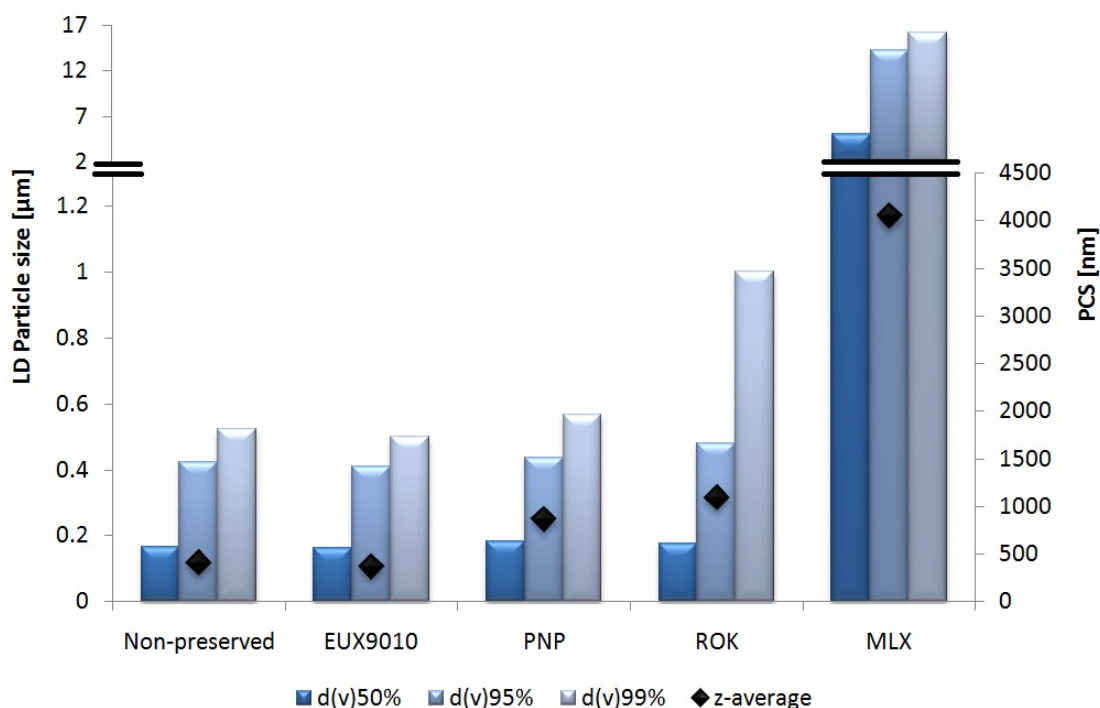


**Fig. 110** Comparative effect of combination of preservatives (EUX9010= Euxyl® PE 9010, PNP= Phenonip®, ROK= Rokonsal® PB-5 and MLX= multiEx naturotics) on mean particle size (PCS diameter) and LD diameters i.e.  $d(v)50\%$ ,  $d(v)95\%$  and  $d(v)99\%$  of apigenin nanosuspension on the day of production.

Phenonip® and Rokonsal® PB-5 are combinations of phenoxyethanol with different parabens of different percentages. They are broad spectrum liquid preservatives. Both of the preservatives resulted in  $d(v)50\%$  particle sizes  $< 200\ \text{nm}$  and  $d(v)95\% < 600\ \text{nm}$ , only for rokonsal PB-5 an increase in the  $d(v)99\%$  to about  $1\ \mu\text{m}$  was observed (Fig. 110). This pretended no effect (Phenonip®) or very little effect (Rokonsal® PB-5) on the size distribution of the nanosuspensions. However, the PCS diameters clearly identified aggregation of the nanocrystals. The PCS diameters were  $870\ \text{nm}$  for Phenonip®, and  $1099\ \text{nm}$  for rokonsal PB-5. Obviously the aggregates are very loose, therefore de-aggregated by the stirring in the LD measuring unit, but detectable in the non-stirred PCS measuring cell. The presence of aggregates was confirmed by light microscopy (Fig. 111). Due to the similar qualitative

chemical composition - despite quantitative differences -, both preservatives had clearly destabilizing effects on the stability, and are not considered as suitable.

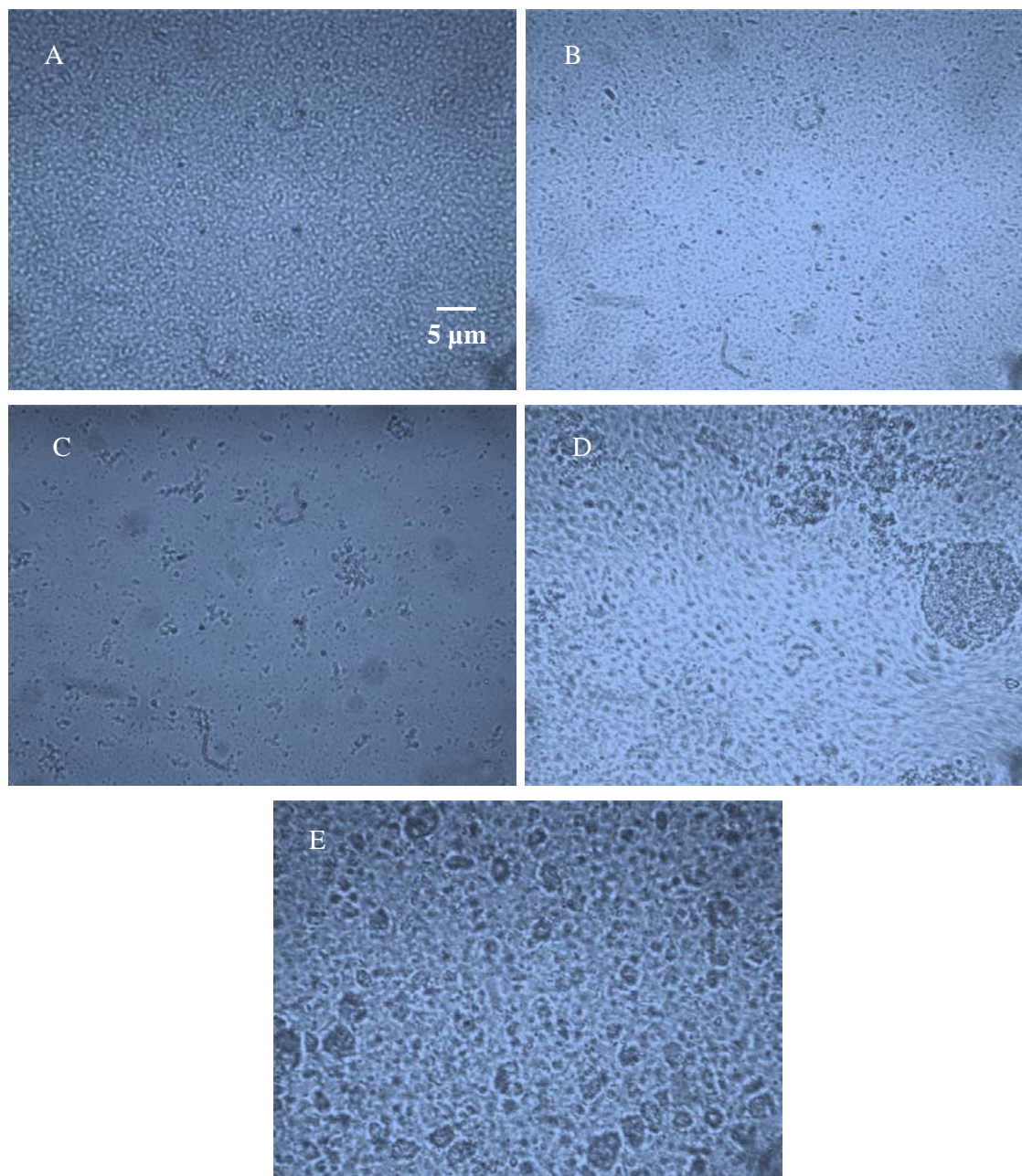


**Fig. 111** Light microscopy images of apigenin smartCrystals® (A) non-preserved and preserved with: (B) EUX9010= Euxyl® PE 9010, (C) Phenonip®, (D) Rokonsal® PB-5, (E) multiEx naturotics directly after admixing (magnification 1000 fold, bar = 5 μm)

MultiEx naturotics is a complex mixture of natural preservatives; major compounds are for example magnolol and honokiol. The addition to the nanosuspension leads to immediate, very pronounced aggregation. The PCS diameter measured was about 4,050 nm (practically outside the measuring range), the LD diameters  $d(v)_{50\%}$  and  $d(v)_{99\%}$  were 5.035 μm and 16.185 μm, respectively (Fig. 110).

#### 4.2.5.4 *Surface active agents*

The cationic surfactants possess distinct antimicrobial, membrane damaging effects. Therefore due to this toxicity effects they are less used for stabilization in pharmaceutical formulations. Main application is the preservative use. Cetylpyridinium chloride (CPC) is a cationic surfactant belonging to the group of quaternary ammonium compounds (QACs), and is a successful antiseptic and disinfectant [156]. The QACs are membrane active agents which are known to lower cellular surface tension, disrupt membranes, and cause loss of selective permeability of the bacterial cell membrane [157]. CPC was used in a concentration of 1%. As side effect, CPC reverses the charge of the nanosuspensions from negative to positive, making the nanocrystals more adhesive to negatively charged membranes.

The other surfactant types are not classical preservatives, but as surface active agents they have negative, damaging effects on bacterial membranes – especially at higher concentrations, which are typically not used for physical stabilization of dispersions. In general stabilizer concentrations are used as low as possible; to minimize side effects (e.g. cell membrane damage). The classical example for such damaging effects is the topical microemulsions, containing high concentrations of surfactants [112]. However in concentrated nanosuspensions such higher surfactant concentrations can be used, because for the final formulation these concentrates (and consequently the contained surfactants) are diluted by a factor 10-50. Therefore a Plantacare<sup>®</sup> 2000 UP concentration of 5% was investigated. Investigating the stability was essential, because sometimes higher stabilizer concentrations can even de-stabilize a suspension (e.g. by bridging, anchoring [158]). As additional surfactant tocopherol polyethylene glycol 1000 succinate (TPGS) was investigated in a concentration of 2.5%. TPGS is of interest, because as additional desired effect it promotes oral absorption of many compounds from the gut [146].

Addition of 4% Plantacare<sup>®</sup> 2000 UP, and addition of CPC (1%) and of TPGS (2.5%) to the nanosuspensions stabilized with 1% Plantacare<sup>®</sup> 2000 UP lead to a de-aggregation of some of the aggregates present, as clearly proven by the decrease in the diameters  $d(v)_{95\%}$  and  $d(v)_{99\%}$  (Fig. 112).



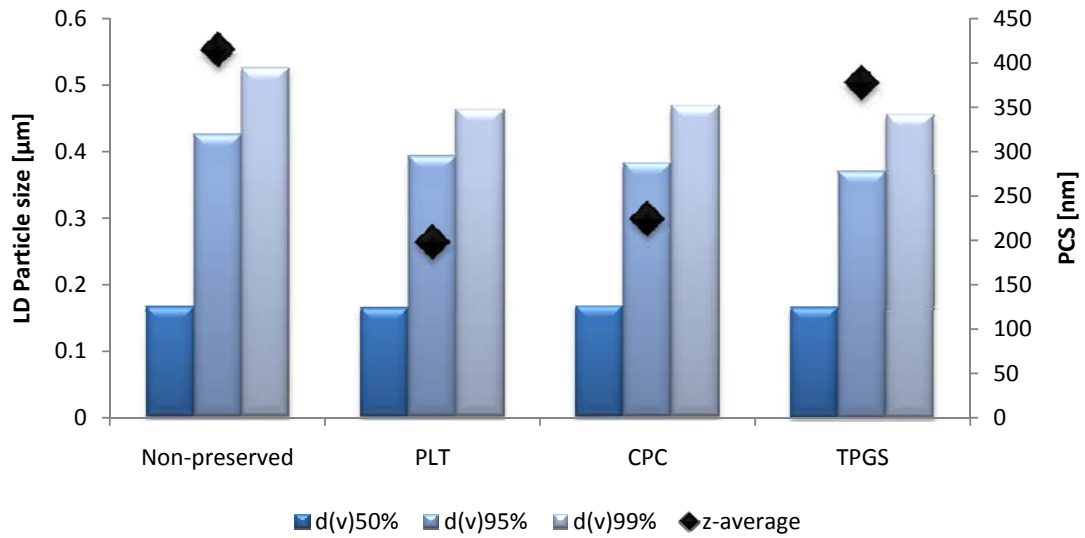


**Fig. 112** Comparative effect of surfactant preservatives (PLT= Plantacare<sup>®</sup> 2000 UP, CPC= cetylpyridinium chloride and TPGS= D-alpha tocopherol polyethylene glycol 1000 succinate) on mean particle size (PCS diameter) and LD diameters i.e. d(v)50%, d(v)95% and d(v)99% of apigenin nanosuspension on the day of production.

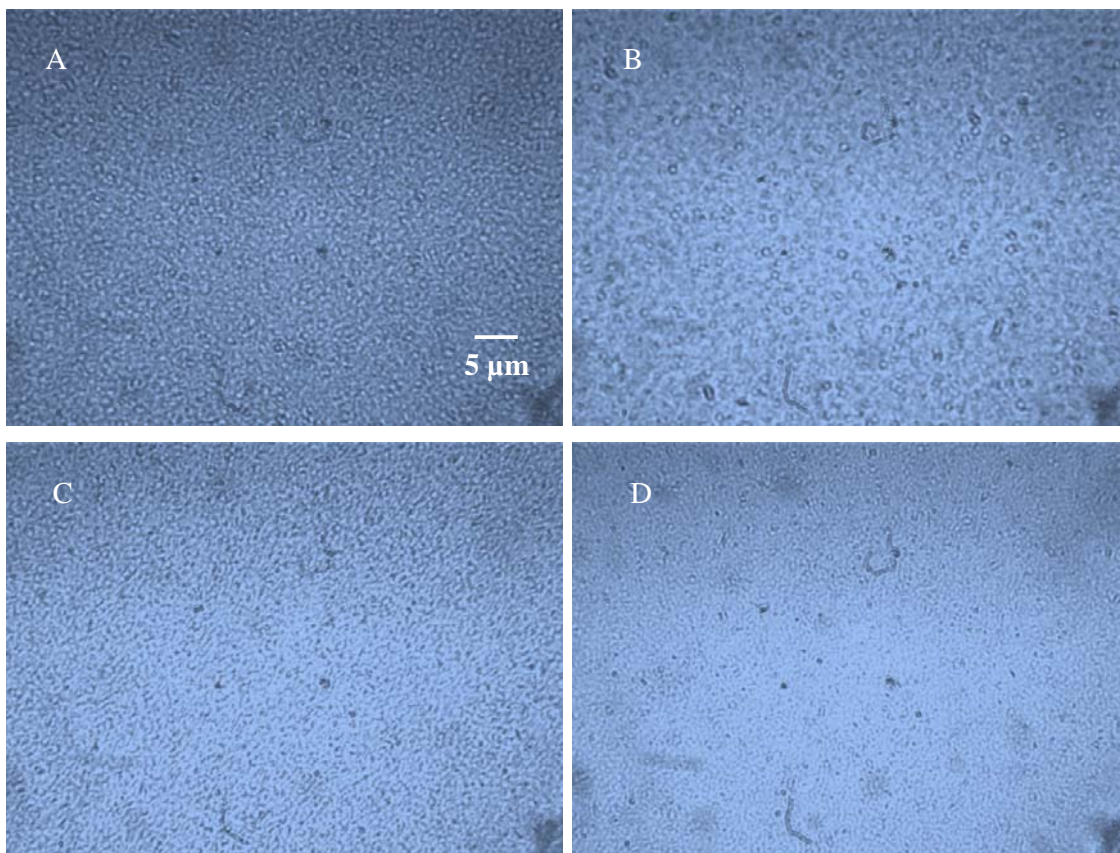


**Fig. 113** Light microscopy images of apigenin smartCrystals<sup>®</sup> (A) non-preserved and preserved with: (B) Plantacare<sup>®</sup> 2000 UP, (C) CPC= cetylpyridinium chloride and (D) TPGS= D-alpha tocopherol polyethylene glycol 1000 succinate directly after admixing (magnification 1000 fold, bar = 5 µm)

The increased Plantacare<sup>®</sup> 2000 UP concentration (4%+1%=5%) and the added CPC had such a de-aggregated effect that also a clear decrease in the PCS diameter to about 200 nm was

observed. To summarize: Addition of additional surfactant, to reach antimicrobial effects, did additionally improve the dispersivity of the nanosuspension by de-aggregation effects (Fig. 113).

#### 4.2.5.5 Zeta potential (ZP)

When measuring in distilled water, or water with very low conductivity, the measured zeta potential (ZP) is identical to the Stern potential. The Stern potential is related to the surface charge (Nernst potential), thus allowing to estimate the charge situation on the particle surface. ZP measurement in the original dispersion medium is a measure for the thickness of the diffuse layer, thus allowing to estimate the physical stability. For a purely electrostatically stabilized dispersion, the absolute value of the ZP should be above 30 mV (Riddick reference). In case steric stabilization is simultaneously present, also dispersion with 20mV and less can be long-term stable.

The ZP in water is in many cases higher, because the original dispersion medium contains often electrolytes, compressing the diffuse layer and leading to a low ZP. In addition when placing the sample in water for the measurement, molecules (non-charged stabilizers) adsorbed on the surface, covering the surface charge can be desorbed, leading to an increase in the ZP. However, most of the apigenin nanosuspensions showed similar ZP values (+/- 2 mV) in both water and original dispersion media (e.g. non-preserved nanosuspension: -42.6 mV in water, -40.0 mV in 1% Plantacare<sup>®</sup> 2000 UP solution). Only three showed a distinctly lower ZP in water (TPGS, multiEx naturotics, glycerol 50%). The reasons for these effects are not easily accessible and outside the scope of this paper. However important is, that the ZP values in the original dispersion media are all above -30 mV. That means theoretically from the ZP theory all the nanosuspensions should be physically stable. Therefore the destabilization is not due to a lack of charge, but obviously due to specific interactions between preservative molecules and the nanocrystals.

A very different behavior was observed for the nanosuspension containing 1% CPC. The measured ZP was +62.5 mV in water (conductivity adjusted) and -12.6 mV in the original dispersion medium (1% Plantacare<sup>®</sup> 2000, 1% CPC). In the original dispersion medium a mixed adsorption layer on the nanocrystals can be assumed, composed of both Plantare 2000 and CPC molecules. The composition is obviously this way, that Plantacare<sup>®</sup> 2000 UP dominates the charge property resulting in a charge still being slightly negative (ZP of non-preserved Plantacare<sup>®</sup> 2000 UP nanosuspension in original dispersion medium: -40.0 mV). Diluting the nanosuspension for the measurement in water seems to lead to a predominant

desorption of Plantacare<sup>®</sup> 2000 UP, while CPC remains, leading to the measured positive ZP of +62.5 mV (Fig. 114).

What are the implications of this for the physical stabilization effect? Due to the low ZP in the original dispersion medium, the nanosuspension is not sufficiently electrostatically stabilized. However, the nanosuspension proved to be stable, which is attributed to the sterically stabilizing effect of the Plantacare<sup>®</sup> 2000 UP. What is the implication for the in vivo situation? After administration, the CPC-preserved nanosuspensions will be diluted with body fluids (e.g. in the gut). A comparable effect can occur as in the measurement in water. The nanocrystals obtain a positive charge, being beneficial for adhesion to negative cell membranes.

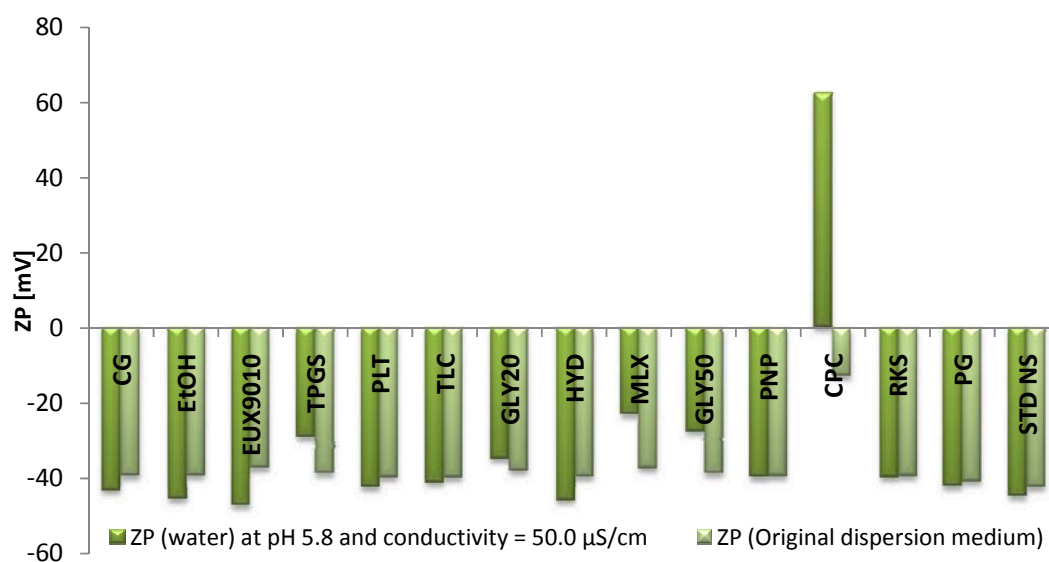


Fig. 114 ZP of the prepared nanosuspensions in conductivity-modified water and in dispersing medium (CG= caprylyl glycol, EtOH= ethanol, EUX9010= Euxyl<sup>®</sup> PE 9010, TPGS= D-alpha tocopherol polyethylene glycol 1000 succinate, PLT= Plantacare<sup>®</sup> 2000 UP, TLC= triclosan, GLY20= glycerol 20%, HYD= Hydrolite<sup>®</sup>-5, MLX= multiEx naturotics, GLY50= glycerol 50%, PNP= Phenonip<sup>®</sup>, CPC= cetylpyridinium chloride, RKS= Rokonsal<sup>®</sup> PB-5, PG= propylene glycol and STD NS= non-preserved nanosuspension)

#### 4.2.6 Incorporation in gels

The apigenin nanosuspensions were incorporated in gels prepared by the same jellifying agents used with hesperetin nanosuspensions. Further, the prepared gels were investigated for their physical characteristics after one month of addition and after one year storage.

#### 4.2.7 Long term physical stability

Stability was observed to all prepared nanosuspensions and smartCrystals in both preserved and nonpreserved forms. All samples were stored at 3 different temperatures 4°C, room temperature, and 40°C.

#### 4.2.7.1 Long term physical stability of lab scale preserved batches

Similarly to hesperetin, caprylyl glycol was not a suitable preservative for preserving apigenin nanosuspensions. The nanocrystals sample stored at 4°C showed no further increase in particle size after the addition of caprylyl glycol. On the other hand, z-average of samples stored at RT and 40°C showed continuous increase in particle size over the time (Fig. 115). By using light microscopy it was found that this inclination in particle size is only a result of particles aggregation (Fig. 116A). This could be due to the low solubility of caprylyl glycol in the nanosuspension, hence the 4°C sample caused less interference in the stability because of the possible crystallization of caprylyl glycol.

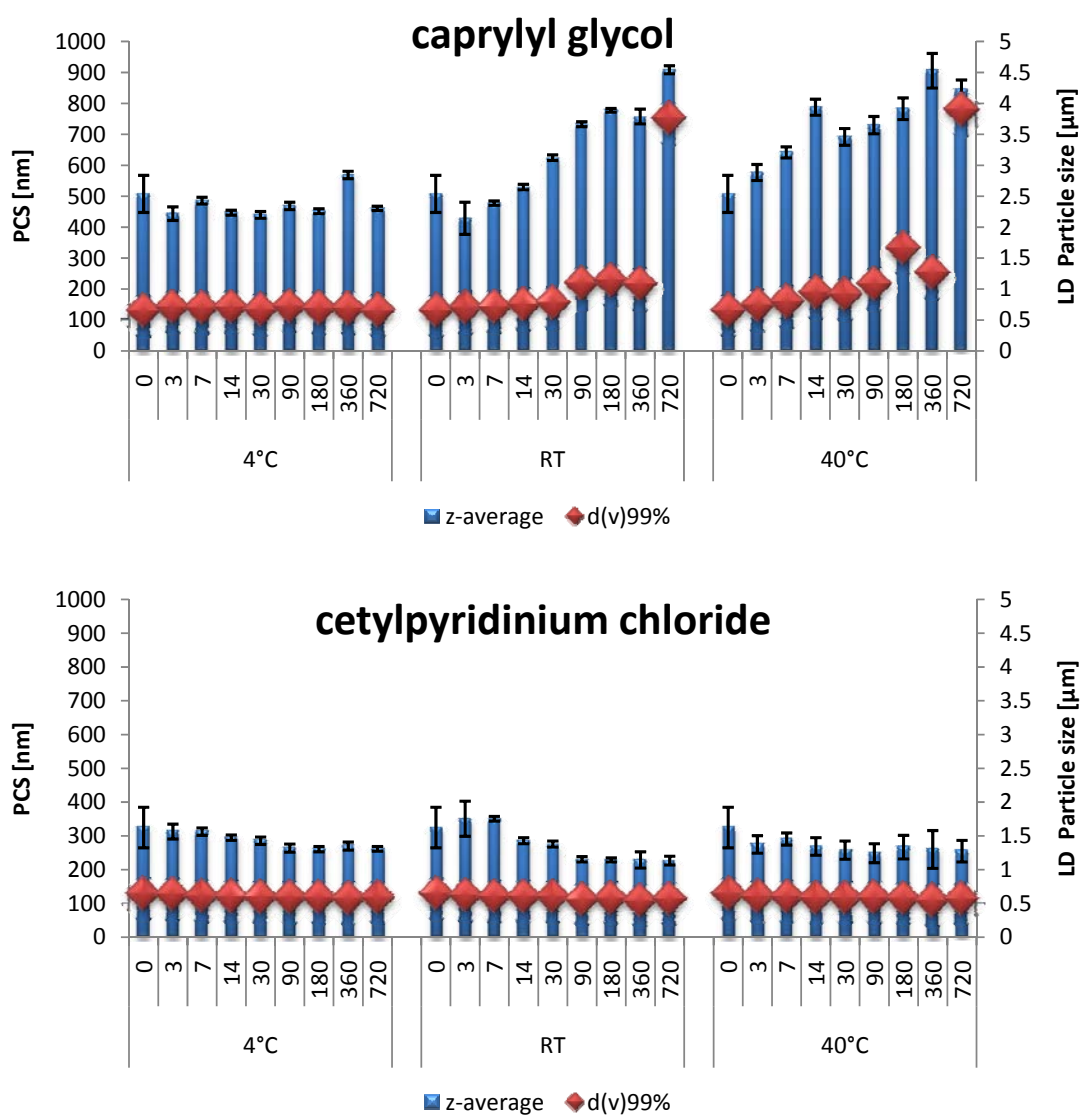
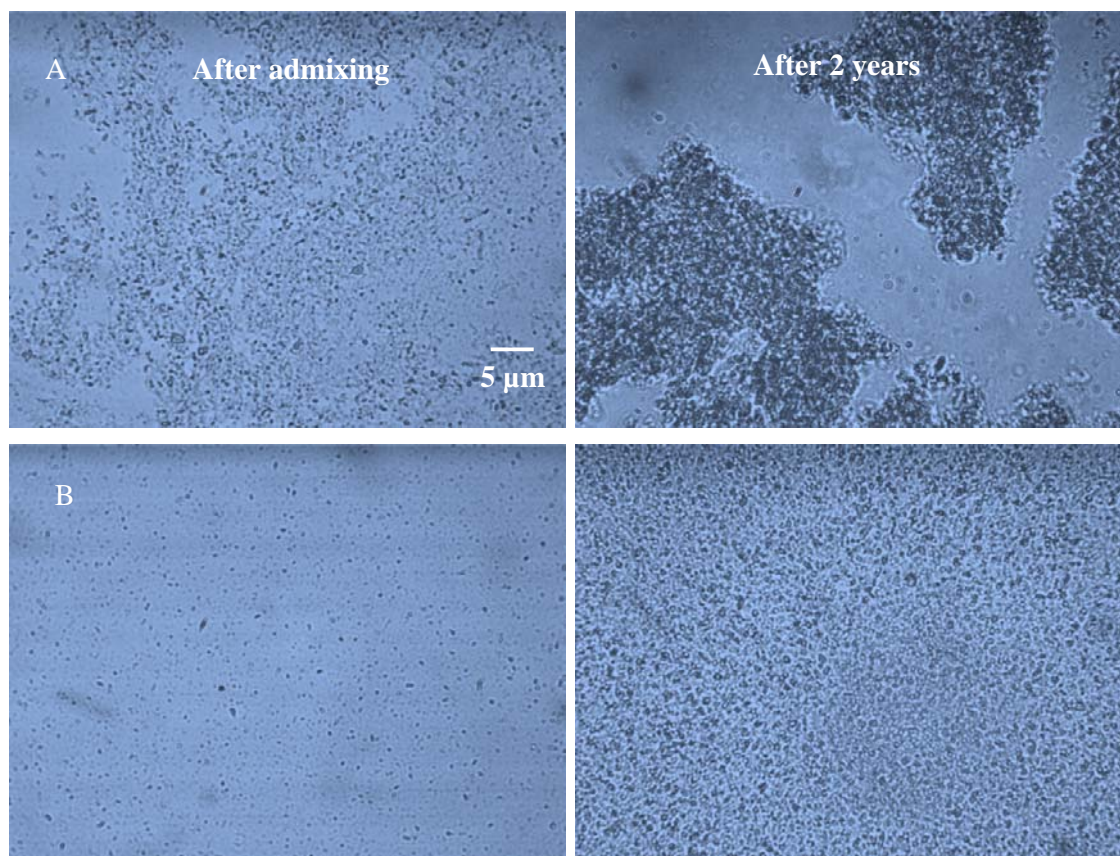


Fig. 115 Particle size of apigenin nanosuspensions preserved with caprylyl glycol and cetylpyridinium chloride stored at three different temperatures (4°C, RT & 40°C) as a function of time (days)

LD data showed the same results as PCS. An increase in  $d(v)99\%$  was seen and in a more obvious way in 40°C sample (Fig. 115).



**Fig. 116** Light microscopy images of nanosuspensions preserved with: (A) caprylyl glycol, (B) cetylpyridinium chloride. (magnification 1000 fold, bar = 5 µm). The right side is directly after production and the right side is after 2 years storage at room temperature

CPC samples were all stable over the storing period. However, the PCS data showed a small decrease in particle size which can be interpreted as increased solubility of the particles without any recrystallization (Fig. 115) [159]. This was confirmed by investigating the nanosuspensions with light microscopy (Fig. 116B).

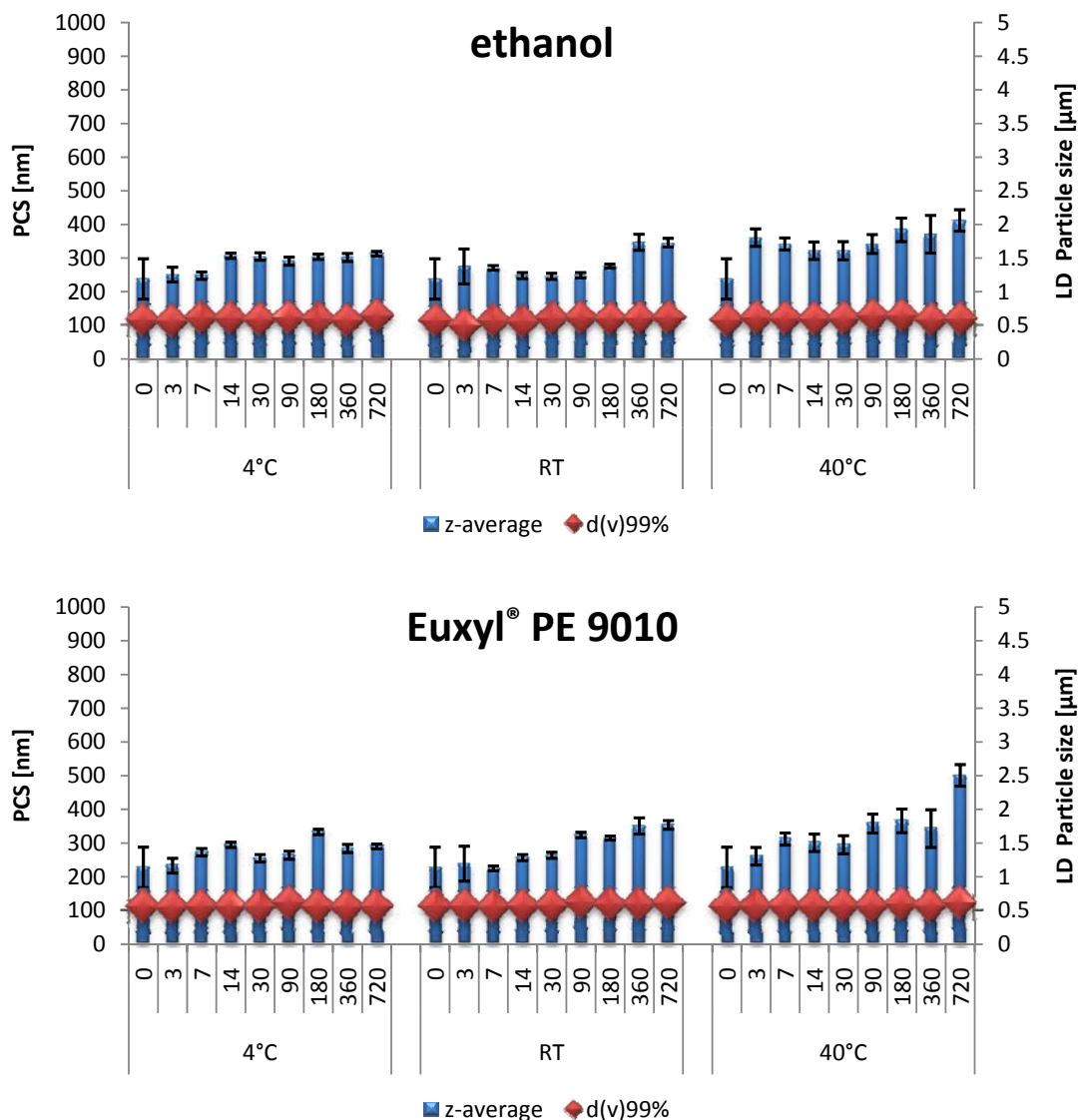
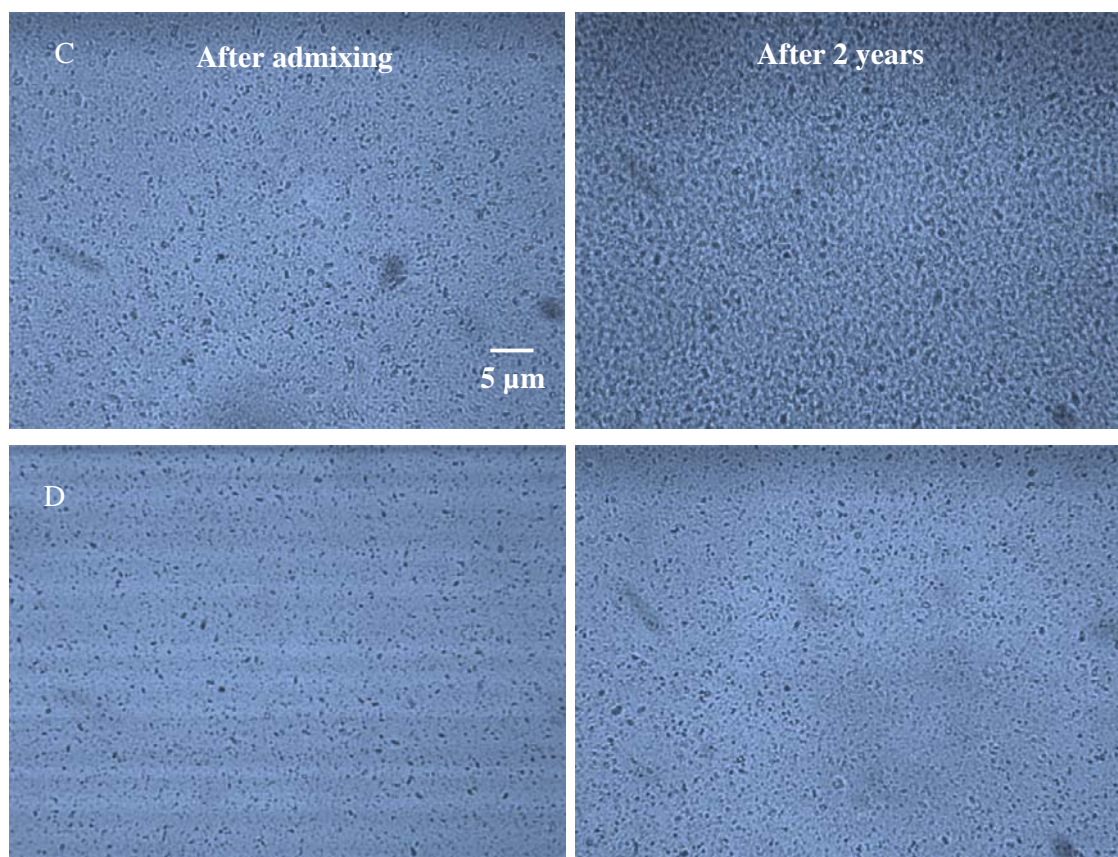


Fig. 117 Particle size of apigenin nanosuspensions preserved with ethanol and Euxyl® PE 9010 stored at three different temperatures (4°C, RT & 40°C) as a function of time (days).

Ethanol & Euxyl® PE 9010 as a hydrophilic preservatives behave as expected with no large increase in z-average or d(v)99% during the storing period (Fig. 117). Light microscopy confirmed the data obtained from PCS and LD for both preservatives (Fig. 118).



**Fig. 118** Light microscopy images of nanosuspensions preserved with: (C) ethanol and (D) Euxyl® PE 9010 (magnification 1000 fold, bar = 5  $\mu\text{m}$ ). The right side is directly after production and the right side is after 2 years storage at room temperature

Glycerol 20% and glycerol 50% had a strong aggregation effect on the nanosuspensions. However, the agglomerating effect of glycerol 20% was less intense than that of glycerol 50%. The increase in z-average was seen at both concentrations, but  $d(v)_{99\%}$  in glycerol 20% was comparable to that of the non-preserved apigenin nanosuspension which proves that these agglomerations are loose at 4°C and RT. At 40°C firmer aggregates can be seen with an increase in  $d(v)_{99\%}$ . However, these aggregates were not that loose in glycerol 50% samples (Fig. 119).

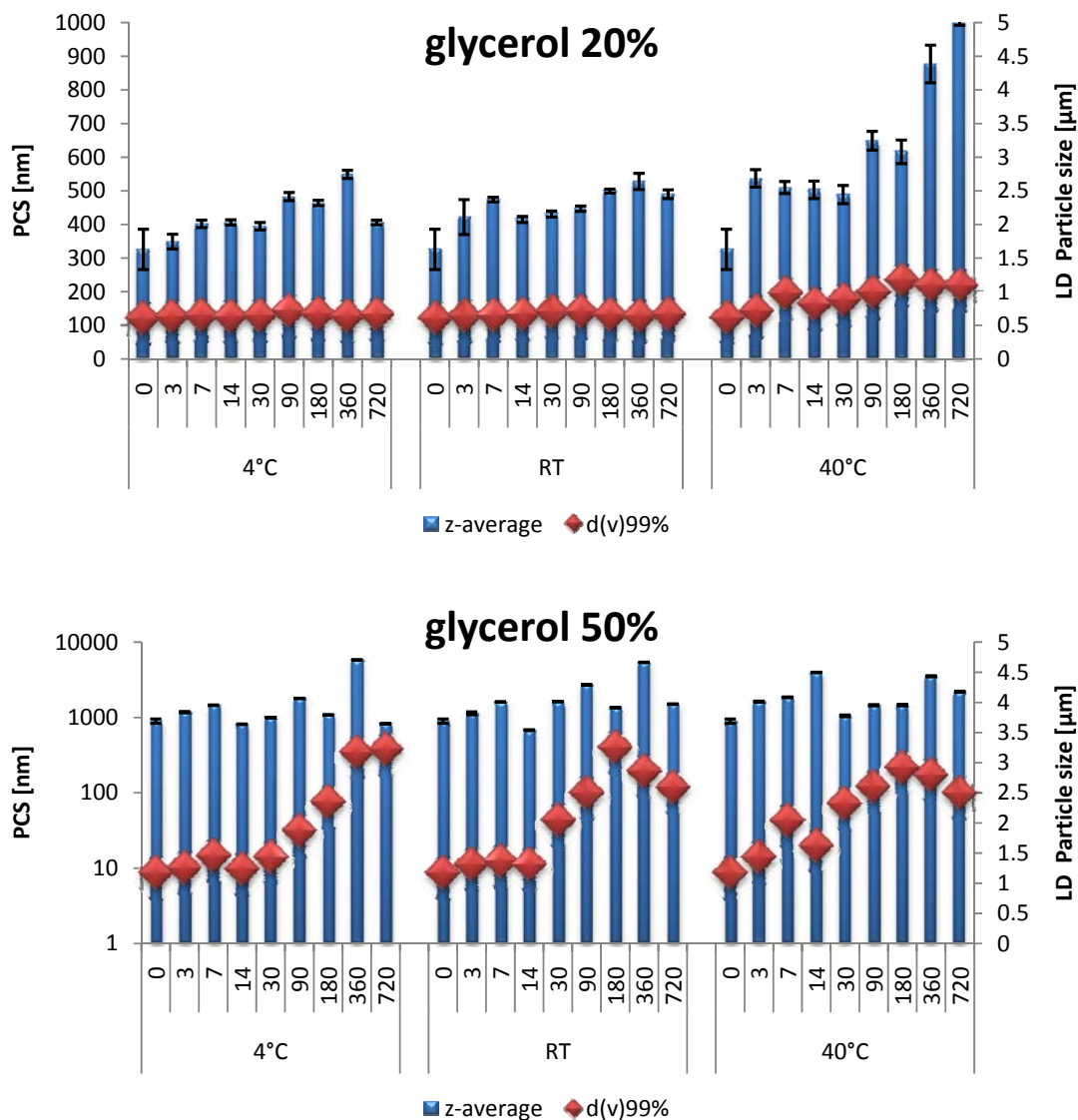


**Fig. 119** Particle size of apigenin nanosuspensions preserved with glycerol 20% and glycerol 50% stored at three different temperatures (4°C, RT & 40°C) as a function of time (days)

This difference was also detected in light microscopy pictures for both preservatives (Fig. 120). Oversized aggregates were found by investigating the apigenin nanosuspension preserved with glycerol 50%.



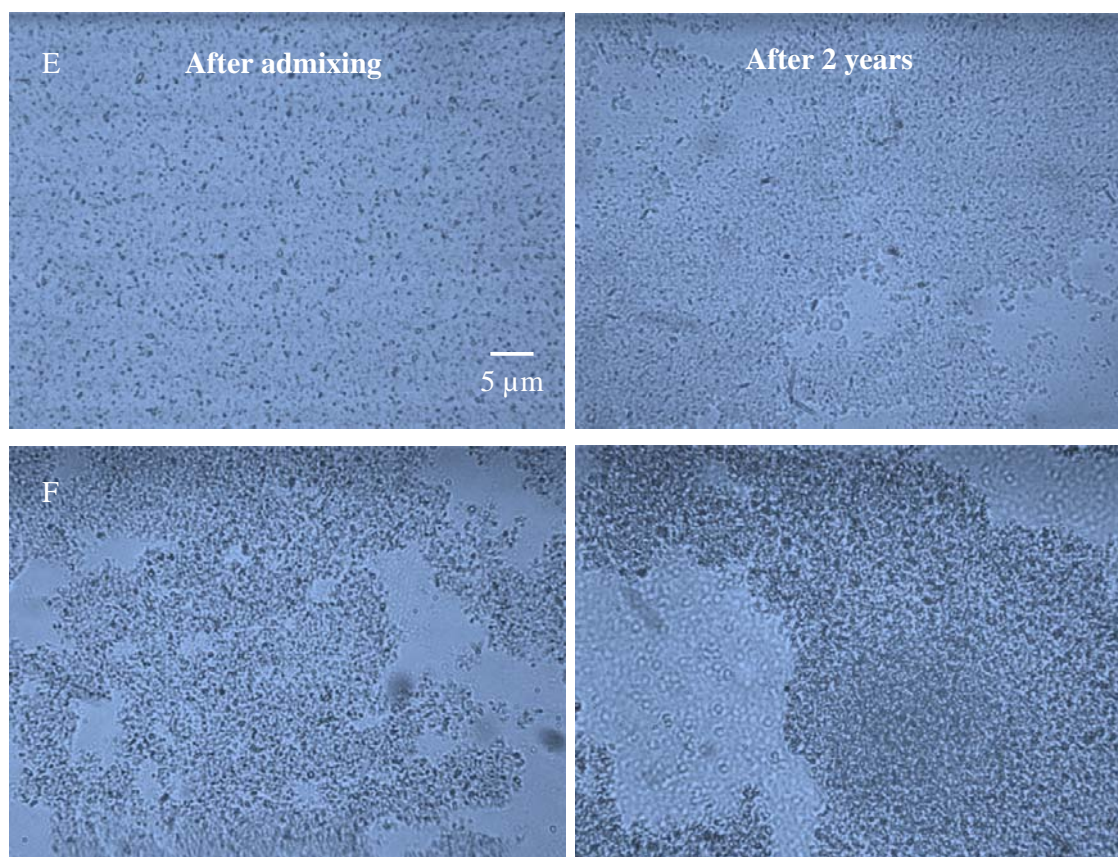


**Fig. 120** Light microscopy images of nanosuspensions preserved with: (E) glycerol 20% and (F) glycerol 50%. (magnification 1000 fold, bar = 5  $\mu\text{m}$ ). The right side is directly after production and the right side is after 2 years storage at room temperature

Apigenin nanosuspensions preserved with Hydrolite<sup>®</sup>-5 were stable the whole period of storage. No change in z-average or in  $d(v)99\%$  was detected except for the last measurement after 2 years where a small increase in particle size was seen (Fig. 121).

MultiEx naturotics preserved apigenin nanosuspensions showed non stable particle size (z-average) and particle size distribution ( $d(v)99\%$ ). This is possibly due to the presence of differently-sized aggregates in comparable results in both PCS and LD (Fig. 121).

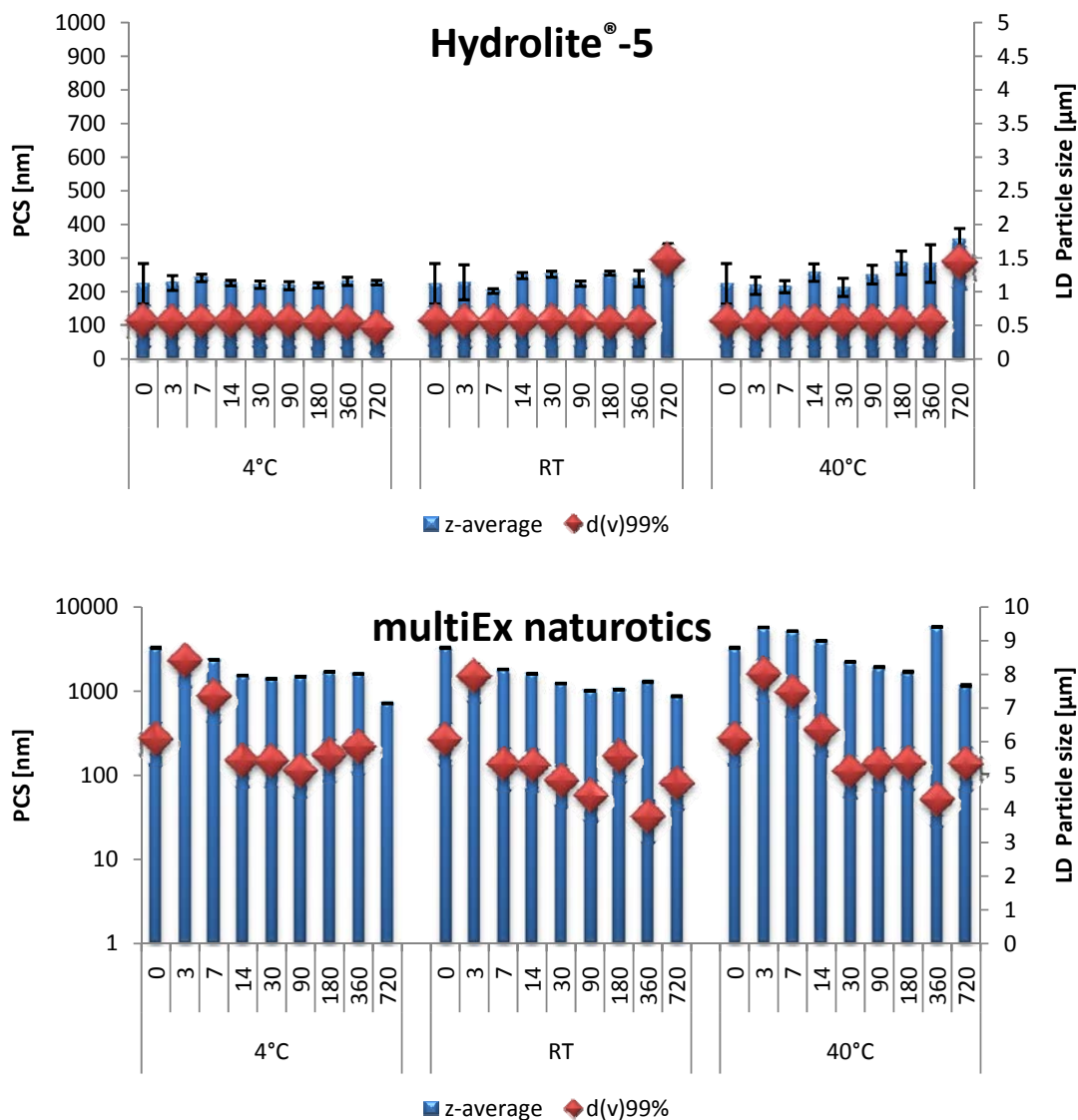


**Fig. 121** Particle size of apigenin nanosuspensions preserved with Hydrolite®-5 and multiEx naturotics stored at three different temperatures (4°C, RT & 40°C) as a function of time (days)

Large aggregates were detected for apigenin preserved nanosuspensions preserved with multiEx naturotics by using the microscope (Fig. 122H). On the contrary, no aggregates were found for Hydrolite®-5 ones (Fig. 122G).

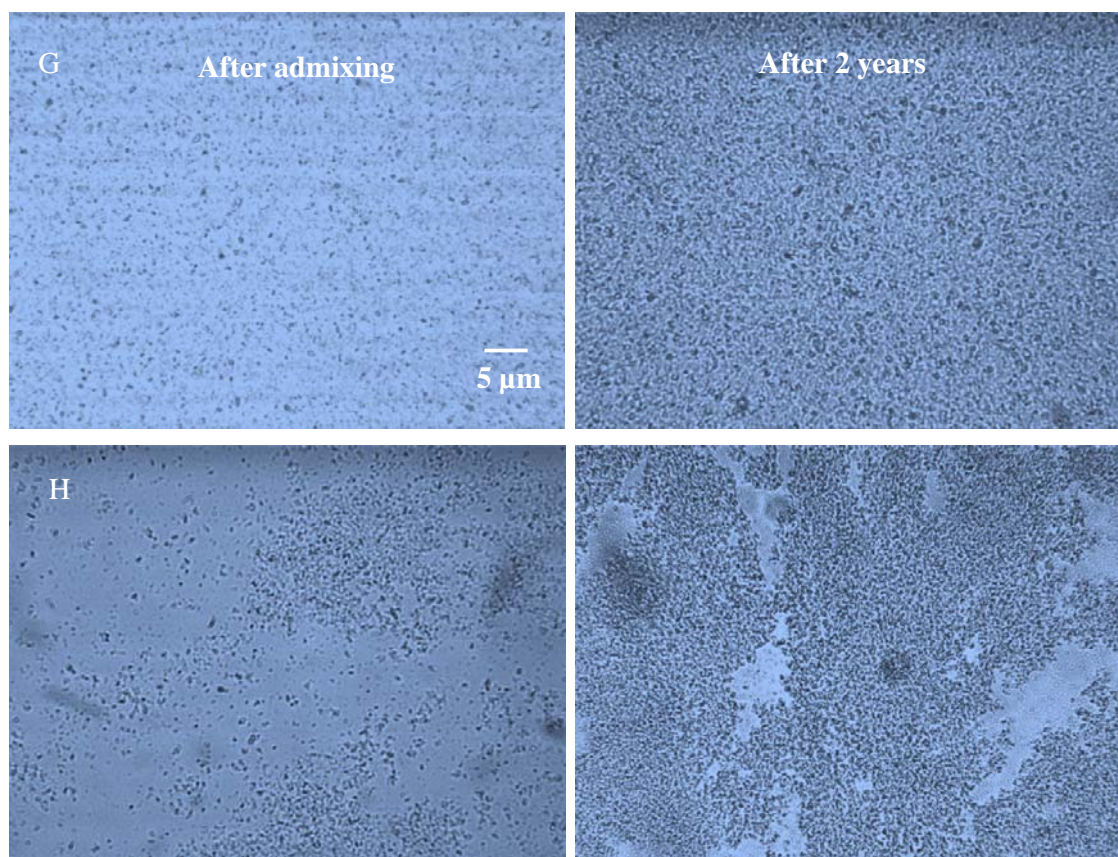


**Fig. 122** Light microscopy images of nanosuspensions preserved with: (G) Hydrolite<sup>®</sup>-5 and (H) multiEx naturotics. (magnification 1000 fold, bar = 5  $\mu\text{m}$ ). The right side is directly after production and the right side is after 2 years storage at room temperature

Apigenin nanosuspensions preserved with propylene glycol showed no significant increase on the particle size. A small increase was noticed in RT sample and 40°C sample. However, this ascending in z-average and d(v)99% can be regarded as a normal augmentation of particle size for nanosuspensions after such a long period of storage (Fig. 123). No difference in micropssscopic pictures were detected (124).

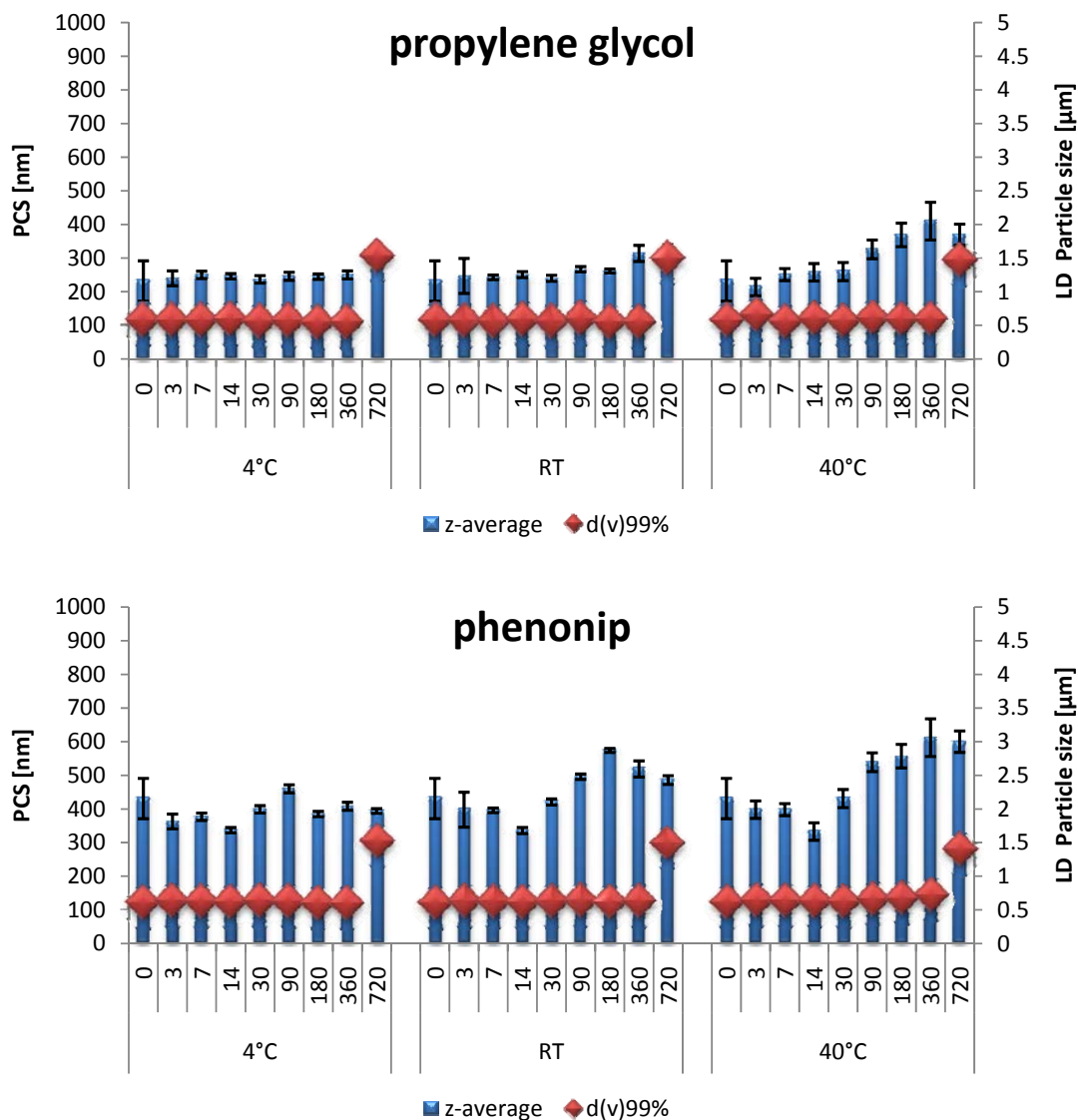
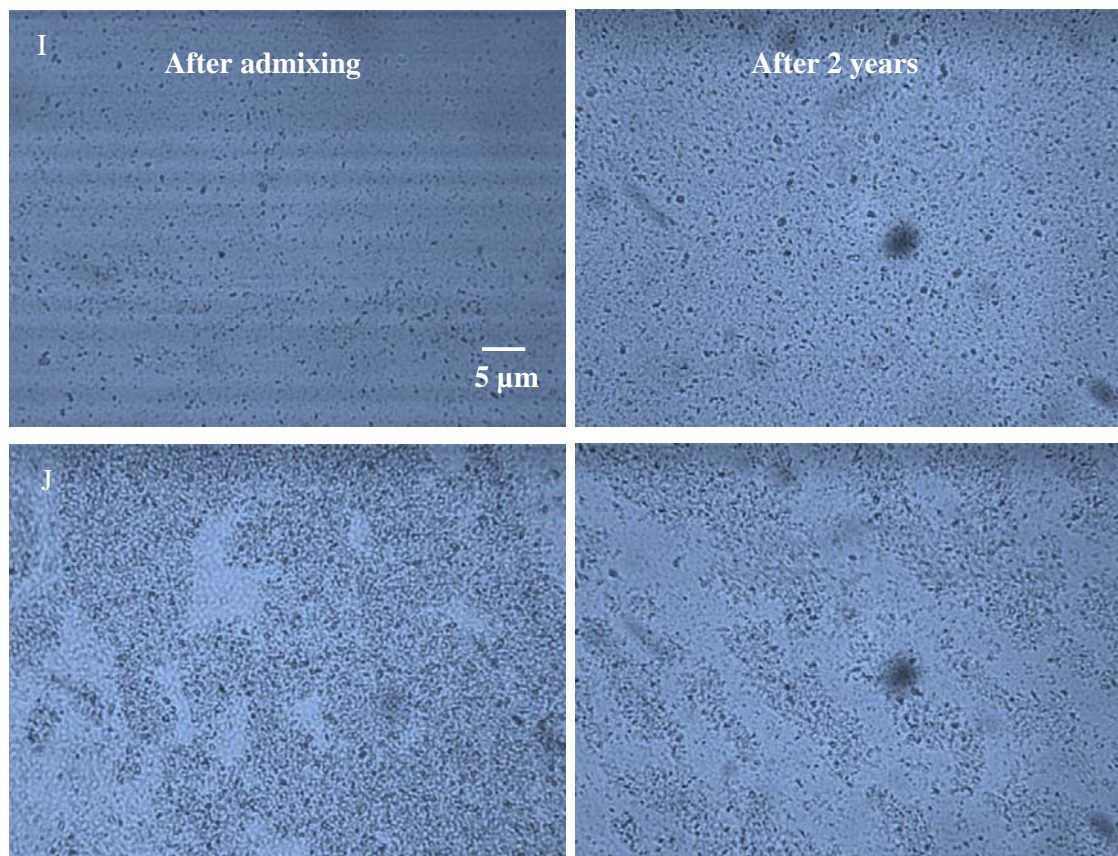


Fig. 123 Particle size of apigenin nanosuspensions preserved with propylene glycol and Phenonip® stored at three different temperatures (4°C, RT & 40°C) as a function of time (days)

Fig. 123 and Fig. 125 show the PCS and LD data of apigenin nanosuspensions preserved with Phenonip® and Rokonsal® PB-5, respectively. Particle size of Phenonip® preserved nanosuspension (z-average) showed no change till 14 days storage. This was followed with an increase in z-average because of agglomeration formation (Fig. 124J).



**Fig. 124** Light microscopy images of nanosuspensions preserved with: (I) propylene glycol and (J) Phenonip<sup>®</sup> (magnification 1000 fold, bar = 5  $\mu\text{m}$ ). The right side is directly after production and the right side is after 2 years storage

Apigenin preserved nanosuspensions with Rokonsal<sup>®</sup> PB-5 followed almost the same pattern but to a lesser extent, because of the enhanced hydrophilicity characteristics. LD data for both preservatives were similar and almost like the LD profile of the non-preserved nanosuspensions (Fig. 125). Agglomeration were detected in microscopic pictures which proves the increase in LD diameter (Fig. 126K)

Although TPGS showed good stabilization properties in hesperetin nanosuspensions but it did not give the same results when used with apigenin nanosuspension. An increase in z-average was noticed over the time reaching 500 nm after 2 years. However, staying under 1  $\mu\text{m}$  is still considered a good sign (Fig. 125).

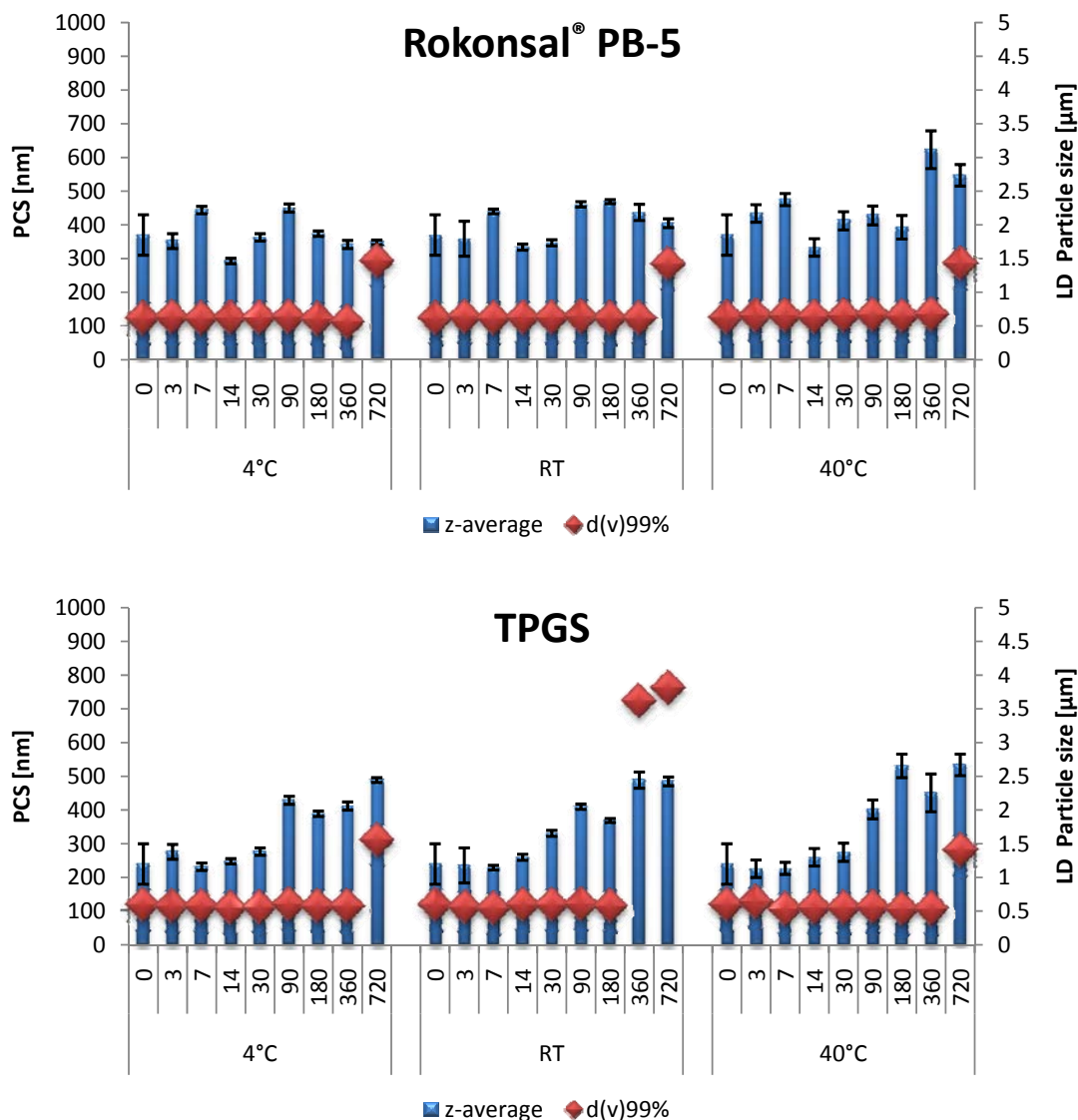


**Fig. 125** Particle size of apigenin nanosuspensions preserved with Rokonsal® PB-5 and TPGS= D-alpha tocopherol polyethylene glycol 1000 succinate stored at three different temperatures (4°C, RT & 40°C) as a function of time (days)

No agglomerates were detected by investigating the nanosuspension using microscopy (Fig. 126L). The d(v)99% stayed small over the storing period with a small decrease in the last measurement, which is comparable to the increase that happened in the non-preserved nanosuspensions (Fig. 127, 128M).

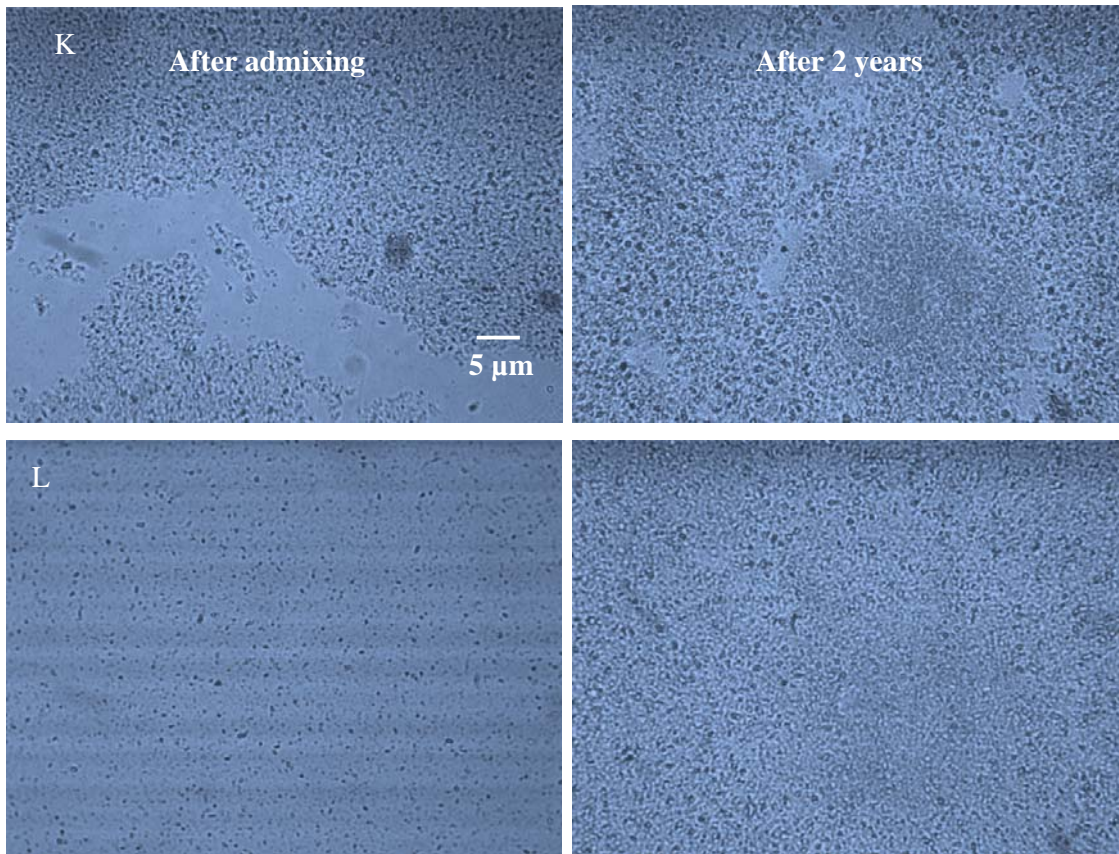


Fig. 126 Light microscopy images of nanosuspensions preserved with: (K) Rokonsal® PB-5 and (L) TPGS= D-alpha tocopherol polyethylene glycol 1000 succinate (magnification 1000 fold, bar = 5 μm). The right side is directly after production and the right side is after 2 years storage

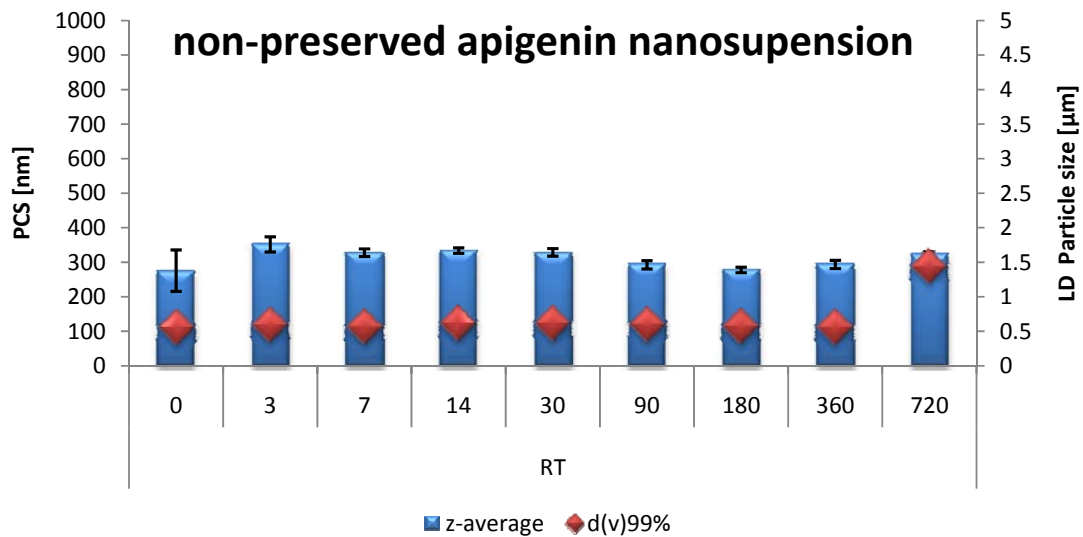


Fig. 127 Particle size of non-preserved apigenin nanosuspensions stored at RT as a function of time (days)

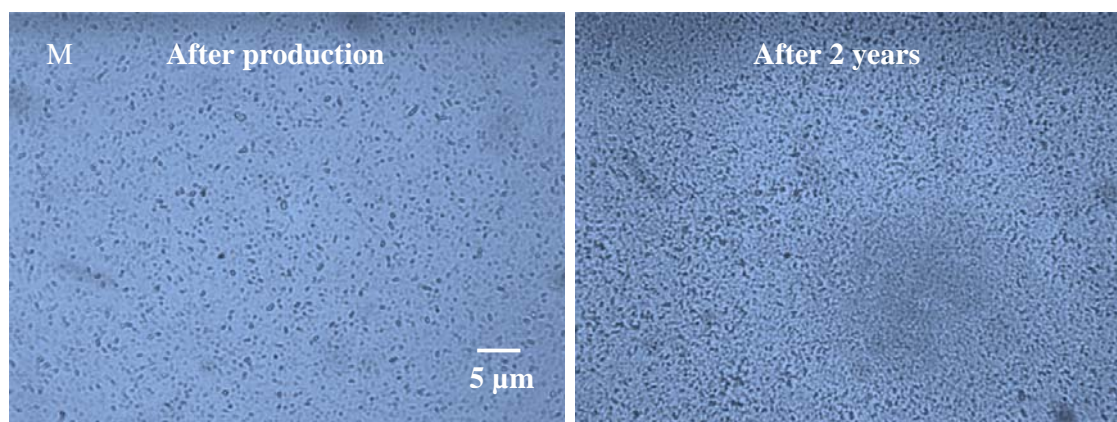


Fig. 128 Light microscopy images of (M) apigenin non-preserved. (magnification 1000 fold, bar = 5  $\mu\text{m}$ ). The right side is directly after production and the right side is after 2 years storage

#### 4.2.7.2 Long term physical stability of apigenin nanosuspensions incorporated in gels

Gels were admixed with water and were left to swell. The particle size (z-average) and LD diameter were measured after one week and after one year.

Apigenin nanosuspension incorporated in Tylose<sup>®</sup> 10000, Tylose<sup>®</sup> 30000 and CMCNa gels tended to agglomerate after admixing and after storing the samples at RT for one year. On the other hand, measuring the mentioned gels in PCS showed an increase in z-average compared to the original nanosuspensions. Using Carbomer<sup>®</sup> derivatives such as Ultrez 10, Ultrez 20 or even Ultrez 21 had no effect on the particle size distribution for the whole period of storage (Table 15).

Table 15 LD diameter for apigenin nanosuspensions incorporated in different gels after 1 month and 1 year

Gelling agent used	Size after 1 month [ $\mu\text{m}$ ]			Size after 1 year [ $\mu\text{m}$ ]		
	z-average	d(v)50%	d(v)99%	z-average	d(v)50%	d(v)99%
Tylose <sup>®</sup> 10000	2.682	28	400	3.493	111	511
Tylose <sup>®</sup> 30000	5.294	12	163	7.426	34	324
CMCNa	1.763	0.186	0.558	2.002	0.330	118
Ultrez 10	0.462	0.178	0.519	0.502	0.181	0.504
Ultrez 20	0.519	0.210	0.522	0.646	0.251	0.537
Ultrez 21	0.482	0.186	0.532	0.620	0.195	0.558

#### 4.2.7.3 Long term physical stability of smartCrystals<sup>®</sup>

The caprylyl glycol smartCrystals<sup>®</sup> had a similar PCS and LD profiles to that of the Micron LAB40 sample. However, the smartCrystals<sup>®</sup> were more affected by caprylyl glycol than the nanosuspension produced with the Micron LAB40. This is because the particle size reached



with smartCrystals<sup>®</sup> technology is smaller than that of Micron LAB40, hence more susceptible to physical changes (Fig. 129). Agglomerates can be distinctly seen using the microscope (Fig. 130A)

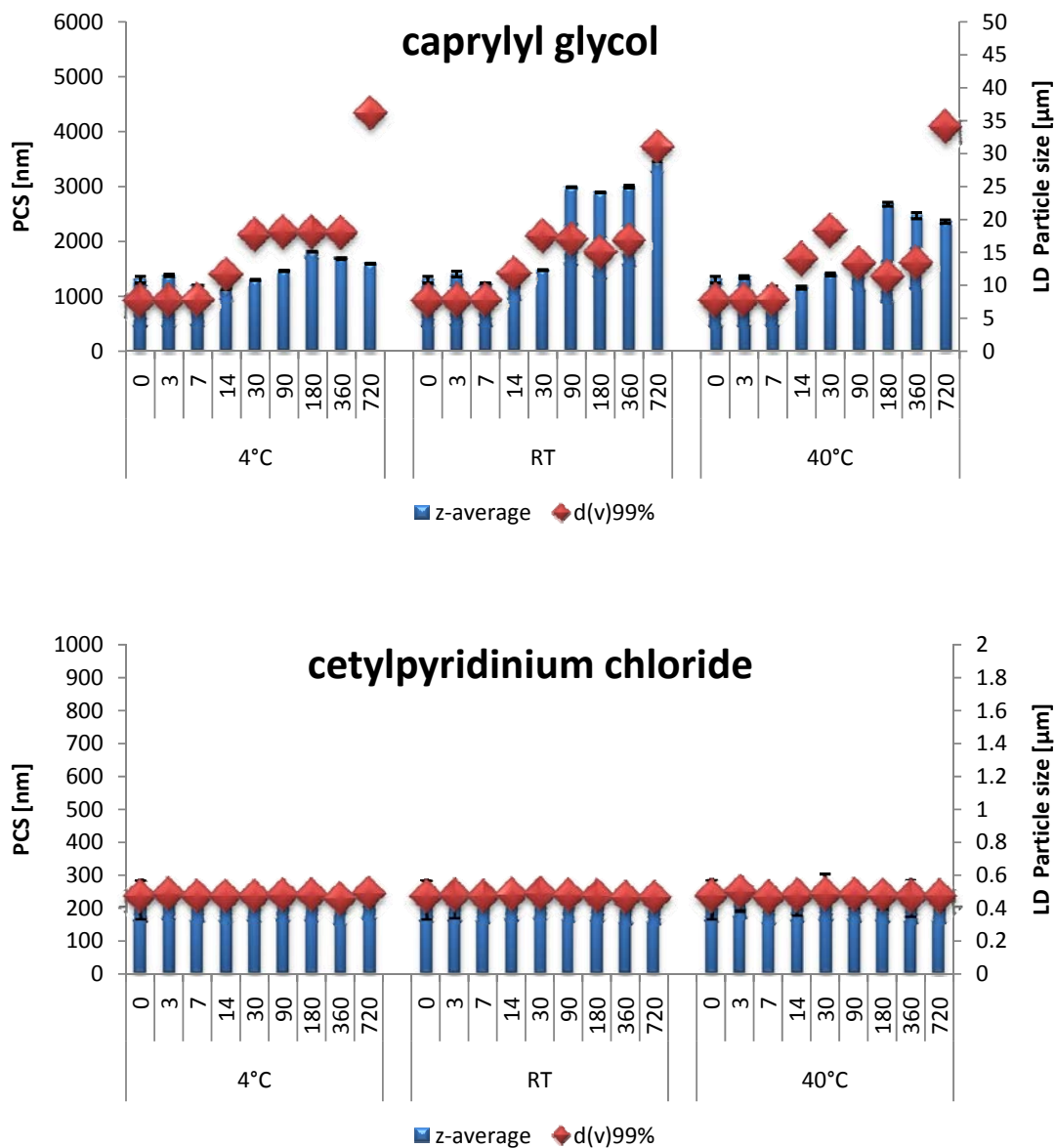
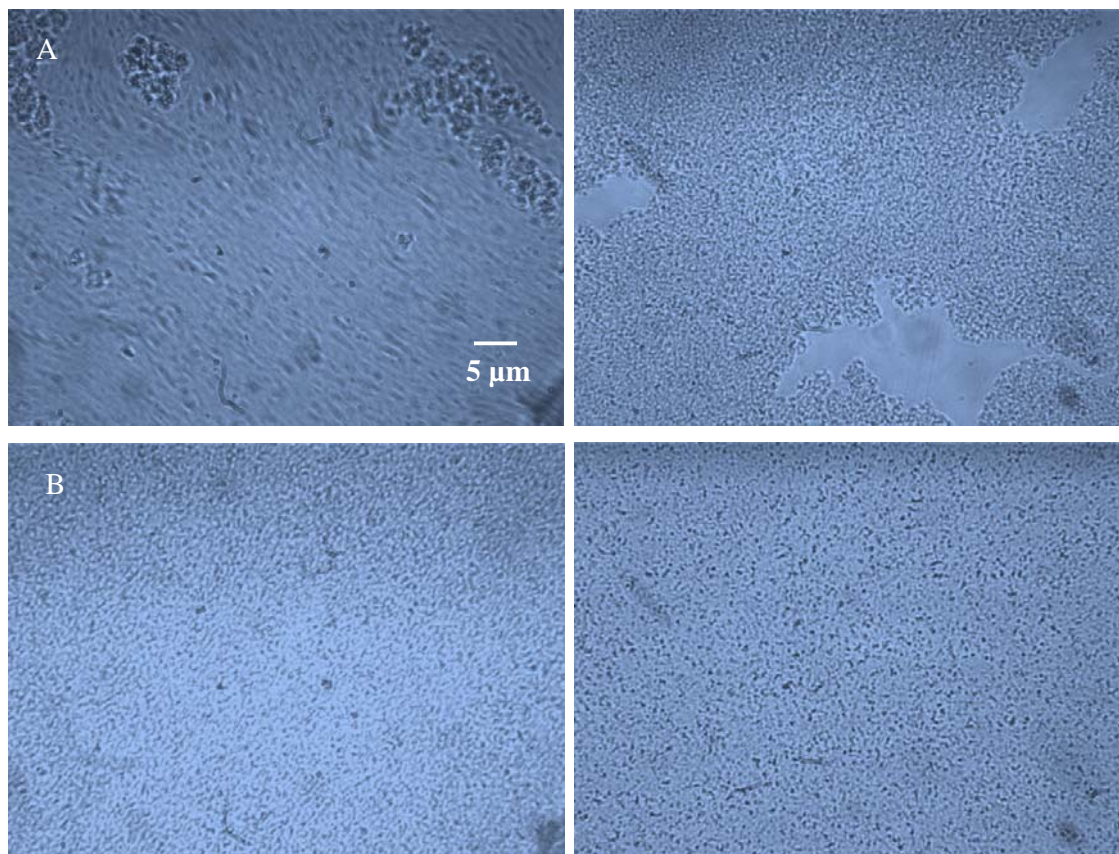


Fig. 129 Particle size of apigenin smartCrystals preserved with caprylyl glycol and CPC= cetylpyridinium chloride stored at three different temperatures (4°C, RT & 40°C) as a function of time (days)



**Fig. 130** Light microscopy images of smartCrystals preserved with: (A) caprylyl glycol and (B) cetylpyridinium chloride. (magnification 1000 fold, bar = 5 µm). The right side is directly after production and the right side is after 2 years storage

Apigenin smartCrystals<sup>®</sup> preserved with CPC were physically stable for the whole period of storage with a steady z-average and d(v)99% (Fig. 129). No changes were detected in microscopic pictures after the addition till 2 years (Fig. 130B).

Ethanol and Euxyl<sup>®</sup> PE 9010 as preservatives did not affect the physical characteristics of the apigenin smartCrystals<sup>®</sup>. No increase in z-average with 400 nm nor in d(v)99% with 0.500 µm was noticed till 2 years storage period (Fig. 131).

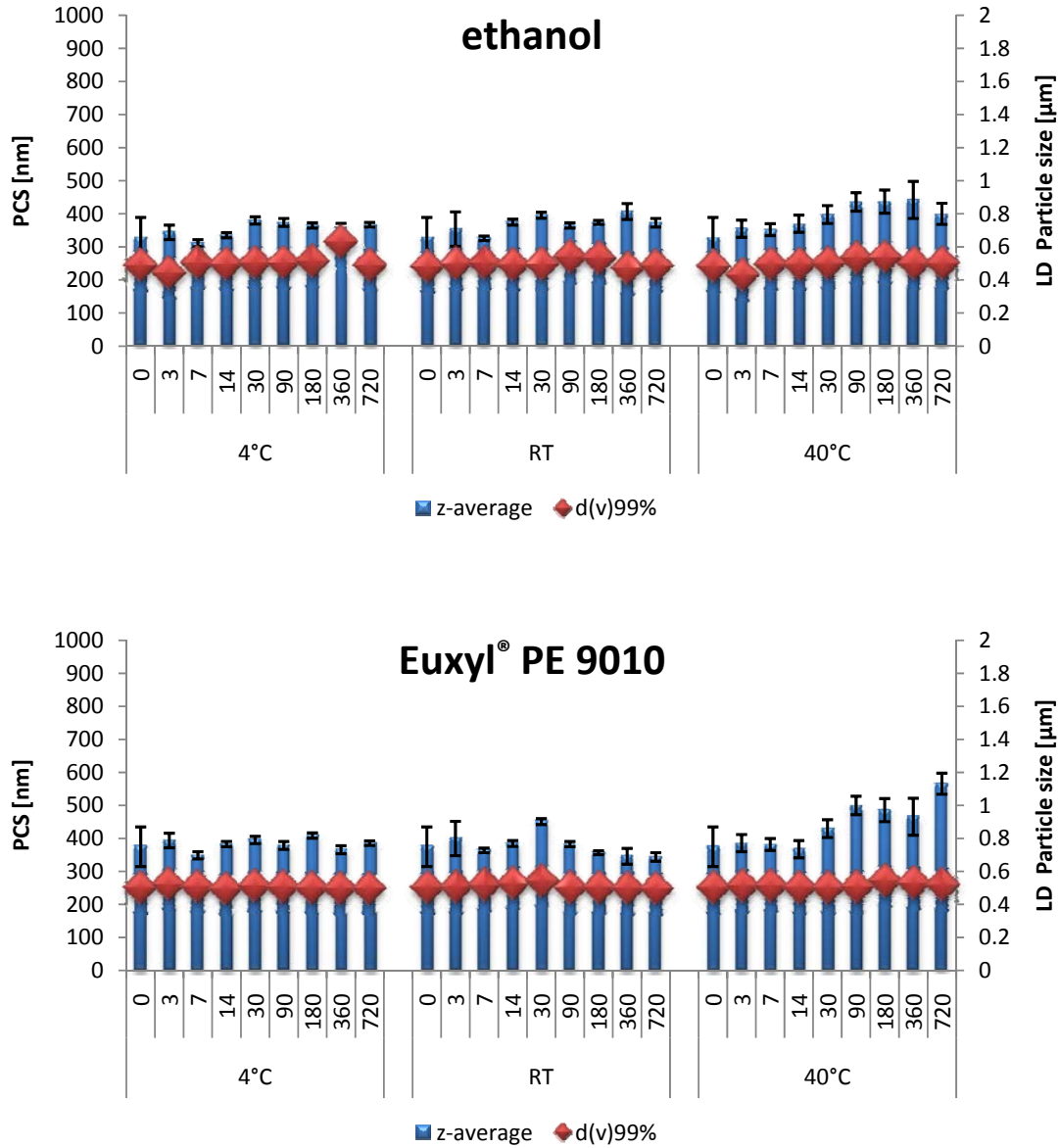
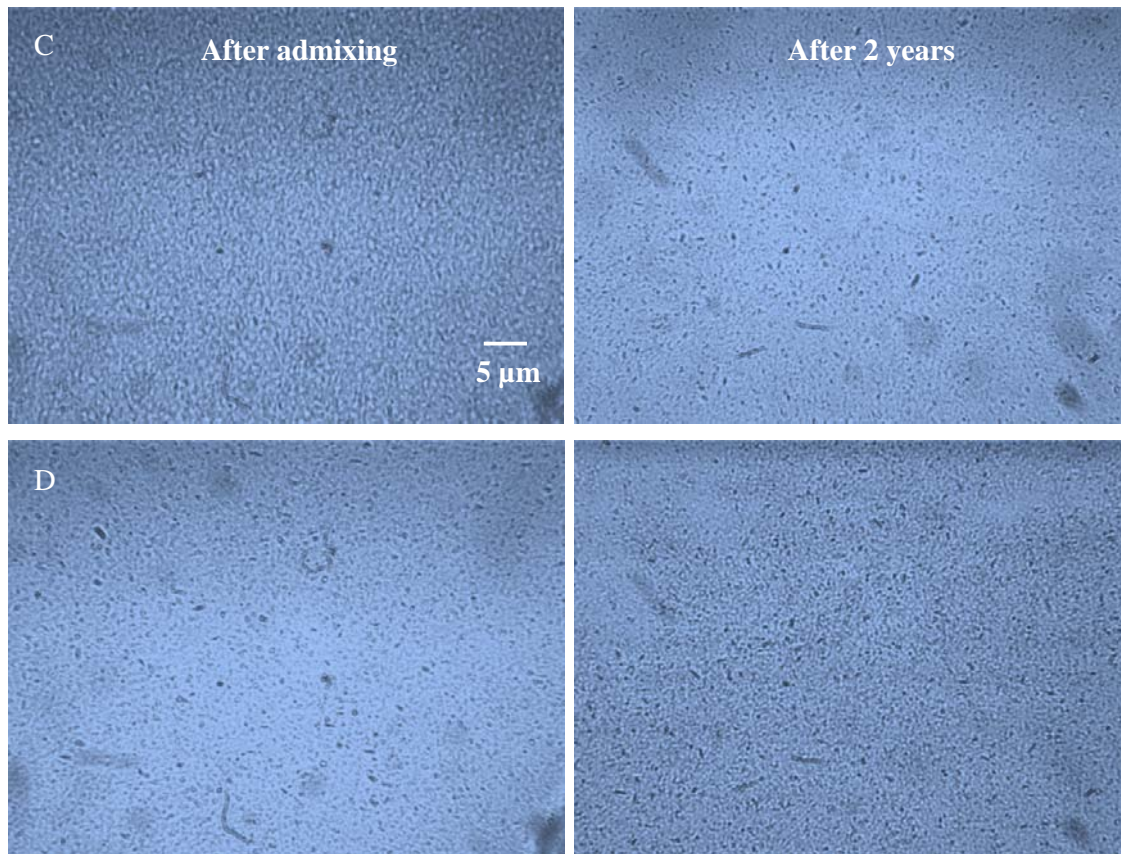


Fig. 131 Particle size of apigenin smartCrystals preserved with ethanol and euxyl PE9010 stored at three different temperatures (4°C, RT & 40°C) as a function of time (days)

Even microscopic pictures showed no difference in the storage period for both preservatives (Fig. 132C, 132D).



**Fig. 132** Light microscopy images of smartCrystals preserved with: (C) ethanol and (D) Euxyl® PE 9010 (magnification 1000 fold, bar = 5  $\mu\text{m}$ ). The right side is directly after production and the right side is after 2 years storage

The effect of glycerol 20% and glycerol 50% was more obvious in the smartCrystals® technology due to the smaller particle size (Fig. 133). The z-average reached around 3,000 nm and a  $d(v)_{99\%}$  of 15  $\mu\text{m}$  for glycerol 20%, where it was around 6,000 nm for PCS and 30 – 35  $\mu\text{m}$  for LD. Distinctive agglomerates were detected with microscopy proving the data obtained from PCS and LD (Fig. 134E, 134F).

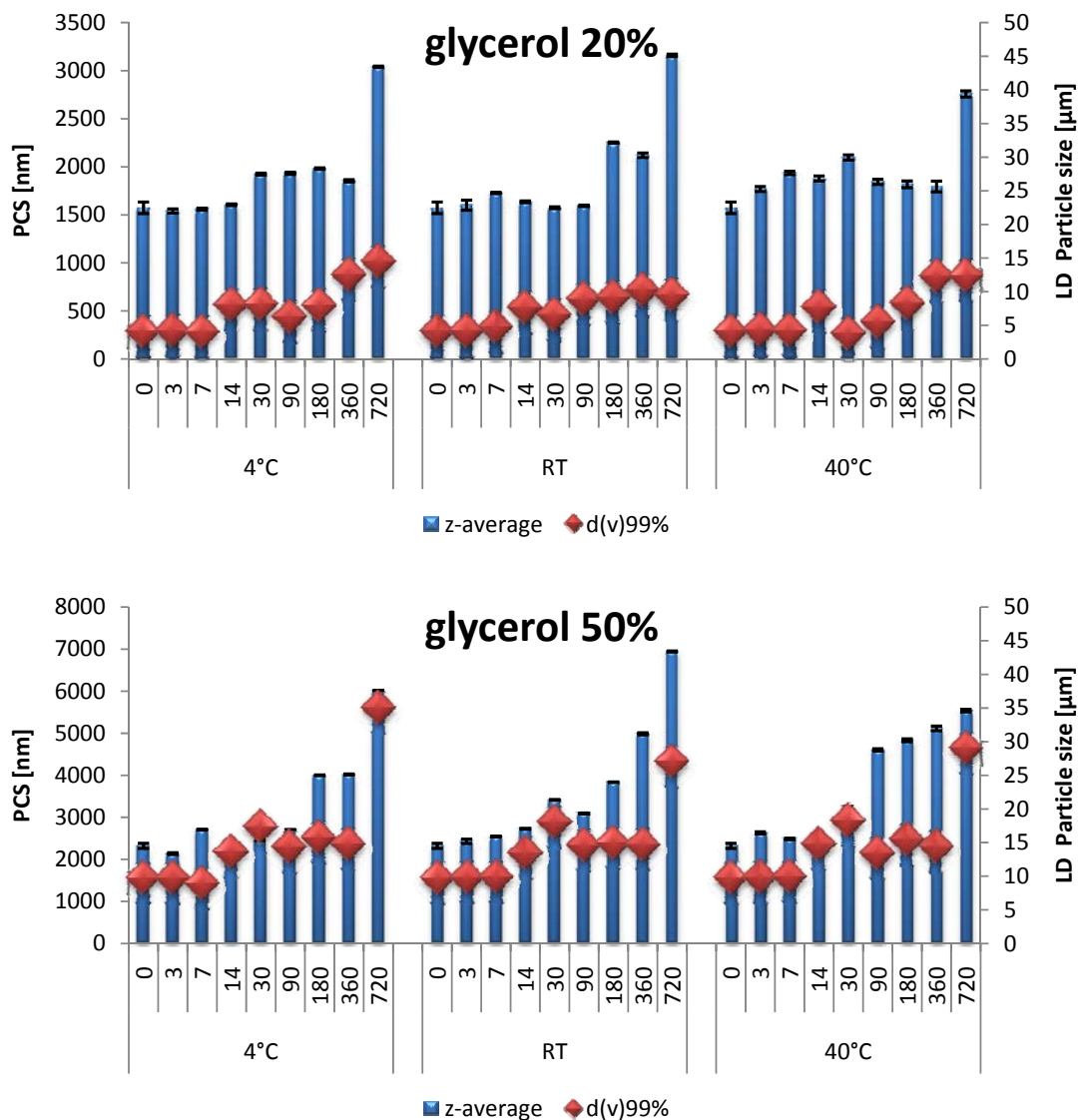


Fig. 133 Particle size of apigenin smartCrystals preserved with glycerol 20% and glycerol 50% stored at three different temperatures (4°C, RT & 40°C) as a function of time (days)

Fig. 135 showed the PCS and LD data for apigenin smartCrystals<sup>®</sup> preserved with Hydrolite<sup>®</sup>-5. No significant increase in z-average was noticed and there was no change in d(v)99% as well for the whole period of storage. Microscopic pictures showed no difference between the nanosuspensions after admixing and the one after storage for 2 years (Fig. 136G).

MultiEx naturotics PCS profile had 2 phases, a descending phase because of the possible solubilizing effect of multiEx naturotics, due to the abundant alcohol groups, followed by an ascending one due to the agglomerating.

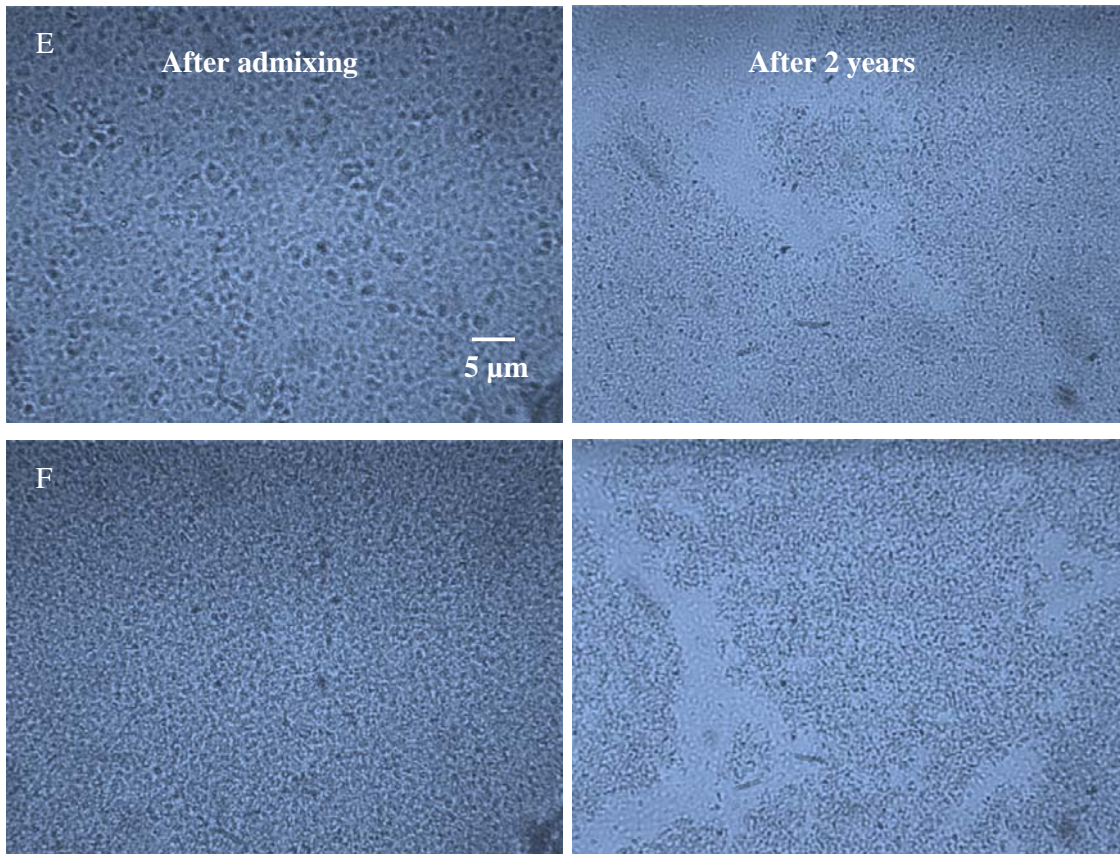
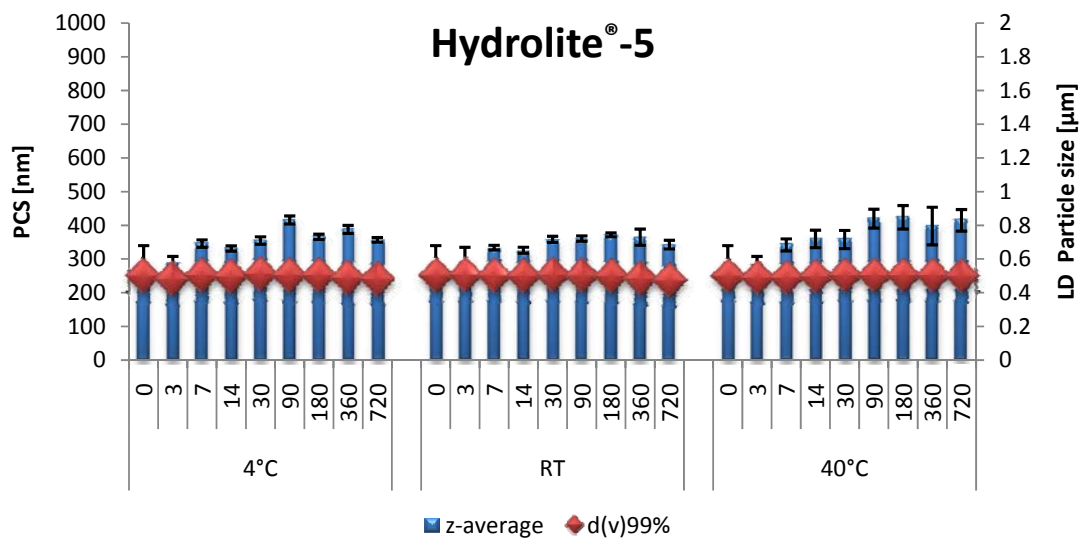


Fig. 134 Light microscopy images of smartCrystals<sup>®</sup> preserved with: (E) glycerol 20% and (F) glycerol 50%. (magnification 1000 fold, bar = 5 μm). The right side is directly after production and the right side is after 2 years storage

LD data remained stable during the descending phase of z-average and the increase was really noticed from 1 year measurement (Fig. 135). Clear aggregates were seen under microscope for these nanosuspensions which confirm the results obtained from LD (Fig. 136H).



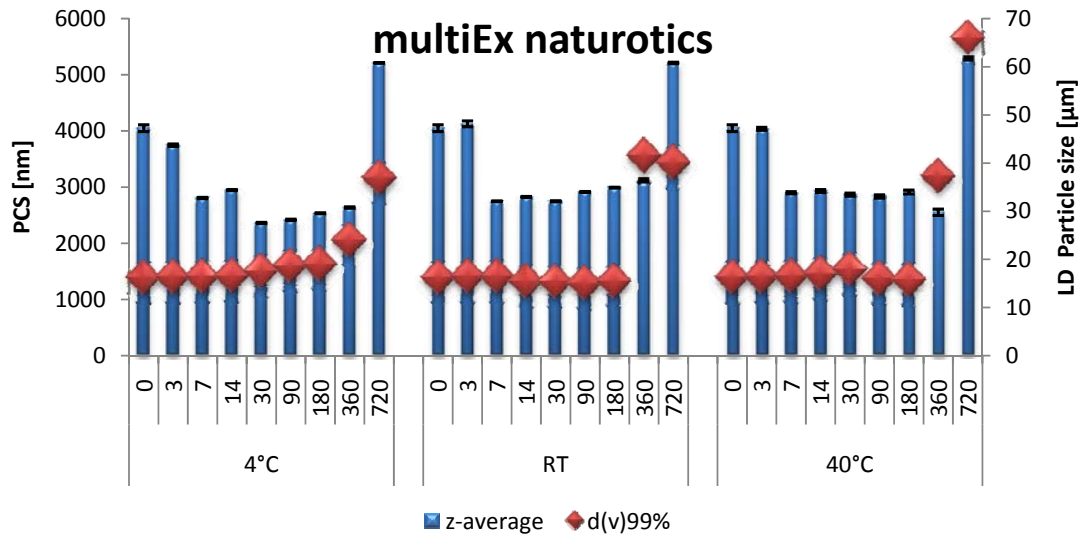


Fig. 135 Particle size of apigenin smartCrystals<sup>®</sup> preserved with Hydrolite<sup>®</sup>-5 and multiEx naturotics stored at three different temperatures (4°C, RT & 40°C) as a function of time (days)

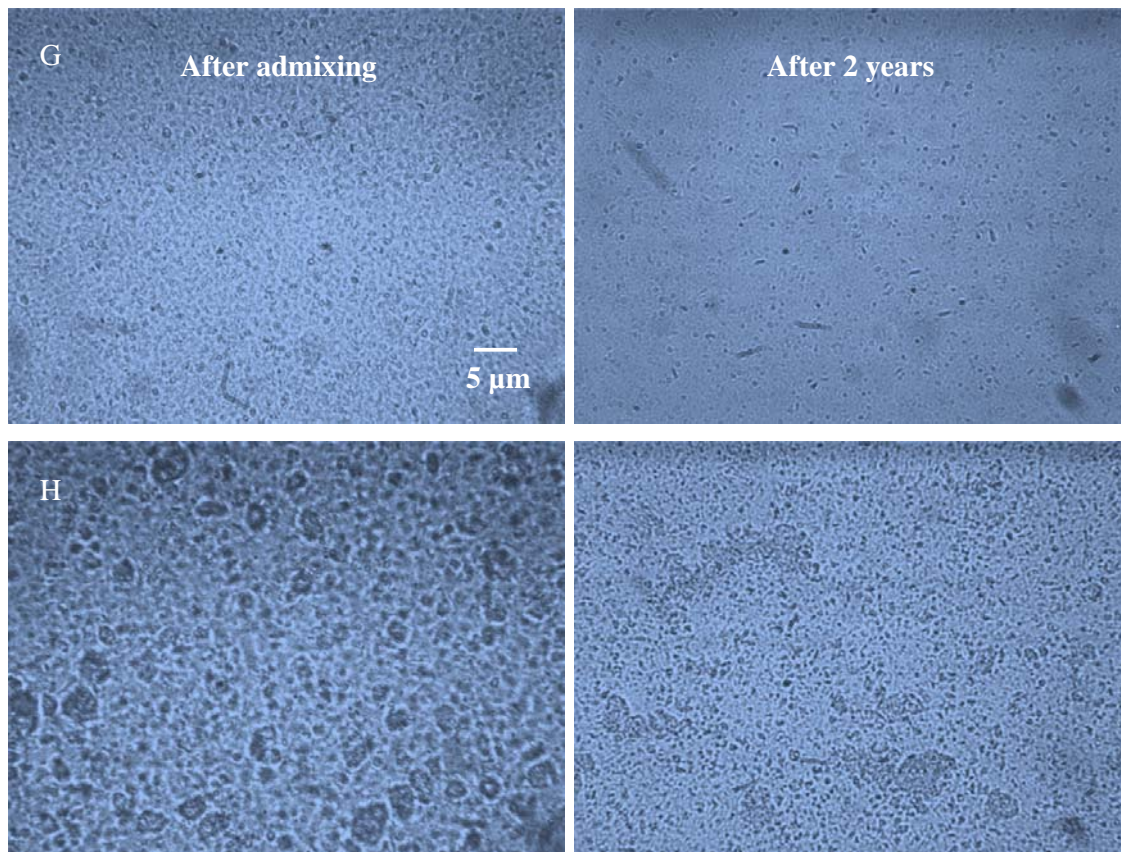


Fig. 136 Light microscopy images of nanosuspensions preserved with: (G) Hydrolite<sup>®</sup>-5 and (H) multiEx naturotics. (magnification 1000 fold, bar = 5 μm). The right side is directly after production and the right side is after 2 years storage

The stability profile of apigenin smartCrystals preserved with propylene glycol remained stable the whole period of storage without any changes in both PCS and LD data (Fig. 137). No agglomerates were detected under microscope after 2 years storage proving high physical stability (Fig. 138I)

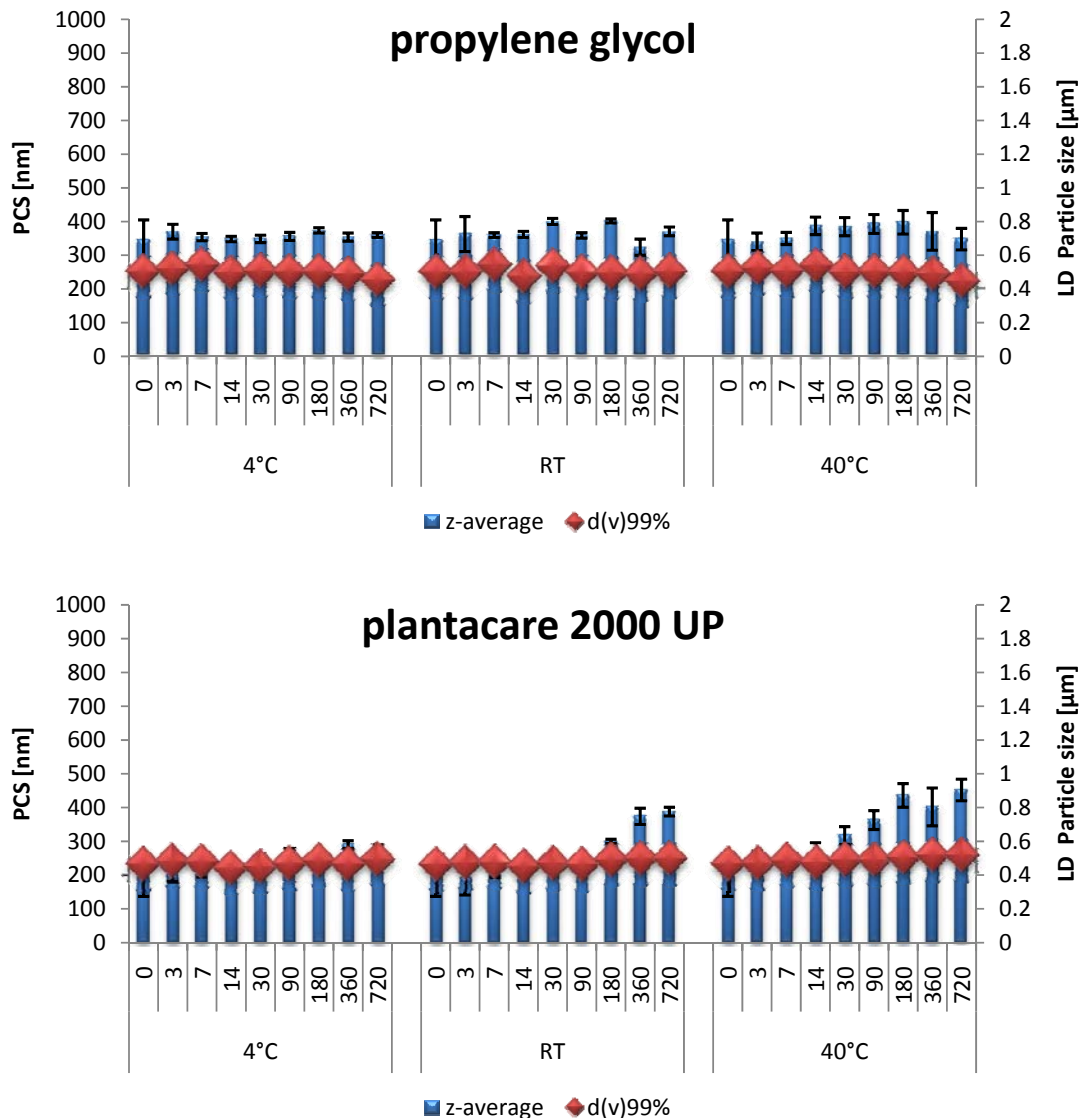
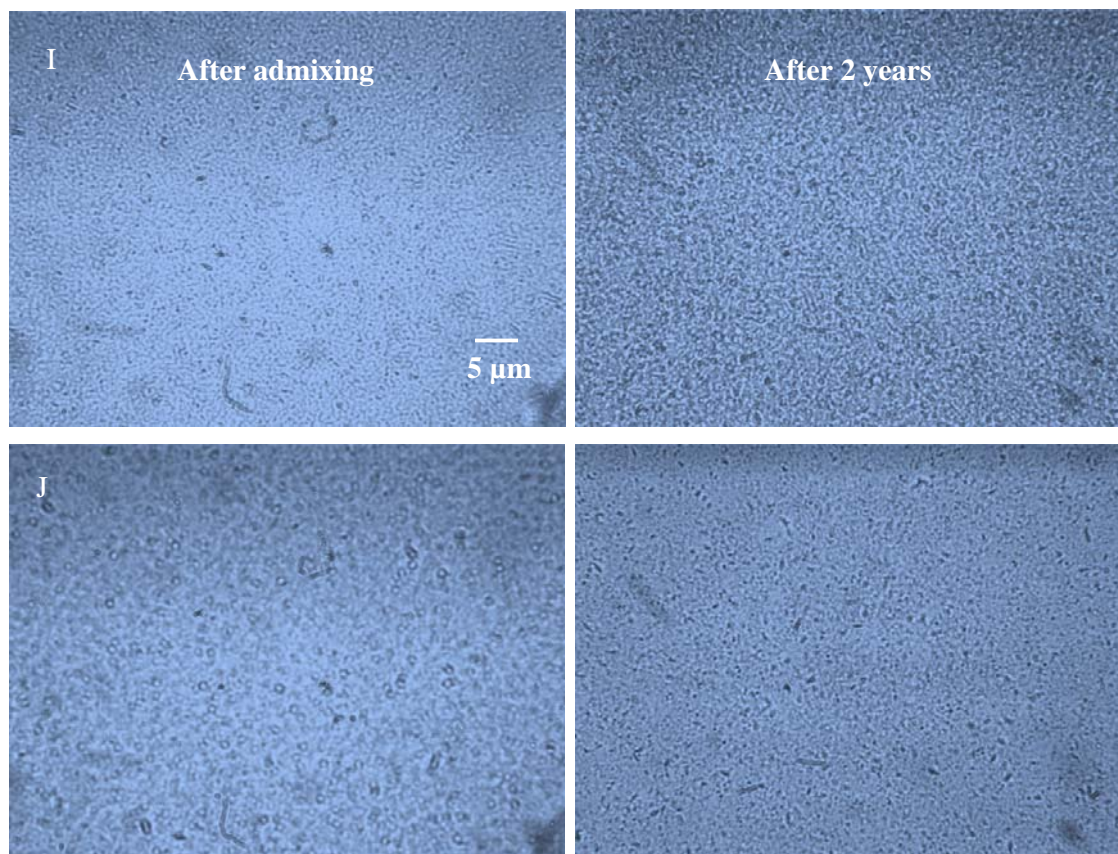


Fig. 137 Particle size of apigenin smartCrystals preserved with propylene glycol and Plantacare® 2000 UP stored at three different temperatures (4°C, RT & 40°C) as a function of time (days)

As for Plantacare® 2000 UP, the PCS data showed no increase for the 4°C samples, whereas a small increase was observed for the 1 year data for RT samples and after 3 months for the 40°C samples. No increase in d(v)99% was noticed in all samples.





**Fig. 138** Light microscopy images of smartCrystals preserved with: (I) propylene glycol and (J) Plantacare<sup>®</sup> 2000 UP. (magnification 1000 fold, bar = 5  $\mu\text{m}$ ). The right side is directly after production and the right side is after 2 years storage

The increase seen in PCS data can be due to the same recrystallization of dissolved particles because of the increased amount of Plantacare<sup>®</sup> 2000 UP (Cf. 4.2.8) (Fig. 137). No agglomerations were detected for both smartCrystals after storing by investigating them using the microscope (Fig. 138I, 138J)

Profiles of Phenonip<sup>®</sup> and Rokonsal<sup>®</sup> PB-5 from apigenin preserved smartCrystals<sup>®</sup> were also alike, with intense effect of instability was seen in Phenonip<sup>®</sup> samples.

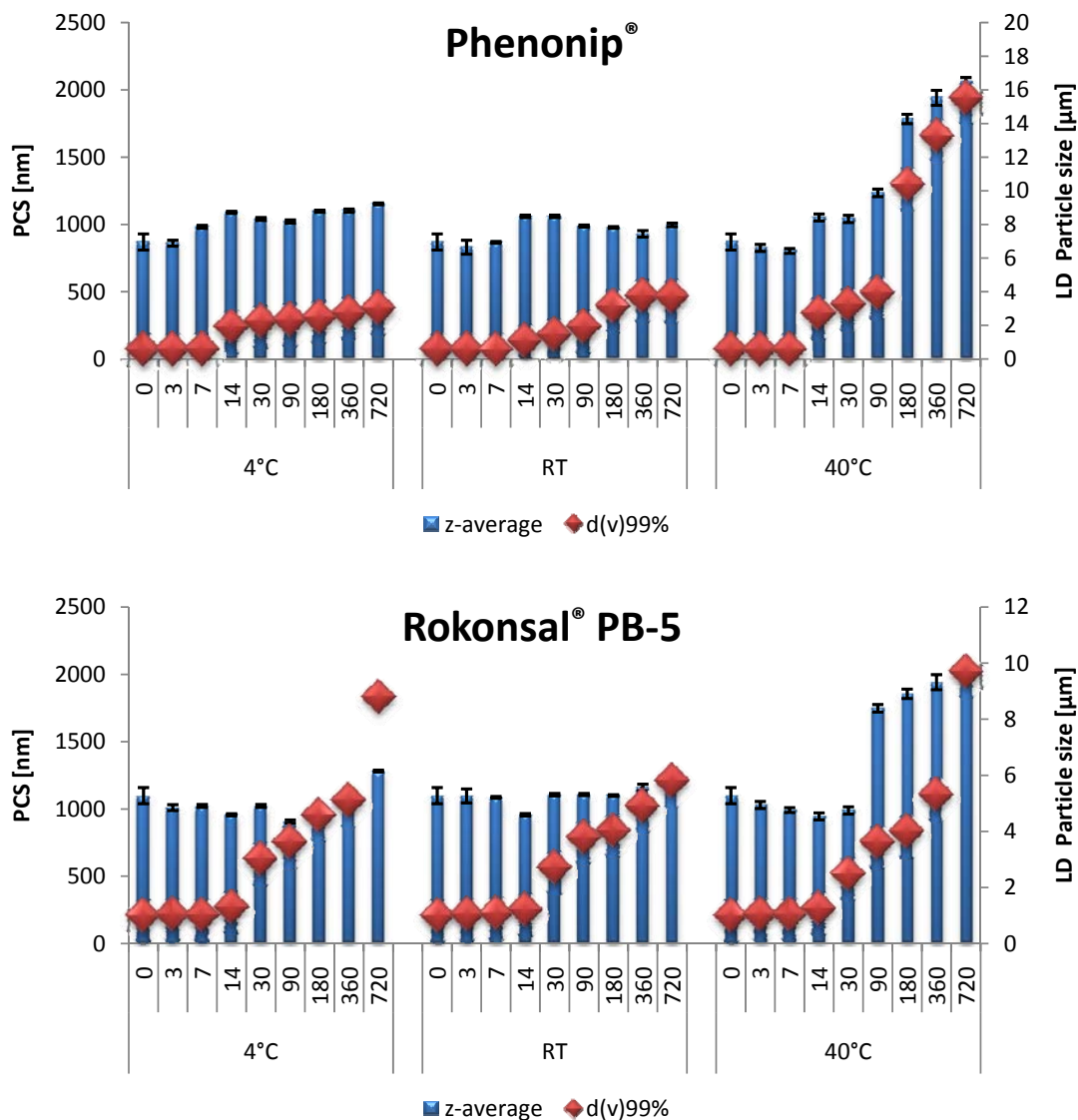
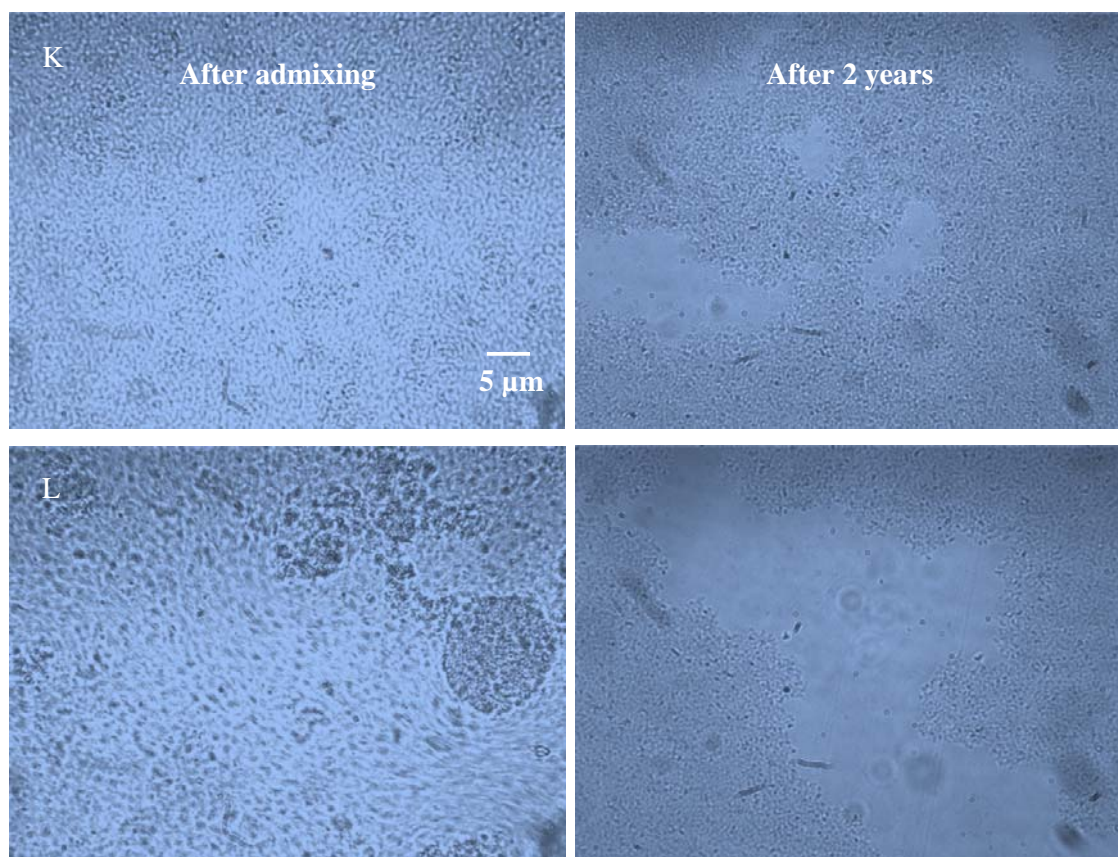


Fig. 139 Particle size of apigenin smartCrystals preserved with Phenonip® and Rokonsal® PB-5 stored at three different temperatures (4°C, RT & 40°C) as a function of time (days)

This instability was detected as an obvious increase in PCS and LD results (Fig. 139). Both preserved smartCrystals® showed huge agglomerates when analyzed using the microscope (Fig. 140K, 140L).



**Fig. 140** Light microscopy images of nanosuspensions preserved with: (K) Phenonip<sup>®</sup> and (L) Rokonsal<sup>®</sup> PB-5. (magnification 1000 fold, bar = 5  $\mu\text{m}$ ). The left side is directly after production and the right side is after 2 years storage

Fig. 141 shows the TPGS stability profile. No increase in particle size was detected for preserved apigenin smartCrystals<sup>®</sup>, neither for PCS nor for LD results. Microscopic pictures showed no aggregation after admixing and after 2 years storage (Fig. 142M).

On the other hand, apigenin nanosuspensions preserved with triclosan had a quite recognizable increase in particle size in both PCS and LD measurements (Fig. 141). The agglomerates were clearly seen by investigating the smartCrystals<sup>®</sup> under microscope (Fig. 142N) unlike the nonpreserved nanosuspension where no aggregates were detected upon microscopic investigation (Fig. 144O). This was predictable as the data measured in the day of the addition was already a lot larger in comparison to the non-preserved smartCrystals<sup>®</sup> (Fig. 143).

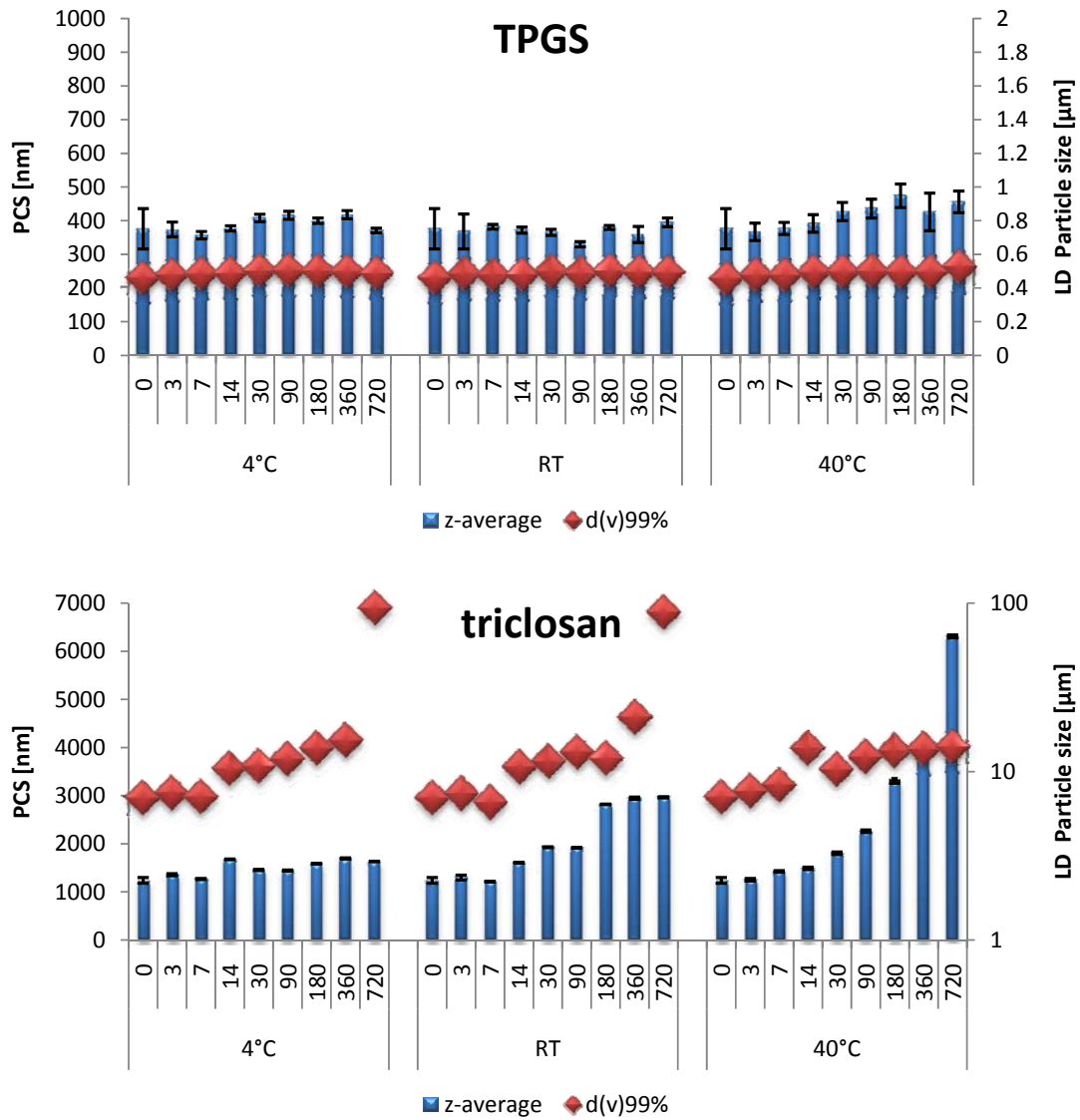
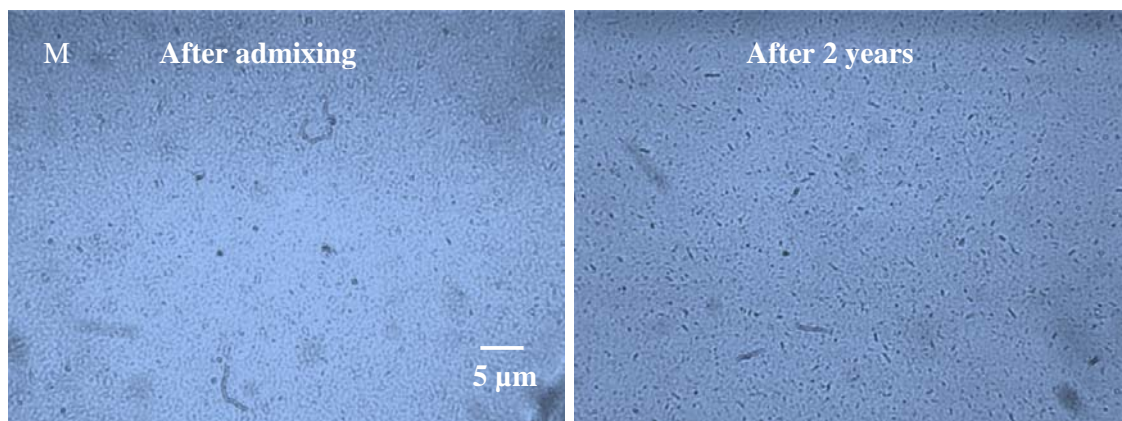


Fig. 141 Particle size of apigenin nanosuspensions preserved with TPGS= D-alpha tocopherol polyethylene glycol 1000 succinate and triclosan stored at three different temperatures (4°C, RT & 40°C) as a function of time (days)



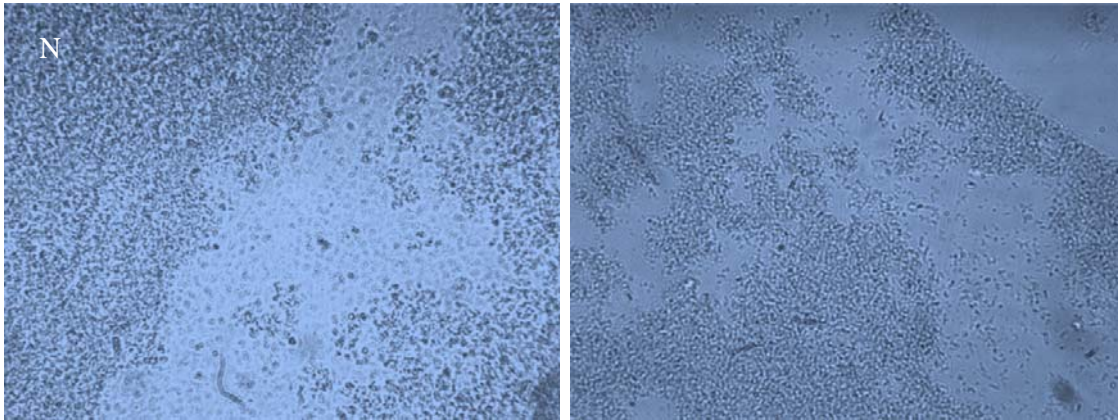


Fig. 142 Light microscopy images of nanosuspensions preserved with: (M) TPGS= D-alpha tocopherol polyethylene glycol 1000 succinate and (N) triclosan. (magnification 1000 fold, bar = 5 μm). The right side is directly after production and the right side is after 2 years storage

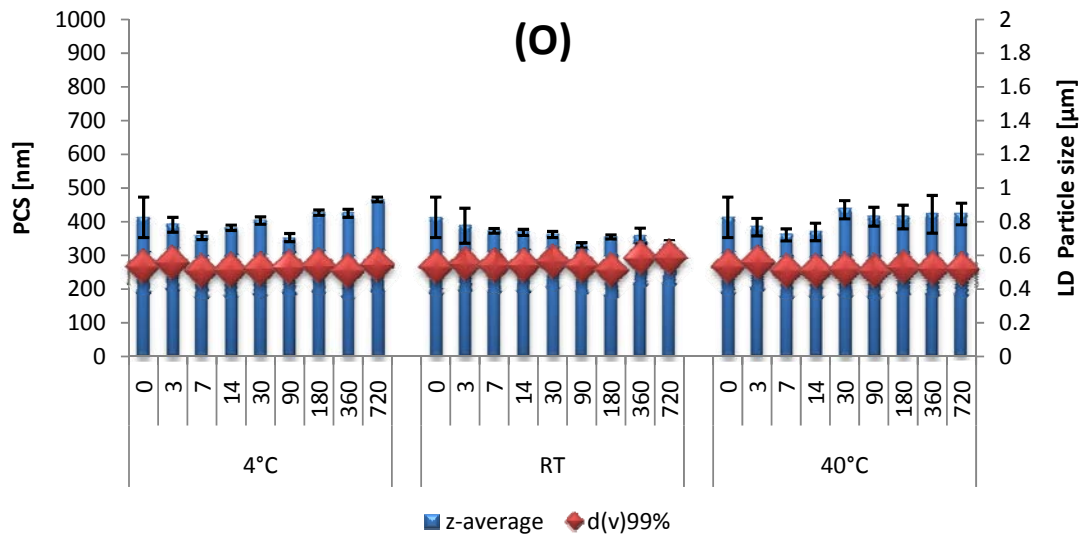


Fig. 143 Particle size of non-preserved apigenin nanosuspensions stored at three different temperatures (4°C, RT & 40°C) as a function of time (days)

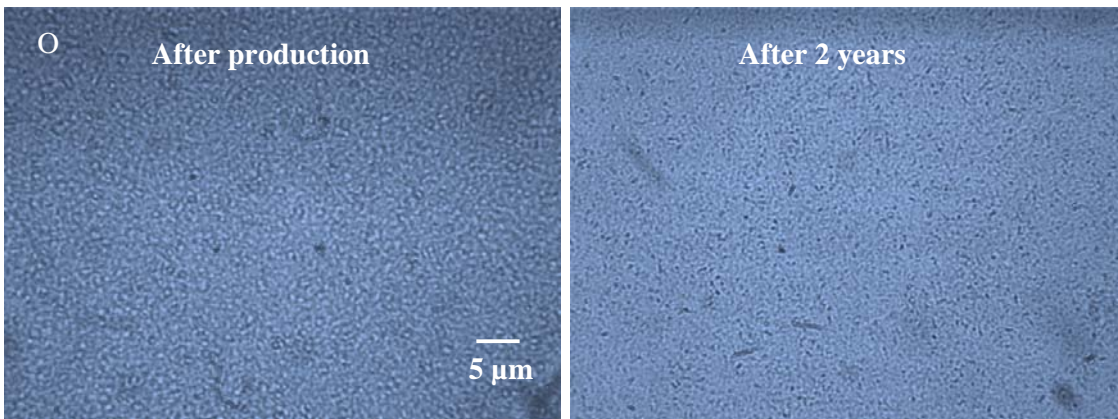
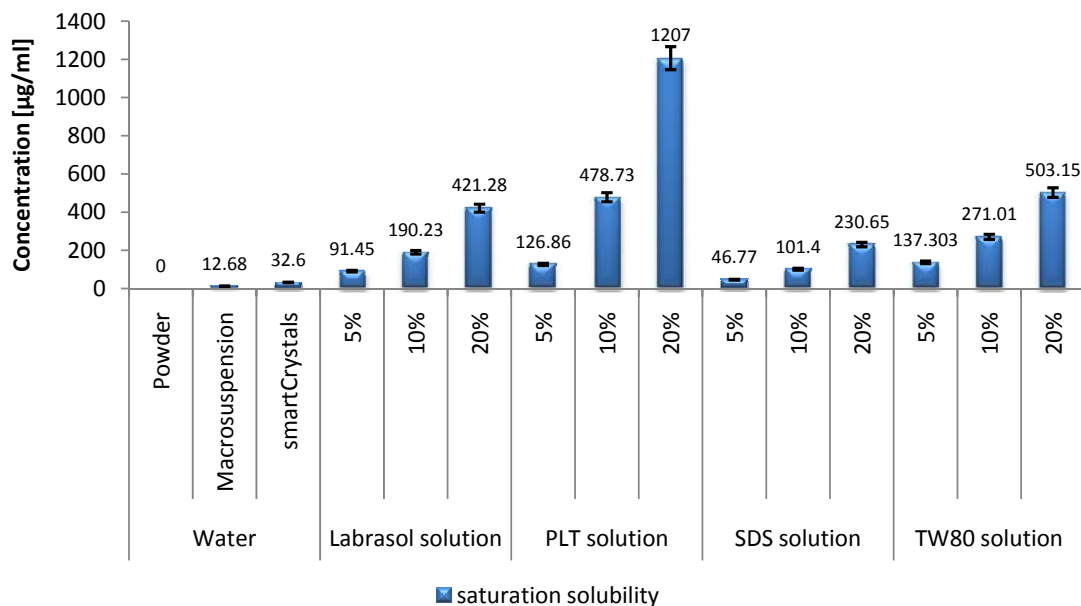


Fig. 144 Light microscopy images of (O) apigenin non-preserved. (magnification 1000 fold, bar = 5 μm). The right side is directly after production and the right side is after 2 years storage

#### 4.2.8 Saturation solubility

Such as in hesperetin, the saturation solubility was determined for apigenin powder, apigenin macrosuspensions (with the presence of 1% Plantacare<sup>®</sup> 2000 UP) and apigenin smartCrystals<sup>®</sup> at 25°C in water. The results were compared to the saturation solubility of apigenin powder in surfactant solutions of different stabilizers and permeation enhancers.



**Fig. 145 Saturation solubility of apigenin powder, macrosuspension, smartCrystals<sup>®</sup> and apigenin powder with different solubilizing agents and different concentration**

In Fig. 145 It can be seen that the smartCrystals<sup>®</sup> technology enhanced the saturation solubility of apigenin powder by 257% than that of the macrosuspensions. Although better saturation solubility was obtained using 5, 10 and 20% of Plantacare<sup>®</sup> 2000 UP but using such a concentration in the formulation is not only impossible due to the irritation effect of the surfactant but also because of the foaming effect of them as well.

#### 4.2.9 Antioxidant activity

As the procedure in hesperetin, DPPH antioxidant activity study was performed on the prepared apigenin products (Fig. 146).

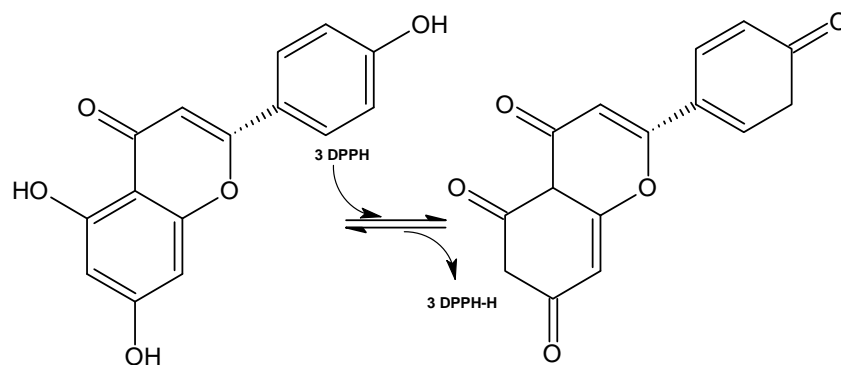


**Fig. 146** Reaction kinetics of DPPH and apigenin

The steady state time ( $T_{\text{steadystate}}$ ) was determined in order to ensure the endpoint of reaction. The reaction between apigenin and  $\text{DPPH}^\bullet$  was slow compared to the reaction with hesperetin. Apigenin, being poorly dissolved in methanolic solutions of  $\text{DPPH}^\bullet$  [106], had a negative effect on the reaction time as the reaction takes place only on the surface of particles (Fig. 147).

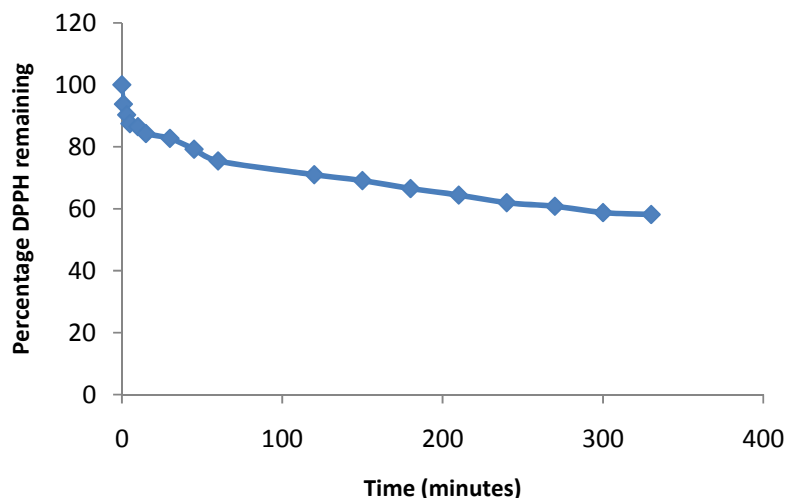


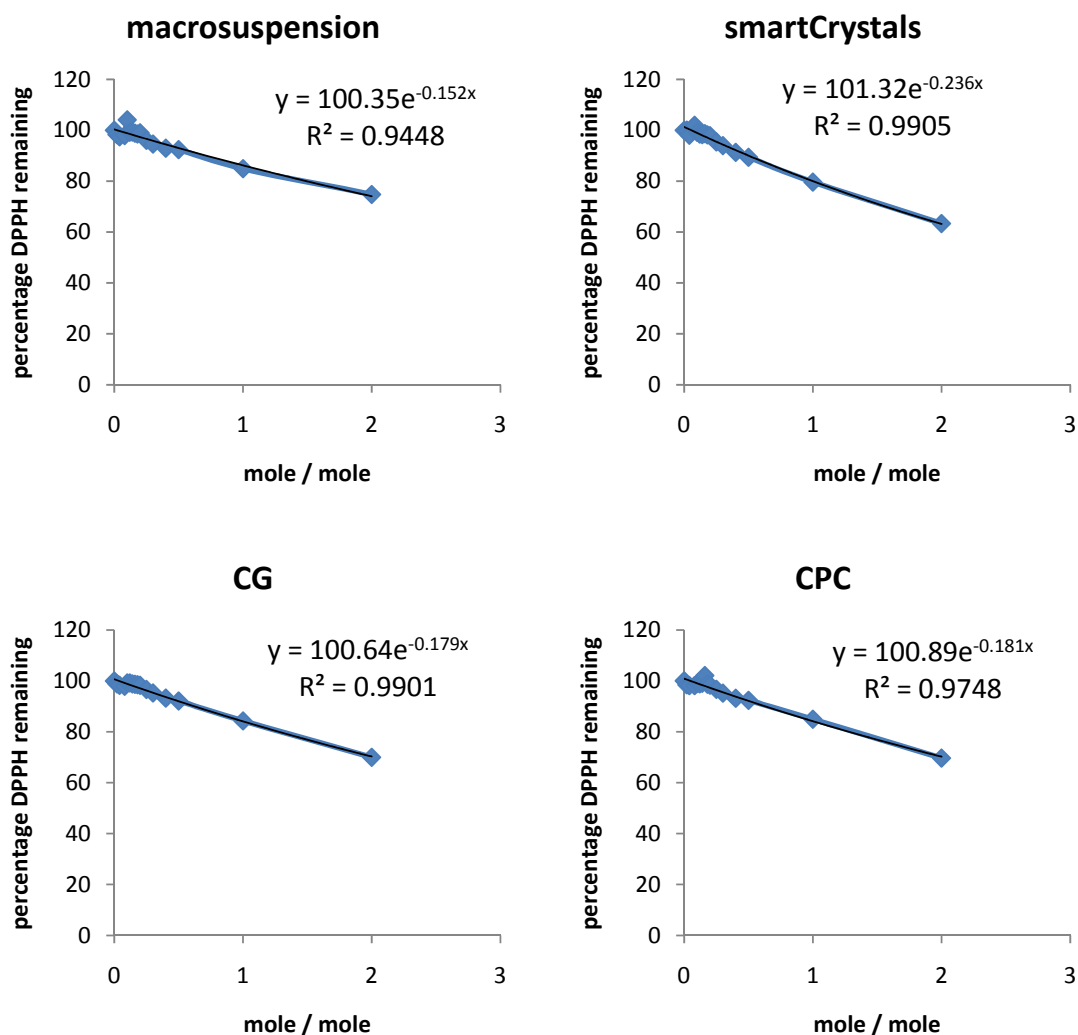
**Fig. 147** The steady state for the antioxidant reaction of apigenin nanosuspension and  $\text{DPPH}^\bullet$

$EC_{50}$  (Efficient concentration required to decrease the  $\text{DPPH}^\bullet$  concentration by 50%) of apigenin macro- and nano-suspensions was calculated by plotting the residual percentage of  $\text{DPPH}^\bullet$  against the molar ratios of the antioxidant to  $\text{DPPH}^\bullet$  (Fig. 148).  $EC_{50}$  of apigenin macro- and nanosuspensions were 4.583 and 2.993, respectively.

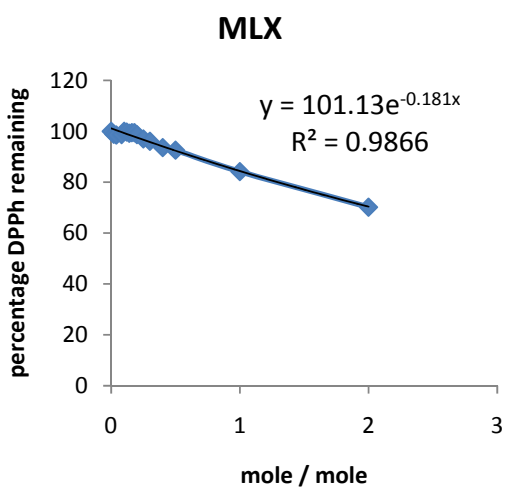
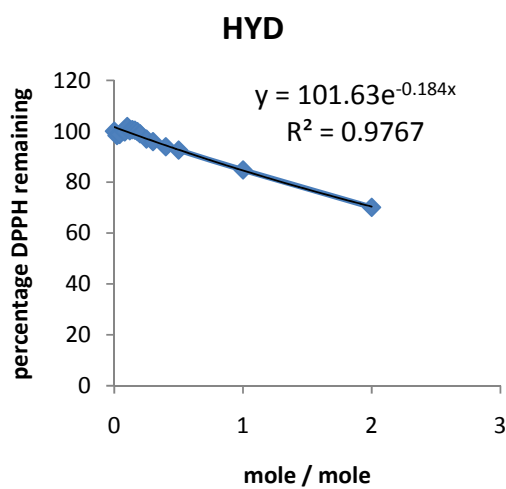
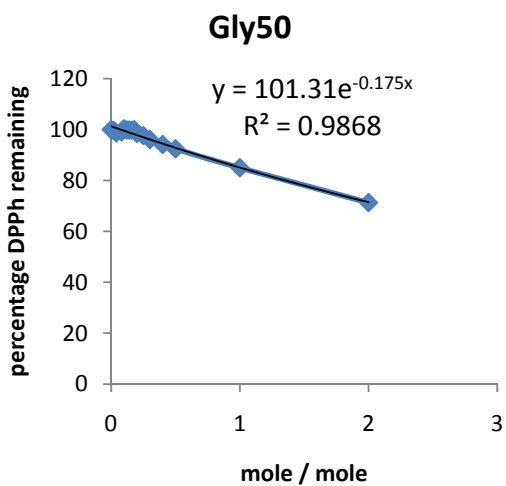
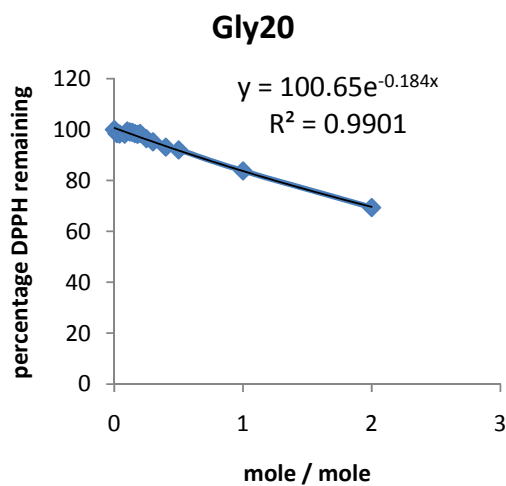
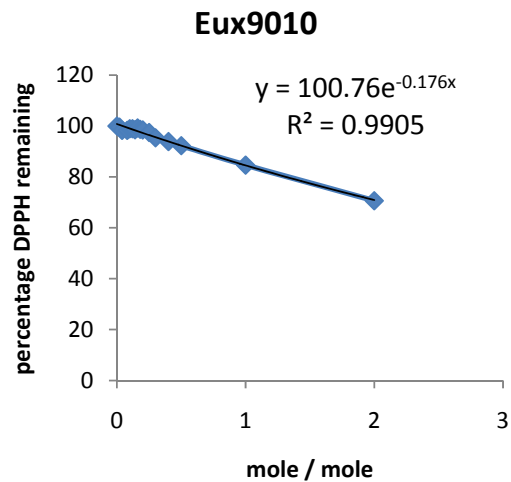
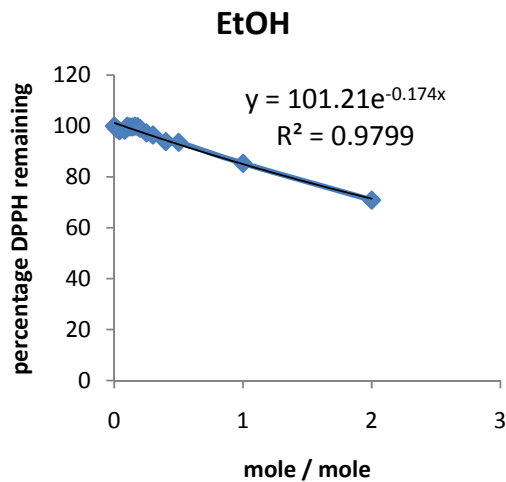
The effect of nanonization can be clearly seen in the case of apigenin macro- ( $EC_{50}=4.583$ ) and nanosuspension ( $EC_{50}=2.993$ ) (Table 16) due to the low solubility in methanol and hence the effect of surface area augmentation on the antioxidant activity was more pronounced. Antioxidant activity was further investigated in preserved nanosuspensions in order to evaluate the possible interference of the preservative on the antiradical activity.

The EC<sub>50</sub> values of apigenin nanosuspension with the addition of preservatives were remarkably higher than the apigenin non-preserved smartCrystals<sup>®</sup>. The negative effect of the preservatives differed from increasing the EC<sub>50</sub> to 3.855 in apigenin smartCrystals<sup>®</sup> preserved with Hydrolite<sup>®</sup>-5 to 4.176 for apigenin smartCrystals<sup>®</sup> preserved with triclosan. TPGS preserved smartCrystals<sup>®</sup> had better EC<sub>50</sub> with 3.546 which could be highly related to self antioxidant efficacy of TPGS.

Despite the negative effect of the preservatives on the antioxidant activity of apigenin smartCrystals<sup>®</sup>, but the preservative addition can be considered more important than increasing the applying dose to cover the loss of activity. On the other hand, preservatives with less effect on the antioxidant such as Hydrolite<sup>®</sup>-5 can be chosen.







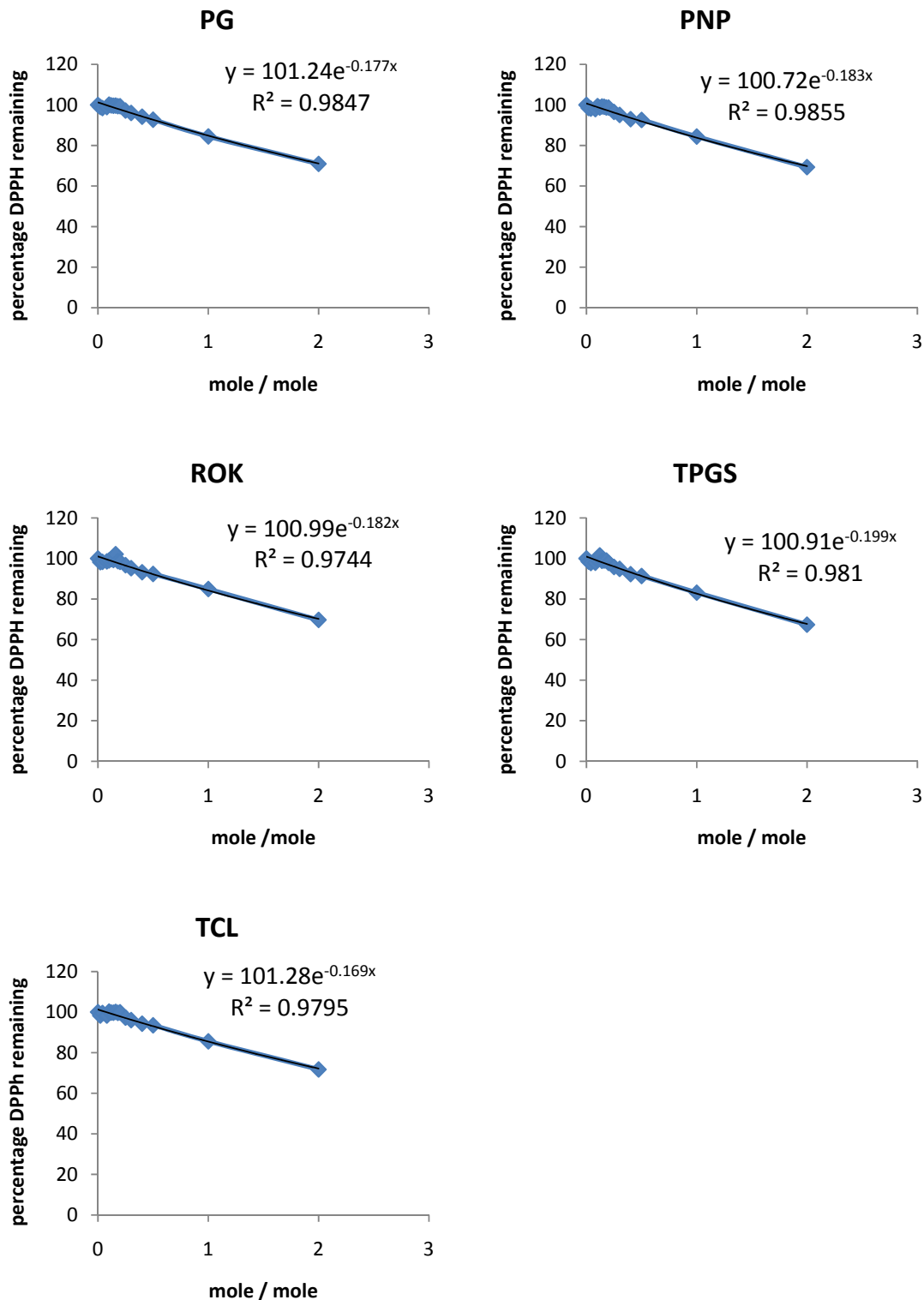


Fig. 148 The declining in DPPH<sup>•</sup> concentration as a function of the number of moles of apigenin / moles of DPPH<sup>•</sup> for apigenin macrosuspension, Non-preserved apigenin smartCrystals and preserved apigenin smartCrystals with (CG= caprylyl glycol, CPC= cetyl pyridinium chloride, EtOH= ethanol, EUX9010= Euxyl<sup>®</sup> PE 9010, GLY20= glycerol 20%, GLY50= glycerol 50%, HYD= Hydrolite<sup>®</sup>-5, MLX= multiEx naturotics, PG= propylene glycol, PNP= Phenonip<sup>®</sup>, ROK= Rokonsal<sup>®</sup> PB-5, TPGS= D-alpha tocopherol polyethylene glycol 1000 and TCL= triclosan)

**Table 16** EC<sub>50</sub> values of apigenin macrosuspension, smartCrystals and preserved hesperetin smartCrystals (CG= caprylyl glycol, CPC= cetyl pyridinium chloride, EtOH= ethanol, EUX9010= Euxyl<sup>®</sup> PE 9010, GLY20= glycerol 20%, GLY50= glycerol 50%, HYD= Hydrolite<sup>®</sup>-5, MLX= multiEx naturotics, PG= propylene glycol, PNP= Phenonip<sup>®</sup>, ROK= Rokonsal<sup>®</sup> PB-5, TPGS= D-alpha tocopherol polyethylene glycol 1000 and TCL= triclosan)

Type of apigenin suspension	EC <sub>50</sub> values
<b>Macrosuspension</b>	4.583
<b>smartCrystals</b>	2.992
<b>CG</b>	3.908
<b>CPC</b>	3.878
<b>EtOH</b>	4.053
<b>EUX9010</b>	3.981
<b>GLY20</b>	3.802
<b>GLY50</b>	4.035
<b>HYD</b>	3.855
<b>MLX</b>	3.892
<b>PG</b>	3.986
<b>PNP</b>	3.827
<b>ROK</b>	3.863
<b>TPGS</b>	3.546
<b>TCL</b>	4.177

#### 4.2.10 X-ray diffraction (XRD)

X-ray diffraction was performed as well to examine the crystalline status of the apigenin particles. The crystallinity of four samples was tested after drying them: apigenin powder dispersed in water, apigenin powder dispersed in a Plantacare<sup>®</sup> 2000 UP aqueous solution, apigenin nanosuspension produced with Micron LAB40 (lab-scale batch) and apigenin smartCrystals<sup>®</sup> (scaled-up batch). All diffractions patterns were depicted in the X-ray diffractogram shown in Fig. 149. It can be clearly seen that no different peaks appeared when the Plantacare<sup>®</sup> 2000 UP was added to the formulation. Not to mention that the peak shapes for both samples of apigenin nanosuspension and apigenin smartCrystals<sup>®</sup> in the diffractogram showed almost total similarity if compared to the macrosuspension. Hence, all produced nanosuspensions on lab- and large-scale have the same crystallinity as the raw material. Applying very high energy to obtain smaller particles such as the case in Micron LAB40 produced nanosuspension or less energy such as the case in smartCrystals<sup>®</sup> did not affect the crystalline status of the formulation. Staying in the crystalline status assure the

stability of the product, as crystalline substances are physically more stable than amorphous ones.

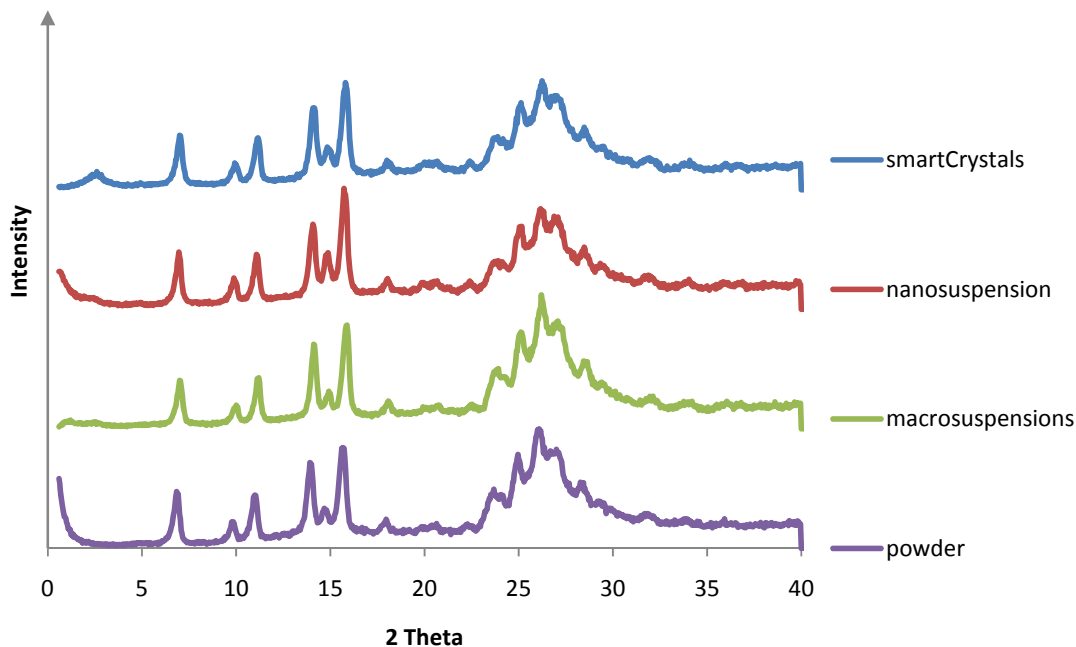


Fig. 149 X-ray diffractogram of dried apigenin coarse suspension, dried apigenin suspension in Plantacare® 2000 UP aqueous solution (macrosuspension), dried apigenin nanosuspension produced with Micron LAB40 and dried apigenin smartCrystals®

#### 4.2.11 *In vitro* release

In order to evaluate the permeation of apigenin the Franz diffusion cells were used. From the experience gained from hesperetin the receptor medium that gave better release characteristics was used. A mixture of PBS : ethanol : PEG 400 (40 : 20 : 40) was used. Although the release rate of apigenin in this medium is expected to be better than that of PBS alone but it was not as good as the results obtained from hesperetin (Fig. 150). A cumulative amount of apigenin can be seen in this graph for 24 hours. Similarly to hesperetin, three different formulations were tested: apigenin powder dispersed in water, apigenin powder dispersed in Plantacare® 2000 UP aqueous solution (apigenin macrosuspension) and apigenin smartCrystals®. This low rate of release can be due to the low solubility of apigenin in this medium. However, an increase in the release has been identified using the apigenin smartCrystals® compared to the release rate obtained from both apigenin macrosuspension and the apigenin powder dispersed directly in water.

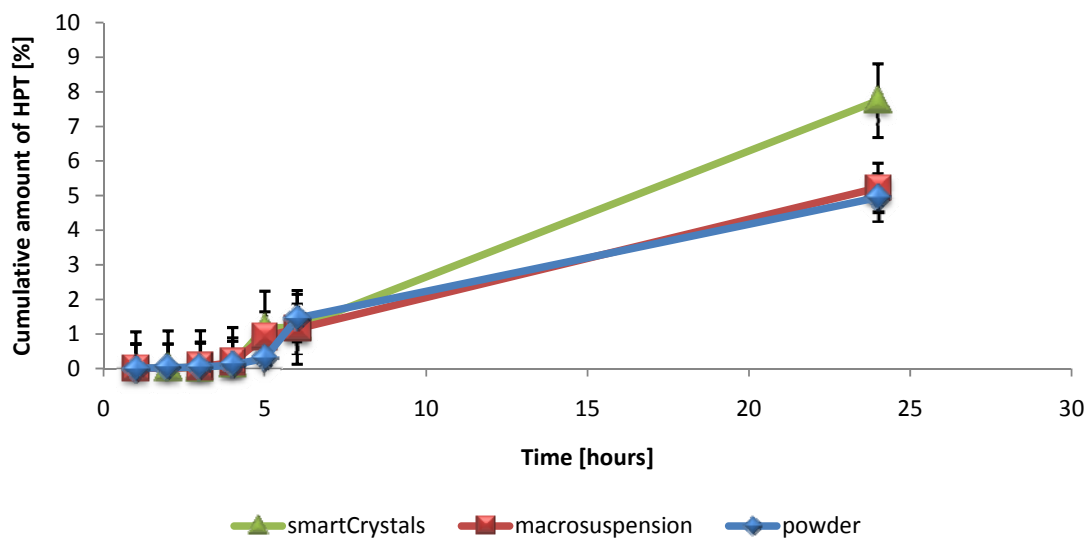


Fig. 150 The cumulative amount of apigenin dissolved from the smartCrystals<sup>®</sup>, macrosuspensions and dispersed powder in water in a mixture of Phosphate buffer saline : ethanol : PEG 400 (40:20:40)

#### 4.2.12 Chemical stability

The chemical stability test was conducted for both batches (lab scale batch and the large scale batch). Fig. 151 shows the HPLC data of the apigenin nanosuspensions prepared with Micron LAB40. All prepared nanosuspensions preserved and non-preserved ones have not had more degradation than 10% after 2 years. This can be a good indicator of the chemical stability of the apigenin nanosuspensions and the good chemical compatibility of the added preservatives with the apigenin particles.

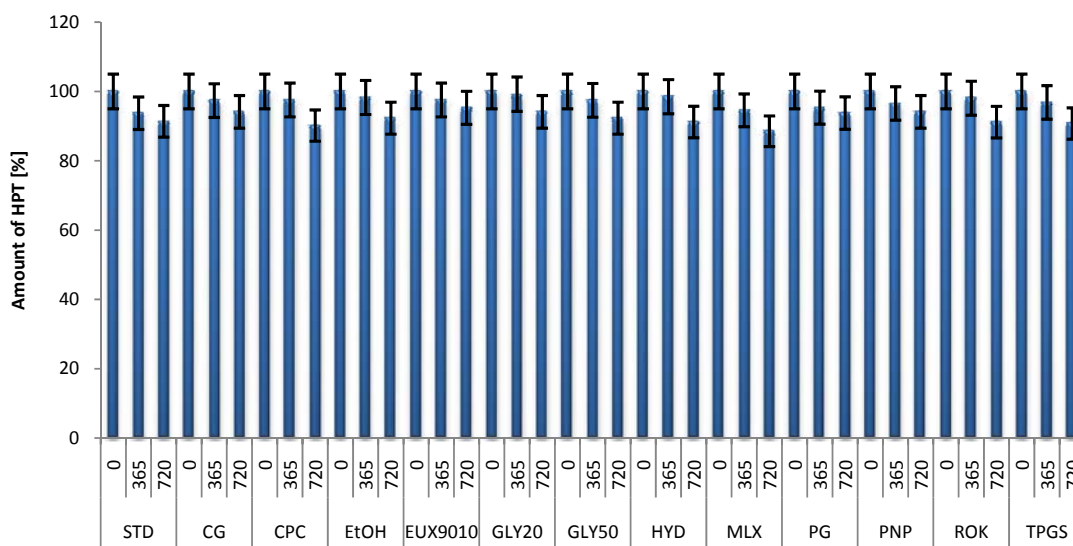
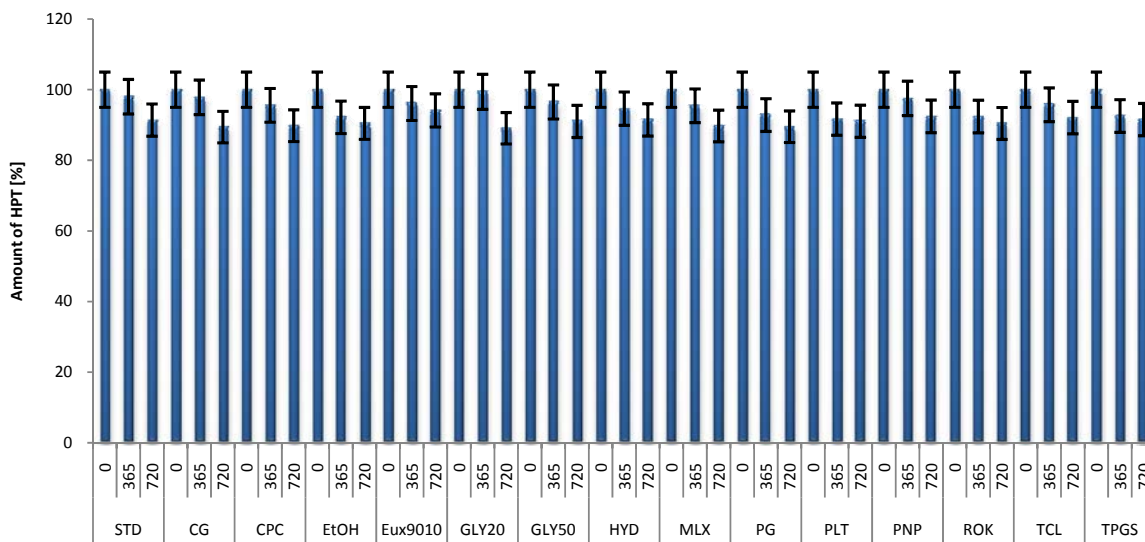


Fig. 151 Amount of apigenin [%] in the non-preserved and preserved apigenin nanosuspension produced with Micron LAB40 using different preservatives (STD= non-preserved, CG= caprylyl glycol, CPC= cetylpyridinium chloride, EtOH= ethanol, EUX9010= Euxyl<sup>®</sup> PE 9010, GLY20= glycerol 20%, GLY50= glycerol 50%, HYD= Hydrolite<sup>®</sup>-5, MLX= multiEx naturotics, PG= propylene glycol, PNP= Phenonip<sup>®</sup>, ROK= Rokonsal<sup>®</sup> PB-5 and TPGS= D-alpha tocopherol polyethylene glycol 1000 succinate) as a function of time (days)

The same observation was noticed with the samples prepared with the smartCrystal technology. No chemical incompatibility was detected for all the samples and they were all in the range of 90-100% concentration over the time of storage (Fig. 152).



**Fig. 152** Amount of apigenin [%] in the non-preserved and preserved apigenin nanosuspension produced with smartCrystals technology using different preservatives (STD= non-preserved, CG= caprylyl glycol, CPC= cetylpyridinium chloride, EtOH= ethanol, Eux9010= Euxyl® PE 9010, GLY20= glycerol 20%, GLY50= glycerol 50%, HYD= Hydrolite®-5, MLX= multiEx naturotics, PG= propylene glycol, PNP= Phenonip®, ROK= Rokonsal® PB-5, TPGS= D-alpha tocopherol polyethylene glycol 1000 succinate and TCL= triclosan) as a function of time (days)

## 5 Summary/Zusammenfassung

### 5.1 Summary

Flavonoids have attracted a considerable interest as active ingredients due to the possession of different biological activities at nontoxic levels. They are considered as potential antioxidants besides their effects as anti-inflammatory, anti-cancer, and anti-viral agents. As they have antioxidant properties they can be incorporated in dermal applied anti-aging products. However, due to their poor aqueous solubility they have limited bioavailability. In order to enhance flavonoids solubility, they can be rendered as nanosuspensions.

The contact angle measurements on compressed tablets of hesperetin and apigenin showed that 1% Plantacare<sup>®</sup> 2000 UP has the best wettability among other surfactants. Therefore, nanosuspensions containing 1% solution of Plantacare<sup>®</sup> 2000 UP were prepared using high pressure homogenization by applying 1,500 bar for 30 cycles. The particle size reached for both flavonoids was less than 1  $\mu\text{m}$ . Both nanocrystals showed good reproducibility of the mean particle size in between the batches. Nanocrystals of both flavonoids were scaled-up using the smartCrystals<sup>®</sup> technology (up to 5 kg). The macrosuspensions were firstly milled using the pearl mill for 7 consecutive passages and subsequently homogenized at 300 bar using high pressure homogenizer. Both stabilized nanocrystals showed excellent long term physical and chemical stability at 4°C and room temperature.

As the prepared smartCrystals<sup>®</sup> are aqueous formulations, preservation is a must. Therefore, Different preservatives with a variety of physical and chemical characteristics were scanned. SmartCrystals<sup>®</sup> were successfully preserved using hydrophilic preservatives without any negative effect on their physical or chemical stability. Agglomerates were detected when hydrophobic preservatives were used, therefore they were discarded as suitable preservatives for our highly dispersed systems.

The effect of an antifoaming agent on the physical and chemical properties of the preserved nanosuspensions was also evaluated and was found that it has a minor effect on these characteristics.

The crystalline status was evaluated using XRD and showed that the used particle size reduction methods did not produce amorphous forms. All peaks and patterns obtained from XRD were similar to that of the original powder.

The saturation solubility for both flavonoids was several times improved. For example, the saturation solubility of hesperetin in water increased from 3 µg/ml for the normal powder to 113 µg/ml for the hesperetin smartCrystals®.

Release studies were conducted using Franz diffusion cells. There was large increase in the dissolved amount of flavonoids by rendering them as nanocrystals when compared to the coarse form.

The antioxidant activity for both flavonoids was examined and evaluated using the DPPH method. An increase in the antioxidant activity was observed by decreasing the particle size and hence increasing the surface area. Nanocrystals showed almost double the activity to that of the micronized powder.

The smartCrystals® were incorporated in gels to obtain a final stable dosage form for dermal application. No sign of instability was detected during and after several months of incorporation.

Thus, stable and preserved flavonoids nanocrystals with enhanced solubility were produced using the combination technology without affecting the crystalline nature of the compounds. These smartCrystals® can be incorporated in gels or creams by simple admixing.

## 5.2 Zusammenfassung

Flavonoide sind interessant als aktive Wirkstoffe aufgrund ihrer verschiedenen biologischen Aktivitäten, ohne die toxische Ebene zu überschreiten. Sie werden als Antioxidantien und entzündungshemmende-, antivirale Arzneimittel verwendet, sowie in der Anti-Krebstherapie eingesetzt. Aufgrund ihrer antioxidativen Eigenschaften können sie in dermalen Anti-Aging Produkten inkorporiert werden. Wegen ihrer geringen Wasserlöslichkeit besitzen sie nur eine begrenzte Bioverfügbarkeit. Um die Löslichkeit zu erhöhen werden sie als Nanosuspensionen eingesetzt.

Die Kontaktwinkel Messungen von komprimiertem Hesperetin und Apigenin zeigten, dass 1% Plantacare® 2000 UP sich als bestes Netzmittel eignet. Deshalb wurden Nanosuspensionen mit 1%iger Plantacare® 2000 UP-Lösung hergestellt unter Verwendung von Hochdruckhomogenisation bei 1.500 bar und 30 Zyklen. Die Teilchengröße betrug für beide Flavonoide weniger als 1 µm. Eine gute Reproduzierbarkeit der mittleren Teilchengröße zwischen den einzelnen Chargen konnte nachgewiesen werden. Mittels der smartCrystals® Technologie wurde von Hesperetin- und Apigenin Nanokristallen ein Scaling-up bis 5 kg durchgeführt. Die Makrosuspensionen wurden zuerst mit einer Perlmühle in 7 aufeinander folgenden Passagen gemahlen und anschließend bei 300 bar mit einem Hochdruck-



homogenisator homogenisiert. Die so hergestellten Nanokristalle zeigten eine hervorragende physikalische und chemische Langzeitstabilität bei der Lagerung bei 4°C und Raumtemperatur.

Wegen der wässrigen Formulierung der hergestellten smartCrystals<sup>®</sup> ist eine Konservierung erforderlich. Deshalb wurden verschiedene Konservierungsstoffe mit einer Vielzahl physikalischer und chemischer Eigenschaften ausprobiert. SmartCrystals<sup>®</sup> wurden erfolgreich mit hydrophilen Konservierungsstoffen versetzt ohne negative Auswirkungen auf ihre physikalische und chemische Stabilität. In Proben mit hydrophoben Konservierungsstoffen bildeten sich Agglomerate und fielen somit als geeignetes Konservierungsmittel für unsere hochdispersen Systeme aus.

Die Auswirkungen von Antischaummittel auf die physikalischen und chemischen Eigenschaften der konservierten Nanosuspensionen wurden ebenfalls untersucht. Es wurde ein geringer Einfluss auf diese Eigenschaften festgestellt.

Der kristalline Zustand wurde mittels Röntgendiffraktometrie untersucht und ergab, dass die durchgeführten Partikelgrößenreduktionsmethoden keine amorphen Formen produzierten. Die Nanosuspensionen wiesen in den Röntgendiffraktometrie -diagrammen ähnliche Muster und Höhen auf wie das ursprüngliche Pulver.

Die Sättigungslöslichkeit für beide Flavonoide wurde verbessert und erhöht, zum Beispiel für Hesperetin in Wasser von 3 µg/ml für grobes Pulver auf 113 µg/ml für die Hesperetin smartCrystals<sup>®</sup>.

In *in vitro* Freisetzungsversuchen an Franz-Diffusionszellen gab es eine große Zunahme der gelösten Menge an Flavonoiden durch Rendering als Nanokristalle im Vergleich zur Pulverform.

Die antioxidative Aktivität für beide Flavonoide mittels DPPH-Methode wurde untersucht und bewertet. Eine Erhöhung der antioxidativen Aktivität wurde durch die Verringerung der Teilchengröße und damit die Vergrößerung der Oberfläche beobachtet. Nanokristalle zeigten fast doppelt so viel Aktivität im Vergleich zum mikronisierten Pulver.

Die smartCrystals<sup>®</sup> wurden in Gele eingearbeitet um eine endgültige stabile Darreichungsform für dermale Applikationen zu finden. Die physikalischen Eigenschaften wurden für diese smartCrystals<sup>®</sup>-Gele untersucht. Es wurden keine Anzeichen von Instabilität nach mehreren Monaten der Einarbeitung festgestellt.

Aufgrund dieser Experimente wurden stabile und konservierte Flavonoid Nanokristalle mit erhöhter Löslichkeit produziert, unter Verwendung der Kombinationstechnologie, ohne die

kristallinen Eigenschaften der Komponenten zu verändern. Diese smartCrystals<sup>®</sup> können in Gele oder Cremes durch einfaches Mischen eingearbeitet werden.

## 6 References

1. Harman, D., *Aging - Prospects for Further Increases in the Functional Life-Span*. Age, 1994. **17**(4): p. 119-146.
2. Harman, D., *Antioxidant supplements: Effects on disease and aging in the United States population*. Journal of the American Aging Association, 2000. **23**(1): p. 25-31.
3. Harman, D., *Free radical theory of aging: an update: increasing the functional life span*. Annals of the New York Academy of Sciences, 2006. **1067**: p. 10-21.
4. Umbach, W., *Kosmetik und Hygiene: Von Kopf bis Fuß*. 3 ed. ed. 2004, Weinheim: Wiley. 569.
5. Pardeike, J., *Nanosuspensions and nanostructured lipid carriers for dermal application*. 2008, Freie Universität Berlin: Berlin.
6. Wiechers, J.W., *The barrier function of the skin in relation to percutaneous absorption of drugs*. Pharm Weekbl Sci, 1989. **11**(6): p. 185-98.
7. Yu, B.P., *Cellular Defenses against Damage from Reactive Oxygen Species*. Physiological Reviews, 1994. **74**(1): p. 139-162.
8. De Paepe, K., et al., *Analysis of epidermal lipids of the healthy human skin: Factors affecting the design of a control population*. Skin Pharmacology and Physiology, 2004. **17**(1): p. 23-30.
9. Rogers, J., et al., *Stratum corneum lipids: The effect of ageing and the seasons*. Archives of Dermatological Research, 1996. **288**(12): p. 765-770.
10. Kent, M.J., N.D. Light, and A.J. Bailey, *Evidence for glucose-mediated covalent cross-linking of collagen after glycosylation in vitro*. Biochemical Journal, 1985. **225**(3): p. 745-52.
11. Stern, R. and H.I. Maibach, *Hyaluronan in skin: aspects of aging and its pharmacologic modulation*. Clinics in Dermatology, 2008. **26**(2): p. 106-122.
12. Ryan, T., *The ageing of the blood supply and the lymphatic drainage of the skin*. Micron, 2004. **35**(3): p. 161-171.
13. Cerami, A., *Hypothesis - Glucose as a Mediator of Aging*. Journal of the American Geriatrics Society, 1985. **33**(9): p. 626-634.
14. Davies, K.J.A., *Oxidative stress: The paradox of aerobic life*. Free Radicals and Oxidative Stress: Environment, Drugs and Food Additives, 1995(61): p. 1-31.
15. Fridovich, I., *Superoxide Radical and Superoxide Dismutases*. Annual Review of Biochemistry, 1995. **64**: p. 97-112.

16. Halliwell, B., *Free-Radicals, Reactive Oxygen Species and Human-Disease - a Critical-Evaluation with Special Reference to Atherosclerosis*. British Journal of Experimental Pathology, 1989. **70**(6): p. 737-757.
17. Lavker, R.M., *Cutaneous aging: chronologic versus photoaging*, in *Photodamage*, G.B. A., Editor. 1995, New York: Blackwell. p. 123–135.
18. Kohen, R. and A. Nyska, *Oxidation of biological systems: oxidative stress phenomena, antioxidants, redox reactions, and methods for their quantification*. Toxicologic Pathology, 2002. **30**(6): p. 620-50.
19. Schabeuter, K.U. and J.M. Wood, *Free radicals in the human epidermis*. FREE RADICAL BIOLOGY AND MEDICINE, 1989. **6**: p. 519-532.
20. Rieger, M.M. and M. Pains, *Oxidative reactions in and on the skin: mechanism and prevention*,. Cosmetic Toiletries, 1993. **108**: p. 43-56.
21. Rittie, L. and G.J. Fisher, *UV-light-induced signal cascades and skin aging*. Ageing Research Reviews, 2002. **1**(4): p. 705-720.
22. Weber, S.U., et al., *Vitamin C, uric acid, and glutathione gradients in murine stratum corneum and their susceptibility to ozone exposure*. Journal of Investigative Dermatology, 1999. **113**(6): p. 1128-32.
23. Hellemans, L., et al., *Antioxidant enzyme activity in human stratum corneum shows seasonal variation with an age-dependent recovery*. Journal of Investigative Dermatology, 2003. **120**(3): p. 434-9.
24. Beckman, K.B. and B.N. Ames, *The free radical theory of aging matures*. Physiol Rev, 1998. **78**(2): p. 547-581.
25. Harman, D., *Free-Radical Theory of Aging - Increasing the Functional Life-Span*. Pharmacology of Aging Processes: Methods of Assessment and Potential Interventions, 1994. **717**: p. 1-15.
26. Medvedev, Z.A., *An attempt at a arational classification of theories of ageing*. Biological Reviews, 1990. **65**: p. 375–398.
27. Hayflick, L., *Limited in Vitro Lifetime of Human Diploid Cell Strains*. Experimental Cell Research, 1965. **37**(3): p. 614-&.
28. Harman, D., *Aging: a theory based on free radical and radiation chemistry*. J Gerontol, 1956. **11**(3): p. 298-300.
29. Hermann, K., *Flavonols and flavones in food plants: a review*. International Journal of Food Science & Technology, 1976. **11**: p. 433-448.
30. Harborne, J.B., *Comparative Biochemistry of Flavonoids .4. Correlations between Chemistry Pollen Morphology and Systematics in Family Plumbaginaceae*. Phytochemistry, 1967. **6**(10): p. 1415-&.

31. RiceEvans, C.A., N.J. Miller, and G. Paganga, *Structure-antioxidant activity relationships of flavonoids and phenolic acids*. Free Radical Biology and Medicine, 1996. **20**(7): p. 933-956.
32. Shahidi, F. and P.K. Wanasundara, *Phenolic antioxidants*. Critical Reviews in Food Science and Nutrition, 1992. **32**(1): p. 67-103.
33. Kandaswami, C. and E. Middleton, Jr., *Free radical scavenging and antioxidant activity of plant flavonoids*. Advances in Experimental Medicine and Biology, 1994. **366**: p. 351-76.
34. Ho, C.T., et al., *Antioxidative Effect of Polyphenol Extract Prepared from Various Chinese Teas*. Preventive Medicine, 1992. **21**(4): p. 520-525.
35. Kinsella, J.E., et al., *Possible Mechanisms for the Protective Role of Antioxidants in Wine and Plant Foods*. Food Technology, 1993. **47**(4): p. 85-89.
36. Duarte, J., et al., *Vasodilatory Effects of Flavonoids in Rat Aortic Smooth-Muscle - Structure-Activity-Relationships*. General Pharmacology, 1993. **24**(4): p. 857-862.
37. Brown, J.P., *A review of the genetic effects of naturally occurring flavonoids, anthraquinones and related compounds*. Mutation Research, 1980. **75**(3): p. 243-77.
38. Middleton, E. and C. Kandaswami, *Effects of Flavonoids on Immune and Inflammatory Cell Functions*. Biochemical Pharmacology, 1992. **43**(6): p. 1167-1179.
39. Jovanovic, S.V., I. Jankovic, and L. Josimovic, *Electron-Transfer Reactions of Alkyl Peroxy-Radicals*. Journal of the American Chemical Society, 1992. **114**(23): p. 9018-9021.
40. Robak, J., et al., *Screening of the Influence of Flavonoids on Lipoxygenase and Cyclooxygenase Activity, as Well as on Nonenzymic Lipid Oxidation*. Polish Journal of Pharmacology and Pharmacy, 1988. **40**(5): p. 451-458.
41. Lindahl, M. and C. Tagesson, *Selective-Inhibition of Group-II Phospholipase-A2 by Quercetin*. Inflammation, 1993. **17**(5): p. 573-582.
42. Elliott, A.J., et al., *Inhibition of glutathione reductase by flavonoids. A structure-activity study*. Biochemical Pharmacology, 1992. **44**(8): p. 1603-8.
43. Chang, W.S., et al., *Inhibitory effects of flavonoids on xanthine oxidase*. Anticancer Research, 1993. **13**(6A): p. 2165-70.
44. Hanasaki, Y., S. Ogawa, and S. Fukui, *The Correlation between Active Oxygens Scavenging and Antioxidative Effects of Flavonoids*. Free Radical Biology and Medicine, 1994. **16**(6): p. 845-850.
45. Cotelle, N., et al., *Scavenger and antioxidant properties of ten synthetic flavones*. Free Radical Biology and Medicine, 1992. **13**(3): p. 211-9.
46. Chen, Y.T., et al., *Flavonoids as Superoxide Scavengers and Antioxidants*. Free Radical Biology and Medicine, 1990. **9**(1): p. 19-21.

47. Zhou, Y.C. and R.L. Zheng, *Phenolic-Compounds and an Analog as Superoxide Anion Scavengers and Antioxidants*. *Biochemical Pharmacology*, 1991. **42**(6): p. 1177-1179.
48. Bors, W., et al., *Flavonoids as Antioxidants - Determination of Radical-Scavenging Efficiencies*. *Methods in Enzymology*, 1990. **186**: p. 343-355.
49. Tsujimoto, Y., H. Hashizume, and M. Yamazaki, *Superoxide Radical Scavenging Activity of Phenolic-Compounds*. *International Journal of Biochemistry*, 1993. **25**(4): p. 491-494.
50. Erbenruss, M., et al., *Absolute Rate Constants of Alkoxy Radical Reactions in Aqueous-Solution*. *Journal of Physical Chemistry*, 1987. **91**(9): p. 2362-2365.
51. Terao, J., M. Piskula, and Q. Yao, *Protective Effect of Epicatechin, Epicatechin Gallate, and Quercetin on Lipid-Peroxidation in Phospholipid-Bilayers*. *Archives of Biochemistry and Biophysics*, 1994. **308**(1): p. 278-284.
52. Mangiapane, H., et al., *The inhibition of the oxidation of low density lipoprotein by (+)-catechin, a naturally occurring flavonoid*. *Biochemical Pharmacology*, 1992. **43**(3): p. 445-50.
53. Riceevans, C.A., et al., *The Relative Antioxidant Activities of Plant-Derived Polyphenolic Flavonoids*. *Free Radical Research*, 1995. **22**(4): p. 375-383.
54. Havsteen, B.H., *The biochemistry and medical significance of the flavonoids*. *Pharmacology and Therapeutics*, 2002. **96**(2-3): p. 67-202.
55. Müller, R.H., B.H.L. Böhm, and M.J. Grau, *Nanosuspensionen - Formulierungen für schwerlösliche Arzneistoffe mit geringer Bioverfügbarkeit: II. Stabilität. biopharmazeutische Aspekte. mögliche Arzneiformen und Zulassungsfragen*. *Pharm. Ind.*, 1999. **61**(2): p. 175-178.
56. Rabinow, B.E., *Nanosuspensions in drug delivery*. *Nat Rev Drug Discov*, 2004. **3**(9): p. 785-96.
57. Stegemann, S., et al., *When poor solubility becomes an issue: From early stage to proof of concept*. *Eur J Pharm Sci*, 2007. **31**(5): p. 249-261.
58. Desai, M.P., et al., *Gastrointestinal uptake of biodegradable microparticles: effect of particle size*. *Pharm Res*, 1996. **13**(12): p. 1838-45.
59. Kasim, N.A., et al., *Molecular properties of WHO essential drugs and provisional biopharmaceutical classification*. *Mol Pharm*, 2004. **1**(1): p. 85-96.
60. Martinez, M.N. and G.L. Amidon, *A mechanistic approach to understanding the factors affecting drug absorption: a review of fundamentals*. *Journal of Clinical Pharmacology.*, 2002. **42**(6): p. 620-43.
61. Buckton, G. and A.E. Beezer, *The relationship between particle size and solubility*. *International Journal of Pharmaceutics*, 1992. **82**(3): p. R7-R10.
62. Hecq, J., et al., *Preparation and characterization of nanocrystals for solubility and dissolution rate enhancement of nifedipine*. *Int J Pharm*, 2005. **299**(1-2): p. 167-177.

63. Jinno, J., et al., *Effect of particle size reduction on dissolution and oral absorption of a poorly water-soluble drug, cilostazol, in beagle dogs*. J Control Release, 2006. **111**(1-2): p. 56-64.
64. Keck, C.M. and R.H. Müller, *Nanodiamanten - Erhöhte Bioaktivität*. Labor & More, 2008. **01/08**: p. 64-65.
65. Müller, R.H., C. Jacobs, and O. Kayser, *Nanosuspensions for the Formulation of Poorly Soluble Drugs*, in *Pharmaceutical Emulsions and Suspensions*, F. Nielloud and G. Marti-Mestres, Editors. 2000, Marcel Dekker. p. 383-407.
66. Müller, R.H., et al., *Pharmaceutical nanosuspensions for medicament administration as systems with increased saturation solubility and rate of solution*. 1999, Medac Gesellschaft für klinische Spezialpräparate mbH: United States.
67. Mishra, P.R., et al., *Production and characterization of Hesperetin nanosuspensions for dermal delivery*. International Journal of Pharmaceutics, 2009. **371**(1-2): p. 182-9.
68. Müller, R.H., B.H.L. Böhm, and G. M.J., *Nanosuspensionen: Formulierungen für schwerlösliche Arzneistoffe mit geringer Bioverfügbarkeit. 2. Mitteilung: Stabilität, biopharmazeutische Aspekte, mögliche Arzneiformen und Zulassungsfragen*. Pharm. Ind. , 1999. **61**(2): p. 175-178.
69. Tommasini, S., et al., *The inclusion complexes of hesperetin and its 7-rhamnoglucoside with (2-hydroxypropyl)-beta-cyclodextrin*. J Pharm Biomed Anal, 2005. **39**(3-4): p. 572-80.
70. Tommasini, S., et al., *Improvement in solubility and dissolution rate of flavonoids by complexation with beta-cyclodextrin*. J Pharm Biomed Anal, 2004. **35**(2): p. 379-87.
71. Willems, L., R. van der Geest, and K. de Beule, *Itraconazole oral solution and intravenous formulations: a review of pharmacokinetics and pharmacodynamics*. J Clin Pharm Ther, 2001. **26**(3): p. 159-169.
72. Müller, R.H. and J.U. Junghanns, *Drug nanocrystals/nanosuspensions for the delivery of poorly soluble drugs*, in *Nanoparticulates as Drug Carriers*, V.P. Torchilin, Editor. 2006, Imperial College Press: London. p. 307-328.
73. Petersen, R.D., *Nanocrystals for use in topical formulations and method of production thereof*, in *PCT/EP2007/009943*. 2006, Abbott GmbH, Petersen, R.D.: Germany.
74. Liversidge, G., *Workshop 'Nanotechnology-solid particles, lipids and nanocomplexes'*, in *IIR Drug Delivery Partnerships™ Meeting*. 2003: Cologne/Germany.
75. Müller, R.H., C.M. Keck, and R.D. Petersen. *Rutin smartCrystals: Bioactivity enhancement and stability against electrolytes*. in *Annual Meeting of the American Association of Pharmaceutical Scientists (AAPS)*. 2008. Atlanta, USA.
76. Keck, C.M., et al., *Second generation of drug nanocrystals for delivery of poorly soluble drugs: smartCrystals technology*. Dosis, 2008. **2**(24): p. 124-128
77. Karavas, E., et al., *Investigation of the release mechanism of a sparingly water-soluble drug from solid dispersions in hydrophilic carriers based on physical state of drug, particle size distribution and drug-polymer interactions*. Eur J Pharm Biopharm, 2007. **66**(3): p. 334-47.

78. Keck, C.M. and R.H. Muller, *Drug nanocrystals of poorly soluble drugs produced by high pressure homogenisation*. European Journal of Pharmaceutics and Biopharmaceutics, 2006. **62**(1): p. 3-16.
79. Müller, R.H. and A. Akkar, *Drug nanocrystals of poorly soluble drugs*, in *Encyclopedia of Nanoscience and Nanotechnology*, H.S. Nalwa, Editor. 2004, American Scientific Publishers. p. 627-638.
80. Müller, R.H. and K. Peters, *Nanosuspensions for the formulation of poorly soluble drugs: I. Preparation by a size-reduction technique* Int. J. Pharm., 1998. **160**(2): p. 229-237.
81. *Megace ES, Rx List -The Internet Drug List Inc.* 2008.
82. Bonina, F., et al., *Flavonoids as potential protective agents against photo-oxidative skin damage*. International Journal of Pharmaceutics, 1996. **145**(1-2): p. 87-94.
83. Choi, E.M. and Y.H. Kim, *Hesperetin attenuates the highly reducing sugar-triggered inhibition of osteoblast differentiation*. Cell Biol Toxicol, 2008. **24**(3): p. 225-231.
84. Choi, E.J., *Antioxidative effects of hesperetin against 7,12-dimethylbenz(a)anthracene-induced oxidative stress in mice*. Life Sci, 2008. **82**(21-22): p. 1059-64.
85. Neung-Kee, L., et al., *Antiallergic Activity of Hesperidin Is Activated by Intestinal Microflora*. Int. J. Exp. Clin. Pharmacology, 2004. **71**(4): p. 174-180.
86. Cha, J.Y., et al., *Effect of hesperetin, a citrus flavonoid, on the liver triacylglycerol content and phosphatidate phosphohydrolase activity in orotic acid-fed rats*. Plant Foods Hum Nutr, 2001. **56**(4): p. 349-58.
87. Longxiao, L. and C. Jun, *Solubility of Hesperetin in Various Solvents from (288.2 to 323.2) K*. J. Chem. Eng., 2008. **53**(7): p. 1649-1650.
88. Jeong, Y.J., et al., *Differential inhibition of oxidized LDL-induced apoptosis in human endothelial cells treated with different flavonoids*. British Journal of Nutrition, 2005. **93**(5): p. 581-591.
89. Vauzour, D., et al., *Activation of pro-survival Akt and ERK1/2 signalling pathways underlie the anti-apoptotic effects of flavanones in cortical neurons*. Journal of Neurochemistry, 2007. **103**(4): p. 1355-1367.
90. Lee, N.K., et al., *Antiallergic activity of hesperidin is activated by intestinal microflora*. Pharmacology, 2004. **71**(4): p. 174-180.
91. deGrey, A.D.N.J., *A proposed refinement of the mitochondrial free radical theory of aging*. Bioessays, 1997. **19**(2): p. 161-166.
92. Yi, L.T., et al., *Antidepressant-like behavioral and neurochemical effects of the citrus-associated chemical apigenin*. Life Sci, 2008. **82**(13-14): p. 741-51.
93. Peterson, J. and J. Dwyer, *Flavonoids: Dietary occurrence and biochemical activity*. Nutrition Research, 1998. **18**(12): p. 1995-2018.



94. Siddique, Y.H. and M. Afzal, *Antigenotoxic effect of apigenin against mitomycin C induced genotoxic damage in mice bone marrow cells*. Food Chem Toxicol, 2009. **47**(3): p. 536-9.
95. Datta, B.K., et al., *Analgesic, antiinflammatory and CNS depressant activities of sesquiterpenes and a flavonoid glycoside from Polygonum viscosum*. Pharmazie, 2004. **59**(3): p. 222-5.
96. Jeong, G.S., et al., *Anti-inflammatory effects of apigenin on nicotine- and lipopolysaccharide-stimulated human periodontal ligament cells via heme oxygenase-1*. Int Immunopharmacol, 2009. **9**(12): p. 1374-80.
97. Romanova, D., et al., *Study of antioxidant effect of apigenin, luteolin and quercetin by DNA protective method*. Neoplasma, 2001. **48**(2): p. 104-7.
98. Kim, H.P., et al., *Effects of naturally-occurring flavonoids and biflavonoids on epidermal cyclooxygenase and lipoxygenase from guinea-pigs*. Prostag Leukotr Ess, 1998. **58**(1): p. 17-24.
99. Wang, W.Q., et al., *Cell-cycle arrest at G2/M and growth inhibition by apigenin in human colon carcinoma cell lines*. Molecular Carcinogenesis, 2000. **28**(2): p. 102-110.
100. Yin, F., A.E. Giuliano, and A.J. Van Herle, *Growth inhibitory effects of flavonoids in human thyroid cancer cell lines*. Thyroid, 1999. **9**(4): p. 369-376.
101. guide, V.h.s. *Bioflavonoids (vitamin P)* <http://www.vitamins-supplements.org/bioflavonoids.php>. 2006.
102. Choi, S.I., et al., *Mechanism of apoptosis induced by apigenin in HepG2 human hepatoma cells: involvement of reactive oxygen species generated by NADPH oxidase*. Archives of Pharmacal Research, 2007. **30**(10): p. 1328-35.
103. Birt, D.F., et al., *Inhibition of ultraviolet light induced skin carcinogenesis in SKH-1 mice by apigenin, a plant flavonoid*. Anticancer Res, 1997. **17**(1A): p. 85-91.
104. Wei, H., et al., *Inhibitory effect of apigenin, a plant flavonoid, on epidermal ornithine decarboxylase and skin tumor promotion in mice*. Cancer Res, 1990. **50**(3): p. 499-502.
105. Ujiki, M.B., et al., *Apigenin inhibits pancreatic cancer cell proliferation through G2/M cell cycle arrest*. Mol Cancer, 2006. **5**: p. 76.
106. Xiao, M., et al., *Measurement and correlation of solubilities of apigenin and apigenin 7-O-rhamnosylglucoside in seven solvents at different temperatures*. Journal of Chemical Thermodynamics, 2011. **43**(3): p. 240-243.
107. Rowe, R.C., et al., *Handbook of pharmaceutical excipients*. 6th ed. 2009, London ; Greyslake, IL Washington, DC: Pharmaceutical Press ; American Pharmacists Association. xxvii, 888 p.
108. Varvaresou, A., et al., *Self-preserving cosmetics*. International Journal of Cosmetic Science, 2009. **31**(3): p. 163-175.

109. Chiori, C.O. and A.A. Ghobashy, *A Potentiating Effect of Edta on the Bactericidal Activity of Lower Concentrations of Ethanol*. International Journal of Pharmaceutics, 1983. **17**(2-3): p. 121-128.
110. NIPA. *Phenonip*.
111. BIOCHEMA, I. *Rokonsal PB-5*.
112. Müller, R.H., *Polydispersität und elektroforetische Beweglichkeit hochdispenser Systeme*. 1983, Christian-Albrechts-Universität: Kiel.
113. Kunlayakorn, L., M. Kanlayavattanakul, and N. Lourith, *Antimicrobial efficacy of caprylyl glycol and ethylhexylglycerine in emulsion*. Journal of Health Research, 2009. **23**(1): p. 1-3.
114. Cutter, C.N., et al., *Antimicrobial Activity of Cetylpyridinium Chloride Washes against Pathogenic Bacteria on Beef Surfaces*. Journal of Food Protection, 2000. **63**: p. 593-600.
115. *Euxyl® K 700. Product information, preservatives for cosmetics*.
116. *Euxyl® K 702. Product information, preservatives for cosmetics*.
117. *Euxyl® PE 9010. Product information, preservatives for cosmetics*.
118. FDA. *The role of glycerol in allergen extracts*. 2002.
119. Obeidat, W.M., et al., *Preservation of nanostructured lipid carriers (NLC)*. European Journal of Pharmaceutics and Biopharmaceutics, 2010. **76**(1): p. 56-67.
120. Park, J., et al., *In vitro antibacterial and anti-inflammatory effects of honokiol and magnolol against Propionibacterium sp.* European Journal of Pharmacology, 2004. **496**(1-3): p. 189-195.
121. *Updated request for a scientific opinion: Triclosan (CAS 3380-34-5) (EINECS 222-182-2) Supplement I (P32)*.
122. Shegokar, R., et al., *Apigenin smartCystals for dermal delivery*. International Journal of Pharmaceutics, 2011. **In press**.
123. Measures, T.I.B.o.W.a., *The International System of Units (SI)*. 8th ed. ed. 2006.
124. Saveyn, H., et al., *Determination of the refractive index of water-dispersible granules for use in laser diffraction experiments*. Particle & Particle Systems Characterization, 2002. **19**(6): p. 426-432.
125. Brandwilliams, W., M.E. Cuvelier, and C. Berset, *Use of a Free-Radical Method to Evaluate Antioxidant Activity*. Food Science and Technology-Lebensmittel-Wissenschaft & Technologie, 1995. **28**(1): p. 25-30.
126. Kanaze, F.I., et al., *A validated solid-phase extraction HPLC method for the simultaneous determination of the citrus flavanone aglycones hesperetin and naringenin in urine*. Journal of Pharmaceutical and Biomedical Analysis, 2004. **36**(1): p. 175-181.

127. Tsai, Y.H., et al., *In vitro permeation and in vivo whitening effect of topical hesperetin microemulsion delivery system*. International Journal of Pharmaceutics, 2010. **388**(1-2): p. 257-262.
128. Fichera, M., S. Wissing, and R.H. Müller. *Effect of 4000 bar homogenisation pressure on particle diminution in drug suspensions*. in *International Meeting on Pharmaceutics, Biopharmaceutics and Pharmaceutical Technology*. 2004. Nürnberg.
129. Fichera, M.A., Keck, C.M., Müller, R.H. *Nanopure technology - drug nanocrystals for the delivery of poorly soluble drugs*. in *Particles*. 2004. Orlando.
130. Peters, K., *Nanosuspensionen - ein neues Formulierungsprinzip für schwerlösliche Arzneistoffe*, in *Dissertation, Pharmazeutische Technologie*. 1999, Freie Universität: Berlin.
131. Müller, R.H., et al. *Nanosuspensions - a novel formulation for the i.v. administration of poorly soluble drugs*. in *1st World Meeting APGI/APV*. 1995. Budapest.
132. Müller, R.H., *Zetapotential und Partikeladung in der Laborpraxis*. Band 37, ed. A. Paperback. 1996, Stuttgart: Wissenschaftliche Verlagsgesellschaft mbH.
133. Riddick, T.M., *Control of colloid stability through zeta potential; with a closing chapter on its relationship to cardiovascular disease*. 1968, Wynnewood, Pa.: Published for Zeta-Meter, inc. v.
134. Grau, M.J., O. Kayser, and R.H. Müller, *Nanosuspensions of poorly soluble drugs--reproducibility of small scale production*. Int J Pharm, 2000. **196**(2): p. 155-9.
135. Lucassen, J., *Anionic Surfactants - Physical Chemistry of Surfactant Action* ed. E.H. Lucassen-Reijnders. 1981, NY: Marcel Dekker.
136. Müller, R.H., *Zetapotential und Partikeladung in der Laborpraxis*. 1996, Stuttgart: Wissenschaftliche Verlagsges.
137. Keck, C.M., J. Hanisch, and S. Kobierski. *Nanosuspensions – New insights through improved characterisation*. in *Annual Meeting of the German Pharmaceutical Society (DPhG)*. 2008. Bonn, Germany.
138. Al Shaal, L., et al., *Preserved nanosuspensions of Hesperetin: Preparation and characterization*. European journal of pharmaceutics and biopharmaceutics.
139. Owen, M.J., *Defoamers*. Kirk-Othmer Encyclopedia of Chemical Technology. 2000: John Wiley & Sons, Inc.
140. Langevin, D., *Aqueous foams: a field of investigation at the frontier between chemistry and physics*. Chemphyschem, 2008. **9**(4): p. 510-22.
141. Al Shaal, L., R.H. Müller, and R. Shegokar, *smartCrystal combination technology--scale up from lab to pilot scale and long term stability*. Pharmazie, 2010. **65**(12): p. 877-84.
142. Rothbard, J.B., et al., *Conjugation of arginine oligomers to cyclosporin A facilitates topical delivery and inhibition of inflammation*. Nature Medicine, 2000. **6**(11): p. 1253-1257.

143. Patravale, V.B., A.A. Date, and R.M. Kulkarni, *Nanosuspensions: a promising drug delivery strategy*. J Pharm Pharmacol, 2004. **56**(7): p. 827-40.
144. Keck, C.M., *Cyclosporine nanosuspensions: Optimised size characterisation & oral formulations* in *Pharmaceutical technology*. 2006, Freie Universität Berlin: Berlin.
145. Huang, Y.B., et al., *The effect of component of cream for topical delivery of hesperetin*. Chemical and Pharmaceutical Bulletin, 2010. **58**(5): p. 611-4.
146. Varma, M.V. and R. Panchagnula, *Enhanced oral paclitaxel absorption with vitamin E-TPGS: effect on solubility and permeability in vitro, in situ and in vivo*. Eur J Pharm Sci, 2005. **25**(4-5): p. 445-53.
147. Shahidi, F. and M. Naczk, *Food phenolics: an overview*, in *Food phenolics: sources, chemistry, effects, applications*, F. Shahidi and M. Naczk, Editors. 1995, echnomic Publishing Company Inc: Lancaster. p. 1-5.
148. Kerč, J., et al. *Influence of different stabilizers on particle size of apigenin nanosuspensions produced by high pressure homogenization*. in *International Symposium on Controlled Release of Bioactive Materials*, 36. 2009. Copenhagen: Controlled Release Society, Inc.
149. Chiou, R.Y., et al., *Ethanol-mediated variations in cellular fatty acid composition and protein profiles of two genotypically different strains of Escherichia coli O157:H7*. Appl Environ Microbiol, 2004. **70**(4): p. 2204-10.
150. Buttke, T.M. and L.O. Ingram, *Ethanol-induced changes in lipid composition of Escherichia coli: inhibition of saturated fatty acid synthesis in vitro*. Arch Biochem Biophys, 1980. **203**(2): p. 565-71.
151. Ingram, L.O. and T.M. Buttke, *Effects of alcohols on micro-organisms*. Adv Microb Physiol, 1984. **25**: p. 253-300.
152. Cook, W.H., *The Physio-medical Dispensatory*. 1869.
153. Bhargava, H.N. and P.A. Leonard, *Triclosan: applications and safety*. Am J Infect Control, 1996. **24**(3): p. 209-218.
154. Giesová, M., J. Chumchalová, and M. Plocková, *Effect of food preservatives on the inhibitory activity of acidocin CH5 and bacteriocin D10*. Eur. Food Res. Technol., 2004. **218**: p. 194-197.
155. Beilfuss, W., M. Leschke, and K. Weber, *A new concept to boost the preservative efficacy of phenoxyethanol*. SÖFW Journal 2005. **11**: p. 30-36.
156. McDonnell, G. and A.D. Russell, *Antiseptics and disinfectants: activity, action, and resistance*. Clin Microbiol Rev, 1999. **12**(1): p. 147-79.
157. Talaro, K. and A. Talaro, *Foundations in Microbiology*. 1st ed. ed. 1993, Dubuque: William C Brown Publishers.

158. Sato, T., *Effects of Surfactant Concentration on Stability of Dispersion*, in *Environmental Fate and Safety Management of Agrochemicals*, J.M. Clark and H. Ohkawa, Editors. 2005, American Chemical Society: Washington, DC. p. 290-296.

## 7 Publication list

### Book Chapter:

1. Keck, C.M., **Al Shaal, L.**, Müller, R.H., “*Intravenous drug nanocrystals: Production & modulation of organ distribution*”, in: *Materials for nanomedicine*, (Torchilin, V., Amiji, M.M., eds.), Pan Stanford Publishing Pte Ltd., Singapore, 2009, (in press).

### Articles in Peer-reviewed Journals:

1. Mishra, P.R., **Al Shaal, L.**, Müller, R.H., Keck, C.M., “*Production and characterization of Hesperetin nanosuspensions for dermal delivery*”, *Int. J. Pharm.* 371, 182-189, 2009.
2. **Al Shaal, L.**, Mishra, P.R., Müller, R.H., Keck, C.M., “*Preserved nanosuspensions of Hesperetin: Preparation and characterization*”, *Eur. J. Pharm. Biopharm.*, 2009, (in press).
3. **Al Shaal, L.**, Müller, R.H., Keck, C.M., “*Preserving Hesperetin nanosuspensions for dermal application*”, *Die Pharmazie*, 65, 86-92, 2010.
4. Shegokar, R., **Al Shaal, L.**, Keck, C.M., “*Production & characterization of Apigenin nanocrystals for cancer therapy*”, (in press).
5. Rachmawati, H., **Al Shaal, L.**, Müller, R.H., Keck, C.M., “*Curcumin nanocrystals for oral bioavailability enhancement: Preparation, characterization and short-term physical stability*”, (in press).
6. **Al Shaal, L.**, Müller, R.H., Shegokar, R., “*smartCrystal combination technology – scale up from lab to pilot scale & long term stability*”, *Die Pharmazie*, 2010, (accepted).
7. Sahoo, N.G., Kakran, M., **Al Shaal, L.**, Li, L., Müller, R.H., Pal, M., Tan, L.P., “*Preparation and characterization of quercetin nanocrystals*”, *J. Pharm. Sci.*, 2010, (accepted).
8. **Al Shaal, L.**, Shegokar, R., Müller, R.H., “*Apigenin smartCrystals for novel UV skin protection formulations*”, *Int. J. Pharm.*, 2010, (in press).

### Proceedings:

1. Kerč, J., Kobierski, S., **Al Shaal, L.**, Keck, C.M., Müller, R.H., “*Ascorbyl Palmitate nanosuspensions: Factors affecting the physical stability*”, in: 7<sup>th</sup> Central European Symposium on Pharmaceutical Technology and Biodelivery systems, Ljubljana, Slovenia, 18-20<sup>th</sup> Sep., *Farmaceutski vestnik* 59, 2008.
2. **Al Shaal, L.**, Müller, R.H., Keck, C.M., “*Preparation of stabilized and preserved Hesperetin nanosuspensions*”, in: 36<sup>th</sup> Annual Meeting & Exposition of the Controlled Release Society (CRS), Copenhagen, Denmark, 18-22<sup>th</sup> Jul., P-227, 2009.

3. **Al Shaal, L.**, Müller, R.H., Keck, C.M., “*Preservation of Hesperetin nanocrystals for dermal application*”, in: 2nd PharmSciFair, Nice, France, 8-12 June, P-316, 2009.

4. Shegokar, R., **Al Shaal, L.**, Singh, K.K., Müller, R.H., “*Oral apigenin nanosuspensions – effect of stabilizers on particle size*”, in: 10<sup>th</sup> annual meeting and exposition of the controlled release society Indian Chapter, Mumbai, India, 17-18 February, 2010.

### Abstracts:

1. **Al Shaal, L.**, Mishra, P.R., Müller, R.H., Keck, C.M., “*Hesperetin nanocrystals for dermal & oral bioavailability enhancement*”, in: Eurobiotech 2008, Krakow, Poland, 16-18 October, P2-37, 2008.

2. Kobiarski, S., **Al Shaal, L.**, Keck, C.M., Kerc, J., Müller, R.H., “*Preparation and physical evaluation of Ascorbyl Palmitate nanosuspensions*”, in: Annual Meeting of the American Association of Pharmaceutical Scientists (AAPS), Atlanta, USA, 16-20 November, 10(S2), 2008.

3. **Al Shaal, L.**, Müller, R.H., Keck, C.M., *Production & stability of dermal Hesperetin nanosuspensions*, in: 5th German – Polish Symposium “New Challenges for Pharmaceutical Sciences”, Poznań, Poland, 15-16 May, P-05, 2009.

4. **Al Shaal, L.**, Keck, C.M., “*Development of Hesperetin nanosuspensions for dermal application*”, in: Jahrestagung der Deutschen Pharmazeutischen Gesellschaft, Jena, Germany, 28 September – 1 October, P-C02, 2009.

5. Rachmawati, H., **Al Shaal, L.**, Keck, C.M., “*Curcumin nanocrystals for oral administration: Preparation, characterization and electrolyte stability*”, in: Jahrestagung der Deutschen Pharmazeutischen Gesellschaft, Jena, Germany, 28 September – 1 October, P-C04, 2009.

6. Shegokar, R., **Al Shaal, L.**, Singh, K.K., Müller, R.H., “*Production and optimization of preserved oral Apigenin nanosuspensions for cancer therapy*”, in: Annual Meeting of the American Association of Pharmaceutical Scientists (AAPS), Los Angeles, USA, 8-12 November, 2009.

7. **Al Shaal, L.**, Shegokar, R., Müller, R.H., “*Production of flavonoid nanosuspension*”, in: COST865 2010 Spring Workshop on Safety Aspects in Bioencapsulation Research & Applications, Cluj Napoca, Romania, 5 – 7 May, 2010.

8. **Al Shaal, L.**, Shegokar, R., Müller, R.H., “*Apigenin smartCrystals for novel UV skin protection formulations*”, in: European workshop on Particulate systems (EWPS), Paris, France, June 4-5, 2010.

9. **Al Shaal, L.**, Shegokar, R., Müller, R.H., “*Herstellung stabiler, konservierter Nanosuspensionen*”, in: 7. Der wissenschaftliche Nachwuchs stellt sich vor, Landesgruppe Berlin-Brandenburg der DPhG, Berlin, Germany, 2 Juli, P-5, 2010.

10. **Al Shaal, L.**, Shegokar, R., Müller, R.H., “*Microfluidics Reaction Technology (H69) zur Herstellung dermalen Flavonoidnanosuspension*”, in: 7. Der wissenschaftliche Nachwuchs stellt sich vor, Landesgruppe Berlin-Brandenburg der DPhG, Berlin, Germany, 2 Juli, P-6, 2010.

11. Müller, R.H., **Al Shaal, L.**, Shegokar, R., “*Injectable extended release lidocaine smartcrystals for dermal application*”, in: Jahrestagung der Deutschen Pharmazeutischen Gesellschaft, Braunschweig, Germany, 4 - 7 October, 2010, (accepted).

12. Sahoo, N.G., **Al Shaal, L.**, Kakran, M., Li, L., Müller, R.H., “*Artimisinin nanocrystals for improved oral bioavailability in malaria treatment*”, in: combined

meeting of the International Pharmaceutical Federation's PSWC and the AAPS Annual Meeting, New Orleans, USA, 14-18 November, T2154, 2010.

13. Sahoo, N.G., **Al Shaal, L.**, Kakran, M., Li, L., Müller, R.H., “*Antioxidant quercetin: preparation and characterization of nanocrystals*”, in: combined meeting of the International Pharmaceutical Federation's PSWC and the AAPS Annual Meeting, New Orleans, USA, 14-18 November, W4134, 2010.

14. Shegokar, R., **Al Shaal, L.**, Müller, R.H., “*Local anaesthetic nanocrystals as prolonged release profile*”, in: combined meeting of the International Pharmaceutical Federation's PSWC and the AAPS Annual Meeting, New Orleans, USA, 14-18 November, W4123, 2010.

15. **Al Shaal, L.**, Shegokar, R., Müller, R.H., “*Hesperetin nanosuspension: comparison of small and large scale homogenizer*”, in: combined meeting of the International Pharmaceutical Federation's PSWC and the AAPS Annual Meeting, New Orleans, USA, 14-18 November, W4088, 2010.

16. **Al Shaal, L.**, Shegokar, R., Müller, R.H., “*Novel UV skin protective antioxidant nanocrystals*”, in: combined meeting of the International Pharmaceutical Federation's PSWC and the AAPS Annual Meeting, New Orleans, USA, 14-18 November, W4089, 2010.

17. Voelker, M.T., Fichtner, F., Hoelman, A., Keck, C.M., **Al Shaal, L.**, Kaisers, U.X., Laudi, S., “*New injectable nanosuspension of BAY 41-2272 as effective treatment option in pulmonary hypertension*”, in: ATS international conference, Denver, USA, 14-19 May, 2011.



## **8 Acknowledgments**

For over than three years of hard working and intense research, I would like to express my gratitude to Prof. Dr. R. H. Müller for giving me the opportunity to do my PhD in such an admirable working group under his supervision and his support and especially on this interesting topic.

He gave me the opportunity to participate my research ideas and results in different conferences and congresses, national and international ones. I am very grateful for his confidence, encouragement and patience. My appreciation for his help in publishing papers and reviewing them will never be enough to cover his favors.

I am very grateful for Dr. Cornelia M. Keck for her help in the scientific guidance and her assistance in paper writing and giving productive ideas to enrich my research.

I would like to thank PharmaSol GmbH (Berlin, Germany) for providing the financial support for purchasing some of the consumables used in this research, and for sponsoring my participation in international congresses.

My gratitude to Freie Universität Berlin Nachwuchsförderung (NaFöG) scholarship for offering their financial support for the last year of my PhD work.

My special thanks to my friends and colleagues in the working group at the Freie Universität Berlin for helping me to complete this work and make it not only scientific work but also a team one.

Many thanks to Dr. Ranjita Shegokar and Dr. Jana Pardeike who both helped me to finish this work in a proper way and gave me many ideas to go on with my research.

To Dr. Aiman Hommoss who helped me at my beginning not only being my friend and colleague but also my room-mate.

I appreciate the help, the warm atmosphere, and the support provided from my friends and colleagues: Szymon Kobiersky, Senem Acar, Ansgar Brinkmann, Mirko Jansch, Rachmat Mauludin.

My deepest appreciation to Ms. Inge Volz and Ms. Corinna Schmidt whose help was not only inside the institute as a laboratory work and assistance but also exceeded it far beyond the department and left a huge impact in my life.

I would like to thank Mrs. Gabriela Karsubke for being helpful in administrative issues.

My appreciation to Dr. Wolfgang Mehnert and Dr. Lothar Schwabe for their support in practical issues.

I would like to show my endless appreciation and gratitude to my friend and second room mate Marwan Semaan.

Last but not least, I would like to dedicate my gratefulness to those who I would never be here without their support, love and faith, my parents and my sister.

## 9 Curriculum Vitae

For reasons of data protection,  
the curriculum vitae is not included in the online version



## 10 List of figures and tables:

### 10.1 Figures:

Fig. 1 The morphology of human skin [5] .....	5
Fig. 2 Chemical structure of the flavonoid family: (A) flavanols, (B) flavanones, (C) anthocyanidins, (D) flavones, (E) flavonols, (F) hydroxycinnamic acid. ....	8
Fig. 3 Left: poor solubility of BCS class II drug due to low-dissolution velocity and low-concentration gradient at membrane; right: improved bioavailability by production of nanocrystals, processing an increased saturation solubility and a high dissolution velocity which leads to a high-concentration gradient at the membranes [67].....	10
Fig. 4 Chemical structure of hesperetin .....	18
Fig. 5 Chemical structure of apigenin .....	19
Fig. 6 Molecular structure of Tween 80.....	20
Fig. 7 Molecular structure of poloxamer 188.....	20
Fig. 8 Molecular structure of Plantacare® 2000 UP.....	20
Fig. 9 Molecular structure of Inutec® SP1 .....	21
Fig. 10 Molecular structure of caprylyl glycol (1,2-Octandiol).....	21
Fig. 11 Molecular structure of CPC .....	22
Fig. 12 Molecular structure of ethanol .....	22
Fig. 13 Molecular structures of compounds present in EUX700: Phenoxyethanol (A), Benzyl alcohol (B), Potassium sorbate (C) and Tocopherol (D).....	23
Fig. 14 Molecular structures of components present in EUX702 containing Phenoxyethanol (A), Benzyl acid (B), Dehydroacetic acid (C) , Ethylhexylglycerin (D) and polyaminopropyl biguanide (E).....	23
Fig. 15 Molecular structures of compounds present in EUX9010: Phenoxyethanol (A) and Ethylhexylglycerin (B).....	24
Fig. 16 Molecular structure of glycerin.....	24
Fig. 17 Molecular structure of Hydrolite-5 .....	24
Fig. 18 Molecular structure of propylene glycol.....	26
Fig. 19 Molecular structures of compounds present in Phenoninp® ( A, Phenoxyethanol, B, Methylparaben, C, Ethylparaben, D, Propylparaben, E, Butylparaben) .....	26

Fig. 20 Molecular structures of components present in Rokonsal <sup>®</sup> PB-5 (A, Phenoxyethanol, B, Methylparaben, C, Ethylparaben, D, Propylparaben, E, Butylparaben) .....	27
Fig. 21 Molecular structure of triclosan .....	27
Fig. 22 Molecular structure of TPGS .....	28
Fig. 23 Molecular structure of DPPH <sup>•</sup> .....	29
Fig. 24 Reduction in z-average (PCS) along with the decrease in polydispersity index (PdI) as function of homogenization cycles for the four stabilizers (INT= Inutec <sup>®</sup> SP1, PLT= Plantacare <sup>®</sup> 2000 UP, PLX= poloxamer 188 and TW80= Tween 80) (PM = pre-milling) .....	40
Fig. 25 Reduction in LD diameter as function of homogenization cycles for the four stabilizers (INT= Inutec <sup>®</sup> SP1, PLT= Plantacare <sup>®</sup> 2000 UP, PLX= poloxamer 188 and TW80= Tween 80) (PM = pre-milling) .....	41
Fig. 26 Microscopic pictures of hesperetin nanosuspensions with the four stabilizers: (A) the original hesperetin macrosuspension, (B) Inutec <sup>®</sup> SP1, (C) Plantacare <sup>®</sup> 2000 UP, (D) poloxamer 188 and (E) Tween 80 (magnification 1000 fold, bar = 20 $\mu$ m) .....	43
Fig. 27 PCS (upper) and LD (lower) particle size of three different batches of hesperetin nanosuspensions produced on the same day using Micron LAB 40 .....	45
Fig. 28 PCS diameter and polydispersityindex (PdI) of the preserved nanosuspension directly after the addition of the preservative (CG= caprylyl glycol, EUX9010= Euxyl <sup>®</sup> PE 9010, HYD= hydrolite <sup>®</sup> -5, MLX= multiEx naturotics, PNP= Phenonip <sup>®</sup> , ROK= Rokonsal <sup>®</sup> PB-5) .....	47
Fig. 29 LD diameters 50%, 90% and 95% of the preserved nanosuspensions directly after addition of the preservative (CG= caprylyl glycol, EUX9010= Euxyl <sup>®</sup> PE 9010, HYD= hydrolite <sup>®</sup> -5, MLX= multiEx naturotics, PNP= Phenonip <sup>®</sup> , ROK= Rokonsal <sup>®</sup> PB-5) .....	48
Fig. 30 Light microscopy images of nanosuspensions preserved with: A) hydrolite-5, B) EUX9010, C) rokonsal PB-5, D) caprylyl glycol, E) multiEx naturotics, F) Phenonip <sup>®</sup> , (magnification 1000 fold, bar = 5 $\mu$ m) .....	49
Fig. 31 Reduction in particle size (PCS) along with the decrease in polydispersity index (PdI) as function of homogenization cycles for the six preservatives (A) EUX9010= Euxyl <sup>®</sup> PE 9010, (B) Hydrolite <sup>®</sup> -5, (C) Rokonsal <sup>®</sup> PB-5, (D) Phenonip <sup>®</sup> , (E) caprylyl glycol, and (F) multiEx naturotics (PM = pre-milling) .....	52
Fig. 32 LD diameters as a function of homogenization cycles for the six preservatives (A) EUX9010= Euxyl <sup>®</sup> PE 9010, (B) Hydrolite <sup>®</sup> -5, (C) Rokonsal <sup>®</sup> PB-5, (D) Phenonip <sup>®</sup> , (E) caprylyl glycol, and (F) multiEx naturotics (PM = pre-milling) .....	53

Fig. 33 Light microscopy images of nanosuspensions preserved with: (A) EUX9010= Euxyl® PE 9010, (B) Hydrolite®-5, (C) Rokonsal® PB-5, (D) Phenonip®, (E) caprylyl glycol, and (F) multiEx naturotics (magnification 1000 fold, bar = 5 µm) .....	54
Fig. 34 Differences in potentials of preserved and non-preserved nanosuspensions [138] .....	57
Fig. 35 Comparison of PCS diameters of preserved hesperetin nanosuspensions using different preservatives (EUX9010= Euxyl® PE 9010, HYD= Hydrolite®-5, ROK= Rokonsal® PB-5, PNP= Phenonip®, CG= caprylyl glycol and MLX= multiEx naturotics) added before or after homogenization (after one month stability stored at room temperature) .....	59
Fig. 36 Comparison of PCS diameters (up) and LD particle size (down) of preserved hesperetin nanosuspensions without or with the addition of antifoaming agent in different concentrations (% w/w) .....	61
Fig. 37 Microscopic pictures of the nanosuspension with antifoaming agents according to the following concentrations: A) nanosuspension without antifoaming agent, B) 0.125% antifoaming agent, C) 0.25% antifoaming agent, D) 0.5% antifoaming agent, & E) 1.0% antifoaming agent. (magnification 1000 fold, bar = 5 µm) .....	62
Fig. 38 Particle size reduction in nanosuspension during homogenization using PCS and LD ....	63
Fig. 39 Comparison between particle size (PCS & LD) after production of nanosuspensions using Micron LAB 40 & Avestin Emulsiflex C50 .....	64
Fig. 40 Particle sizes measured using PCS (up) and LD (down) of preserved nanosuspensions produced using Avestin Emulsiflex C50 for 3 kg batch (CG= caprylyl glycol, EtOH= ethanol, EUX700= Euxyl® K700, EUX702= Euxyl® K702, EUX9010= Euxyl® PE 9010, HYD= Hydrolite®-5, MLX= multiEx naturotics, PG= propylene glycol, PG-GLY= propylene glycol & glycerol mixture 14% & 11%, PG-HYD= propylene glycol & Hydrolite®-5 mixture 5% & 3%, PNP= Phenonip®, ROK= Rokonsal® PB-5) .....	65
Fig. 41 Light microscopy images of nanosuspensions preserved with: A) caprylyl glycol, B) ethanol, C) EUX700= Euxyl® K700, D) EUX702= Euxyl® K702, E) EUX9010= Euxyl® PE 9010, F) Hydrolite®-5, G) multiEx naturotics, H) propylene glycol, I) propylene glycol-glycerol 14% & 11%, J) propylene glycol-Hydrolite®-5 5% & 3%, K) Phenonip®, L) Rokonsal® PB-5, (magnification 1000 fold, bar = 5 µm) .....	67
Fig. 42 Particle size reduction measured with PCS (upper) & LD (lower) according to number of passages (1 to 7) starting with the pearl mill and ending with Avestin C50 (Raw= raw material) .....	70
Fig. 43 Microscopic pictures of hesperetin nanosuspensions using LAB 40 and the combination technology (magnification 160 fold, bar = 100 µm) .....	71

- Fig. 44 Particle size using PCS (upper) and LD (lower) after the addition of different preservatives to the produced smartCrystals<sup>®</sup> (CG= caprylyl glycol, CPC= cetylpyridinium chloride, EtOH= ethanol, EUX9010= Euxyl<sup>®</sup> PE 9010, GLY20= glycerol 20%, GLY50= glycerol 50%, HYD= Hydrolite<sup>®</sup>-5, MLX= multiEx naturotics, PG= propylene glycol, PNP= Phenonip<sup>®</sup>, ROK= Rokonsal<sup>®</sup> PB-5 and TPGS= D-alpha tocopherol polyethylene glycol 1000 succinate )..... 72
- Fig. 45 Light microscopy images of hesperetin smartCrystals<sup>®</sup> preserved with: A) caprylyl glycol, B) CPC= cetylpyridinium chloride, C) ethanol, D) EUX9010= Euxyl<sup>®</sup> PE 9010, E) glycerol 20%, F) glycerol 50%, G) Hydrolite<sup>®</sup>-5, H) multiEx naturotics, I) propylene glycol, J) Rokonsal<sup>®</sup> PB-5, K) TPGS, L) Non-preserved nanosuspension directly after admixing (magnification 1000 fold, bar = 5  $\mu$ m)..... 74
- Fig. 46 The physical stability of nanosuspensions, stabilized with the four different stabilizers (INT= Inutec<sup>®</sup> SP1, PLT= Plantacare<sup>®</sup> 2000 UP, PLX= poloxamer 188 and TW80= Tween 80), measured by PCS (z-average) and LD [d(v)99%] in fridge (4°C), room temperature (RT), and in oven (40°C) ..... 77
- Fig. 47 Microscopic pictures of hesperetin nanosuspensions with the four stabilizers: (A) Inutec<sup>®</sup> SP1, (B) Plantacare<sup>®</sup> 2000 UP, (C) poloxamer 188 and (D) Tween 80 (magnification 1000 fold, bar = 5  $\mu$ m). The left side is directly after production and the right side is after 2 years storage at room temperature ..... 79
- Fig. 48 Particle size of hesperetin nanosuspensions preserved with CG= caprylyl glycol and EUX9010= euxyl PE 9010 stored at three different temperatures (4°C, RT & 40°C) as a function of time (days) ..... 80
- Fig. 49 Light microscopy images of nanosuspensions preserved with: (A) caprylyl glycol, (B) EUX9010. (magnification 1000 fold, bar = 5  $\mu$ m). The left side is directly after production and the right side is after 2 years storage at room temperature..... 81
- Fig. 50 Particle size of hesperetin nanosuspensions preserved with Hydrolite<sup>®</sup>-5 and multiEx naturotics stored at three different temperatures (4°C, RT & 40°C) as a function of time (days) ..... 82
- Fig. 51 Light microscopy images of nanosuspensions preserved with: (C) Hydrolite<sup>®</sup>-5, (D) multiEx naturotics. (magnification 1000 fold, bar = 5  $\mu$ m). The left side is directly after production and the right side is after 2 years storage at room temperature ..... 83
- Fig. 52 Particle size of hesperetin nanosuspensions preserved with Phenonip<sup>®</sup> and Rokonsal<sup>®</sup> PB-5 stored at three different temperatures (4°C, RT & 40°C) as a function of time (days)..... 84



Fig. 53 Light microscopy images of nanosuspensions preserved with: (E) Phenonip <sup>®</sup> , (F) Rokonsal <sup>®</sup> PB-5. (magnification 1000 fold, bar = 5 μm). The right side is directly after production and the right side is after 2 years storage at room temperature .....	85
Fig. 54 Particle size of hesperetin nanosuspensions preserved with caprylyl glycol and EUX9010= Euxyl <sup>®</sup> PE 9010 stored at three different temperatures (4°C, RT & 40°C) as a function of time (days) .....	86
Fig. 55 Light microscopy images of nanosuspensions preserved with: (A) caprylyl glycol, (B) EUX9010. (magnification 1000 fold, bar = 5 μm). The right side is directly after production and the right side is after 2 years storage at room temperature.....	87
Fig. 56 Particle size of hesperetin nanosuspensions preserved with Hydrolite <sup>®</sup> -5 and multiEx naturotics stored at three different temperatures (4°C, RT & 40°C) as a function of time (days) .....	88
Fig. 57 Light microscopy images of nanosuspensions preserved with: (C) Hydrolite <sup>®</sup> -5, (D) multiEx naturotics. (magnification 1000 fold, bar = 5 μm). The right side is directly after production and the right side is after 2 years storage at room temperature .....	89
Fig. 58 Particle size of hesperetin nanosuspensions preserved with Phenonip <sup>®</sup> and Rokonsal <sup>®</sup> PB-5 stored at three different temperatures (4°C, RT & 40°C) as a function of time (days).....	90
Fig. 59 Light microscopy images of nanosuspensions preserved with: (E) Phenonip <sup>®</sup> , (F) Rokonsal <sup>®</sup> PB-5. (magnification 1000 fold, bar = 5 μm). The right side is directly after production and the right side is after 2 years storage at room temperature .....	91
Fig. 60 Particle size of hesperetin nanosuspensions preserved with hydrolite-5 with the addition of different concentration of antifoaming agent (Antifoam B Emulsion). 0.125% w/w, 0.250%, 0.500%, 1.000% stored at three different temperatures (4°C, RT & 40°C) as a function of time (days) .....	93
Fig. 61 Light microscopy images of nanosuspensions preserved with Hydrolite <sup>®</sup> -5 with the addition of different concentration of antifoaming agent (Antifoam B Emulsion). B1 (0.125% w/w), B2 (0.250%), B3 (0.500%), B4 (1.000%) (magnification 1000 fold, bar = 5 μm). The right side is directly after production and the right side is after 2 years storage at room temperature.....	94
Fig. 62 Particle size of hesperetin nanosuspensions preserved with caprylyl glycol and ethanol stored at three different temperatures (4°C, RT & 40°C) as a function of time (days).....	96
Fig. 63 Light microscopy images of nanosuspensions preserved with: (A) caprylyl glycol, (B) ethanol (magnification 1000 fold, bar = 5 μm). The right side is directly after production and the right side is after 2 years storage at room temperature.....	97

Fig. 64 Particle size of hesperetin nanosuspensions preserved with EUX700= Euxyl <sup>®</sup> K700 and EUX702= Euxyl <sup>®</sup> K702 stored at three different temperatures (4°C, RT & 40°C) as a function of time (days) .....	98
Fig. 65 Light microscopy images of nanosuspensions preserved with: (C) EUX700= Euxyl <sup>®</sup> K700 and (D) EUX702= Euxyl <sup>®</sup> K702. (magnification 1000 fold, bar = 5 µm). The right side is directly after production and the right side is after 2 years storage at room temperature ....	99
Fig. 66 Particle size of hesperetin nanosuspensions preserved with EUX9010= Euxyl <sup>®</sup> PE 9010 and Hydrolite <sup>®</sup> -5 stored at three different temperatures (4°C, RT & 40°C) as a function of time (days).....	100
Fig. 67 Light microscopy images of nanosuspensions preserved with: (E) EUX9010= Euxyl <sup>®</sup> PE 9010 and (F) Hydrolite <sup>®</sup> -5. (magnification 1000 fold, bar = 5 µm). The right side is directly after production and the right side is after 2 years storage at room temperature .....	101
Fig. 68 Particle size of hesperetin nanosuspensions preserved with multiEx naturotics and propylene glycol - glycerol mixture (14% & 11%) stored at three different temperatures (4°C, RT & 40°C) as a function of time (days) .....	102
Fig. 69 Light microscopy images of nanosuspensions preserved with: (G) multiEx naturotics and (H) propylene glycol - glycerol mixture (14% & 11%). (magnification 1000 fold, bar = 5 µm). The right side is directly after production and the right side is after 2 years storage at room temperature.....	103
Fig. 70 Particle size of hesperetin nanosuspensions preserved with PG (G) and PG-Hydrolite <sup>®</sup> -5 (5% & 3%) (H) stored at three different temperatures (4°C, RT & 40°C) as a function of time (days).....	104
Fig. 71 Light microscopy images of nanosuspensions preserved with: (I) propylene glycol, (H) propylene glycol –Hydrolite <sup>®</sup> -5 mixture (5% & 3%). (magnification 1000 fold, bar = 5 µm). The right side is directly after production and the right side is after 2 years storage at room temperature.....	105
Fig. 72 Particle size of hesperetin nanosuspensions preserved with Phenonip <sup>®</sup> and Rokonsal <sup>®</sup> PB-5 stored at three different temperatures (4°C, RT & 40°C) as a function of time (days).....	106
Fig. 73 Light microscopy images of nanosuspensions preserved with: Phenonip <sup>®</sup> and Rokonsal <sup>®</sup> PB-5. (magnification 1000 fold, bar = 5 µm). The right side is directly after production and the right side is after 2 years storage at room temperature.....	107
Fig. 74 Particle size of hesperetin nanosuspensions preserved with caprylyl glycol stored at three different temperatures (4°C, RT & 40°C) as a function of time (days) .....	108

- Fig. 75 Light microscopy images of nanosuspensions preserved with (A) caprylyl glycol (magnification 1000 fold, bar = 5  $\mu\text{m}$ ). The right side is directly after production and the right side is after 2 years storage at room temperature ..... 108
- Fig. 76 Particle size of hesperetin nanosuspensions preserved with CPC= cetylpyridinium chloride, ethanol and EUX9010= Euxyl<sup>®</sup> PE 9010 stored at three different temperatures (4°C, RT & 40°C) as a function of time (days) ..... 109
- Fig. 77 Light microscopy images of nanosuspensions preserved with: (B) CPC= cetylpyridinium chloride, (C) ethanol and (D) EUX9010= Euxyl<sup>®</sup> PE 9010. (magnification 1000 fold, bar = 5  $\mu\text{m}$ ). The right side is directly after production and the right side is after 2 years storage at room temperature ..... 110
- Fig. 78 Particle size of hesperetin nanosuspensions preserved with glycerol 20% and glycerol 50% stored at three different temperatures (4°C, RT & 40°C) as a function of time (days) . 111
- Fig. 79 Light microscopy images of nanosuspensions preserved with: (E) glycerol 20% and (F) glycerol 50% (magnification 1000 fold, bar = 5  $\mu\text{m}$ ). The right side is directly after production and the right side is after 2 years storage at 40°C..... 112
- Fig. 80 Particle size of hesperetin nanosuspensions preserved with Hydrolite<sup>®</sup>-5 and multiEx naturotics stored at three different temperatures (4°C, RT & 40°C) as a function of time (days) ..... 113
- Fig. 81 Light microscopy images of nanosuspensions preserved with: (G) Hydrolite<sup>®</sup>-5 and (H) multiEx naturotics. (magnification 1000 fold, bar = 5  $\mu\text{m}$ ). The right side is directly after production and the right side is after 2 years storage at room temperature ..... 114
- Fig. 82 Particle size of hesperetin nanosuspensions preserved with propylene glycol and Rokonsal<sup>®</sup> PB-5 stored at three different temperatures (4°C, RT & 40°C) as a function of time (days) ..... 115
- Fig. 83 Light microscopy images of nanosuspensions preserved with: (I) propylene glycol and (J) Rokonsal<sup>®</sup> PB-5. (magnification 1000 fold, bar = 5  $\mu\text{m}$ ). The right side is directly after production and the right side is after 2 years storage at room temperature ..... 116
- Fig. 84 Particle size of hesperetin nanosuspensions preserved with TPGS= D-alpha tocopherol polyethylene glycol 1000 succinate and non-preserved stored at three different temperatures (4°C, RT & 40°C) as a function of time (days)..... 117
- Fig. 85 Light microscopy images of nanosuspensions preserved with: (K) TPGS= D-alpha tocopherol polyethylene glycol 1000 succinate and (L) Non-preserved. (magnification 1000 fold, bar = 5  $\mu\text{m}$ ). The right side is directly after production and the right side is after 2 years storage at room temperature ..... 118

Fig. 86 Saturation solubility of hesperetin powder, macrosuspension, smartCrystals <sup>®</sup> and hesperetin powder with different solubilizing agents and different concentration. ....	119
Fig. 87 Reaction kinetics of DPPH <sup>•</sup> and hesperetin.....	120
Fig. 88 The steady state for the antioxidant reaction of hesperetin nanosuspension and DPPH <sup>•</sup>	120
Fig. 89 The declining in DPPH <sup>•</sup> concentration as a function of the number of moles of hesperetin / moles of DPPH <sup>•</sup> for hesperetin macrosuspension, Non-preserved hesperetin smartCrystals and preserved hesperetin smartCrystals <sup>®</sup> with (CG= caprylyl glycol, CPC= cetyl pyridinium chloride, EtOH= ethanol, EUX9010= Euxyl <sup>®</sup> PE 9010, GLY20= glycerol 20%, GLY50= glycerol 50%, HYD= Hydrolite <sup>®</sup> -5, MLX= multiEx naturotics, PG= propylene glycol, PNP= Phenonip <sup>®</sup> , ROK= Rokonsal <sup>®</sup> PB-5 and TPGS= D-alpha tocopherol polyethylene glycol 1000 succinate).....	123
Fig. 90 X-ray diffractogram of dried hesperetin coarse suspension, dried hesperetin suspension in Plantacare <sup>®</sup> 2000 UP aqueous solution (macrosuspension), dried hesperetin nanosuspension produced with Micron LAB40 and dried hesperetin smartCrystals <sup>®</sup> .....	125
Fig. 91 The cumulative amount of hesperetin dissolved from the smartCrystals <sup>®</sup> , macrosuspensions and dispersed powder in water in (A) PBS as a receptor medium or (B) a mixture of PBS : ethanol : PEG 400 (40:20:40).....	126
Fig. 92 Amount of hesperetin [%] in the produced nanosuspension produced with Micron LAB40 using different stabilizers (INT= Inutec <sup>®</sup> SP1, PLT= Plantacare <sup>®</sup> 2000 UP, PLX= poloxamer 188 and TW80= Tween 80) as a function of time (days).....	127
Fig. 93 Amount of hesperetin [%] in the preserved hesperetin nanosuspension produced with Micron LAB40 using different preservatives (CG= caprylyl glycol, EUX9010= Euxyl <sup>®</sup> PE 9010, HYD= Hydrolite <sup>®</sup> -5, MLX= multiEx naturotics, PNP= Phenonip <sup>®</sup> and ROK= Rokonsal <sup>®</sup> PB-5) as a function of time (days) either added before (A) or after (B) homogenization .....	128
Fig. 94 Amount of hesperetin [%] in the hesperetin nanosuspension produced with Micron LAB40 with the addition of an antifoaming agent as a function of time (days).....	129
Fig. 95 Amount of hesperetin [%] in the hesperetin nanosuspension produced with Avestin C50 as a function of time (days) after mixing the nanosuspension with different preservatives (CG= caprylyl glycol, EtOH= ethanol, EUX700= Euxyl <sup>®</sup> K700, EUX702= Euxyl <sup>®</sup> K702, EUX9010= Euxyl <sup>®</sup> PE 9010, HYD= Hydrolite <sup>®</sup> -5, MLX= multiEx naturotics, PG= propylene glycol, PG-GLY= propylene glycol - glycerin mixture, PG-HYD= propylene glycol – Hydrolite <sup>®</sup> -5 mixture, PNP= Phenonip <sup>®</sup> , ROK= Rokonsal <sup>®</sup> PB-5).....	129

Fig. 96 Amount of hesperetin [%] in the hesperetin nanosuspension produced with the smartCrystals technology preserved with different preservatives (CG= caprylyl glycol, CPC= cetylpyridinium chloride, EtOH= ethanol, EUX9010= Euxyl <sup>®</sup> PE 9010, GLY20= glycerol 20%, GLY50= glycerol 50%, HYD= Hydrolite <sup>®</sup> -5, MLX= multiEx naturotics, PG= propylene glycol, PNP= Phenonip <sup>®</sup> , ROK= Rokonsal <sup>®</sup> PB-5 and TPGS= D-alpha tocopherol polyethylene glycol 1000 succinate) as a function of time (days) .....	130
Fig. 97 PCS particle size (z-average) and polydispersity index (PdI) of three different batches of apigenin nanosuspensions .....	132
Fig. 98 LD particle size of three different batches of apigenin nanosuspensions .....	132
Fig. 99 Reduction in particle size (PCS) along with the decrease in polydispersity index (PdI) as a function of homogenization cycles (PM = pre-milling).....	133
Fig. 100 Reduction in LD diameter as function of homogenization cycles (PM = pre-milling).	133
Fig. 101 Particle size (z-average) and PdI after addition of various preservatives (CG= caprylyl glycol, CPC= cetylpyridinium chloride, EtOH= ethanol, EUX9010= Euxyl <sup>®</sup> PE 9010, GLY20= glycerol 20%, GLY50= glycerol 50%, HYD= Hydrolite <sup>®</sup> -5, MLX= multiEx naturotics, PNP= Phenonip <sup>®</sup> , PG= propylene glycol, ROK= Rokonsal <sup>®</sup> PB-5 and TPGS= D-alpha tocopherol polyethylene glycol 1000 succinate) .....	135
Fig. 102 LD diameter [ $\mu\text{m}$ ] after addition of various preservatives (CG= caprylyl glycol, CPC= cetylpyridinium chloride, EtOH= ethanol, EUX9010= Euxyl <sup>®</sup> PE 9010, GLY20= glycerol 20%, GLY50= glycerol 50%, HYD= Hydrolite <sup>®</sup> -5, MLX= multiEx naturotics, PNP= Phenonip <sup>®</sup> , PG= propylene glycol, ROK= Rokonsal <sup>®</sup> PB-5 and TPGS= D-alpha tocopherol polyethylene glycol 1000 succinate) .....	135
Fig. 103 Light microscopy images of apigenin nanosuspensions preserved with: (A) caprylyl glycol, (B) CPC, (C) ethanol, (D) Euxyl <sup>®</sup> PE 9010 , (E) glycerol 20%, (F) glycerol 50%, (G) Hydrolite <sup>®</sup> -5, (H) multiEx naturotics, (I) Phenonip <sup>®</sup> , (J) propylene glycol, (K) Rokonsal <sup>®</sup> PB-5, (L) TPGS= D-alpha tocopherol polyethylene glycol 1000, (M) Non-preserved nanosuspension directly after admixing (magnification 1000 fold, bar = 5 $\mu\text{m}$ ).....	137
Fig. 104 Particle size reduction measured with PCS (z-average) along with PdI reduction by producing using the pearl mill and followed with Avestin C50 .....	138
Fig. 105 Particle size reduction measured with PCS (z-average) along with PdI reduction by producing using the pearl mill and followed with Avestin C50 .....	139
Fig. 106 Comparative effect of alcohol and glycol preservatives (EtOH= ethanol, PG= propylene glycol, GLY20= glycerol 20%, CG= caprylyl glycol and GLY50= glycerol 50%) on mean	

particle size (PCS diameter) and LD diameter i.e. d(v)50%, d(v)95% and d(v)99% of apigenin nanosuspension on the day of production .....	141
Fig. 107 Light microscopy images of apigenin smartCrystals <sup>®</sup> (A) non-preserved and preserved with: (B) ethanol, (C) propylene glycol, (D) glycerol 20%, (E) caprylyl glycol and (F) glycerol 50% directly after admixing (magnification 1000 fold, bar = 5 $\mu$ m).....	142
Fig. 108 Comparative effect of synthetic established preservatives (HYD= Hydrolite <sup>®</sup> -5 and TCL= triclosan) on mean particle size (PCS diameter) and LD diameters i.e. d(v)50%, d(v)95% and d(v)99% of apigenin nanosuspension on the day of production .....	143
Fig. 109 Light microscopy images of apigenin smartCrystals <sup>®</sup> (A) non-preserved and preserved with: (B) Hydrolite <sup>®</sup> -5, (C) triclosan directly after admixing (magnification 1000 fold, bar = 5 $\mu$ m) .....	144
Fig. 110 Comparative effect of combination of preservatives (EUX9010= Euxyl <sup>®</sup> PE 9010, PNP= Phenonip <sup>®</sup> , ROK= Rokonsal <sup>®</sup> PB-5 and MLX= multiEx naturotics) on mean particle size (PCS diameter) and LD diameters i.e. d(v)50%, d(v)95% and d(v)99% of apigenin nanosuspension on the day of production. ....	145
Fig. 111 Light microscopy images of apigenin smartCrystals <sup>®</sup> (A) non-preserved and preserved with: (B) EUX9010= Euxyl <sup>®</sup> PE 9010, (C) Phenonip <sup>®</sup> , (D) Rokonsal <sup>®</sup> PB-5, (E) multiEx naturotics directly after admixing (magnification 1000 fold, bar = 5 $\mu$ m) .....	146
Fig. 112 Comparative effect of surfactant preservatives (PLT= Plantacare <sup>®</sup> 2000 UP, CPC= cetylpyridinium chloride and TPGS= D-alpha tocopherol polyethylene glycol 1000 succinate) on mean particle size (PCS diameter) and LD diameters i.e. d(v)50%, d(v)95% and d(v)99% of apigenin nanosuspension on the day of production. ....	148
Fig. 113 Light microscopy images of apigenin smartCrystals <sup>®</sup> (A) non-preserved and preserved with: (B) Plantacare <sup>®</sup> 2000 UP, (C) CPC= cetylpyridinium chloride and (D) TPGS= D-alpha tocopherol polyethylene glycol 1000 succinate directly after admixing (magnification 1000 fold, bar = 5 $\mu$ m) .....	148
Fig. 114 ZP of the prepared nanosuspensions in conductivity-modified water and in dispersing medium (CG= caprylyl glycol, EtoH= ethanol, EUX9010= Euxyl <sup>®</sup> PE 9010, TPGS= D-alpha tocopherol polyethylene glycol 1000 succinate, PLT= Plantacare <sup>®</sup> 2000 UP, TLC= triclosan, GLY20= glycerol 20%, HYD= Hydrolite <sup>®</sup> -5, MLX= multiEx naturotics, GLY50= glycerol 50%, PNP= Phenonip <sup>®</sup> , CPC= cetylpyridinium chloride, RKS= Rokonsal <sup>®</sup> PB-5, PG= propylene glycol and STD NS= non-preserved nanosuspension).....	150

Fig. 115 Particle size of apigenin nanosuspensions preserved with caprylyl glycol and cetylpyridinium chloride stored at three different temperatures (4°C, RT & 40°C) as a function of time (days) .....	151
Fig. 116 Light microscopy images of nanosuspensions preserved with: (A) caprylyl glycol, (B) cetylpyridinium chloride. (magnification 1000 fold, bar = 5 µm). The right side is directly after production and the right side is after 2 years storage at room temperature .....	152
Fig. 117 Particle size of apigenin nanosuspensions preserved with ethanol and Euxyl® PE 9010 stored at three different temperatures (4°C, RT & 40°C) as a function of time (days).....	153
Fig. 118 Light microscopy images of nanosuspensions preserved with: (C) ethanol and (D) Euxyl® PE 9010 (magnification 1000 fold, bar = 5 µm). The right side is directly after production and the right side is after 2 years storage at room temperature .....	154
Fig. 119 Particle size of apigenin nanosuspensions preserved with glycerol 20% and glycerol 50% stored at three different temperatures (4°C, RT & 40°C) as a function of time (days).....	155
Fig. 120 Light microscopy images of nanosuspensions preserved with: (E) glycerol 20% and (F) glycerol 50%. (magnification 1000 fold, bar = 5 µm). The right side is directly after production and the right side is after 2 years storage at room temperature .....	156
Fig. 121 Particle size of apigenin nanosuspensions preserved with Hydrolite®-5 and multiEx naturotics stored at three different temperatures (4°C, RT & 40°C) as a function of time (days) .....	157
Fig. 122 Light microscopy images of nanosuspensions preserved with: (G) Hydrolite®-5 and (H) multiEx naturotics. (magnification 1000 fold, bar = 5 µm). The right side is directly after production and the right side is after 2 years storage at room temperature .....	158
Fig. 123 Particle size of apigenin nanosuspensions preserved with propylene glycol and Phenonip® stored at three different temperatures (4°C, RT & 40°C) as a function of time (days) .....	159
Fig. 124 Light microscopy images of nanosuspensions preserved with: (I) propylene glycol and (J) Phenonip® (magnification 1000 fold, bar = 5 µm). The right side is directly after production and the right side is after 2 years storage.....	160
Fig. 125 Particle size of apigenin nanosuspensions preserved with Rokonsal® PB-5 and TPGS= D-alpha tocopherol polyethylene glycol 1000 succinate stored at three different temperatures (4°C, RT & 40°C) as a function of time (days).....	161
Fig. 126 Light microscopy images of nanosuspensions preserved with: (K) Rokonsal® PB-5 and (L) TPGS= D-alpha tocopherol polyethylene glycol 1000 succinate (magnification 1000 fold,	

bar = 5 $\mu\text{m}$ ). The right side is directly after production and the right side is after 2 years storage .....	162
Fig. 127 Particle size of non-preserved apigenin nanosuspensions stored at RT as a function of time (days).....	162
Fig. 128 Light microscopy images of (M) apigenin non-preserved. (magnification 1000 fold, bar = 5 $\mu\text{m}$ ). The right side is directly after production and the right side is after 2 years storage .....	163
Fig. 129 Particle size of apigenin smartCrystals preserved with caprylyl glycol and CPC= cetylpyridinium chloride stored at three different temperatures (4°C, RT & 40°C) as a function of time (days) .....	164
Fig. 130 Light microscopy images of smartCrystals preserved with: (A) caprylyl glycol and (B) cetylpyridinium chloride. (magnification 1000 fold, bar = 5 $\mu\text{m}$ ). The right side is directly after production and the right side is after 2 years storage.....	165
Fig. 131 Particle size of apigenin smartCrystals preserved with ethanol and euxyl PE9010 stored at three different temperatures (4°C, RT & 40°C) as a function of time (days) .....	166
Fig. 132 Light microscopy images of smartCrystals preserved with: (C) ethanol and (D) Euxyl <sup>®</sup> PE 9010 (magnification 1000 fold, bar = 5 $\mu\text{m}$ ). The right side is directly after production and the right side is after 2 years storage .....	167
Fig. 133 Particle size of apigenin smartCrystals preserved with glycerol 20% and glycerol 50% stored at three different temperatures (4°C, RT & 40°C) as a function of time (days).....	168
Fig. 134 Light microscopy images of smartCrystals <sup>®</sup> preserved with: (E) glycerol 20% and (F) glycerol 50%. (magnification 1000 fold, bar = 5 $\mu\text{m}$ ). The right side is directly after production and the right side is after 2 years storage.....	169
Fig. 135 Particle size of apigenin smartCrystals <sup>®</sup> preserved with Hydrolite <sup>®</sup> -5 and multiEx naturotics stored at three different temperatures (4°C, RT & 40°C) as a function of time (days) .....	170
Fig. 136 Light microscopy images of nanosuspensions preserved with: (G) Hydrolite <sup>®</sup> -5 and (H) multiEx naturotics. (magnification 1000 fold, bar = 5 $\mu\text{m}$ ). The right side is directly after production and the right side is after 2 years storage.....	170
Fig. 137 Particle size of apigenin smartCrystals preserved with propylene glycol and Plantacare <sup>®</sup> 2000 UP stored at three different temperatures (4°C, RT & 40°C) as a function of time (days) .....	171



Fig. 138 Light microscopy images of smartCrystals preserved with: (I) propylene glycol and (J) Plantacare <sup>®</sup> 2000 UP. (magnification 1000 fold, bar = 5 $\mu$ m). The right side is directly after production and the right side is after 2 years storage.....	172
Fig. 139 Particle size of apigenin smartCrystals preserved with Phenonip <sup>®</sup> and Rokonsal <sup>®</sup> PB-5 stored at three different temperatures (4°C, RT & 40°C) as a function of time (days).....	173
Fig. 140 Light microscopy images of nanosuspensions preserved with: (K) Phenonip <sup>®</sup> and (L) Rokonsal <sup>®</sup> PB-5. (magnification 1000 fold, bar = 5 $\mu$ m). The right side is directly after production and the right side is after 2 years storage.....	174
Fig. 141 Particle size of apigenin nanosuspensions preserved with TPGS= D-alpha tocopherol polyethylene glycol 1000 succinate and triclosan stored at three different temperatures (4°C, RT & 40°C) as a function of time (days) .....	175
Fig. 142 Light microscopy images of nanosuspensions preserved with: (M) TPGS= D-alpha tocopherol polyethylene glycol 1000 succinate and (N) triclosan. (magnification 1000 fold, bar = 5 $\mu$ m). The right side is directly after production and the right side is after 2 years storage .....	176
Fig. 143 Particle size of non-preserved apigenin nanosuspensions stored at three different temperatures (4°C, RT & 40°C) as a function of time (days).....	176
Fig. 144 Light microscopy images of (O) apigenin non-preserved. (magnification 1000 fold, bar = 5 $\mu$ m). The right side is directly after production and the right side is after 2 years storage.	176
Fig. 145 Saturation solubility of apigenin powder, macrosuspension, smartCrystals <sup>®</sup> and apigenin powder with different solubilizing agents and different concentration.....	177
Fig. 146 Reaction kinetics of DPPH and apigenin.....	178
Fig. 147 The steady state for the antioxidant reaction of apigenin nanosuspension and DPPH <sup>•</sup>	178
Fig. 148 The declining in DPPH <sup>•</sup> concentration as a function of the number of moles of apigenin / moles of DPPH <sup>•</sup> for apigenin macrosuspension, Non-preserved apigenin smartCrystals and preserved apigenin smartCrystals with (CG= caprylyl glycol, CPC= cetyl pyridinium chloride, EtOH= ethanol, EUX9010= Euxyl <sup>®</sup> PE 9010, GLY20= glycerol 20%, GLY50= glycerol 50%, HYD= Hydrolite <sup>®</sup> -5, MLX= multiEx naturotics, PG= propylene glycol, PNP= Phenonip <sup>®</sup> , ROK= Rokonsal <sup>®</sup> PB-5, TPGS= D-alpha tocopherol polyethylene glycol 1000 and TCL= triclosan).....	181
Fig. 149 X-ray diffractogram of dried apigenin coarse suspension, dried apigenin suspension in Plantacare <sup>®</sup> 2000 UP aqueous solution (macrosuspension), dried apigenin nanosuspension produced with Micron LAB40 and dried apigenin smartCrystals <sup>®</sup> .....	183

Fig. 150 The cumulative amount of apigenin dissolved from the smartCrystals <sup>®</sup> , macro-suspensions and dispersed powder in water in a mixture of Phosphate buffer saline : ethanol : PEG 400 (40:20:40).....	184
Fig. 151 Amount of apigenin [%] in the non-preserved and preserved apigenin nanosuspension produced with Micron LAB40 using different preservatives (STD= non-preserved, CG= caprylyl glycol, CPC= cetylpyridinium chloride, EtOH= ethanol, EUX9010= Euxyl <sup>®</sup> PE 9010, GLY20= glycerol 20%, GLY50= glycerol 50%, HYD= Hydrolite <sup>®</sup> -5, MLX= multiEx nатурotics, PG= propylene glycol, PNP= Phenonip <sup>®</sup> , ROK= Rokonsal <sup>®</sup> PB-5 and TPGS= D- alpha tocopherol polyethylene glycol 1000 succinate) as a function of time (days) .....	184
Fig. 152 Amount of apigenin [%] in the non-preserved and preserved apigenin nanosuspension produced with smartCrystals technology using different preservatives (STD= non-preserved, CG= caprylyl glycol, CPC= cetylpyridinium chloride, EtOH= ethanol, EUX9010= Euxyl <sup>®</sup> PE 9010, GLY20= glycerol 20%, GLY50= glycerol 50%, HYD= Hydrolite <sup>®</sup> -5, MLX= multiEx nатурotics, PG= propylene glycol, PNP= Phenonip <sup>®</sup> , ROK= Rokonsal <sup>®</sup> PB-5, TPGS= D-alpha tocopherol polyethylene glycol 1000 succinate and TCL= triclosan) as a function of time (days).....	185

## 10.2 Tables:

Table 1 Different types of flavonoids used as antioxidants .....	9
Table 2 MultiEx Naturotics compounds .....	25
Table 3 List of preservatives and preservative mixtures used and their concentration ranges .....	29
Table 4 Calculated and measured RI for hesperetin. For the standard curve [y = RI related to the concentration of the substance, x = concentration of the material in the defined solvent (mg/100 mL)] .....	38
Table 5 Contact angle of different aqueous surfactant solutions (1% w/w) and pure water with the compressed discs of hesperetin .....	39
Table 6 Formulations of hesperetin nanosuspensions with different stabilizers (w/w) .....	39
Table 7 Zeta potential data for the hesperetin nanosuspensions using four different stabilizers... 44	44
Table 8 ZP values of the preserved hesperetin nanosuspensions .....	50
Table 9 ZP values of the preserved nanosuspensions in distilled water and in original dispersion medium.....	56
Table 10 ZP values of the preserved nanosuspensions in distilled water and in original dispersion medium.....	68

Table 11 ZP values of the preserved and nonpreserved smartCrystals <sup>®</sup> .....	72
Table 12 LD diameter for hesperetin nanosuspensions incorporated in different gels after 1 month and 1 year .....	95
Table 13 EC <sub>50</sub> values of hesperetin macrosuspension, smartCrystals <sup>®</sup> and preserved hesperetin smartCrystals (CG= caprylyl glycol, CPC= cetyl pyridinium chloride, EtOH= ethanol, EUX9010= Euxyl <sup>®</sup> PE 9010, GLY20= glycerol 20%, GLY50= glycerol 50%, HYD= Hydrolite <sup>®</sup> -5, MLX= multiEx naturotics, PG= propylene glycol, PNP= Phenonip <sup>®</sup> , ROK= Rokonsal <sup>®</sup> PB-5 and TPGS= D-alpha tocopherol polyethylene glycol 1000 succinate).....	124
Table 14 calculated and measured RI for apigenin. For the standard curve [y = RI related to the concentration of the substance, c = concentration of the material in the defined solvent (mg/100 mL)]. .....	131
Table 15 LD diameter for apigenin nanosuspensions incorporated in different gels after 1 month and 1 year .....	163
Table 16 EC <sub>50</sub> values of apigenin macrosuspension, smartCrystals and preserved hesperetin smartCrystals (CG= caprylyl glycol, CPC= cetyl pyridinium chloride, EtOH= ethanol, EUX9010= Euxyl <sup>®</sup> PE 9010, GLY20= glycerol 20%, GLY50= glycerol 50%, HYD= Hydrolite <sup>®</sup> -5, MLX= multiEx naturotics, PG= propylene glycol, PNP= Phenonip <sup>®</sup> , ROK= Rokonsal <sup>®</sup> PB-5, TPGS= D-alpha tocopherol polyethylene glycol 1000 and TCL= triclosan) .....	182